



HAL
open science

Vibrotactile feedback to support kinesthetic motor imagery in a brain-computer interface for post-stroke motor rehabilitation

Altamira Gabriela Herrera

► **To cite this version:**

Altamira Gabriela Herrera. Vibrotactile feedback to support kinesthetic motor imagery in a brain-computer interface for post-stroke motor rehabilitation. Computer Science [cs]. Université de Lorraine, 2024. English. NNT: 2024LORR0002 . tel-04540310

HAL Id: tel-04540310

<https://hal.univ-lorraine.fr/tel-04540310>

Submitted on 9 Sep 2024

HAL is a multi-disciplinary open access archive for the deposit and dissemination of scientific research documents, whether they are published or not. The documents may come from teaching and research institutions in France or abroad, or from public or private research centers.

L'archive ouverte pluridisciplinaire **HAL**, est destinée au dépôt et à la diffusion de documents scientifiques de niveau recherche, publiés ou non, émanant des établissements d'enseignement et de recherche français ou étrangers, des laboratoires publics ou privés.



**UNIVERSITÉ
DE LORRAINE**

**BIBLIOTHÈQUES
UNIVERSITAIRES**

AVERTISSEMENT

Ce document est le fruit d'un long travail approuvé par le jury de soutenance et mis à disposition de l'ensemble de la communauté universitaire élargie.

Il est soumis à la propriété intellectuelle de l'auteur. Ceci implique une obligation de citation et de référencement lors de l'utilisation de ce document.

D'autre part, toute contrefaçon, plagiat, reproduction illicite encourt une poursuite pénale.

Contact bibliothèque : ddoc-theses-contact@univ-lorraine.fr
(Cette adresse ne permet pas de contacter les auteurs)

LIENS

Code de la Propriété Intellectuelle. articles L 122. 4

Code de la Propriété Intellectuelle. articles L 335.2- L 335.10

http://www.cfcopies.com/V2/leg/leg_droi.php

<http://www.culture.gouv.fr/culture/infos-pratiques/droits/protection.htm>

Vibrotactile feedback to support kinesthetic motor imagery in a brain-computer interface for post-stroke motor rehabilitation

THÈSE

présentée et soutenue publiquement le 10 Janvier 2024

pour l'obtention du

Doctorat de l'Université de Lorraine
(mention informatique)

par

Gabriela Herrera Altamira

Composition du jury

Président : François Cabestaing, Professeur à l'Université de Lille, France

Rapporteurs : François Cabestaing, Professeur à l'Université de Lille, France
Géry Casiez, Professeur à l'Université de Lille, France

Examineurs : Maryam Alimardani, Assistant Professor at Tilburg University, The Netherlands
Ines di Loreto, Maître de conférences à l'Université de Technologie de Troyes, France

Directeurs : Patrick Hénaff, Professeur à l'Université de Lorraine / Mines Nancy, France

Co-Encadrant : Laurent Bougrain, Maître de conférences à l'Université de Lorraine, France

Invités : Stéphanie Fleck, Maître de conférences à l'Université de Lorraine, France
Anatole Lécuyer, Directeur de recherche, Inria, Rennes, France

Mis en page avec la classe thesul.

Remerciements

Je n'aurais pas pu en arriver là sans le soutien inconditionnel de plusieurs personnes dont les contributions méritent d'être reconnues dans ces pages de remerciements.

Tout d'abord, je tiens à remercier les membres du jury qui m'ont fait l'honneur de lire et d'évaluer ce manuscrit en l'enrichissant de leurs commentaires. Merci à François Cabestaing, Géry Casiez et Inès di Loreto. Thank you very much professor Maryam Alimardani for taking the time to be part of the jury.

Merci à mes encadrants, Laurent Bougrain, Stéphanie Fleck et Anatole Lécuyer pour m'avoir transmis leur passion pour la recherche, leur curiosité et leur rigueur scientifique. Merci Laurent de m'avoir donné cette opportunité de collaborer à cet incroyable projet et de m'avoir transmis ton savoir. Merci Anatole pour avoir toujours trouvé un moment de disponible, pour ton optimisme et pour tes commentaires précieux et pertinents. Merci Stéphanie de m'avoir transmis tes connaissances avec patience et dévouement, et merci pour toutes les expériences professionnelles et personnelles que nous avons partagées. Ce fut un honneur de travailler avec vous trois, et j'espère continuer à le faire.

Merci aux autres partenaires du projet GraspIT. Merci à Sébastien Rimbart, un des pionniers de ce projet, merci pour tes conseils et pour les moments où nous avons pu échanger. Merci à Thomas Prampart, qui a toujours su m'aider à résoudre les problèmes que j'avais avec OpenViBE et qui s'est assuré que je puisse faire des expériences à Rennes. Merci à l'équipe de l'IRR - Lay Saint-Christophe pour nous avoir permis de réaliser des tests et des études dans leurs locaux, ainsi que pour leurs retours sur chaque nouveau dispositif que nous leur avons présenté.

Je tiens à remercier les partenaires industriels. Tout d'abord à l'équipe de la société Octarina, avec qui nous avons travaillé en étroite collaboration sur le développement de l'interface graphique. Merci pour votre engagement et votre patience. Votre contribution à ce projet a été très précieuse. Merci à l'équipe d'OpenEdge, merci Nathalie, Kevin et Yannick pour votre contribution au développement du dispositif tangible et pour m'avoir aidé à améliorer mon prototype de dispositif vibrotactile.

Merci à tous les membres des équipes NeuroRhythms, PErSEUs et Hybrid pour leur accueil chaleureux et tous les moments passés ensemble. Merci à Lætitia, Stéphane et Lauriane pour les nombreuses discussions qui ont rendu cette expérience encore plus agréable. Merci aux stagiaires Emilie, Chaïma, Mathilde, Cédric et Kevin, dont la participation à ce projet a été précieuse. Merci pour votre professionnalisme et votre engagement, ce travail ne serait certainement pas le même sans vous.

Je voudrais également remercier tous les volontaires qui ont participé à mes expériences. Merci d'avoir contribué à mes travaux pour que je puisse obtenir des données sur lesquelles travailler. Sans vous, cette thèse n'aurait certainement pas été possible !

Gracias Mariana Díaz, por además de mostrar un gran interés en mi proyecto, motivarme a participar en actividades más allá de la tesis, a comunicar mi trabajo a todo tipo de público y enriquecer mi experiencia. Gracias por todas esas conversaciones *autour d'un café*, y por los tips de la vida en Francia.

Por último, quiero expresar mi más sincero agradecimiento a aquellos que llevo más cerca del corazón.

Gracias a Cra, Ferst, Jaks, Cristy G, Lars, Miri, Diego, y a todos aquellos que han estado conmigo a distancia, sepan que los llevo siempre conmigo.

Gracias a mi fiel amiguito peludo, Pablito(u), por siempre sacarme una sonrisa.

A mi increíble hermana, Fer, por siempre estar a mi lado, por esas llamadas interminables, esos stickers divertidos de WhatsApp, y por compartir consejos deportivos y de vida. Tu presencia ilumina mis días de una manera única.

A mis papás, les debo un agradecimiento infinito. Mamá y papá, son mis mayores modelos a seguir. Agradezco su creencia constante en mí, su apoyo incondicional a lo largo del tiempo y la distancia. Papá, agradezco especialmente que hayas compartido conmigo el valor del trabajo, la organización, y la importancia de seguir mis pasiones. Mamá, gracias por enseñarme a siempre dar lo mejor de mí, respaldarme en cada paso, confiar en mis decisiones y mostrarme con tu ejemplo lo que significa ser una mujer trabajadora y, al mismo tiempo, dedicada a su familia. Siempre han estado presente, atentos y pendientes de mí, y eso significa el mundo para mí. Los dos me han enseñado todo lo que sé, y les agradezco por permitirme llegar hasta este día. Espero que se sientan contentos y orgullosos de su hija que tanto los ama. Gracias por todo.

Thanks to my husband, Léo, for being the solid rock in my life and my ultimate cheerleader. Your unwavering support since day one means the world to me. Thank you for patiently enduring my countless repetitions of the same stories, for standing by me during the intense months of writing, and for gently reminding me that life extends beyond the confines of a computer screen. Your comforting presence and the laughter you have brought into my life during the moments of need are invaluable. Your role in my journey is beyond measure. I love you.

*"We keep moving forward, opening up new doors and doing new things, because we're curious. . .
and curiosity keeps leading us down new paths." - Walt Disney*

Contents

List of Figures	xi
List of Tables	xv
Acronyms	xvii
Résumé en Français	xix
General Introduction	xxv

Part I BCIs for Upper Limb Rehabilitation After Stroke: State-of-the-Art, Research Methodology, and Technical Platform

Chapter 1 A Brief Introduction to Stroke	1
1.1 Introduction	1
1.2 Definition and Types of Stroke	2
1.3 Effects of Stroke: Motor and Sensory Deficits	2
1.3.1 Motor deficits	3
1.3.2 Sensory deficits	3
1.3.3 Psychosocial complications	4
1.4 Post-Stroke Recovery	4
1.5 Current Therapies for Upper Limb Motor Recovery	5
1.5.1 Vibration therapy	5
1.6 Conclusion	6
Chapter 2 Brain-Computer Interfaces for Post-Stroke Rehabilitation of the Upper Limb	7
2.1 Introduction	8

2.2	Acquisition of the Brain Activity	9
2.3	Mental Tasks in Post-Stroke BCIs	13
2.3.1	Action observation	13
2.3.2	Motor attempt	13
2.3.3	Motor imagery	13
2.4	Signal Processing and Classification	14
2.4.1	Preprocessing	14
2.4.2	Feature extraction	16
2.4.3	Classification	17
2.5	Feedback Modalities	18
2.5.1	Visual Feedback	20
2.5.2	Virtual reality	21
2.5.3	Haptic Feedback	21
2.5.4	Multimodal Feedback	25
2.5.5	Feedback Timing	27
2.5.6	Conclusion on the Feedback	28
2.6	Focus on Vibrotactile Stimulation in Other BCI Applications	28
2.6.1	Event-Related Potentials	28
2.6.2	Motor Imagery	29
2.7	Conclusion	35
 Chapter 3 Design-Based Research Methodology for the Novel Design of Vibrotactile Feedback in KMI-Based BCIs		37
3.1	Introduction	37
3.2	Focus Phase	40
3.3	Understand Phase	40
3.4	Define Phase	41
3.5	Conceive and Build Phases	41
3.6	Test Phase	42
3.7	Conclusion	43
 Chapter 4 Building the Vibrotactile Device and Description of the Technical Platform		45
4.1	GraspIt V1: a BCI to improve kinesthetic motor imagery	46
4.1.1	Components of the BCI	46
4.1.2	Functioning of the BCI	47
4.2	GraspIt V2: further gamification and integration of haptic feedback	48

4.2.1	Adding movements and everyday life situations	48
4.2.2	OpenViBE communication and incorporation of haptic feedback . . .	51
4.3	Conception and Building of a Novel Vibrotactile Device	52
4.3.1	Components of the vibrotactile device	53
4.3.2	Anatomical location of the motors	54
4.3.3	Summary of the challenges addressed by the vibrotactile device . . .	56
4.3.4	FeelIt: a KMI-based BCI integrating visual and vibrotactile feedback	57
4.4	Conclusion	57

Part II Design and Evaluation of Vibrotactile Feedback to Support Kinesthetic Motor Imagery of Grasping **59**

Chapter 5 Identifying the Sensory Thresholds of a Vibrotactile Device for a KMI-Based BCI **61**

5.1	Introduction	62
5.2	Material and Methods	63
5.2.1	Experimental protocol	63
5.2.2	Questionnaires	65
5.3	Results	65
5.3.1	Minimum Sensory Threshold	65
5.3.2	Uncomfortable Threshold	68
5.3.3	User Experience	69
5.4	Discussion	70
5.4.1	The minimum sensory threshold varies according to age and placement	71
5.4.2	Participants' tolerance toward high vibration intensities	72
5.4.3	A first user evaluation of the vibrotactile device	72
5.5	Conclusion	74

Chapter 6 Design and Evaluation of the Vibrotactile Stimulation as Feedback for a KMI-Based BCI **75**

6.1	Introduction	76
6.2	Design of the Vibrotactile Stimulation	78
6.2.1	Sequential Vibration Pattern	78
6.2.2	Simultaneous Vibration Pattern	80
6.3	Material and Methods	81
6.3.1	Experimental Setup	81

6.3.2	Questionnaires	83
6.3.3	Statistical Tests of the User Evaluation	84
6.3.4	EEG offline analysis	85
6.4	Results	85
6.4.1	User’s subjective evaluation	85
6.4.2	Participants’ emotional state, fatigue level, and mental workload	88
6.4.3	System’s elicited emotions and attractiveness	89
6.4.4	Time-frequency analysis of EEG activity	91
6.4.5	Topographical analysis of EEG activity	96
6.4.6	Activity in delta and theta	100
6.5	Discussion	101
6.5.1	User preference for the three-motor sequential configuration	101
6.5.2	Positive user experience and system’s attractiveness	101
6.5.3	EEG activity in the alpha, mu, and beta frequency bands	102
6.5.4	Activity in delta and theta: a potential indicator of attention and surprise	104
6.6	Limitations and Future Work	105
6.7	Conclusion	105

Chapter 7 Evaluation of a KMI-Based BCI Integrating Visual and Vibrotactile Feedback **107**

7.1	Introduction	108
7.2	Material and Methods	109
7.2.1	Participants	109
7.2.2	Experimental Setup	110
7.2.3	Questionnaires	110
7.2.4	Experimental Procedure	111
7.2.5	Online Classification	115
7.2.6	EEG Offline Analysis	116
7.2.7	Statistical Analyses of Behavioral Data and BCI Performance	117
7.3	Results	117
7.3.1	BCI Performance Across Feedback Modalities	117
7.3.2	Participants’ Subjective Assessment of the Bimodal BCI	121
7.3.3	Evaluation of the Participants’ Well-Being	125
7.3.4	Influence of Participant’s Characteristics on BCI Performance	131
7.3.5	System’s Elicited Emotions and Attractiveness	135
7.3.6	EEG Analysis	139

7.4	Discussion	146
7.4.1	BCI performance is comparable in all feedback modalities	146
7.4.2	Participants' preference for the bimodal feedback	146
7.4.3	Factors influencing the performance	147
7.4.4	The bimodal BCI offers a positive user experience	149
7.4.5	EEG activity	150
7.5	Conclusion	151
 Chapter 8 Toward a Post-Stroke Evaluation of a KMI-Based BCI Integrating Visual and Vibrotactile Feedback: Experimental Protocol		153
8.1	Introduction	154
8.2	Objectives	155
8.2.1	Primary Objective	155
8.2.2	Secondary Objectives	156
8.3	Participants	157
8.3.1	Inclusion and Non-Inclusion Criteria	157
8.3.2	Pseudo-Anonymization	158
8.4	Study Procedure	158
8.4.1	Experimental Setup	158
8.4.2	Procedure	158
8.4.3	Study Duration	164
8.5	Statistical Tests	164
8.6	Benefits and Risks	165
8.7	Withdrawal	165
8.8	Management of Adverse Events	165
8.8.1	Evaluation and report of adverse events	165
8.9	Data Archiving and Access to Documents	166
8.10	Conclusion and Study Limitations	166
 Chapter 9 General Discussion and Perspectives		169
9.1	General Summary	169
9.2	Future Work	172
9.3	Primary Takeaways	173
9.3.1	The importance of a user-centered design	173
9.3.2	The importance of adapting the BCI to the patient	173
 Appendix		175

Appendix A Questionnaires for the user evaluation of the vibration patterns	175
Appendix B Questionnaire Participants' Characteristics	185
Appendix C Questionnaire for the user evaluation of the feedback modalities	189
Appendix D Questionnaires for the user evaluation with post-stroke patients	193
Bibliography	205
My publications	227

List of Figures

1.1	Motor and sensory cortices of the human brain.	3
2.1	The Brain-Computer Interface Loop	9
2.2	Visual feedback covering the participant’s hand, extracted from [1].	20
2.3	Visual feedback consisting of a boat’s race, extracted from [2].	20
2.4	Hand exoskeleton developed by Ramos-Murguialday et al. [3]	22
2.5	Neuroolution’s IpsiHand for post-stroke recovery.	23
2.6	Tendon vibration applied during MI, extracted from [4].	24
2.7	g.tec’s recoveriX BCI system for post-stroke motor rehabilitation with visual and FES feedback.	26
2.8	Soft glove and visual feedback extracted from [5].	26
2.9	Congruent locations of vibrotactile feedback on the wrist and hand.	30
2.10	Congruent location of vibrotactile feedback on the biceps and fingertip.	31
2.11	Non-congruent vibrotactile feedback on the lower neck.	32
2.12	Visual and Vibrotactile Feedback Extracted From [6]	33
2.13	Vibration Patterns by Leeb et al. [7].	34
3.1	Example of a design-based research process comprising six iterative phases, extracted from [8].	38
3.2	Methodology for the design and evaluation of the vibrotactile feedback.	39
4.1	Evolution of GraspIt	46
4.2	Virtual environment of GraspIt V1.	47
4.3	Hand movements in GraspIt.	48
4.4	Grasping games.	49
4.5	Grasping of a ketchup bottle. The visual feedback includes an animated hand and a gauge. A progress bar indicates the current trial.	49
4.6	GraspIt User Parameters	50
4.7	Calibration Parameters of the BCI.	51
4.8	Feedback Parameters of the BCI.	52
4.9	Advanced Parameters of the BCI.	53
4.10	First version of the vibrotactile device.	55
4.11	Second version of the vibrotactile device.	56
5.1	Methodology for the design and evaluation of vibrotactile feedback: Build phase - Identification of the vibrotactile sensorial thresholds.	62
5.2	Box plots of the minimum sensory thresholds.	66
5.3	Box plots of the uncomfortable thresholds. RPM stands for revolutions per minute.	68

5.4	Participants' fatigue level and emotions.	70
5.5	AttrakDiff questionnaire results 1.	71
6.1	Methodology for the design and evaluation of vibrotactile feedback. Build phase - Design of the vibrotactile stimulation.	76
6.2	Sequential vibration patterns	79
6.3	Simultaneous vibration patterns	80
6.4	Experimental setup to define the vibrotactile activation patterns	82
6.5	Participant's description of the vibrotactile stimulation on the hand and forearm.	86
6.6	Box plots of the Likert evaluation of the four vibration configurations	87
6.7	Participants forced choice: three versus two motors	87
6.8	Participants forced choice: three motors, sequential versus simultaneous	88
6.9	Participants forced choice: two motors, sequential versus simultaneous	88
6.10	Participant's fatigue, mental workload, and emotions during the session.	89
6.11	meCUE's positive emotions	90
6.12	meCUE's negative emotions	91
6.13	AttrakDiff questionnaire results 2.	92
6.14	ERSPs grand average time-frequency analysis of the primary motor and so- matosensory cortices.	93
6.15	ERSPs grand average time-frequency analysis of the occipital cortex.	94
6.16	Average 2-second topographies in alpha + low beta grouped by device configura- tions.	96
6.17	Average 2-second topographies in high beta grouped by device configurations.	97
6.18	Average 2-second topographies in alpha + low beta grouped by stimulation intensity.	97
6.19	Average 2-second topographies in high beta grouped by stimulation intensity.	98
6.20	Post-stimulation topographies in alpha + low beta grouped by stimulation intensity.	99
6.21	Post-stimulation topographies in high beta grouped by stimulation intensity.	99
6.22	One-second average topographies in delta.	100
6.23	One-second average topographies in theta.	100
7.1	Methodology for designing and evaluating vibrotactile feedback: Test phase - Evaluation of the feedback.	108
7.2	Calibration run consisting of 20 trials. Participants performed KMI without any feedback during the calibration. <i>s</i> stands for seconds.	112
7.3	Feedback run consisting of 15 trials. Participants performed KMI and received visual, vibrotactile, or bimodal feedback. <i>s</i> stands for seconds.	113
7.4	Traffic light provides instructions for the participants when visual feedback is inactive.	114
7.5	39 electrodes (in green) selected from the original 64-electrode setup.	115
7.6	BCI performance across the three feedback modalities grouped by presentation order.	118
7.7	BCI performance across the three feedback modalities.	119
7.8	BCI performance grouped by order of presentation, regardless of feedback modality.	120
7.9	Ranking of feedback modalities	121
7.10	Chart depicting the users' perception of the feedback modality that helped the most to imagine the movement.	122
7.11	Chart depicting the users' preference of the most entertaining feedback.	122
7.12	Chart depicting the users' preference of the most realistic feedback.	123

7.13	Users' perception on the easiest feedback modality to understand.	123
7.14	Users' perception on the hardest feedback modality to understand.	124
7.15	Temporal evolution of fatigue levels across the session.	125
7.16	Emotional states of participants before and after the session. *** $p < 0.001$	126
7.17	Raw mental workload score of the NASA-TLX questionnaire for each feedback modality.	126
7.18	Scores of each item of the NASA-TLX questionnaire for the calibration and feedback modalities.	127
7.19	Mental workload score of the NASA-TLX questionnaire by presentation order.	128
7.20	NEXT-Q: Score for the <i>Mood</i> dimension per feedback modality. The average for each modality is shown in gray. * $p < 0.05$, ** $p < 0.01$	129
7.21	NEXT-Q: Score for the <i>Motivation</i> dimension per feedback modality. The average for each modality is shown in gray. ** $p < 0.01$	130
7.22	NEXT-Q: Score for the <i>Mindfulness</i> dimension per feedback modality. The average for each modality is shown in gray.	130
7.23	NEXT-Q: Score for the <i>Cognitive Load</i> dimension per feedback modality. The average for each modality is shown in gray.	131
7.24	NEXT-Q: Score for the <i>Agency</i> dimension per feedback modality. The average for each modality is shown in gray. ** $p < 0.01$	131
7.25	Grand average of self-efficiency score.	133
7.26	Correlation between self-efficiency and average feedback score.	134
7.27	Results from the Freiburg Mindfulness Inventory.	134
7.28	Visualization of meCUE's positive emotional responses during the third experiment.	136
7.29	Visualization of meCUE's negative emotional responses during the third experiment.	136
7.30	AttrakDiff score dimensions for the third experiment.	137
7.31	AttrakDiff portfolio for the third experiment.	138
7.32	AttrakDiff word pairs diagram for third experiment.	139
7.33	Time-frequency analysis (ERSP) of left-hand MI (n=28) for electrode C_4 during the calibration and three feedback conditions.	139
7.34	Time-frequency analysis (ERSP) of left-hand MI (n=28) for electrode C_3 during the calibration and three feedback conditions.	140
7.35	Time-frequency analysis (ERSP) of right-hand MI (n=3) for electrode C_4 during the calibration and three feedback conditions.	141
7.36	Time-frequency analysis (ERSP) of right-hand MI (n=3) for electrode C_3 during the calibration and three feedback conditions.	142
7.37	Scalp topographies of the average of left-hand KMI (t=0 – 4s) for the 8-30 Hz frequency band for the calibration and feedback phases.	143
7.38	Scalp topographies of the average of left-hand KMI (t=0–4s) for a) μ and b) beta frequency bands for the calibration and feedback phases.	144
7.39	Scalp topographies of the average of right-hand KMI (t=0–4s, n=3) for the 8-30 Hz frequency band for the calibration and feedback phases.	145
7.40	Scalp topographies of the average of the feedback phase (t=4–6s) for the 8-30 Hz frequency band.	145
8.1	Methodology for designing and evaluating vibrotactile feedback: Test phase - User evaluation with post-stroke patients.	154
8.2	Sessions of the Clinical Protocol	159
8.3	Calibration run timeline for study among post-stroke participants.	162

List of Figures

8.4	Image depicting the screen participants will see during the calibration. The virtual arm will match the participant's affected limb.	162
8.5	Feedback run timeline for study among post-stroke participants.	163
8.6	Schedule of the study sessions for eight post-stroke participants.	164

List of Tables

2.1	Summary of articles on EEG-based BCIs for upper limb motor rehabilitation of post-stroke patients.	11
2.2	Summary of feedback modalities in EEG-based BCIs for upper limb motor rehabilitation of post-stroke patients.	19
4.1	Challenges and solutions of the vibrotactile device	57
5.1	Mean and standard deviation of the minimum sensory threshold for each motor and age group. Units are revolutions per minute (rpm).	66
5.2	p-values corresponding to the comparison among the locations of the motors. . .	67
5.3	MST Pearson’s correlation coefficient for each motor and participant’s characteristics.	67
5.4	Mean and standard deviation of the uncomfortable threshold for each motor and age group individually. Units are revolutions per minute (rpm).	68
5.5	UT Pearson’s correlation coefficient for each motor and participant’s characteristics. BMI stands for body mass index.	69
6.1	Number of trials and duration of the bimodal stimulation intensities	83
6.2	Vibration intensity approximate equivalencies: pulse width modulation (PWM), revolutions per minute (RPM), and hertz (Hz).	83
7.1	Four levels of visual feedback corresponding to the participant’s performance . .	113
7.2	Four levels of vibrotactile feedback corresponding to the participant’s performance	114
7.3	Four levels of bimodal feedback corresponding to the participant’s performance .	114
7.4	Mean feedback scores and standard deviation for the three feedback modalities.	120
7.5	Mean performance scores and standard deviation by order of presentation.	121
7.6	Average and standard deviation of the temporal evolution of fatigue levels across the session.	125
7.7	Raw scores of the NASA-TLX questionnaire across feedback modalities.	129
7.8	Linear model of participant’s characteristics as predictors for KMI performance.	133
7.9	Correlation between mindfulness (FMI) and BCI performance.	135
7.10	Spearman correlation coefficients and p-values between the feedback scores and the AttrakDiff dimensions.	138
8.1	Study plan and outcome measures	160
8.2	Lowest vibration intensities to test with post-stroke participants.	160

Acronyms

BCI Brain-Computer Interface.

CAR Common Average Reference.

CSP Common Spatial Patterns.

EEG Electroencephalography.

ERD Event-Related Desynchronization.

ERP Event-Related Potential.

ERS Event-Related Synchronization.

ERSP Event-Related Spectral Perturbation.

fMRI Functional Magnetic Resonance Imaging.

fNIRS Functional Near-Infrared Spectroscopy.

ICA Independent Component Analysis.

KMI Kinesthetic Motor Imagery.

LDA Linear Discriminant Analysis.

MEG Magnetoencephalography.

MI Motor Imagery.

ML Machine Learning.

MST Minimum Sensory Threshold.

SMR Sensory-Motor Rhythms.

UT Uncomfortable Threshold.

VMI Visual Motor Imagery.

Résumé en Français

Dans cette thèse, l'objectif est de concevoir et d'évaluer un nouveau retour d'information vibrotactile pour soutenir l'exécution d'une imagerie motrice kinesthésique afin d'interagir avec une interface cerveau-ordinateur destinée à la rééducation motrice après un accident vasculaire cérébral. Cette thèse a été réalisée dans le cadre du projet ANR Grasp-IT.

L'accident vasculaire cérébral (AVC) est un problème de santé publique important et la deuxième cause de décès dans le monde. Une personne sur quatre âgée de plus de 25 ans sera victime d'un AVC au cours de sa vie [9]. Plus de 60% des AVC concernent des personnes âgées de moins de 70 ans, et 57% des décès et des handicaps liés à l'AVC touchent des personnes du même âge, ce qui représente une perte considérable d'années de vie en bonne santé [10, 9].

L'impact socio-économique de l'AVC est considérable, avec un coût mondial estimé à 861 milliards de dollars américains. La majorité (89%) des cas d'AVC surviennent dans des pays à faible ou moyen revenu. L'incidence de l'AVC a augmenté dans ces pays entre 1990 et 2019, alors qu'elle a diminué dans les pays à revenu élevé [10]. En plus, dans les pays à revenu élevé, comme la France, les AVC sont plus fréquents et moins pris en charge pour les personnes à revenu modeste, ce qui augmente leur risque de présenter des complications post-AVC [11].

Les accidents vasculaires cérébraux sont aussi la troisième cause d'incapacité permanente acquise dans le monde [9]. Les survivants d'un AVC peuvent être confrontés à toute une série de complications médicales, psychosociales et musculo-squelettiques, qui persistent même des années après l'événement [12]. Les troubles liés à l'AVC comprennent la parésie et la paralysie, les déficits sensoriels qui ont un impact significatif sur le contrôle des mouvements, les déficiences cognitives et les limitations articulaires [13]. Parmi les déficits moteurs, 60% concernent la main [14], ce qui a des répercussions sur les activités de la vie quotidienne puisque la préhension et la manipulation d'objets sont considérablement affectées [15]. Environ 38% des patients récupèrent légèrement la dextérité du bras six mois après l'AVC, et seulement 12% récupèrent complètement après une thérapie de réadaptation. Par conséquent, la nécessité de thérapies visant à améliorer la récupération motrice de l'AVC est très significative.

Une gamme de thérapies a été développée pour traiter la récupération motrice de l'AVC, y compris l'entraînement bilatéral, la thérapie du mouvement induit par la contrainte, la thérapie du miroir, l'observation de l'action, la thérapie robotique, la stimulation électrique fonctionnelle (FES), la stimulation tactile, la réalité virtuelle et l'imagerie mentale [16, 17, 18]. Parmi ces techniques, l'imagerie mentale se distingue comme une approche difficile à comprendre et à exécuter, avec un retour d'information souvent insuffisant pour les patients et les thérapeutes. Malgré ces difficultés, l'imagerie mentale a gagné en importance dans le contrôle des interfaces cerveau-ordinateur (ICO), promettant ainsi une technologie pour la rééducation motrice.

Une interface cerveau-ordinateur (ICO ou brain-computer interface, BCI, en anglais) est un système conçu pour enregistrer l'activité cérébrale d'un individu, et traduire ses intentions en commandes d'interaction avec l'ordinateur [19]. Les ICOs ont été utilisées comme technologies d'assistance dans diverses applications, par exemple pour contrôler un fauteuil roulant [20], sélectionner les touches d'un clavier visuel [21, 22, 23], et contrôler une prothèse [24, 25]. Plus récemment, les ICOs sont considérées comme une technologie prometteuse pour la rééducation post-AVC [26, 27, 28, 29, 30, 31].

Les thérapies de rééducation du membre supérieur existantes requièrent souvent le mouvement de la main affectée, ce qui limite leur application aux patients souffrant de déficits moteurs sévères. Les ICOs basées sur l'imagerie motrice (IM, motor imagery, MI, en anglais) offrent une solution potentielle pour ces patients en proposant une thérapie de rééducation basée sur leurs

besoins et capacités individuels. L'ICO enregistre l'activité cérébrale pendant la tâche mentale, puis utilise des algorithmes de traitement du signal pour extraire les caractéristiques les plus importantes afin de détecter l'IM. L'une de ces caractéristiques comprend les désynchronisations/synchronisations associées à un événement (event-related de/synchronization, ERD/ERS, en anglais), qui correspondent à une diminution/augmentation de la puissance dans les bandes de fréquences mu et bêta de l'activité neuronale pendant l'imagerie motrice [32, 33, 34]. En conséquence, le système active un dispositif externe, créant un système en boucle fermée qui stimule le membre paralysé, favorisant ainsi la neuroplasticité [27]. La technique la plus courante pour enregistrer l'activité cérébrale est l'électroencéphalographie (EEG), une technique non invasive qui consiste à placer des électrodes sur le cuir chevelu.

Deux types d'imagerie motrice ont été identifiés et différenciés : l'imagerie motrice visuelle, où les utilisateurs visualisent mentalement le mouvement sous différentes perspectives, et l'imagerie motrice kinesthésique (IMK), où les utilisateurs se souviennent des sensations kinesthésiques et proprioceptives liées au mouvement, telles que les contractions musculaires, la température, la pression, la rugosité, l'étirement de la peau, entre autres [35]. L'IMK rappelle donc des sensations sans générer de mouvements. Néanmoins, la stratégie employée lors d'une rééducation utilisant une ICO est souvent insuffisamment expliquée dans les protocoles de réadaptation [36].

L'IMK possède la singularité d'activer les régions du cerveau liées à la motricité [37], ce qui la rend particulièrement pertinente pour la rééducation motrice post-AVC. L'un des principaux défis associés à cette technique est que, bien que l'accent soit mis sur les sensations de mouvement, il n'y a pas de retour kinesthésique et proprioceptif, ce qui fait que les patients ont des difficultés à l'exécuter correctement. Ce problème peut être résolu en fournissant un retour d'information pertinent aux patients, ce qui leur permet d'évaluer leur réussite dans la génération de l'IMK et donc d'apprendre à moduler leur activité cérébrale et d'améliorer leur récupération.

Pour aider les patients et les thérapeutes à évaluer l'exécution de l'IMK, un retour d'information est souvent fourni par le biais de différentes modalités. Le retour haptique s'est principalement concentré sur la facilitation du mouvement, ce qui a donné de meilleurs résultats que d'autres modalités de retour [31]. D'autres options, comme le retour vibrotactile, n'ont pas été suffisamment explorées. Malheureusement, les systèmes de retour d'information existants donnent souvent la priorité aux aspects technologiques plutôt qu'aux considérations centrées sur l'utilisateur, et négligent parfois les besoins et préférences individuels des utilisateurs au-delà de leur récupération physique.

Nous avons exploré les applications du retour vibrotactile dans les paradigmes basés sur l'imagination motrice, en reconnaissant son potentiel à produire des performances ICO similaires à celles du retour visuel [38, 39, 40]. Un avantage supplémentaire justifiant le choix de ce retour réside dans la libération du canal visuel [7], permettant aux utilisateurs de se concentrer sur la tâche mentale à exécuter plutôt que sur le traitement du retour d'information visuel. Néanmoins, les choix de conception de la stimulation vibrotactile demandent à être éclaircis, ce qui soulève d'importantes questions, par exemple sur la séquence d'activation des dispositifs impliquant plusieurs moteurs de vibration et sur les intensités de vibration appropriées. C'est pourquoi une approche centrée sur l'utilisateur a été proposée pour la conception de la stimulation vibrotactile. La stimulation résultante peut ensuite être intégrée à des animations visuelles pour créer un retour d'information bimodal plus complet, qui peut être testé en tant que modalité de retour d'information pour une ICO basé sur l'IMK.

L'objectif principal de cette thèse est **la conception et l'évaluation d'un nouveau retour**

vibrotactile pour soutenir l'exécution de l'IMK afin d'interagir avec une ICO destiné à la rééducation motrice après un AVC. Dans le chapitre 3, une méthodologie de recherche basée sur le design est présentée pour atteindre cet objectif. Cette méthodologie réunit des méthodes scientifiques et des méthodes de design afin de créer des solutions technologiques qui génèrent des connaissances. Ainsi, cette méthodologie nous a permis d'introduire une nouvelle solution soigneusement conçue pour répondre spécifiquement aux besoins des patients post-AVC. Dans un premier temps, le dispositif vibrotactile et la stimulation ont été construits en suivant une approche centrée sur l'utilisateur. Dans un deuxième temps, la phase de test a consisté à évaluer le dispositif et la stimulation initialement auprès d'une population neurotypique, puis auprès de patients ayant subi un AVC.

Dans le chapitre 4, nous présentons la plateforme technologique utilisée dans le cadre de cette thèse. Initialement, la première version De l'ICO GraspIt [41] a été introduite, qui a comme objectif améliorer l'IMK des mouvements de préhension en fournissant un retour d'information visuel. Cette version a servi de base scientifique et technique à la deuxième version développée et utilisée dans cette thèse. La deuxième version a intégré des améliorations basées sur les tests préliminaires de GraspIt V1, y compris un retour visuel personnalisable et ludique, en intégrant des scènes des activités de la vie quotidienne correspondant à quatre mouvements pour une expérience d'entraînement plus complète. Ces améliorations visuelles ont nécessité d'importantes modifications du logiciel afin d'intégrer le retour haptique sous forme vibrotactile, tangible et de stimulation électrique fonctionnelle.

Ce chapitre détaille également le développement du dispositif vibrotactile. Trois moteurs de vibration ont été placés stratégiquement en fonction des principaux muscles actifs lors d'un mouvement de préhension, afin d'assurer la cohérence entre la stimulation vibrotactile et le mouvement physique. Les moteurs ont été attachés à des bracelets réglables, facilitant l'interchangeabilité entre les membres gauche et droit. Le dispositif vibrotactile a été intégré dans l'interface GraspIt V2, ce qui a donné lieu à une nouvelle ICO nommée FeelIt. FeelIt fait référence à une ICO basé sur l'IMK qui intègre un retour visuel et vibrotactile pour soutenir l'exécution de l'IMK. Avant de tester la facilité d'utilisation de ce nouveau retour, la stimulation vibrotactile a dû être développée et synchronisée avec l'environnement visuel, selon les détails présentés dans les deux chapitres suivants.

La première contribution expérimentale, présentée dans le chapitre 5, consiste à identifier les seuils sensoriels de vibration en fonction de l'âge pour notre dispositif vibrotactile. Les participants ont été regroupés par âge et ont indiqué les intensités de vibration les plus faibles qu'ils pouvaient identifier et les plus élevées qui étaient encore confortables. Les principaux résultats ont révélé des variations liées à l'âge pour le seuil sensoriel minimal, permettant une généralisation en fonction des groupes pour une configuration plus rapide de l'appareil. Le seuil maximal de vibration ne diffère pas de manière significative entre les groupes d'âge, ce qui suggère la sécurité et le confort du niveau de vibration le plus élevé. Néanmoins, il est conseillé de ne pas utiliser la valeur maximale pour éviter d'éventuels effets indésirables, en particulier chez les personnes ayant subi un accident vasculaire cérébral. Ces résultats mettent en évidence les différences sensorielles tactiles en fonction de l'âge. De plus, ils soulignent l'importance d'ajuster l'intensité de la stimulation pour la perception de la stimulation et le confort sans compromettre l'objectif de retour d'information de l'ICO qui est de fournir des informations sur la performance de la tâche mentale.

Le chapitre 6 présente la deuxième contribution expérimentale, qui vise à comparer quatre modèles d'activation de la vibration afin d'identifier celui qui convient le mieux pour compléter



Interface-cerveau ordinateur FeelIt, qui intègre un retour vibrotactile et un retour visuel. Image issue du chapitre 6.

l'animation visuelle d'une main qui presse une bouteille. L'objectif était de créer une stimulation vibrotactile pertinente qui transmette des informations tactiles correspondant à l'image affichée. Le défi était de comparer les modèles et de garantir la cohérence et la synchronisation avec l'animation visuelle de la main. Un nouveau modèle séquentiel a été conçu, inspiré par l'activation naturelle des principaux muscles lors d'un mouvement de préhension. Les tests ont impliqué deux et trois moteurs de vibration. La stimulation bimodale ainsi créée, qui intègre dans une forme bimodale des éléments visuels et vibrotactiles sur quatre niveaux d'intensité, a été évaluée par les utilisateurs.

L'activité EEG pendant la stimulation a été étudiée dans les bandes de fréquences alpha et bêta. Les ERD observées dans les zones cérébrales sensorimotrices pendant la stimulation bimodale dans tous les modèles de vibration suggèrent une excitation du cortex sensorimoteur, ce qui est important pour promouvoir la neuroplasticité dans la rééducation motrice après un accident vasculaire cérébral. Des différences significatives entre les quatre niveaux d'intensité de la stimulation ont été observées dans l'EEG, le plus haut niveau provoquant des ERD plus importants.

L'étude a confirmé qu'un modèle séquentiel avec trois moteurs ressemblant au mouvement réel est perçu comme cohérent et synchronisé avec une animation visuelle de la main. Lors de la conception d'une stimulation tactile, la prise en compte de la tâche peut fournir des informations plus significatives aux utilisateurs. L'expérience positive de l'utilisateur souligne le potentiel de la stimulation en tant que signal de retour pour les ICOs. La stimulation et l'exécution simultanées de la tâche mentale peuvent également entraîner la superposition des activités EEG, ce qui complique la détection de l'IMK. Bien que cela puisse être bénéfique pour détecter l'IMK dans certaines applications, ce n'est peut-être pas le cas dans la neuroréhabilitation motrice, ce qui souligne la nécessité d'encourager le patient à effectuer la tâche d'imagerie motrice pour

stimuler efficacement le cortex sensorimoteur.

Dans le chapitre 7, nous présentons la troisième étude expérimentale, axée sur l'évaluation de l'ICO bimodale *FeelIt* au sein d'une population neurotypique. L'évaluation a porté sur trois modalités de retour d'information (visuelle, vibrotactile et bimodale) afin de comprendre leur impact sur l'exécution de l'IMK. Les résultats ont montré que les performances de l'ICO étaient similaires pour les trois modalités de retour d'information, ce qui suggère que le choix de la modalité devrait prendre en compte d'autres aspects qui s'alignent sur les compétences, les objectifs, les besoins et les préférences de l'utilisateur.

Les oscillations EEG ont révélé une activité cohérente du cortex sensorimoteur pour toutes les modalités. Cela souligne la possibilité d'adapter l'ICO aux limitations de l'utilisateur, par exemple en utilisant un retour d'information uniquement visuel pour les utilisateurs souffrant de déficits sensoriels. De plus, l'activité ERD était plus importante pendant le retour d'information bimodal, avec une mobilisation plus importante des zones sensorimotrices que pour les modalités de retour d'information uniquement visuel et uniquement vibrotactile.

Les participants ont indiqué une forte préférence pour le retour d'information bimodal, qu'ils considèrent comme plus complet et détaillé. De plus, le retour d'information bimodal a eu des effets positifs plus importants sur l'humeur, la motivation et le sens de contrôle de l'interface. Ces aspects sont particulièrement importants pour la rééducation motrice post-AVC, qui est un processus long et laborieux. Une évaluation holistique tenant compte du point de vue de l'utilisateur est cruciale, en complément des évaluations techno-centrées et pour faciliter un choix plus clair et mieux justifié en matière de retour d'information. L'expérience positive de l'utilisateur et l'attractivité du système sont encourageants pour l'étude à venir avec des patients post-AVC.

Un protocole expérimental est défini dans le chapitre 8 pour l'évaluation initiale par l'utilisateur de l'ICO basé sur l'IMK et intégrant un retour d'information visuel et vibrotactile. L'étude, qui se déroulera au CHU de Rennes en 2024, vise à évaluer trois modalités de retour d'information (visuelle, vibrotactile et bimodale) pour faciliter l'exécution efficace et effective des mouvements de préhension par l'ICM chez les personnes ayant subi un accident vasculaire cérébral (AVC). Cette étude permettra d'évaluer l'utilité, l'utilisabilité et la désirabilité de l'ICO au sein de la population cible, une étape nécessaire avant une étude thérapeutique longitudinale. La flexibilité du protocole permet de remplacer facilement la modalité vibrotactile par le retour tangible ou la stimulation électrique fonctionnelle, développés par les partenaires du projet *GraspIt*. Cette adaptabilité permet une analyse comparative complète des différentes modalités de retour haptique en utilisant le même protocole expérimental.

En conclusion, dans cette thèse, un retour vibrotactile pour une ICO basée sur l'IMK pour la rééducation post-AVC a été conçu en adoptant une approche centrée sur l'utilisateur. Le dispositif vibrotactile a été construit en tenant compte des caractéristiques physiques des patients post-AVC. Ensuite, la stimulation a été conçue et synchronisée avec un environnement visuel en tenant compte du mouvement auquel elle est destinée et de l'avis des utilisateurs. Le résultat est un retour d'information qui fournit des informations significatives à l'utilisateur sur l'exécution de l'IMK, ce qui se reflète dans les bonnes performances de l'ICO et les résultats encourageants de l'évaluation de l'utilisateur. Cette nouvelle conception du retour d'information a mis en évidence l'importance d'une approche centrée sur l'utilisateur, ainsi que l'importance d'un retour d'information bimodal pour soutenir l'IMK dans les ICO.

General Introduction

The global impact of stroke and promising rehabilitation techniques

Stroke, a significant public health problem, ranks as the second leading cause of death globally. Shockingly, one out of four individuals over the age of 25 will experience stroke at one point in their lives [9]. Despite the common perception that stroke primarily affects the elderly, it is worth noting that over 60% of strokes occur in individuals under the age of 70. Additionally, a staggering 57% of stroke-related deaths and disabilities impact individuals within the same age range, resulting in a considerable loss of healthy life years [10, 9]. Consequently, stroke can no longer be considered a disease of the elderly. The socioeconomic impact of stroke is also profound, with a worldwide estimated cost of \$861 billion USD. It is noteworthy that the majority (89%) of stroke cases occur in low-to-middle-income countries. Alarming, its incidence has been on the rise in these countries between 1990 and 2019, while high-income countries have experienced a decline [10]. In high-income countries, such as France, stroke is most common among individuals of modest income, thus increasing their risk of presenting post-stroke complications [11].

Furthermore, stroke is the third leading cause of acquired permanent disability in the world [9]. Stroke survivors may encounter a range of medical, psychosocial, and musculoskeletal complications, persisting even years after the event [12]. Stroke-related deficiencies include paresis-paralysis, sensory deficits that significantly impact movement control, cognitive impairments, and joint limitations [13]. Within motor skills deficiencies, 60% of them are present in the hand [14], which has an impact on daily life activities since grasping and object manipulation are greatly affected [15]. About 38% of patients lightly recover arm dexterity six months after stroke, while only 12% fully recover after rehabilitation therapy. Therefore, the necessity for therapies aimed at enhancing stroke motor recovery is highly significant. A range of therapies has been developed to address stroke motor recovery, including bilateral training, constrain-induced movement therapy, mirror therapy, task-oriented therapy, robotic therapy, functional electrical stimulation (FES), tactile stimulation, soft tissue mobilization, passive movements, action observation, virtual reality, and mental imagery [16, 17, 18]. Among these techniques, mental imagery stands out as a challenging approach that may be difficult to understand and execute, often lacking sufficient feedback for both patients and therapists. Despite these challenges, mental imagery has gained prominence in the control of brain-computer interfaces (BCIs), thereby holding promise as a technology for motor rehabilitation.

Brain-computer interfaces as an alternative to traditional post-stroke motor rehabilitation therapies

A brain-computer interface is a system designed to record and monitor an individual's brain activity, translating their intentions into commands for computer interaction [19]. BCIs have been used as assistive technologies in various applications, such as to control a wheelchair [20], select the keys of a visual keyboard [21, 22, 23], and control a prosthesis [24, 25]. More recently, BCIs have emerged as a promising technology for post-stroke rehabilitation [26, 27, 28, 29, 30, 31].

Existing upper-limb rehabilitation therapies often require movement of the affected hand, limiting their application to patients with severe motor deficits. However, motor imagery (MI)-based BCIs offer a potential solution for these patients by enabling rehabilitation therapy based on their individual needs and abilities. Motor imagery-based BCIs record the brain activity and

use it to activate an external device, creating a closed-loop system that stimulates the paralyzed limb, thereby promoting neuroplasticity [27]. Nevertheless, motor imagery may be challenging to understand and perform, and is often inadequately explained in rehabilitation protocols [36]. Two types of motor imagery have been identified and differentiated: visual motor imagery, where users mentally visualize the movement from different perspectives, and kinesthetic motor imagery (KMI), where users recall the kinesthetic and proprioceptive sensations related to movement, such as muscle contractions, pressure temperature, skin stretching, among others [35]. KMI has the unique ability to activate motor-related brain regions [37], making it particularly relevant for post-stroke rehabilitation. One significant challenge associated with this technique is that although the focus is on movement sensations, it lacks kinesthetic and proprioceptive feedback, therefore patients encounter difficulties in executing it correctly. This challenge may be addressed by providing meaningful feedback to patients, allowing them to evaluate their KMI performance, learn to modulate their brain activity, and improve their recovery.

The ANR-project Grasp-It ¹ addresses the challenge of improving stroke recovery with BCIs. The project aims to recover upper limb control by improving the performance of kinesthetic motor imagery of post-stroke patients using a tangible and haptic interface within a gamified BCI training environment. To achieve its objective, the project comprises multidisciplinary research, integrating the knowledge of researchers, engineers, medical doctors, physical therapists, and post-stroke patients. Notably, eight partners, including academic and research institutions, hospitals, and an industry partner, make up the team that currently develops three distinct haptic feedback modalities to integrate with a common gamified visual environment. Within the framework of this project, the objective of the present thesis is to develop one of the haptic solutions, involving vibrotactile feedback and integrate it with the visual environment.

Vibrotactile feedback to support the execution of KMI in BCIs

Different types of feedback may be provided to help KMI execution. For instance, visual feedback shows a visual representation of the KMI, yet it lacks kinesthetic and proprioceptive feedback. Haptic techniques such as functional electrical stimulation and exoskeletons may provide the missing movement sensations by artificially moving the limb. Although they have been proven to be efficient in stroke recovery [31], these solutions may not always be suitable for patients who present very limited mobility. Other feedback modalities that stimulate the patient without requiring movement may be considered, such as vibrotactile feedback.

Vibrotactile feedback stimulates the mechanoreceptors found on the skin, thus it is possible to convey information, for example, regarding the motor imagery performance. Indeed, previous work has demonstrated its use in MI-based BCIs, resulting in acceptable BCI performances [38, 7, 42], and enhanced classification of MI [39, 40]

Furthermore, most of the feedback modalities have been designed centered on the technology, often overlooking the user's needs, preferences, and well-being when interacting with the system. It is important to develop solutions that are tailored to their needs, and rehabilitation goals, but that also take into consideration their personal preferences and their well-being.

In this thesis, we present a novel BCI for post-stroke rehabilitation that integrates both visual and vibrotactile feedback. By incorporating these two types of feedback, users can receive information about their performance visually and kinesthetically. We expect that sensory stimulation

¹<http://graspit.loria.fr/>

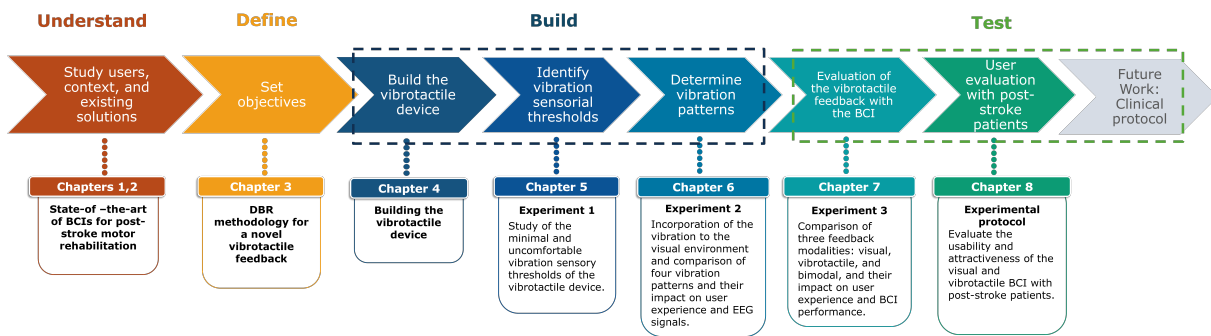
will assist post-stroke patients in developing awareness of the affected limb and facilitate the execution of KMI. Furthermore, the development is user-centered taking into consideration the user's perspective of the proposed solution and constantly performing a user evaluation in order to identify improvement areas rapidly.

Objective of the thesis The main objective of this thesis is to design and evaluate vibrotactile feedback for a brain-computer interface based on kinesthetic motor imagery intended for post-stroke rehabilitation. The vibrotactile feedback should be compatible with a visual modality to create a bimodal feedback that should:

1. support the performance of kinesthetic motor imagery.
2. improve the rehabilitation process of post-stroke motor rehabilitation of the hand.

The main hypothesis is that the bimodal feedback, consisting of visual and vibrotactile modalities, supports the execution of KMI, manifested in increased BCI performance, increased cortical excitability in sensorimotor areas, and a positive user experience.

To accomplish the objective, a design-based research (DBR) methodology was proposed, grounded on a user-centered approach, in figure 3.2.



Methodology for designing and evaluating vibrotactile feedback. Figure extracted from chapter 3

Structure of the thesis

Part 1

This part starts with a brief introduction to stroke, the motor deficiencies it generates, and rehabilitation therapies. Then, the concept of brain-computer interfaces is presented, as well as their role in post-stroke rehabilitation. The current feedback modalities used in post-stroke motor rehabilitation are discussed, and an introduction to vibrotactile stimulation is given. Next, the DBR methodology used to design and evaluate a novel vibrotactile feedback is introduced. Finally, the technical platform and the design of the vibrotactile device are presented.

Chapter 1: Introduction to stroke

This first chapter provides an overview of stroke, including its basic elements, the motor skill impairments it may cause, and current therapeutic approaches.

Chapter 2: State-of-the-art of BCIs in post-stroke motor rehabilitation

In this chapter, we discuss the current state of the art of BCIs for the motor rehabilitation of the upper limb of post-stroke patients. We present how they work, the elements that compose

them, and the challenges these technologies face. Furthermore, the current feedback modalities are examined, with a focus on vibrotactile feedback. Although this feedback has not been fully explored in post-stroke motor rehabilitation, other applications are presented, as well as the existing gaps in the domain.

Chapter 3: *Design-based research methodology for the design of vibrotactile feedback*

In this third chapter, we outline the design-based research methodology employed to design and evaluate a novel vibrotactile feedback. Following the DBR and user-centered methodology, the main objective and hypothesis of the thesis are presented.

Chapter 4: *Presentation of the technological platforms*

This chapter begins by presenting the original BCI GraspIt, which laid the groundwork for the present study. GraspIt consisted of a visual interface to support the execution of KMI. Numerous modifications were made to improve it, resulting in a second version of GraspIt. Then, the novel brain-computer interface FeelIt is introduced, which aims to enhance kinesthetic motor imagery by integrating visual and vibrotactile feedback. Furthermore, the building phase of the vibrotactile device is presented, highlighting the challenges it addresses.

Part 2

This part delves into the methodology for designing and evaluating the novel BCI integrating visual and vibrotactile feedback. The first two chapters correspond to the building phase of the vibrotactile stimulation, while the next two chapters focus on evaluating the BCI, along with the vibrotactile feedback, with healthy users and post-stroke patients, respectively. The final chapter provides a general discussion encompassing all the studies and their contributions to the design and evaluation of the bimodal BCI, as well as the perspectives.

Chapter 5: *Study of the minimum and uncomfortable sensory thresholds of the vibrotactile stimulation*

In this first chapter, we present the study conducted to determine the minimum and uncomfortable sensory thresholds specific to the vibrotactile device. This step was crucial to ensure that participants could perceive the vibrotactile stimulus while also experiencing a comfortable vibration intensity, ultimately resulting in a positive user experience.

Chapter 6: *Design and evaluation of the vibration activation patterns and integration with the visual interface*

Building upon the previous chapter, we investigated the merging of visual and vibrotactile feedback. Four different configurations of the vibrotactile device, varying the number of motors and activation patterns of the vibration stimulation. More specifically, a sequential vibration pattern was designed, inspired by the muscle activation of the muscles involved in a grasping movement. The vibrotactile stimulation was merged with the visual animating of a grasping hand, ensuring its congruence and synchronization. Additionally, an analysis of the electroencephalography signals was conducted to gain a deeper understanding of the effect of the vibration on brain oscillations.

Chapter 7: *Evaluation of the vibrotactile feedback with healthy participants*

In this chapter, we present the study concerning the assessment of three feedback modalities: visual, vibrotactile, and bimodal feedback. Healthy neurotypical subjects participated in this

experiment to evaluate the acceptability, usability, and reliability of the BCI. This study serves as the foundation for subsequent evaluations involving post-stroke patients.

Chapter 8: *Evaluation of the vibrotactile feedback with post-stroke patients*

This chapter outlines the experimental protocol developed to assess the usability and acceptability of the BCI FeelIt among post-stroke patients. Additionally, this study aims to identify the most efficient and user-preferred feedback modality among visual, vibrotactile, and bimodal. The results from this study will lay the basis for a future long-term clinical trial to measure the therapeutic effects of the system. This experimental protocol is intended to take place at the University Hospital in Rennes during the course of the year 2024.

Chapter 9: *General Discussion and Perspectives*

In this last chapter, we engage in a discussion of the results obtained from the various studies and their implications for the design of a novel BCI for post-stroke rehabilitation. Furthermore, the possibility of integrating the vibrotactile solution with other feedback modalities developed for the GraspIT project is presented. Additionally, potential avenues for future research involving the BCI with visual and vibrotactile feedback are discussed.

Part I

BCIs for Upper Limb Rehabilitation After Stroke: State-of-the-Art, Research Methodology, and Technical Platform

Chapter 1

A Brief Introduction to Stroke

Contents

1.1	Introduction	1
1.2	Definition and Types of Stroke	2
1.3	Effects of Stroke: Motor and Sensory Deficits	2
1.3.1	Motor deficits	3
1.3.2	Sensory deficits	3
1.3.3	Psychosocial complications	4
1.4	Post-Stroke Recovery	4
1.5	Current Therapies for Upper Limb Motor Recovery	5
1.5.1	Vibration therapy	5
1.6	Conclusion	6

1.1 Introduction

Stroke is a significant public health problem and the second leading cause of death globally. Shockingly, one out of four individuals over 25 years old will experience stroke at one point in their lives [9]. Despite the common perception that stroke primarily affects senior individuals, it can no longer be considered a disease of the elderly, as more than 60% of strokes occur in individuals under the age of 70. Additionally, 57% of stroke-related deaths and disabilities impact individuals within the same age range, resulting in a considerable loss of healthy life years [10, 9].

Furthermore, stroke is the third leading cause of acquired permanent disability in the world [9]. Stroke survivors may encounter a range of medical, psychosocial, and musculoskeletal complications, persisting even years after the event [12]. Stroke-related deficiencies include paresis-paralysis, cognitive impairments, sensory deficits, and joint limitations that significantly impact movement control [13]. Motor impairments due to stroke are a major cause of diminished performance in daily life activity, resulting in an increased socioeconomic burden. Thus, rehabilitation must be performed to maximize the patient's recovery and improve their daily life performance. Consequently, the need for therapies to enhance stroke motor recovery is highly significant.

There are various therapies such as bilateral training, constraint-induced movement therapy, mirror therapy, action observation, task-oriented therapy, robotic therapy, functional electrical stimulation, tactile stimulation, passive movements virtual reality, and mental imagery [16, 17, 18]. Among these techniques, mental imagery stands out as a challenging approach, difficult to understand and execute, and often lacks sufficient feedback for both patients and therapists. Despite these challenges, mental imagery has gained prominence in the control of brain-computer interfaces (BCIs), thereby holding promise as a technology for motor rehabilitation.

Before delving into the role of BCI's in post-stroke motor rehabilitation, it is important to establish a foundational understanding of stroke, its repercussions, and traditional motor rehabilitation therapies. This chapter first gives an overview of stroke, encompassing its definition, typology, consequences, and existing rehabilitation modalities. Subsequently, we present the role of BCIs in post-stroke motor rehabilitation. Throughout our exploration, we introduce vibrotactile stimulation in both the context of post-stroke rehabilitation and BCIs, as well as the possibility of merging in with visual stimulation. We finalize with a presentation of the potential of vibrotactile stimulation within BCI-based post-stroke motor rehabilitation.

1.2 Definition and Types of Stroke

The brain relies on a steady supply of oxygen delivered via the circulatory system from the heart through arteries. A stroke occurs when the oxygen supply is disrupted due to the blockage or rupture of one of these arteries. This disruption leads to the death of brain cells because they do not receive enough oxygen to function properly [43]. Stroke may be classified into two categories:

- *Ischemic Stroke*: It is the most common type [44], and it occurs when the blood flow to the brain is obstructed. There are two subtypes:
 - Embolic: A plaque or a blood clot forms in a different location within the body and migrates to the brain, causing a blockage in its arteries.
 - Thrombotic: A blood clot forms directly in the arteries, impeding the flow of blood.
- *Hemorrhagic Stroke*: It occurs when a brain blood vessel in the brain bursts, leading to the leakage of blood into or around the brain. This bleeding causes brain pressure to increase, resulting in damage to the brain cells.

Once a patient has suffered a stroke and received the appropriate medical attention, a multidisciplinary medical team will be in charge of assessing its effects and defining a recovery plan.

1.3 Effects of Stroke: Motor and Sensory Deficits

Stroke survivors may present a variety of effects depending on the location and the extent of the brain damage. When the left side of the brain is impacted by a stroke, it can result in difficulties related to speech, language, reasoning, and analytical abilities. Conversely, strokes occurring on the right side of the brain may impact spatial orientation, creativity, and insight [43]. Stroke may also result in motor and sensory deficiencies, ranging from mild to severe. These deficits typically manifest when the stroke has affected the motor cortex, responsible for movement, and/or the somatosensory cortex, responsible for processing sensory inputs (refer to figure 1.1 for a visual depiction of these brain regions).

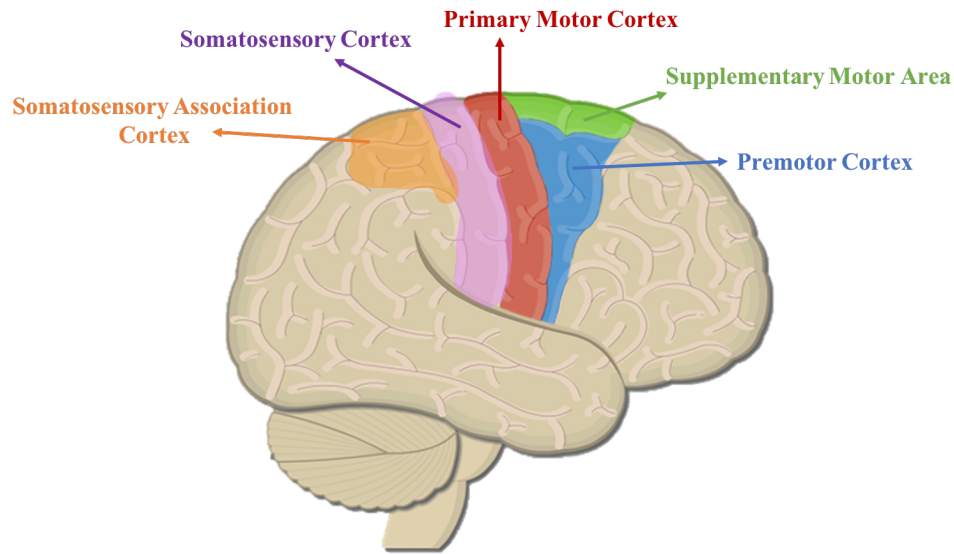


Figure 1.1: Motor and sensory cortices of the human brain.

1.3.1 Motor deficits

Motor deficits manifest as a loss of control over movement on the side of the body opposite to the brain lesion, resulting in a decrease in muscle strength or a complete inability to execute certain movements. These deficits are often associated with joint limitations, abnormal movements, and a condition known as spasticity, characterized by abnormal muscle tightness caused by sustained contractions. Motor impairments are the most common deficits observed in post-stroke patients [45]. These impairments can affect various parts of the body, with the hand being particularly susceptible. In fact, approximately 60% of motor deficits affect the hand [14], significantly impacting daily life activities due to the impairment of grasping and object manipulation [15]. Despite rehabilitation efforts, only around 38% of patients lightly recover arm dexterity six months after stroke, and a mere 12% fully recover after rehabilitation therapy. Therefore, the need for therapies to enhance stroke motor recovery of the hand is highly significant.

1.3.2 Sensory deficits

Sensory deficits resulting from stroke include loss or reduced sense of proprioception, touch (impacting object and texture recognition), temperature and pain perception, as well as heightened sensitivity, known as hypersensitivity. These sensory deficits are especially relevant because they can adversely impact motor performance. For example, proprioception, which involves sensing the position, movement, and orientation of one's own body and limbs, without relying on any visual or auditory cues, plays a crucial role in controlling limb movement, object manipulation, and posture [46, 47]. Similarly, the sense of touch plays an essential role for tasks such as estimating the size and texture of objects during manipulation. Consequently, when the sensorimotor cortex is affected by stroke, the inability to process sensory stimuli can have a negative impact on motor coordination during activities such as reaching and grasping [48]. It is then important to recognize that motor impairments may often coexist with sensory deficiencies, needing a holistic approach to post-stroke upper-limb motor rehabilitation that addresses both dimensions.

1.3.3 Psychosocial complications

In addition to the prevalent motor and sensory deficits experienced by post-stroke individuals, approximately one-third of patients face psychosocial complications, such as depression, anxiety, or apathy [49]. These issues may manifest either as a direct consequence of the brain injury itself or as a natural response to the challenges caused by the event. Irrespective of their origin, these psychosocial complications influence significantly the recovery process, underscoring the importance of recognizing and addressing them as integral components of stroke rehabilitation.

Among the psychosocial complications, post-stroke depression stands out, affecting approximately 25% to 30% of stroke survivors [50]. The presence of depression can have a negative impact on a patient's motivation to engage in and adhere to rehabilitation therapies, thereby impeding the overall recovery. Moreover, patients may exhibit mood fluctuations and difficulty in managing emotions such as frustration and anger [51]. Therefore, it is important to take these emotions into consideration during the rehabilitation process.

Addressing these complications involves the requirement of therapeutic strategies and technologies that not only target the physical aspects of recovery but also attend to the emotional well-being of the patient. Such approaches should be designed to mitigate the worsening of emotional distress and ideally contribute positively to the patient's emotional state. Recognizing and addressing these psychosocial complexities is key to optimizing the overall efficacy of stroke rehabilitation therapies.

1.4 Post-Stroke Recovery

The timeline of post-stroke recovery is delineated into five distinct phases [52]:

1. *Hyper-acute*: This initial phase encompasses the first 24 hours following a stroke.
2. *Acute*: Extending from one to seven days post-stroke, this phase is a crucial period in the early response to the event.
3. *Early sub-acute*: Seven days to three months, this phase marks the early stages of recovery, where some spontaneous improvements may be observed.
4. *Late sub-acute*: The following three to six months are characterized by therapeutic interventions.
5. *Chronic*: beyond six months, the permanent effects of stroke become more visible.

The rationale behind this classification is that the processes related to post-stroke recovery are time-dependent. Patients with mild and severe upper limb paresis may recover within three to six weeks after stroke (subacute phase). Consequently, most rehabilitative therapies are strategically designed to target this time period, aiming to harness their potential for maximizing recovery. However, it has been suggested that although early training is more effective, the learning window never really closes, it only diminishes because the mechanisms underlying stroke recovery are very similar to those involved in neuronal development [53].

Post-stroke recovery is based on the principle of neuroplasticity, which is the remarkable ability of the nervous system to reorganize its structure, functions, and connections [15]. Although neuroplasticity can manifest spontaneously in the immediate days following a stroke, it can be significantly augmented through targeted training interventions. The extent and efficacy of this

neuroplasticity depend on various factors, including the nature of the task and the motivation of the individual.

1.5 Current Therapies for Upper Limb Motor Recovery

Post-stroke motor rehabilitation encompasses a diverse range of therapeutic strategies to facilitate recovery. These therapies use various techniques and technologies to address the challenges faced by stroke patients. Here, we present an overview of some of these approaches:

- **Constraint-induced movement therapy (CIMT):** This method involves moving the impaired limb while constraining the unaffected one [54]. It encourages intensive use of the affected limb to promote recovery.
- **Mirror therapy:** Here, the patient moves the unaffected limb while the affected limb is hidden behind a mirror, creating the illusion of movement in the affected limb [55].
- **Functional Electrical Stimulation (FES):** during this therapy, the patient's impaired limb is stimulated through an electrical current delivered via electrodes, triggering functional movements such as grasping [56].
- **Robot-assisted therapy:** Robotic therapies use electronic-based robots to intensify repetitions of movements, in contrast to physical therapists-based therapy [15, 57]. These robotic systems offer precise control and feedback to enhance recovery.
- **Virtual Reality (VR):** These interventions immerse patients in computer-generated environments, enabling increased repetition of movements and engagement in real-life scenarios [58].
- **Motor Imagery (MI):** It consists of imagining movement execution without any body movement. It harnesses cognitive processes and working memory, proving effective in improving motor function in stroke patients when combined with other therapies [59, 60].
- **Vibration Therapy:** Mechanical vibration treats motor deficits, especially to decrease spasticity [61, 62]. In this thesis, the focus is on this approach with distinct benefits and potential sustainability.

1.5.1 Vibration therapy

Vibration therapy is a non-invasive therapeutic intervention for stroke rehabilitation that uses mechanical vibrations to decrease muscle spasticity [61, 62]. Vibration stimulus can trigger cutaneous sensory receptors and muscle fibers without causing any physical movement. Two types of vibration therapy may be distinguished: whole body vibration (WBV), and focal muscle vibration (FMV).

- **WBV:** It conveys mechanical vibrations to the body from the feet through a vibrating platform. WBV has the advantage of being a safe therapy to reduce spasticity and improve bone mineral density in stroke survivors [63].
- **FMV:** This approach applies the vibration to a specific muscle or tendon, inducing an involuntary contraction and inhibiting the antagonist muscle, known as tonic vibration reflex [61, 64]. FMV has proved to reduce post-stroke spasticity of the upper limbs [62], improve motor function [65], and increase awareness of the affected limb [66].

Vibratory stimulation is not limited to muscle contraction, but it can also create an illusion of movement, avoiding any physical motion. In order to achieve the illusion effect, this vibration must follow specific parameters, such as a frequency between 80 and 100 hertz, two to four G-force, and a duration of at least 10 seconds [67, 68, 69].

While vibratory devices are available in the market, their accessibility can be limited due to cost and the need for a specialist for their manipulation. Additionally, most of them are not wearable, restricting their use to specific clinical environments and limiting the patient's mobility. Therefore, there is a need for affordable, wearable, and adjustable vibration devices. Vibration therapy is more accessible than other therapies, such as FES and robotic therapy, which require more specialized and advanced technologies and personnel. As vibrotactile stimulation requires little to no movement, it may result in better comfort and a more positive experience for the patients.

1.6 Conclusion

In conclusion, stroke is a prevalent and impactful health issue affecting individuals of different ages, resulting in significant motor, sensory, and psychosocial deficits. Post-stroke motor recovery has several phases, each one presenting unique challenges and opportunities for rehabilitation. Traditional therapies such as CIMT, mirror therapy, FES, robot-assisted therapy, and virtual reality, have demonstrated their efficacy in promoting motor recovery.

However, in this chapter, we have highlighted the potential of another approach: vibrotactile stimulation. By targeting both motor and sensory deficits, vibrotactile stimulation offers a promising complementary avenue for enhancing post-stroke rehabilitation. Its non-invasive nature, conceivable accessibility, and potential for wearable devices make it an attractive option for stroke survivors to regain their motor skills.

Finally, traditional therapies may be merged or complemented with brain-computer interfaces to maximize their potential. In the following chapter, we will delve deeper into BCIs for post-stroke motor rehabilitation, exploring their functioning and how they have been used to promote recovery.

Chapter 2

Brain-Computer Interfaces for Post-Stroke Rehabilitation of the Upper Limb

Contents

2.1	Introduction	8
2.2	Acquisition of the Brain Activity	9
2.3	Mental Tasks in Post-Stroke BCIs	13
2.3.1	Action observation	13
2.3.2	Motor attempt	13
2.3.3	Motor imagery	13
2.4	Signal Processing and Classification	14
2.4.1	Preprocessing	14
2.4.2	Feature extraction	16
2.4.3	Classification	17
2.5	Feedback Modalities	18
2.5.1	Visual Feedback	20
2.5.2	Virtual reality	21
2.5.3	Haptic Feedback	21
2.5.4	Multimodal Feedback	25
2.5.5	Feedback Timing	27
2.5.6	Conclusion on the Feedback	28
2.6	Focus on Vibrotactile Stimulation in Other BCI Applications .	28
2.6.1	Event-Related Potentials	28
2.6.2	Motor Imagery	29
2.7	Conclusion	35

Related publication

- Le Franc, S., **Herrera Altamira, G.**, Guillen, M., Butet, S., Fleck, S., Lécuyer, A., Bougrain, L., & Bonan, I. (2022). “Toward an Adapted Neurofeedback for Post-stroke Motor Rehabilitation: State of the Art and Perspectives.” *Frontiers in Human Neuroscience* 16:917909. doi: 10.3389/fnhum.2022.917909

2.1 Introduction

A brain-computer interface is a system designed to record and monitor an individual’s brain activity, translating their intentions into commands for computer interaction [19]. Over the years, BCIs have found diverse applications, revolutionizing fields such as mobility assistance, communication, and rehabilitation. For instance, they have enabled individuals to control wheelchairs [20], select the keys of a visual keyboard [21, 22, 23], and manipulate prosthetic devices [24, 25]. More recently, BCIs have emerged as a promising technology in post-stroke rehabilitation, offering new possibilities for patients on the path to recovery [26, 27, 28, 29, 30, 31].

Post-stroke motor rehabilitation BCIs operate as intricate closed-loop systems. They record the neural activity of patients as they engage in specific mental tasks, and then employ dedicated algorithms to provide real-time feedback, as depicted in figure 2.1. This feedback empowers users to assess their actions and modulate their brain activity, thereby optimizing their performance. Such modulation plays a crucial role in facilitating neuroplasticity, potentially enhancing the motor recovery of post-stroke patients. Furthermore, post-stroke BCIs should meet the needs and expectations of the users as much as possible, and support them in carrying out their tasks.

In this chapter, we present the current BCIs tailored for post-stroke rehabilitation. Given that a significant majority of motor impairments affect the upper limb, as discussed in the previous chapter, the focus will be directed toward technologies designed to facilitate the recovery of this vital component of human mobility. The chapter starts by describing the acquisition systems employed to capture brain activity, with a special emphasis on the significance of electroencephalography (EEG). Subsequently, following the trajectory of the BCI loop, we discuss the mental tasks frequently employed in post-stroke rehabilitation and the associated challenges.

The narrative then progresses into the description of the signal processing algorithms to discern the brain activity corresponding to the mental task. Subsequently, the diverse feedback modalities that are provided to post-stroke patients are discussed, with a special focus on the potential of multimodal feedback. Within this section, we introduce the potential of vibrotactile feedback as a noteworthy innovation.

Moreover, other applications of vibrotactile stimulation within the domain of BCIs are briefly introduced. Notably, particular attention is given to its role as a feedback mechanism in motor-imagery-based BCIs. This section examines pivotal considerations in the design of vibrotactile feedback and unveils encouraging research avenues for its implementation in BCIs dedicated to post-stroke motor rehabilitation.

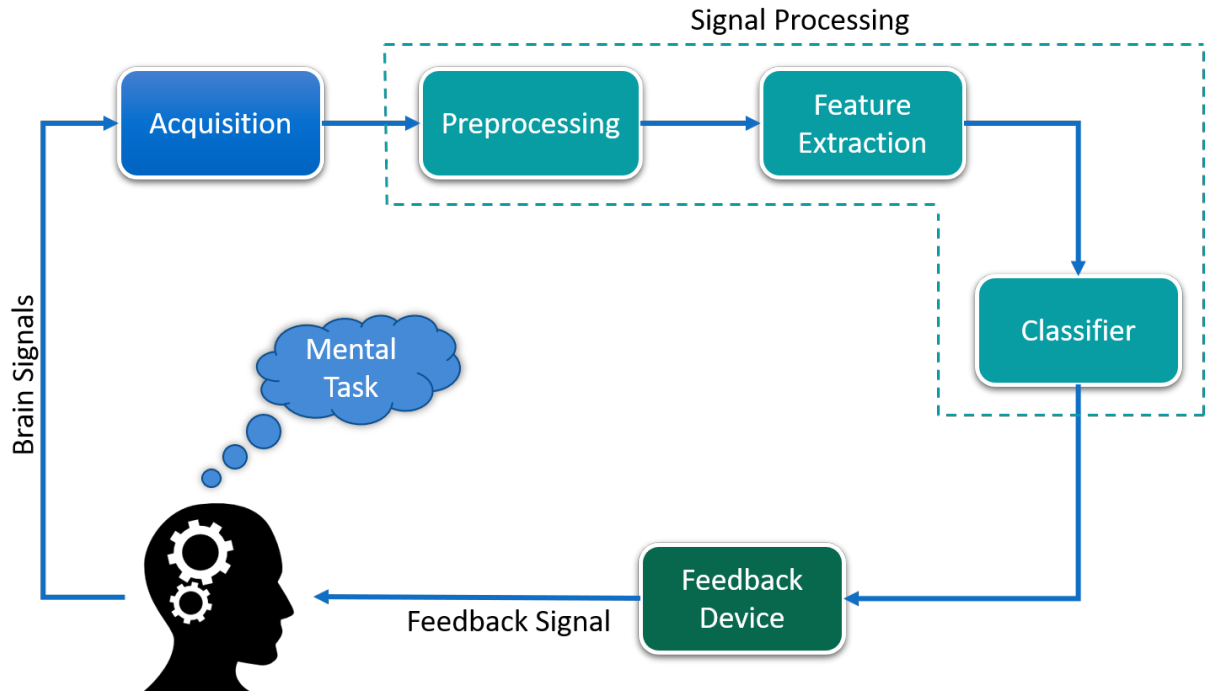


Figure 2.1: The BCI loop. The user’s brain activity is recorded while performing a mental task. The signals are then processed to convert them to a feedback signal that the user may interpret to modulate their brain activity.

2.2 Acquisition of the Brain Activity

In BCIs, the acquisition of brain activity can be achieved through invasive or non-invasive means. Invasive techniques use implanted electrodes to record intracranial brain activity, offering exceptional spatial resolution by capturing signals from single or multiple neurons [70]. However, the invasive nature of this approach introduces surgical risks, making it primarily reserved for medical indications and research in assistive BCIs, particularly those focused on replacing motor and/ or sensory functions rather than facilitating recovery.

Conversely, non-invasive BCIs record the brain activity from the surface of the scalp. While these techniques do not offer the same advantages as invasive recordings, they are safer and offer signals of satisfactory quality. Various imaging technologies facilitate non-invasive brain activity recording, including magnetoencephalography (MEG), functional near-infrared spectroscopy (fNIRS), functional magnetic resonance imaging (fMRI), and electroencephalography (EEG) [71].

Both fNIRS and fMRI, measure changes in the brain’s metabolic activity in response to changes in cognitive states [72]. They rely on monitoring changes in blood oxygenation, with fNIRS using near-infrared spectroscopy and fMRI using magnetic fields. Both methods offer good spatial resolution but have limited temporal resolution. Additionally, fMRI has significant drawbacks, including elevated costs, lack of portability, and the necessity for specialized personnel to operate the equipment.

In clinical practice, MEG has been used mainly for the diagnosis of epileptic loci and for guiding the placement of intracranial electrodes. MEG captures magnetic fields generated by neuronal

activity and shows promise in BCI applications for post-stroke rehabilitation [73, 74]. Nevertheless, MEG is associated with elevated costs, lacks portability, and demands a specialized multidisciplinary team for its manipulation, limiting its widespread clinical deployment.

EEG stands out as the most commonly used technology in post-stroke rehabilitation due to its minimal risk to the patients, high temporal resolution, portability, and relatively low cost compared to other imaging techniques [75, 31]. During EEG recordings, electrodes are placed on the user's scalp, typically following international conventions such as the 10-10 system, involving 75 electrodes [76]. EEG measures electrical brain activity at the surface level, providing insight into the activity of groups of neurons rather than single-neuron activity. Despite its poor spatial resolution, EEG's high temporal resolution makes it a good solution for real-time applications. Furthermore, it does not require specialized technicians for operation, and it boasts portability, enabling use in clinical settings or at the patient's bedside. However, a potential drawback is the time-consuming setup process, which becomes longer with high-density recordings due to the need to place electrodes individually.

Currently, EEG appears to offer the most favorable cost-benefit balance for BCI rehabilitation. As technology evolves, new approaches, such as bimodal acquisition systems, are emerging. However, for the present studies, EEG was selected due to its numerous advantages, allowing for a more comprehensive exploration of the use of BCIs in post-stroke rehabilitation. A summary of 25 studies involving controlled trials of EEG-based BCIs for upper limb post-stroke motor rehabilitation is provided in table 2.1. These studies were extracted from the following reviews and meta-analyses: Bai, et al. [29], Baniqued, et al. [77], Carvalho, et al. [28], Cervera, et al. [78], Khan, et al. [79], Kruse, et al.[80], López-Larraz, et al.[27], Mansour, et al. [31], Monge-Pereira, et al. [26], and Yang, et al. [81]

Table 2.1: Summary of articles on EEG-based BCIs for upper limb motor rehabilitation of post-stroke patients. AO: Action Observation, MI: Motor Imagery, KMI: Kinesthetic Motor Imagery, CSP: Common Spatial Patterns, FBCSP: Filter-Bank Common Spatial Patterns, CAR: Common Average Reference, SMR: SensoriMotor Rhythm, ERD: Event-Related Desynchronization, ERS: Event-Related Synchronization, PSD: 1111, PSO: particle swarm optimization, LDA: Linear Discriminant Analysis, SVM: Support Vector Machine, LAM: Linear Autoregressive Model, NS: Not Specified

Study	Electrodes	Mental Task	Spatial Filter	Temporal Filter	Features	Classifier
Ang et al., 2014 [82]	27	KMI	CSP	Band-pass	FBCSP	Calibration model (unspecified)
Ang et al., 2015 [83]	27	MI	CSP	Band-pass	FBCSP	Calibration model (unspecified)
Barsotti et al., 2015 [84]	13	MI	CSP	Band-pass	ERD mu, beta	SVM with linear kernel
Biasiucci et al., 2018 [85]	16	MA	Laplace	Band-pass	Band power (PSD)	Gaussian Classifier
Bundy et al., 2017 [86]	8	MI	NS	NS	ERD mu, beta	LAM
Carino-Escobar et al., 2019 [87]	11	MA	CSP	Band-pass, Notch	FBCSP, PSO	LDA
Chen et al., 2020 [88]	31	MA	NS	Band-pass	CSP	LDA
Cheng et al., 2020 [5]	24	KMI	CSP	Band-pass	FBCSP	Fisher's linear discriminant
Chowdhury et al., 2018a [89]	12	MI	CSP	Band-pass	CSP, ERD/ERS mu, beta	SVM with linear kernel
Chowdhury et al., 2018b [90]	12	MA	CSP	Band-pass	CSP	SVM
Curado et al., 2015 [91]	NS	MA	NS	NS	SMR power desynchronization	NS
Frolov et al., 2017 [92]	32	KMI	NS	Band-pass	Band power	Bayesian classifier
Jang et al., 2016	NS	AO	NS	NS	Concentration index	Threshold

[93]						
Kasashima-Shindo et al., 2015 [94]	2	MI	NS	NS	Band power mu	NS
Kim et al., 2016 [95]	4	AO	NS	NS	Band power SMR (12-15Hz), mid-beta(16-20Hz)	Threshold
Miao et al., 2020 [96]	16	MI	NS	Band-pass	CSP	LDA
Norman et al., 2018 [97]	16	MI	NS	NS	Band power	Elastic Net Regression
Ono et al., 2016 [98]	9	AO+MI		Band-pass, Notch	Band power (7-15Hz), ERD mu	LDA
Pichiorri et al., 2015 [1]	31	KMI	CAR	Band-pass	Band power	NS
Ramos-Murguialday et al., 2013 [3]	16	MA	NS	Band-pass	SMR power	LAM
Rayegani et al. 2014 [2]	19	KMI	NS	Band-pass	SPD	Threshold
Tsuchimoto et al., 2019 [99]	5	KMI	NS	NS	Band power alpha, beta	NS
Várkuti et al., 2013 [100]	27	MI	CSP	NS	FBCSP	NS
Wang et al., 2018 [101]	16	AO+MI	NS	NS	Band power in mu	Threshold
Wu et al., 2020 [102]	8	MI	NS	Band-pass, Notch	Band power beta	NS

2.3 Mental Tasks in Post-Stroke BCIs

In the context of post-stroke rehabilitation, patients engage in a mental task aimed at stimulating brain activity and fostering neuroplasticity. This section explores three primary mental tasks commonly employed in BCIs for motor rehabilitation: motor imagery, motor attempt, and action observation.

2.3.1 Action observation

Action observation (AO), involves BCI users passively observing physical movements, typically through video presentation or within a virtual environment. This technique requires minimal mental effort from the patients, emphasizing concentration on the observed movements. AO takes advantage of the mirror neuron system, a network of neurons responsible for both executing and observing actions, which activates the motor cortex during movement observation [103]. This activation can be used to initiate feedback signals of the BCI.

Despite being less frequently used in post-stroke BCIs, AO has demonstrated its effectiveness when combined with FES to improve arm recovery [95]. Furthermore, AO has been integrated with motor imagery in some studies [98, 101] with the potential to enhance motor imagery and plasticity by facilitating corticomotor excitability [104]. Nevertheless, during AO, patients may feel too passive, thus other techniques have been employed.

2.3.2 Motor attempt

Motor attempt (MA) is a technique commonly used among post-stroke patients to interact with a BCI, as shown by six studies in table 2.1. In this approach, patients may not be able to fully perform upper limb movement, such as reaching or grasping, but they can make concerted attempts to do so, thereby activating the motor cortex. In response, the BCI can interpret their intentions and trigger FES systems or robotic devices to complete the intended movements.

The recent review by Bai et al. [29], suggested that MA may be slightly more effective than motor imagery in post-stroke recovery of the upper limb. However, it's worth noting that only one study has directly compared both techniques in stroke patients, concluding that while MA improved BCI performance, i.e., better detection of the EEG activity, both methods presented similar cortical activation [105]

MA is well-suited for patients with residual movement capabilities. For those unable to perform any physical movements, alternative techniques, such as motor imagery, may be more appropriate.

2.3.3 Motor imagery

Motor imagery (MI) is a widely used technique in post-stroke recovery, particularly in the domain of BCIs. MI involves mentally simulating the execution of a movement without physically performing it [106]. MI-based BCIs record and translate the corresponding brain activity to activate external devices, creating a closed-loop system that stimulates the paralyzed limb, thus promoting neuroplasticity [27]. It has also been used to improve the performance of athletes and musicians and proves more effective when accompanied by physical practice of the imagined movement [107].

MI elicits brain activity similar to that observed during motor execution, activating the primary sensorimotor areas [108]. However, this activation is less intense and lateralized than that seen during motor execution [109].

Two distinct forms of MI exist: visual motor imagery (VMI), where users mentally visualize the movement from various perspectives, and kinesthetic motor imagery (KMI), which involves recalling kinesthetic and proprioceptive sensations related to movements, such as muscle contractions, pressure temperature, skin stretching, among others [35]. Although they are different, not all studies report which type of MI was implemented. Out of the 15 studies employing MI, only six indicated using KMI. As the others did not report this information, it is not possible to conclude which technique was employed, thus it is not possible to compare them. The differences in VMI and KMI rely not only on the mental strategy but it is also observed in the brain activity associated with each of them. Firstly, VMI shows larger activity in the visual cortex located in the occipital lobe. [110]. An fMRI study revealed that KMI has the unique ability to activate primarily motor-related brain regions, such as the premotor cortex, SMA, and the anterior parietal lobe, while VMI presented more activity in the occipital and posterior parietal regions [37]. A study with transcranial direct stimulation demonstrated that, unlike VMI, KMI modulates corticomotor excitability, making it particularly relevant for post-stroke rehabilitation [111]. Nonetheless, this must be taken carefully as fMRI studies have demonstrated that both, VMI and KMI overlap brain areas [112].

Although KMI seems more appropriate than VMI for rehabilitation purposes, it can pose challenges, as it lacks the proprioceptive and sensory feedback present in physical movements. To address this, providing meaningful haptic feedback that triggers proprioceptive sensations, rather than visual feedback, may enhance KMI's effectiveness in post-stroke rehabilitation. Furthermore, merging visual and haptic feedback engages more senses, thus, it may offer more information to the patients. This thesis focuses on delivering such feedback to maximize post-stroke recovery.

In summary, three mental tasks are mainly used in post-stroke BCIs, each with its own suitability depending on the patient's capabilities. The selection of the appropriate task should align with the patient's physical abilities, adapting the task as they progress to maximize the benefits of BCI training.

2.4 Signal Processing and Classification

Following the acquisition of EEG signals, a crucial step involves their processing to extract relevant information and subsequent classification. The signal processing pipeline consists of three main stages: preprocessing, feature extraction, and classification.

2.4.1 Preprocessing

EEG signals are susceptible to various artifacts stemming from sources like muscle activity, eye movements, cardiac activity, respiration, or other external factors such as line noise. In order to reduce or eliminate these artifacts, signal preprocessing employs spatial and temporal algorithms. Table 2.1, provides an overview of the most prevalent spatial and temporal filters used in post-stroke BCIs. It is essential to note, that several studies did not report this information. In fact, 15 of them did not mention using any spatial filters, while nine did not detail temporal filters. This omission may be due to non-application, or even a matter of technical omission, given that

these studies primarily focus on assessing BCI training efficacy.

2.4.1.1 Spatial Filters

Spatial filters aim to manipulate the amplitude of an EEG electrode based on predefined weightings of neighboring electrodes. Their purpose is to extract or enhance specific features within the recorded EEG signals. In the context of BCIs for stroke, three prominent spatial filters emerge: Common Average Reference (CAR), Laplacian filter, and Common Spatial Patterns (CSP).

2.4.1.1.1 Common Average Reference CAR is a basic filter that computes the mean of all the recording electrodes and then subtracts it from each electrode individually [113]. The objective here is to eliminate common noise present across all electrodes and enhance the signal-to-noise ratio.

2.4.1.1.2 Laplacian Filter The Laplacian filter is commonly applied to improve the spatial resolution of the EEG and accentuate localized brain activity. In its computation, the average of a selected group of neighboring electrodes is subtracted from the value of the target electrode [113].

2.4.1.1.3 Common Spatial Patterns CSP facilitates the discrimination of different mental tasks by extracting spatial patterns associated with each task. By maximizing the variance of signal components linked to one task while minimizing it for the other class, CSP enhances the separation between task-related features. [114, 115]. The computation involves constructing a covariance matrix of the EEG data, which describes the relationship between the EEG signals recorded at different electrodes. Thus, the size of the matrix depends on the number of electrodes.

2.4.1.2 Temporal Filters

Temporal filters are employed to extract or eliminate information proper to specific frequency components. For instance, notch filters serve to eliminate interference from power lines, typically operating at 50 or 60 hertz, depending on the region. High-pass filters, set around 0.5 or 1 hertz, are used to remove direct current noise, typically observed EEG signal offsets.

In the domain of post-stroke motor rehabilitation BCIs, the focus shifts to band-pass filters, catering to specific EEG frequency bands associated with motor-related tasks. These bands and their respective characteristics are outlined:

- **Alpha:** These waves are in the frequency range of 7-12 Hz. They are mainly observed in the occipital lobe and have been associated with the processing of visual information and attention [116, 117].
- **Mu:** Mu waves are often used interchangeably with alpha waves because they are found within a similar frequency range (8-12 Hz). However, they are more present among sensorimotor areas, thus they are rather associated with the processing of sensorimotor activities. In fact, mu rhythms are attenuated by movement [118, 119], reduced or desynchronized by contralateral movements [120] and MI [121], and increased in the ipsilateral hemisphere [108].

- **Beta:** Beta oscillations, falling within the 15-30 Hz range over sensorimotor areas, frequently coexist with mu waves. They are present during motor execution and MI [108]. Some studies, such as [95], differentiate low-beta, mid-beta, and high-beta sub-frequencies. In this manuscript, beta refers primarily to the 15-30Hz range, with specific sub-bands and frequencies specified as needed.
- **Theta:** Although less common in MI-based BCIs, theta waves (3-7 Hz) offer insights into attention and concentration levels [122, 123, 93].

2.4.2 Feature extraction

After pre-processing, the next step involves the extraction of the most relevant EEG features associated with the mental task. Table 2.1 identifies the most common approaches, with Filter Bank-CSP (FBCSP), CSP, and band power features emerging and prominent choices. Notably, a meta-analysis in [29] emphasized the impact of feature selection on the long-term recovery of post-stroke patients, with FBCSP favoring BCI accuracy and band power features promoting upper-limb recovery.

2.4.2.1 Common Spatial Patterns and Filter Bank CSP

CSP spatial filters are employed to extract spatial patterns specific to different frequency bands, projecting EEG data onto these filters for feature extraction. FBCSP is an extension of CSP that incorporates a filter bank approach, facilitating robust and effective feature extraction from EEG data across multiple frequency bands [124]. The advantage of FBCSP is that it leverages the information from multiple frequency bands to enhance the discrimination power of the features. In this way, it can capture distinct neural patterns associated with different mental tasks.

2.4.2.2 Band Power Features

Band power features are considered the gold standard for MI-based BCI, quantifying the power of EEG signals within specific frequency bands and designated time windows in a given channel [125]. This method is well-established and widely adopted in the MI-BCI field as it offers valuable insights into the underlying neural activity during motor-related cognitive tasks.

In MI-BCI studies, researchers frequently focus on specific frequency bands of interest, notably the mu, alpha, and beta bands. These bands are particularly relevant because they contain information pertinent to motor tasks, making them instrumental in deciphering user intent. Furthermore, three studies in table 2.1 report using the power in sensorimotor rhythms (SMR), which encompass the mu, beta, and gamma (>30Hz) EEG oscillations recorded over the sensorimotor cortex [126, 127]. While these articles might not explicitly specify the frequency bands involved, it is reasonable to infer that when referring to SMR power features, they refer to the set of mu, beta, and gamma oscillations.

Various techniques exist for computing power, including power spectral density, wavelets, and time-frequency energy distributions, as described in [128, 129]. In this manuscript, we primarily focus on the approach proposed in [120, 32]. This method involves squaring the EEG signal and aligning trials to the mental task. A baseline period, typically a few milliseconds before the task, is computed and subtracted from the trial average. This results in a decrease or increase of power concerning the baseline, a concept known as event-related de/synchronization.

2.4.2.3 Event-related synchronization/desynchronization

Event-related desynchronization (ERD) and event-related synchronization (ERS) are crucial metrics in MI studies, providing insights into the temporal and spectral dynamics of EEG signals during motor-related cognitive tasks. These measures are instrumental in assessing changes in spectral power across different frequency bands concerning a baseline period.

ERD denotes a decrease in spectral power within a specific frequency band relative to a baseline period, whereas ERS signifies an increase in power. ERD/ERS capture changes in the activity of local interactions between neurons responsible for modulating the frequency components of the ongoing EEG. They serve as an electrophysiological representation of cortical network activity during the processing of sensorimotor information, indicating enhanced excitability of cortical neurons engaged in this cognitive process [32, 33, 34].

During voluntary motor execution, an ERD is predominantly observed in the mu and beta frequency bands. It typically begins one to two seconds before the initiation of muscular contraction and reaches its peak during the execution phase. Following the completion of the movement, the mu power returns to its baseline value, while in beta an ERS is present [130, 32].

A similar phenomenon is observed in MI tasks, although the strength of the signals may be lower than that from motor execution [131] or MA [105]. However, with training, the imagery-induced activity can surpass that of motor execution [131]. Before and during MI, a progressive ERD is evident in the mu and beta frequency bands, primarily over the contralateral sensorimotor cortex [132, 108]. Furthermore, mu desynchronization has been observed bilaterally in the sensorimotor cortex [121]. After MI ends, beta activity returns to baseline, followed by an increase in power (ERS) known as beta rebound, predominantly observed in the contralateral hemisphere [133, 134, 135, 136]. The ERS is also present in the mu band. Although early studies suggested minimal significance of mu ERS during hand MI [137], more recent study indicates that mu exhibits notable ERS, particularly during extended MI tasks [138]. Consequently, both mu and beta ERS can potentially be observed, providing further insights into the dynamic neural processes underlying MI.

ERD/ERS analysis is a robust method for detecting changes in brain activity during MI tasks, making it a common choice for feature extraction in MI-based BCIs for post-stroke recovery. Additionally, it is a valuable method for offline EEG signal analysis, confirming the engagement of the targeted sensorimotor cortex during neurorehabilitation.

2.4.3 Classification

After extracting the most pertinent features from EEG signals, specialized algorithms are employed to discriminate the signals associated with the mental task, such as motor imagery of the impaired hand. The most used classification algorithms in controlled studies (table 2.1) are linear approaches, such as linear discriminant analysis (LDA) and support vector machines (SVM). Additionally, four studies adopted a threshold-based approach, while it is worth noting that six studies omitted details regarding their chosen classification method.

2.4.3.1 Linear Discriminant Analysis

Linear discriminant analysis (LDA), also known as Fisher's linear discriminant (as in [5]), is a supervised machine learning technique extensively used in BCIs. Its primary role is to decode patterns in brain activity associated with different cognitive tasks. LDA uses hyperplanes to

separate the data of different classes. In the two-class scenario, such as in post-stroke MI-BCIs, the resultant class assignment depends on the location of the feature vector relative to the hyperplane. LDA's objective is to determine a linear discriminant function that maximizes the distance between class means while minimizing within-class variance [139]. Despite its popularity in MI-BCIs, it may exhibit limitations when dealing with nonlinear EEG data.

2.4.3.2 Support Vector Machines

Support vector machines (SVM), are similar to LDA in the way that they also perform two-class classification by proposing a hyperplane that best separates the data. This hyperplane, known as the decision boundary, dictates the classification outcome, with data falling on one side categorized as one class and those on the other side as the second class. SVM attempts to identify the best hyperplane, i.e., the one that maximizes the margins from both classes. In cases where data falls within the margin, a tolerance or regularization constant must be chosen. This leads to two variations: a "hard-margin SVM", where the support vectors lie precisely on the border of the margin, and a "soft-margin SVM" where the support vectors are on the margin or on its borders. When the classes cannot be linearly separable, a kernel may be used, which is a function that transforms the features so that they may be separated. Various kernels, including polynomial, Gaussian, and linear, are available [140].

2.4.3.3 Threshold Approach

In contrast to the discrimination of mental states, four studies opted for a threshold approach. In this strategy, the threshold was defined, either based on the extracted features or chosen arbitrarily. The threshold was related to the concentration index [93] or to band power features [95, 2, 101]. Whenever the threshold was exceeded, the feedback signal was triggered.

In summary, the CSP+LDA approach remains the most popular classifier amongst post-stroke BCIs. The most used features are band power in the mu and beta frequency bands as they contain information associated with motor activity such as MI. Nonetheless, critical aspects such as temporal and spatial filters, features, and classifiers are not consistently reported, posing challenges for comprehensive comparative analyses. This information gap complicates the decision-making process for the signal-processing phase of BCI design.

Once the EEG signals have been processed and classified, they are translated into a control signal to trigger the activation of the feedback device and provide the feedback signal to the patient. We will discuss the feedback in the next section.

2.5 Feedback Modalities

The classification results are translated into an output signal to the patient, for example, a visual stimulus, a robotic orthosis that moves the paretic hand, or activation of a functional electrical stimulation system. In this way, patients and clinicians may know if they are executing the mental task correctly and patients may learn to modulate their brain activity [141]. Moreover, providing feedback results in a closed-loop interface that establishes a link between the intended or imagined movement and the patient's body by generating proprioceptive activity in the affected limb, stimulating neuroplasticity, and having an important effect on motor recovery [27]. A summary of the feedback modalities is presented in table 2.2

Table 2.2: Summary of feedback modalities in EEG-based BCIs for upper limb motor rehabilitation of post-stroke patients.

Study	Feedback Modality	Feedback Timing
Ang et al., 2014 [82]	Haptic Knob	Discrete
Ang et al., 2015 [83]	MIT-Manus Robot	Discrete
Barsotti et al., 2015 [84]	Exoskeleton	Discrete
Biasiucci et al., 2018 [85]	FES	Discrete
Bundy et al., 2017 [86]	Exoskeleton	Continuous, not clear
Carino-Escobar et al., 2019 [87]	Exoskeleton	Discrete
Chen et al., 2020 [88]	Exoskeleton	Discrete
Cheng et al., 2020 [5]	Soft glove and visual	Discrete
Chowdhury et al., 2018a [89]	Exoskeleton	Discrete
Chowdhury et al., 2018b [90]	Exoskeleton	Continuous (updated every 0.5 seconds)
Curado et al., 2015 [91]	Orthosis	NS
Frolov et al., 2017 [92]	Exoskeleton and visual	Continuous (updated every 100ms)
Jang et al., 2016 [93]	FES	Discrete
Kasashima-Shindo et al., 2015 [94]	Motor driven	Discrete
Kim et al., 2016 [95]	FES	Discrete, not clear
Miao et al., 2020 [96]	FES and visual	Discrete
Norman et al., 2018 [97]	Visual and robotic	Continuous (updated every 50 ms)
Ono et al., 2016 [98]	Visual, exoskeleton	Discrete
Pichiorri et al., 2015 [1]	Visual	Discrete
Ramos-Murguialday et al., 2013 [3]	Orthosis	Continuous (updated every 200ms)
Rayegani et al. 2014 [2]	Visual and auditory	Discrete
Tsuchimoto et al., 2019 [99]	Robot and NMES	Not clear
Várkuti et al., 2013 [100]	Robot	NS
Wang et al., 2018 [101]	Robot hand	Discrete
Wu et al., 2020 [102]	Exoskeleton	Continuous, not clear

2.5.1 Visual Feedback

Visual feedback provides users with information about their performance through a graphical interface, typically via a screen. Despite its simplicity, this type of feedback has not been broadly explored in control trials for stroke rehabilitation and has been further studied in combination with other modalities.

The visual feedback can take the form of the participant's limbs. For instance, in Pichiorri et al. [1], 28 subacute patients received feedback consisting of a visual representation of the participant's hands on a white blanket covering them, as shown in figure 2.2. When KMI activity was detected, the virtual hands performed a grasp and finger extension movement.

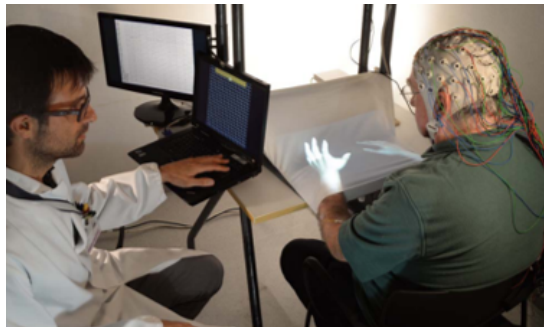


Figure 2.2: Visual feedback covering the participant's hand, extracted from [1].

Conversely, the feedback can be different from the participant's anatomy. The study by Rayegani et al. [2], proposed a gamified feedback consisting of a three-boat race, shown in figure 2.3. If the participant kept the SMR power above a predefined threshold and the beta and theta power below another threshold, then the participant's boat would advance further than the other two boats. This BCI approach resulted in similar hand improvements to conventional therapy and electromyography-based biofeedback. However, the BCI modality showed an improvement in SMR power, suggesting the gamified visual feedback helped the MI task.

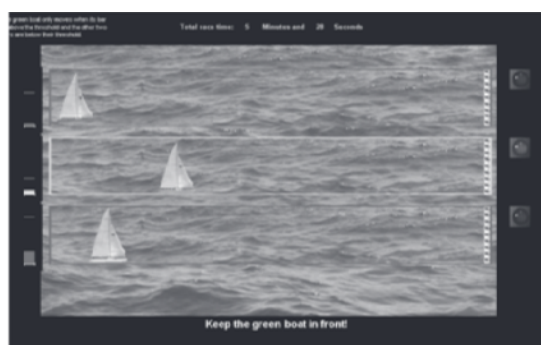


Figure 2.3: Visual feedback consisting of a boat's race, extracted from [2].

Another example is the feasibility study by Prasad et al., [142], where five chronic stroke participants were presented with a visual environment with the objective of placing a ball inside a basket by performing MI of the left or right hand. Despite the moderate BCI performance, participants showed an improvement in clinical rehabilitation measures.

These studies aimed at giving visual feedback, sometimes in the form of virtual hands or in

a gamified way, providing either abstract or realistic feedback regarding the movement to be performed. A way to adapt this feedback to the participants' needs is to take into consideration their preferences, for instance, preferred colors or the participant's physical characteristics to create a similar human avatar. With the rise of virtual reality, more complex and controlled environments have emerged, which provide better engagement than simple stimuli and better control over multisensory stimulation.

2.5.2 Virtual reality

BCIs merged with a virtual reality (VR) environment also aim to promote neuroplasticity and motor recovery by controlling virtual or real devices [143]. Although the feedback in VR is visual, immersive VR (IVR) requires a head-mounted device (HMD), representing a challenge when coupling it with BCI technology. The VR-HMD must be carefully positioned to not interfere with the electrodes placed on the scalp.

An example of IVR for post-stroke motor rehabilitation is the system REINVENT, which uses an Oculus Rift headset to display arm movement associated with MI [144]. Besides proving the feasibility of VR-based BCIs for stroke participants, they showed an increase in the clinical assessment scores after using the device and verified users' acceptability. Nonetheless, the system's costs and technical complexity must be considered carefully. In addition, some people may report vertigo, nausea, and/or dizziness when using VR, and participants with visual impairments may not benefit from this solution.

Overall, through VR, researchers may have more controlled environments, some of them closer to a real-life situation, which might increase patient engagement towards the therapy. Further studies are required to evaluate the therapeutic effects, as well as to verify the compatibility between the VR headsets and the EEG headsets.

Visual feedback may not be suitable for all post-stroke patients because some may present visual impairments. Moreover, when performing MI, participants are demanded great abstraction and concentration, where visual feedback may interfere with the attention necessary to perform MI. In this case, haptic feedback may be considered, as it may offer more intuitive feedback to the user [38].

2.5.3 Haptic Feedback

The term "haptic" refers to "sensory and/or motor activity of the skin, muscles, joints, and tendons" (ISO 9241-910:2011, 2011 244: 1 in [145]). A survey on haptic interfaces in BCIs [145] proposed based on the tactile sense, which involves the mechanoreceptors found on the skin, and the kinesthetic sense, associated with the receptors found in muscles, tendons, and joints. By stimulating these two senses, haptic feedback presents a closed-loop, which may result in better BCI performances and motor recovery.

Until now, most controlled trials involving haptic feedback with stroke participants have tested mainly two types of interfaces: FES and robotic devices, which stimulate the kinesthetic sense. The profile of the post-stroke participant, i.e. their needs, rehabilitation objectives, and physical and cognitive limitations, may influence the choice of the device that will deliver the haptic feedback.

2.5.3.1 FES Feedback

FES is a subtype of neuromuscular electrical stimulation (NMES) that delivers electrical stimulus to muscles through surface electrodes to produce functional movement that might be used for daily life activities [146, 147]. Its intensity can be varied to determine the level of contraction of the muscles. This includes sensory threshold FES [148], a type of electrical stimulation that will not induce movement, but rather a superficial stimulation; yet its effects on stroke participants are to be explored. During the assessment of BCIs with FES feedback, the control groups are typically also stroke patients, but the FES system is triggered independently of the mental task.

FES has been used for upper limb rehabilitation involving reaching and grasping movements. The protocol in Biasiucci et al. [85] aimed to help recover the hand extensors by triggering the FES every time MI was detected. A control group had FES triggered independently of the brain activity, while the BCI-FES group activated the system according to the MI activity. Contrary to the control group, the BCI-FES group showed significant functional motor recovery.

Shoulder subluxation can also be treated with BCI-FES, as presented by Jang et al. [93]. The participants in the BCI-FES performed a combination of AO and MA of shoulder motions. When EEG patterns corresponding to the MA were detected, the FES system was activated. After using the BCI-FES system, four scores of clinical assessments improved, while only three scores of the FES-only group improved. These results suggest the BCI training may help in the motor recovery of the shoulder in stroke participants.

Furthermore, FES can be complemented with AO, as suggested in [95] where 30 chronic-stroke participants observed videos of daily life tasks. Fifteen participants had an EEG system that was used to measure attention level and MI. Whenever these two reached a defined threshold, FES was triggered to stimulate the extensors of the wrist. Their results showed a significant increment in clinical assessments of the participants using the BCI-FES system versus the control group following conventional therapy.

FES feedback systems have proved to be relevant for the motor recovery of stroke participants and superior to other techniques [29, 31]. Nevertheless, they present some limitations such as the need for specific devices that also require specialized personnel for operation, and the limb muscles should be available, which could be a problem when spasticity is present. Some participants may experience pain and discomfort when presented with the electrical stimulation, impeding them from using it. Moreover, individuals with pacemakers cannot benefit from FES.

2.5.3.2 Exoskeletons and Robot-Assisted Feedback



Figure 2.4: Hand exoskeleton developed by Ramos-Murguialday et al. [3]

BCIs coupled with exoskeletons and robots are used to help the participants to perform a specific movement. They are placed under the same category as they require a motorized intervention. Eleven studies from table 2.2 used exoskeletons or motor-driven orthoses, resulting in the most employed feedback modality, followed by robot-assisted feedback present in eight studies. This approach allows for an increased number of movement repetitions in a more controlled way than with a physical therapist. In this context, most of the controlled groups are presented with sham feedback where the exoskeleton or robot movement is independent of the mental task.

Exoskeletons assist the participant in performing the movement and offer some proprioceptive feedback. Most of these devices train finger extension because stroke participants commonly present spasticity in the form of a closed hand. One example is the study by Ramos-Murguialday et al. [3], which investigated the effects of the hand exoskeleton in figure 2.4 that performed reaching and grasping movements corresponding to the MA of post-stroke subjects. The clinical assessment scores improved significantly among the subjects that followed the BCI protocol rather than the control group.

Some of these devices may be taken out of the clinical environment, as described in [86]. This study was carried out at the participant's home, where BCI training was performed with a powered exoskeleton opened and closed the hemiparetic hand. An increase in the primary clinical assessment demonstrated the feasibility of successfully performing the BCI training at home with a hand exoskeleton. This study laid the foundations for the recently FDA-cleared IpsiHand by Neuroolutions², depicted in figure 2.5, which is a wearable non-invasive MI-BCI that can be used at home by post-stroke patients.



Figure 2.5: Neuroolution's IpsiHand for post-stroke recovery. The system consists of a BCI with proprioceptive feedback from an exoskeleton that can be employed at the patient's home. Extracted from: <https://www.neuroolutions.com/>

One example of robotic-assisted therapy is the study by Várkuti et al. [100] with the MIT-Manus robot used for shoulder and elbow recovery. The robot was activated whenever MI was detected

²<https://www.neuroolutions.com/>

or 2 seconds after no activity was detected. Their results showed an improvement in clinical scores and in functional connectivity, measured by resting-state fMRI.

One difference between exoskeletons and robots is their portability. While most robots are grounded to the floor or a base, and cannot be taken out of the hospital environment, some exoskeletons are portable. In this case, the participants may take the device to their home and follow the rehabilitation process in a familiar and more comfortable environment, which may increase technology acceptability and adherence to the therapy. Additionally, the patients perform their rehabilitation therapy in an independent manner, thus the physical therapists may allocate time to more patients at the time.

These devices should be designed taking into consideration the user's morphology, especially for those presenting hand spasticity. In these particular cases, the hand muscles are tightened, keeping it firmly closed and limiting mobility. Thus, fixating the exoskeleton on the limb may be challenging and even painful for some individuals. Moreover, they must be adapted to the environment, at home or at the hospital, as well as the patient's needs and limitations. Both FES and robot-assisted feedback require some mobility from the patients. Some of them, especially in early recovery stages, may present too much pain, not being able to benefit from these therapies. In this case, another type of proprioceptive feedback may be provided, such as vibrotactile stimulation.

2.5.3.3 Vibrotactile Feedback

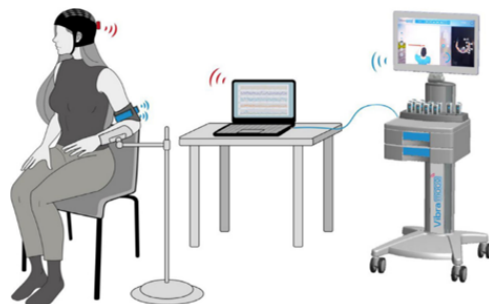


Figure 2.6: Tendon vibration applied during MI, extracted from [4].

Despite its simplicity and potential use in stroke motor rehabilitation, vibrotactile stimulation has been minimally explored as a feedback modality for post-stroke MI-based BCIs. At the moment of writing this thesis, we identified only one study by Shu et al. [149] employing vibrotactile feedback with post-stroke patients. Eleven post-stroke participants participated in the study where they were presented with three conditions: vibrotactile stimulation, MA, and vibrotactile stimulation + MA. The vibrotactile stimulation was given on the paretic wrist of the participants during the idle state and the MA or tactile sensation stage. This study resulted in better BCI performance during the vibrotactile stimulation + MA condition and greater motor-related cortical activation. There are two main limitations of this study. First, the vibration was given at the same time as the MA was given, regardless of their performance, hence it is not possible to consider it as feedback because it did not depend on the participant's brain activity. Second, the therapeutic effects of the vibrotactile stimulation were not assessed, thus further studies are necessary to evaluate its effect on motor recovery.

On the other hand, tendon vibration results in an illusion of movement that can also be used in

MI-BCIs. Tendon vibration has been explored to improve BCI performance [150, 4], as shown in figure 2.6. Currently, there is an ongoing study with post-stroke patients to evaluate its therapeutic effects [151]. No further studies were identified that explore the effects of tendon vibration in MI-BCIs among stroke patients. However, the fixed duration and intensity of the vibration may limit its flexibility in BCI applications, where adaptive, dynamic, and short-latency feedback may be more beneficial.

Finally, vibrotactile stimulation is an alternative haptic feedback modality that has been understudied in post-stroke rehabilitation MI-BCIs. However, it has been investigated in other BCI applications and it has shown promising results in enhancing BCI performance. This will be discussed in the upcoming section 2.6.

2.5.4 Multimodal Feedback

Multimodal feedback within the context of BCIs involves the activation of two or more sensory modalities as a response to changes in brain activity. Primarily, research efforts have concentrated on combining visual feedback with a haptic one, driven by the expectation of delivering a better experience to the user, improving overall performance, and enhancing embodiment and user engagement [152]. A recent systematic review has revealed that relying solely on visual feedback is ineffective for BCI control. However, the integration of multiple modalities, thereby creating multimodal feedback, offers significant advantages across various BCI paradigms, including MI [153]. Moreover, multimodal feedback has demonstrated its potential in assisting users to better modulate sensorimotor rhythms compared to unimodal feedback [154].

Haptic feedback, particularly feedback resulting in physical movements, such as FES, robots, and exoskeletons, has the capacity to replicate limb movements, enabling participants to both perceive and observe their limb's motion. This fusion of sensory information results in a combination of the visual and haptic modalities, even when the visual does not require a third device such as a screen or a VR-HMD. Isolating these modalities could be achieved by concealing the participant's limbs behind a screen or opaque material; however, most studies have overlooked this distinction, making it challenging to evaluate the distinct effects of visual stimuli.

Within the reviewed studies presented in table 2.2, eight of them implemented bimodal feedback. Specifically, six studies combined haptic modalities with visual feedback, one integrated visual and auditory feedback, and one merged two haptic modalities, using both robotic and NMES feedback.

In cases where haptic and visual feedback are combined, the visual modality can assume various forms. Some implementations significantly differ from the mental task, such as altering the color of a fixation marker [92], changing the color saturation of a square box [97], or employing a cursor that moves horizontally [94]. Nevertheless, these visual modalities may be considered less natural as they diverge significantly from the intended mental task, potentially impacting embodiment and agency.

Alternatively, visual feedback can take the form of an avatar resembling the participant's limbs, as demonstrated in Miao et al.'s study [96], who used the commercial g.tec's recoveriX BCI system³ (see figure 2.7). This system combines FES and non-immersive virtual reality to provide feedback for MI tasks involving the left and right hands. A feasibility study with 51 stroke patients, demonstrated that this bimodal BCI effectively enhanced the motor function of the

³<https://recoverix.com/>



Figure 2.7: g.tec’s recoveriX BCI system for post-stroke motor rehabilitation with visual and FES feedback.

paretic arm, underscoring the advantages of multimodal BCI training [155]. However, there was no assessment involving the unimodal feedback, hence no conclusion can be made regarding the superiority of multimodal feedback.

A particularly interesting example is the study in [5], where participants were equipped with a soft glove depicted in figure 2.8 that facilitated hand movement following the detection of MI related to specific daily activities. Simultaneously, a virtual hand within a realistic virtual environment mirrored these movements. The virtual scenarios included activities of daily life such as pouring water on a glass or eating, offering meaningful activities that could improve the patient’s recovery. However, the reliance on virtual environments may not always be feasible; hence, an alternative approach could involve coupling haptic feedback with video displays of actual hand movements corresponding to the imagined actions, as in [98].

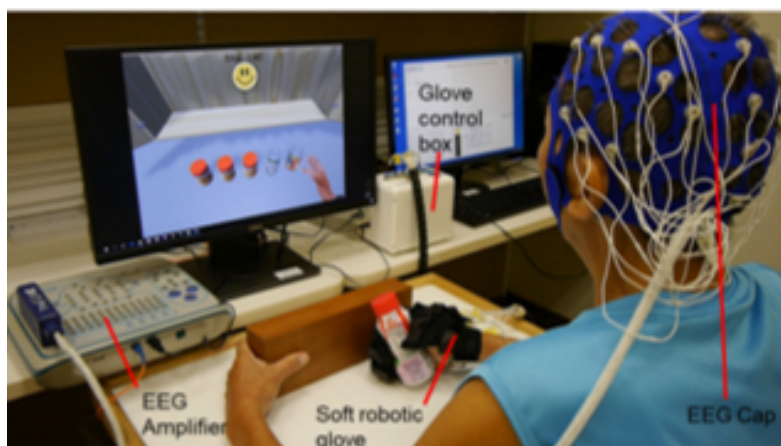


Figure 2.8: Soft glove and visual feedback extracted from [5].

In addition to the boat race study previously mentioned [2], auditory feedback was also offered to the patients. Unfortunately, the specifics of the auditory stimulation were not detailed, limiting further discussion of this particular feedback type.

Future directions in multimodal feedback could explore combinations with other feedback types, such as coupling visual feedback with vibrotactile feedback, as explored in previous studies [7, 156, 42], although this approach must undergo testing within the stroke population. This approach has demonstrated the potential to free up the visual channel, allowing users to allocate attention to other events, including distractors [38, 7, 42]. Furthermore, combining vibrotactile feedback with robots, exoskeletons, or auditory cues presents exciting avenues for exploration.

In conclusion, multimodal feedback, by leveraging multiple sensory modalities, has the potential to enhance the user experience, rendering interaction with the BCI more engaging and intuitive, ultimately leading to improved BCI performance, which has been associated with enhanced motor recovery [155]. Multimodal feedback offers advantages such as conveying a richer stream of information to the user, providing redundancy to mitigate errors, reducing cognitive workload, and enabling customization based on individual preferences and needs. Additionally, it offers flexibility to adapt to specific user constraints, whether physical or cognitive in nature.

2.5.5 Feedback Timing

An important question arises regarding the optimal moment to deliver the feedback. It can be provided in mainly two ways:

- **Continuously:** Feedback is given constantly to the patient and it is updated every certain period of time. This gives the impression to the patient that they are controlling the feedback signal in real-time. However, when it is not working correctly it may result in frustration, and it leaves little time for the patient to reflect on their strategy and adapt it correctly. Continuous feedback can serve as guidance and maintain the user's interest and attention, but it might as well act as a distractor from the mental task [157]
- **Discretely:** Feedback is given after a period dedicated solely to performing the mental task. In this case, patients have enough time to first focus on the mental task, then to interpret the feedback signal, and finally to reflect and adjust their strategy if necessary. Indeed, motor learning has proved to be better when the feedback is delayed by a few seconds [158]. Nevertheless, because the feedback is delayed, it may be perceived as unnatural, for example, a robotic hand moving after thinking of it instead of immediately.

In the studies presented in table 2.2, we observed that discrete feedback is the most used one, with 15 studies opting for this modality, while only four were purely continuous. On the other hand, two studies did not specify the timing, and four were not clear. The ambiguity and underreporting of feedback timing represent a challenge when trying to compare techniques and reproduce studies. Therefore, it is recommended to report as many details as possible to develop technologies that may benefit the patients.

Furthermore, in the context of post-stroke MI-BCIs, the main interest is that patients learn to perform mental imagery, which is considered a skill that can improve with training [159]. Although none of the controlled studies compared the feedback timing, it is highly likely for stroke individuals to present low tolerance to fatigue as well as cognitive impairments. Therefore, continuous feedback demanding high concentration levels to perform the mental task and process the feedback at the same time may be detrimental to the patients. This may explain the preferred use of discrete feedback among the various studies.

2.5.6 Conclusion on the Feedback

As we have seen, the choice of the feedback modality has been independent of the participants' profiles. The diversity of solutions, including visual, haptic, or multimodal feedback, opens up possibilities for adaptation to the singularity of patients. Indeed, the feedback can be informational (score, performance gauge, boat race, etc.), embodied (first-person view of virtual hands and haptic feedback), or assistive devices (exoskeletons and robotic devices). However, homogenization of the participants' profiles and the protocols (training sessions per week, overall duration) should be done so that studies may be compared. Questions arise regarding the possible mental load or dissociation of attention in the face of multimodality for patients who are tired and have a reduced attentional capacity. The synchronization within feedback modalities is also a path worth exploring, where both of them are given at the same time and are proportional, increasing congruence among them. An additional dimension to be evaluated is the effect of the feedback on the participants' motivation and overall user experience, which is commonly overlooked in post-stroke protocols. We should take into consideration the personal, emotional, and pragmatic experiences of the participants as they may have an important role in the BCI training outcome.

In summary, different feedback modalities are proposed for post-stroke motor rehabilitation. Most controlled trials focus on delivering haptic feedback in an attempt to stimulate proprioception and improve motor skills. Since stroke patients may present spasticity that does not allow them to perform movements, it is important to adapt the feedback to their abilities and limits. Consequently, this thesis will aim to propose an alternative or complementary feedback modality based on vibrotactile stimulation that provides meaningful information about the performance of KMI. As discussed previously, little work has been done within BCIs with vibrotactile feedback for stroke. Therefore, an exploration was made in other BCI applications in order to orient the solution. In fact, tactile vibration has been used in other BCI applications, presented briefly in the following section.

2.6 Focus on Vibrotactile Stimulation in Other BCI Applications

Vibrotactile stimulation has found applications in two primary types of Brain-Computer Interfaces (BCIs): reactive BCIs and active BCIs. Reactive BCIs detect changes in brain activity in response to external stimuli, while active BCIs rely on intentional mental tasks performed by the user, such as MI [160]. In the context of reactive BCIs, Event-Related Potentials (ERPs) serve as a common measure of electrical brain activity recorded in response to specific events or stimuli. Vibrotactile stimulation has been employed as an alternative to visual stimuli in cases where patients have limited visual capabilities or to free up the visual channel for other tasks. In this section, we briefly outline the applications of vibrotactile stimulation in ERP paradigms and then delve into its use in MI paradigms.

2.6.1 Event-Related Potentials

ERPs correspond to changes in EEG voltage due to external events or stimuli and are associated with the sense being stimulated, such as visual evoked-potentials (VEP), auditory evoked-potentials (AEP), and somatosensory evoked-potentials (SEP). SEPs are responses to mechanical or electrical skin stimulation, which activates the skin mechanoreceptors. When

ERPs are generated in response to repetitive sustained stimulation at a fixed frequency, they are called steady-state-evoked potentials (SSEP), also associated with the stimulated sense. A well-known SSEP application is steady-state visual evoked potentials (SSVEPs), where users are presented with a series of visual stimuli at different frequencies to detect the SSVEP provoked by them and locate the user's target in a speller [161], but also to control wheelchairs [162] and robotic arms [163]. However, SSVEPs-BCIs can induce visual fatigue, negatively affecting BCI performance [164, 165]. To address these issues and liberate the visual channel, steady-state somatosensory-evoked potentials (SSSEPs) have been explored.

While electrical stimulation has been used to elicit SSSEPs, this technique can be unpleasant and result in low-amplitude potentials [166]. Efforts have been made to develop vibrotactile stimulation as a more suitable and comfortable alternative for prolonged use. Early work by Muller-Putz et al. [167], stimulated index fingers with varying vibration frequencies, prompting users to focus on one finger at a time. The resulting brainwave patterns classified the user's attention to the left or right finger. This study laid the foundations for further SSSEP applications, for example, to control a wheelchair [168], where users had to focus on the vibration on the left or right hands, as well as the right foot, to turn left, right, or move forward, respectively.

In SSSEPs, the EEG frequency of interest is typically the vibration intensity. Nevertheless, the authors in [169] demonstrated, that vibrotactile stimulation applied on the wrist can elicit responses on the somatosensory cortex and within the SMR frequency bands. Thus, the vibrotactile stimulation results in a similar activity as the motor execution or imagery, which is important to consider when the stimulation is given at the same time as the execution of such tasks.

It is important to note that while SSSEPs rely on user attention to stimulation, this may not be ideal for neurorehabilitation, where patients are required to actively modulate their brain activity to encourage neuroplasticity. In post-stroke rehabilitation, the goal is to promote sensorimotor cortex activation through mental tasks and provide feedback for learning. Consequently, vibrotactile stimulation is of greater interest as a feedback signal for motor imagery, rather than a stimulation feedback, as discussed in the following section.

2.6.2 Motor Imagery

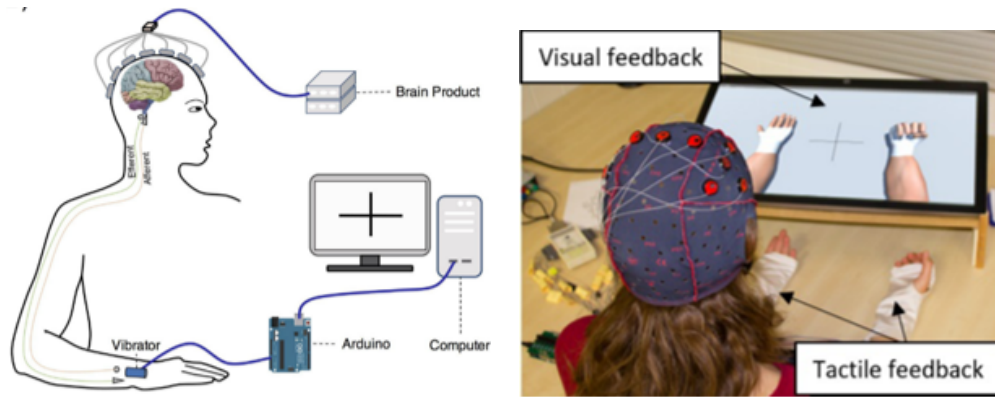
Vibrotactile stimulation has been incorporated into MI-BCIs, primarily in two ways: as a tool for guiding or enhancing MI independently of MI performance, and as a feedback mechanism that adjusts based on the user's brain activity. We aim to develop a vibrotactile stimulation used to provide feedback to the user about their execution of KMI, thus, in this section, the focus is mainly on studies that have used vibrotactile stimulation as feedback rather than a stimulation that reinforces the classification of KMI. Indeed, various studies [170, 171, 172, 173, 174, 175], have taken advantage of the evoked potentials of the vibrotactile stimulation to enhance the classification of MI.

Tactile vibration has been explored as a feedback modality in MI-BCIs. In our objective of improving upper limb motor rehabilitation, we present some examples of BCIs using tactile vibration as feedback for motor imagery of the upper limb. The effectiveness of vibrotactile feedback in post-stroke rehabilitation relies on careful consideration of the spatial location, the activation and deactivation pattern, and the intensity of the vibration. However, it is important to note that some design choices in previous studies lack adequate justification.

2.6.2.1 Spatial Location

In MI-based BCIs, various locations of the vibrotactile stimulation have been proposed and can be broadly categorized into two types: congruent and non-congruent locations. Congruent locations, involve applying vibrotactile stimulation to the same limb the user is imagining moving, while non-congruent locations use areas unrelated to the imagined limb.

For instance, the study by Shu et al. [149] applied feedback to the wrist (see figure 2.9(a)), which was congruent with the MA task involving the paretic hand, but it did not rely on the user’s brain activity. In contrast, the study in [42] applied the stimulation to the left/right palm in response to MI of the corresponding hands, as shown in figure 2.9(c). They demonstrated that continuous vibrotactile feedback can improve BCI performances in a multitasking effect. Similarly, the authors in [156] used the same device to deliver vibrotactile feedback on the wrist in response to KMI of left/right-hand movement. Furthermore, the stimulation was coupled with realistic visual feedback consisting of virtual arms to enhance embodiment, depicted in figure 2.9(b). The study demonstrated that the bimodal feedback was more efficient than the visual feedback alone and that there was an effect due to the presentation order of the feedback modalities.



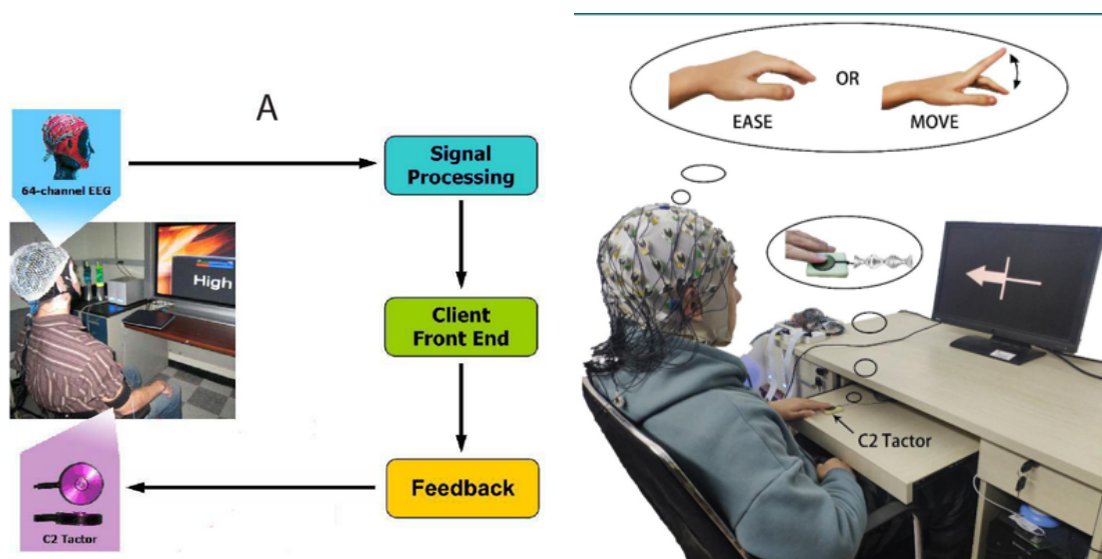
(a) Vibrotactile motor placed on the wrist, extracted from [149] (b) Vibrotactile motors on the hand coupled with visual feedback, extracted from [156]



(c) Vibrotactile motors placed on the hand, extracted from [42]

Figure 2.9: Congruent locations of vibrotactile feedback on the wrist and hand.

Another approach, explored in [176], evaluated the use of vibrotactile stimulus on the left or right biceps after left or right-hand MI. They observed the BCI would better discriminate the left/right MIs when the vibration was given on the same limb that was being imagined, advocating for a congruent location. The feedback has also been given in a smaller area, as suggested in [40], where it was applied on the index fingertip in response to MI of the finger. The stimulus was given continuously or in a closed-loop manner, synchronized with the rise or fall of the alpha



(a) Vibrotactile motor on the biceps, extracted from [176] (b) Vibrotactile stimulus given to the fingertip, extracted from [40]

Figure 2.10: Congruent location of vibrotactile feedback on the biceps and fingertip.

wave related to the MI. The authors demonstrated that the closed-loop stimulation provided at the fall phase of the alpha wave resulted in an enhanced MI reflected in higher classification performance.

The feedback can also be applied to the upper and lower limbs as in [177], where six participants performed MI of both hands, right hand, left hand, or feet. The vibrotactile feedback was given at the same location of the imagined limb, and it was coupled with a visual modality consisting of a cursor moving up, right, left, or down. The results demonstrated that the vibrotactile stimulation improved the classification accuracy of MI.

On the other hand, less congruent locations have been used to give feedback to upper-limb MI, such as the lower neck. In one study [38], six participants imagined left and hand movements. The vibrotactile feedback was delivered either to the left or the right side of the neck (see figure 2.11(a)) and it was compared to a visual feedback consisting of an arrow. Although there were no differences between the feedback modalities, the participants reported the vibrotactile feedback felt more natural than the visual. They also suggested that short-term learning is viable through vibrotactile feedback. However, this modality was reported as more disturbing in the case of misclassification.

A second study applying vibration on the lower neck was performed by Leeb et al. in [7] and shown in figure 2.11(b). In this case, six participants performed left and right-hand MI, and the vibration was given either on the left or the right side of the lower neck depending on the BCI performance. The authors also coupled the vibrotactile feedback with visual feedback in the form of a horizontal bar that would move to the left or right. All participants were able to control the BCI with excellent BCI online performances.

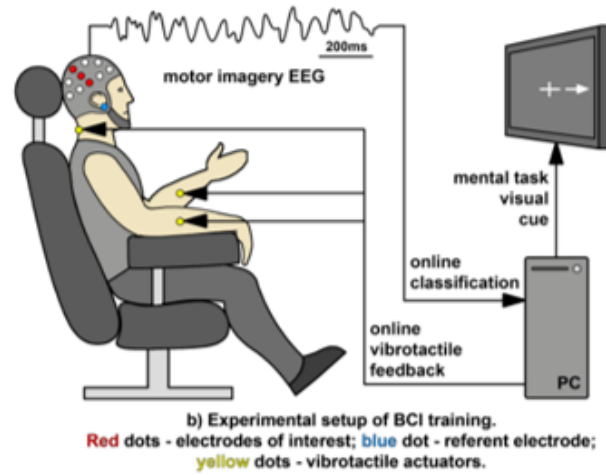
The study in [178] provided feedback on the forearm in response to left/right MI, and vibration on the neck to indicate the participants were in a resting condition, as described in figure 2.11(c).



(a) Vibrotactile feedback on the lower neck extracted from [38].



(b) Vibrotactile feedback on the lower neck extracted from [7].



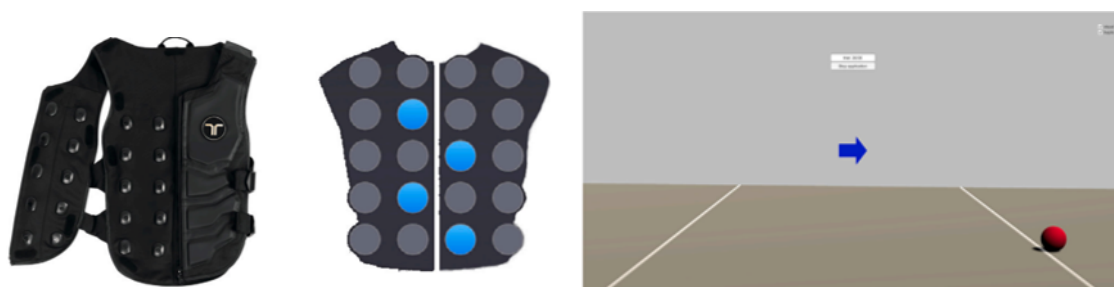
(c) Vibrotactile feedback on the forearm and lower neck extracted from [178].

Figure 2.11: Non-congruent vibrotactile feedback on the lower neck.

Hence, this study employed a combination of congruent and non-congruent locations.

Lastly, the authors in [6] used a commercial vibrotactile vest to deliver the stimulation on the front and back of the torso in response to MI of the left/right hand. The vest is composed of 4 columns of five motors that were activated to the left or right side, starting from the front center, as shown in figure 2.12(a). The vibrotactile feedback was coupled with visual feedback of a ball that was displaced to the left or the right according to the MI performance, as depicted in figure 2.12(b). Although an increase in classification was observed when feedback was provided versus no feedback condition, no difference was observed between the visual, haptic, and multimodal feedback modalities.

Although it is well-established that congruent feedback yields better results [179], sometimes a non-congruent location is well-justified. For instance, patients with limb amputation or severe sensory deficiencies after spinal cord injury cannot benefit from the stimulation on the imagined limb. In these cases, another location is necessary for them to interact with the stimulation.



(a) Haptic vest to deliver vibrotactile feedback by [6]. (b) Visual feedback by [6]. The ball moved to the left or right according to MI performance. The blue circles show the employed vibration motors.

Figure 2.12: Visual and Vibrotactile Feedback Extracted From [6]

In the context of post-stroke rehabilitation, considering the potential benefits of vibration on spasticity, applying congruent vibrotactile feedback on the affected limb remains relevant and necessary. Additionally, visual feedback that is also congruent, for instance, a virtual arm that mimics the imagined movement, may be better to support KMI as it improves embodiment [156], rather than a visual animation of a different task, such as moving a ball, an arrow, or a bar indicating left/right.

2.6.2.2 Activation and Deactivation Patterns

In cases involving multiple vibration motors within a stimulation device, the choice of activation and deactivation patterns becomes a crucial consideration. Two primary patterns come to the front, a simultaneous pattern, where all motors activate and deactivate simultaneously, and a sequential pattern, where motors follow a specific order for activation and deactivation. In selecting either pattern, it is imperative that the choice is well-justified and ideally aligns with the mental task at hand.

For instance, in one study [38], four vibration motors were placed around the lower neck. A simple approach was employed where one motor was activated at a time, either to the left or the right. No sequential pattern was used in this study.

Conversely, in [42], two patterns were proposed: first, a localized pattern, involving the activation of a single motor out of five, and a simultaneous pattern where all motors were activated at the same time. Participants favored the localized pattern due to the perception of excessive intensity associated with the simultaneous pattern. This underscores the importance of considering the number of motors, as it directly impacts perceived intensity. No sequential pattern was proposed in this study.

In a different context, two different patterns were proposed in the study by Leeb et al. [7], involving six motors located at the base of the neck. These patterns are visually described in figure 2.13 The first was a point-based pattern, creating an illusory tactile sensation at a single point to align with visual feedback (represented as a bar). The second was a movement-based pattern that modulated the speed of the illusory tactile sensation across all motors based on the BCI output, resulting in a sweeping sensation. The study found the point-based feedback to be more intuitive, primarily because the movement-based pattern suffered interruptions, especially at extreme BCI output values, causing the interruption of the study. This could potentially have been mitigated through a preliminary design phase that tested the stimulation pattern.

Notably, this study did not propose a simultaneous pattern involving all six motors.

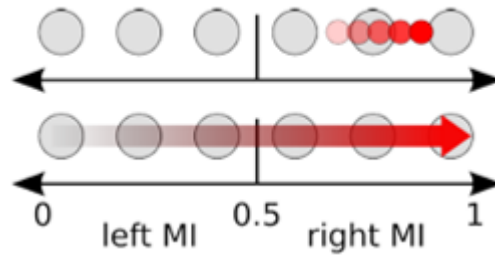


Figure 2.13: Vibration Patterns by Leeb et al. [7]. On top, a point-based pattern is shown. On the bottom, a movement-based pattern is displayed.

In another study [6], a combination of simultaneous and sequential patterns was employed because the device involved a matrix of motors (5×4), allowing for more complex stimulation. In this study, all five motors within one column were activated simultaneously, initiating the stimulation from the center row and expanding to the sides. Interestingly, no other complex sequential pattern was presented in this study.

While many studies lean toward the use of simultaneous patterns, the unexploited potential of employing multiple motors often results in vibration patterns that remain relatively simplistic, predominantly involving movements in one direction or the other. The exploration of sequential vibration patterns in congruent locations, such as the forearm and hand, warrants further investigation.

Furthermore, existing research frequently lacks robust justifications for the chosen vibrotactile patterns and their design. Additionally, sequential patterns are often introduced without comprehensive justifications. Notably, none of the studies have conducted comparisons between sequential and simultaneous patterns, making it challenging to determine which pattern may better facilitate the execution of motor imagery tasks. Lastly, there is an unexplored area concerning the impact of different vibration patterns on EEG signals, paving the way for investigations into various vibration patterns related to upper limb movements.

2.6.2.3 Vibration Intensities

Previous work has predominantly relied on maintaining a constant vibration intensity, offering users only a single feedback level. However, varying the vibration intensity can introduce diverse feedback levels, potentially aiding users to modulate their activity and enhance overall performance. For instance, in one study [156], five levels of intensity were implemented, with the intensity proportionally tied to BCI performance. Consequently, superior classifier results corresponded to stronger vibration intensities. A similar approach was adopted in [7] where the intensity of the vibration related to the probability resulting from the classifier.

In contrast, the study by Chatterjee et al. [176] employed a low vibration intensity to indicate the recognition of left-hand MI and a high intensity for right-hand imagery. However, this vibration intensity was not related to the performance levels.

Furthermore, the impact of different vibration intensities across the alpha, mu, and beta frequency bands remains unclear. While an fMRI study has suggested that vibration can influence

brain activity, particularly in the ERD and ERS domains [180], somatosensory evoked potentials studies have demonstrated that the brain's response to vibrotactile stimuli aligns with the frequencies of the stimulus vibration [166]. However, given that MI-based BCIs focus on frequencies within the alpha, mu, and beta bands [108], exploring the potential impact of varying vibration intensities within these specific frequency ranges is imperative.

Finally, it is necessary to remember that regardless of whether the vibration intensity remains fixed or variable, it must adhere to two fundamental principles: it should be perceptible by the user and comfortable. Strong vibrations should not pose a distraction during MI tasks or cause discomfort. To achieve these dual objectives, an initial calibration process may be employed, although it is essential to recognize that this may consume valuable training time within the BCI paradigm. Therefore, identifying intensity values that can be provided to the majority of users is a crucial need.

2.7 Conclusion

In this chapter, we have presented an overview of current EEG-MI-based BCIs designed for post-stroke upper limb motor rehabilitation. The primary focus has been on the feedback signal provided to users, recognizing its crucial role in both the rehabilitation process and the learning of the associated mental task. While FES is considered the most beneficial modality for feedback, it is important to acknowledge the significant variability among patients. Some individuals can easily interact with the BCI, while others encounter challenges, posing a hurdle to the widespread clinical adoption of these technologies.

Although KMI holds immense potential for activating the sensorimotor cortex essential for motor recovery, it can be challenging for some patients to comprehend and execute due to the absence of haptic feedback. Additionally, reduced mobility may render certain patients unprepared for the use of FES or robotic systems. In such cases, an alternative approach involving haptic feedback through vibrotactile stimulation becomes viable. This feedback modality has been explored within the BCI domain, both in ERP and MI paradigms, demonstrating significant potential, particularly for enhancing MI. Nevertheless, its application in the context of post-stroke rehabilitation remains relatively unexplored, offering exciting research opportunities.

Furthermore, the rationale behind design choices related to vibrotactile stimulation, such as spatial location, activation patterns, and vibration intensities, has not always been clearly ascribed, emphasizing the need for dedicated research efforts in the stimulation design phase before its integration as a feedback signal for optimizing MI-BCIs.

Chapter 3

Design-Based Research Methodology for the Novel Design of Vibrotactile Feedback in KMI-Based BCIs

Contents

3.1	Introduction	37
3.2	Focus Phase	40
3.3	Understand Phase	40
3.4	Define Phase	41
3.5	Conceive and Build Phases	41
3.6	Test Phase	42
3.7	Conclusion	43

3.1 Introduction

This Chapter presents the methodology used to develop a novel vibrotactile feedback to support the execution of kinesthetic motor imagery in a brain-computer interface for post-stroke rehabilitation. The present work seeks to conduct research through design, where the focus is to make the *right thing*: to make artifacts, or solutions, that intend to transform the world from its current state to its preferred state [181]. To accomplish this, we must first study the world, in this case, the current post-stroke rehabilitation therapies with motor imagery BCIs, and then make artifacts that affect change. More specifically, the artifact to be developed is a BCI that integrates visual and vibrotactile feedback to improve KMI execution and enhance user experience, ultimately aiming to improve motor rehabilitation in post-stroke patients.

Rather than producing a commercially viable product, the intention is to make an artifact that produces knowledge. The solution will improve the understanding of developing meaningful feedback within BCIs for a target population and how the carefully crafted BCI may improve the execution of KMI and, eventually, post-stroke rehabilitation. By following a design-based research (DBR) approach, the user's needs are constantly in focus during the entire development of the artifact [181]. This approach is, therefore, a generative research methodology that, at

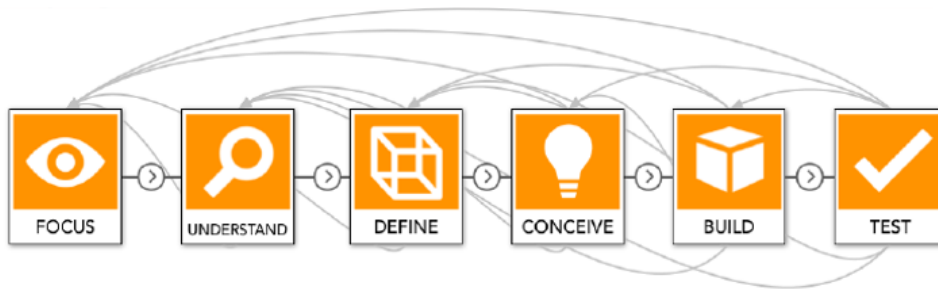


Figure 3.1: Example of a design-based research process comprising six iterative phases, extracted from [8].

each stage of the process, feeds new knowledge and theories, and produces new technological solutions.

Easterday et al. defined DBR “as a process that integrates design and scientific methods to allow researchers to generate useful products and effective theory for solving individual and collective problems of education” [8, p. 319]. Although this model was originally conceived for education, it is smoothly transferable to the BCI application, as demonstrated in the next section. In our particular case, the aim is to identify effective ways of supporting the mastery of a difficult-to-learn mental task. The DBR process, displayed in figure 3.1 consists of six iterative phases:

1. Focusing the topic
2. Understanding the topic
3. Defining the objectives and hypotheses
4. Conceiving the solution
5. Building the solution
6. Testing the solution

It is important to note that the DBR process may involve nested research processes. This means that in designing an artifact, other sub-design processes may be conducted depending on the complexity of the problem and/or the solution, as seen in the next section.

The present work follows the DBR process [8] to develop a solution that may support the execution of KMI in BCIs for post-stroke motor rehabilitation. The process is displayed in figure 3.2. The focus and conceive phase have been omitted in the figure for clarity. In this section, each phase of the DBR process is presented.

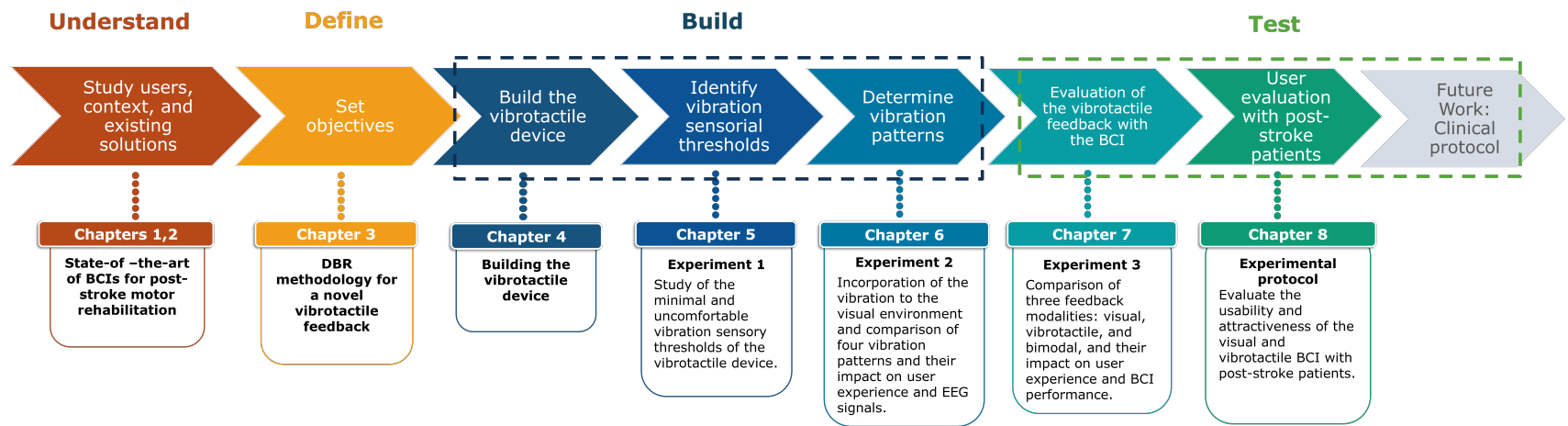


Figure 3.2: Methodology for the design and evaluation of the vibrotactile feedback.

3.2 Focus Phase

The *focus* phase sets the project's direction while establishing the target audience, the topic, and the scope.

Audience: This research is directed toward post-stroke patients dealing with upper limb motor disabilities and the physical therapists involved in their rehabilitation process.

Topic: A pressing issue in MI-BCIs is the challenges users encounter in understanding, learning, and executing KMI. Consequently, some post-stroke patients face difficulties in effectively interacting with BCI systems, hindering their access to these promising technologies for motor rehabilitation.

Moreover, BCI-based motor rehabilitation programs are often lengthy and repetitive, potentially leading to decreased motivation and interest, thereby negatively impacting the rehabilitation process. Consequently, there is a critical need for an MI-BCI that facilitates KMI and offers a satisfying user experience to maintain patient motivation and engagement in motor rehabilitation therapy. In post-stroke rehabilitation, a positive user experience implies that the BCI system does not induce discomfort, excessive fatigue, or negative emotions in the users. Instead, patients eagerly anticipate interacting with and using the device for their rehabilitation.

Scope: The project's scope is centered on developing and validating haptic feedback to integrate into the KMI-based BCI system described in Chapter 4. The development and validation process is thorough to ensure the creation of a robust solution; therefore, a clinical evaluation is not within the scope of this thesis. However, it is essential to note that the clinical evaluation will be a part of the Grasp-It ANR project.

During this early development phase, the primary testing will be conducted with a healthy and neurotypical population, as it presents fewer risks. Early testing with neurotypical users enables the rapid identification of potential solutions and eliminates suboptimal designs, ultimately leading to a more robust and reliable prototype for eventual testing with post-stroke patients.

Furthermore, while the current solution can potentially be extended to other populations, such as individuals with traumatic brain injury or multiple sclerosis, as well as other applications like virtual reality, this project exclusively targets the post-stroke population. Focusing on this user group allows for a clear understanding and identification of their specific needs and preferences, leading to the development of a solution tailored to their requirements.

3.3 Understand Phase

In the *understand* phase, the comprehensive solution of the problem is undertaken, encompassing an investigation into users, the domain, context, and current solutions. This phase corresponds to the content covered in the preceding Chapters 1 and 2.

As discussed in the previous Chapter 2, vibrotactile stimulation has been used in BCIs, primarily in ERP and SSSEP paradigms. However, the application of vibrotactile stimulation in MI paradigms has received relatively limited attention. This may be attributed to the heightened cognitive demands associated with MI compared to other paradigms. To address this challenge, the present work concentrates on delivering feedback to users based on their brain activity related to KMI. As KMI inherently lacks kinesthetic or proprioceptive feedback, we propose two

feedback modalities- visual and vibrotactile- which may be employed separately or in combination. Leveraging the two sensory modalities aims to close the sensorimotor loop and enhance the execution of KMI.

Moreover, the rationale behind the design choices of the vibrotactile stimulation remains insufficiently clarified. These choices encompass the vibration intensity, the number of vibration motors for administering stimulation, the specific anatomical location where the vibration is applied, as well as the patterns governing the activation and deactivation of the vibration. When these choices are inadequately explained or justified, there exists the possibility that poor performance in KMI execution can be attributed to a deficiency in the feedback design, rendering it ineffective, meaningless, and incongruent with the task.

On the other hand, post-stroke patients may encounter challenges in actively engaging in rehabilitation training. As discussed in Chapter 1, a significant proportion of patients experience psychosocial complications, including depression and difficulties in emotional management, such as frustration [50, 51]. These adverse emotions can hinder adherence to rehabilitation therapy, potentially leading to a loss of interest and discontinuation of the treatment.

3.4 Define Phase

The *define* phase consists of setting the principal objective and hypothesis of the project.

Objective

The principal objective of this thesis is to design and evaluate a novel vibrotactile feedback to support the execution of KMI to interact with a BCI intended for post-stroke motor rehabilitation.

Hypothesis

The main hypothesis of the project is that bimodal feedback, combining visual and vibrotactile modalities, aids users in executing an efficient KMI. Furthermore, it is also hypothesized that the KMI-based bimodal BCI guarantees a good user experience, ensuring users remain engaged and motivated during the whole training session.

As it is seen in the present thesis, each building phase also had its own sub-hypotheses linked to the main objective of the phase. These hypotheses are presented in each chapter accordingly.

To accomplish the objective and test the hypothesis, the solution was first built, and then it was tested to evaluate its efficiency, as described in the upcoming sections.

3.5 Conceive and Build Phases

During the *conceive* phase, an outline of the vibrotactile device was developed, presented in Chapter 4. The subsequent *build* phase encompassed the practical realization of this device, which consists of two essential components: the physical device itself and the vibrotactile stimulation. This phase was executed through a series of three key steps:

- Building the vibrotactile device: this step encompassed the physical realization of the device, further elaborated upon in Chapter 4 of Part 1.
- Building the vibrotactile stimulation:

- The first study, detailed in Chapter 5, was dedicated to establishing the minimal and uncomfortable sensory thresholds specific to the vibrotactile device for three distinct age groups. The aim was to generalize these thresholds for an age-dependent population in future studies.
- The second study, documented in Chapter 6, involved the design and a comparative analysis of four distinct vibration patterns. These patterns varied in the number of motors and activation/deactivation sequence. During this phase, the vibrotactile stimulation was seamlessly integrated with the GraspIt visual environment (for additional information, refer to Chapter 4) and evaluated the synchronization and coherence of the proposed vibration patterns with the visual animation. Additionally, the effects of the vibrotactile and visual stimulation on the EEG signals were explored.

Notably, building the vibrotactile stimulation required a nested DBR process. This involved a comprehension of the problem, the formulation of objectives and hypotheses, the conceptualization of an experimental protocol, and testing of the constructed artifact. By exploring, building, and testing various ideas within small samples, it was possible to identify promising solutions and eliminate ineffective designs rapidly. Consequently, at the conclusion of the *build* phase, the meticulously crafted vibrotactile device and stimulation were ready for testing their effectiveness as feedback for the KMI-based BCI with two different populations.

3.6 Test Phase

During the *test* phase, the effectiveness of the proposed solution was examined. This phase comprises three distinct testing steps, as illustrated in figure 3.2.

1) Initial Validation of the BCI with Bimodal Feedback

The initial testing phase focused on assessing the feasibility, reliability, and usability of the BCI integrating visual and vibrotactile feedback with a cohort of healthy neurotypical participants who did not exhibit motor or sensory impairments. This initial evaluation is detailed in Chapter 7. By first validating the solution within a neurotypical population, potential issues may be identified and addressed before conducting tests with post-stroke patients. Additionally, this phase aimed to substantiate or refute the hypothesis regarding the impact of unimodal and bimodal feedback on the execution of the KMI. This foundational test provides a robust basis for the subsequent user evaluation involving post-stroke patients.

2) User Evaluation with Post-Stroke Patients

The second testing step involved a user evaluation exclusively with post-stroke patients. This evaluation will occur only after the BCI system has been tested and validated with the neurotypical population. The principal objective of this study is to estimate the solution's potential in facilitating effective and efficient KMI execution for post-stroke patients, thereby offering a high-quality user experience before evaluating its therapeutic effects. This step allows for uncovering any issues that may not be apparent during the initial neurotypical user evaluation and identifying potential areas for improvement within the post-stroke population. The experimental protocol developed for this test is presented in Chapter 8. This initial protocol will lay the groundwork for a subsequent study to assess the therapeutic impact of the solution.

3) Efficacy Assessment in Post-Stroke Rehabilitation

Upon validation of the BCI with visual and vibrotactile feedback, the third and final test centered on quantifying its efficacy in post-stroke rehabilitation will be performed. This evaluation will be carried out as a randomized controlled trial and will involve post-stroke patients as well as their physical therapists. The primary focus will be on evaluating the therapeutic effects of the BCI with bimodal feedback in the restoration of upper-limb movement. Furthermore, this long-term study will encompass the assessment of the user experience of both patients and therapists. It is important to note that this evaluation extends beyond the scope of this thesis and is discussed as a topic for future research in the concluding Chapter 9.

3.7 Conclusion

In summary, the main objective of the thesis is to design and evaluate a novel vibrotactile feedback to support the execution of KMI to interact with a BCI intended for post-stroke motor rehabilitation, while ensuring an enriching and satisfactory overall user experience for post-stroke patients. Employing a DBR methodology, a novel carefully designed solution is introduced, with a clear focus on the specific needs and requirements of the patients. Consequently, this solution is anticipated to play a pivotal role in not only improving the rehabilitation journey of the patients but also positively influencing the daily practices of physical therapists.

Notably, the studies conducted in this project have employed a mixed approach, encompassing both quantitative and qualitative assessments. While certain evaluations have involved quantitative measurements, such as BCI performance metrics, ERD/ERS analyses, and questionnaire scores, a qualitative evaluation has also been incorporated, delving into the user's perceptions and emotional responses during their interactions with the BCI. This innovative combination represents a departure from the traditional quantitative-centric and techno-centered evaluation approach seen in most prior studies of BCI systems.

In essence, this thesis tackles the pressing challenge of improving the KMI execution within BCIs by prioritizing the delivery of meaningful feedback. Through a careful design and evaluation of vibrotactile feedback, the objective is to not only boost KMI performance and user experience but, in the foreseeable future, to lead to improvements in post-stroke rehabilitation through the adoption of the proposed solution.

Chapter 4

Building the Vibrotactile Device and Description of the Technical Platform

Contents

4.1 GraspIt V1: a BCI to improve kinesthetic motor imagery . . .	46
4.1.1 Components of the BCI	46
4.1.2 Functioning of the BCI	47
4.2 GraspIt V2: further gamification and integration of haptic feedback	48
4.2.1 Adding movements and everyday life situations	48
4.2.2 OpenViBE communication and incorporation of haptic feedback . .	51
4.3 Conception and Building of a Novel Vibrotactile Device	52
4.3.1 Components of the vibrotactile device	53
4.3.2 Anatomical location of the motors	54
4.3.3 Summary of the challenges addressed by the vibrotactile device . .	56
4.3.4 FeelIt: a KMI-based BCI integrating visual and vibrotactile feedback	57
4.4 Conclusion	57

Related publication

- **Herrera Altamira, G.**, Bougrain, L., Lécuyer, A., & Fleck, S. (2022). "Grasp-IT Xmod: A Multisensory Brain-Computer Interface for Post-Stroke Motor Rehabilitation." *33ème Conférence Francophone Pour l'Interaction Humain-Machine IHM'22*. April 2022. Namur, Belgium

This chapter presents the evolution of the technical platform used and developed for this thesis, as depicted in figure 4.1. The first section corresponds to the presentation of the initial version of the KMI-based BCI GraspIt, which was the foundation for the rest of the platforms. Section 2 introduces GraspIt V2, consisting of a more gamified interface that offers multiple movements and the possibility to integrate haptic feedback. In this new version, visual and technical modifications were implemented, ensuring the correct functioning of the BCI.

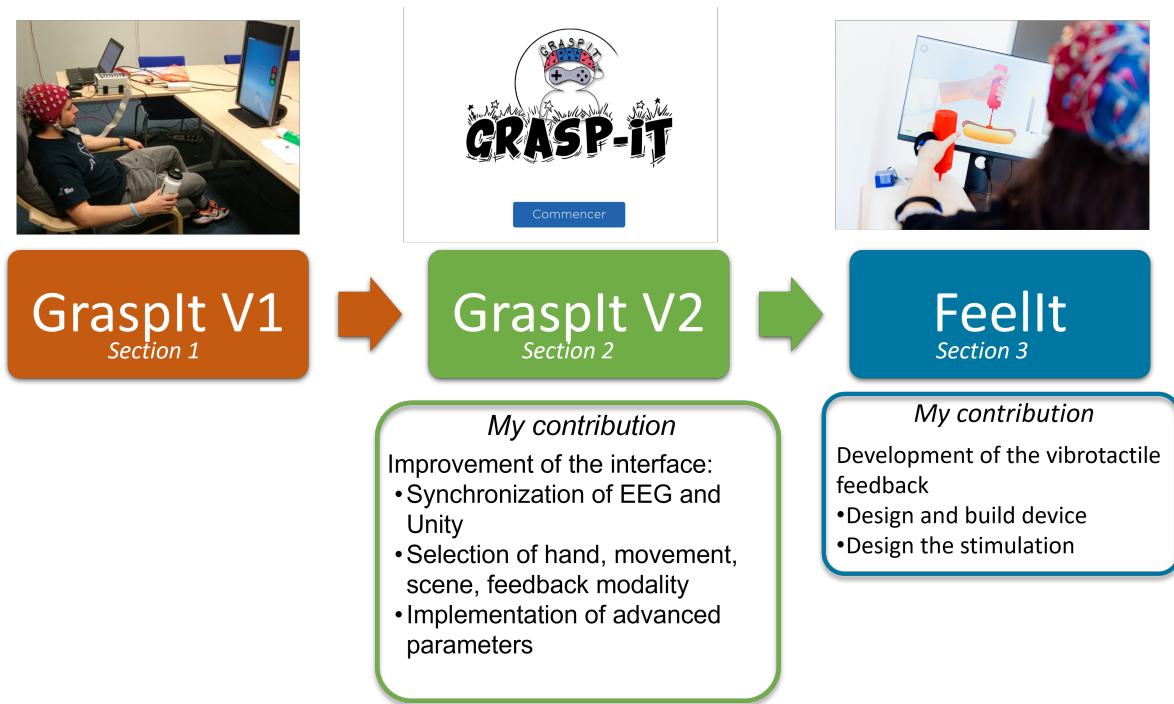


Figure 4.1: Evolution of the technical platforms and contributions to Grasplt V2 and FeelIt

The third section corresponds to the conception and building phases of the vibrotactile device. It presents the innovative design and implementation of the device tailored to provide responsive vibrotactile stimulation, as introduced in the methodology in Chapter 3. The device is easily paired with the BCI Grasplt, in which case, it is called FeelIt, a novel BCI that integrates visual and vibrotactile feedback to support KMI for the motor rehabilitation of post-stroke patients.

4.1 Grasplt V1: a BCI to improve kinesthetic motor imagery

Grasplt is a kinesthetic motor imagery-based brain-computer interface that aims to improve motor rehabilitation following a stroke and to facilitate the execution of KMI tasks [41, 182], developed by the *Neurorhythms* team from the LORIA laboratory in collaboration with the PErSEUs laboratory. The initial version of Grasplt addresses the issue of the lack of sensory feedback during KMI by providing gamified visual feedback. This approach enables users to learn KMI of the upper limb and evaluate their performance during the training.

4.1.1 Components of the BCI

Grasplt comprises three main elements: a screen for presenting a non-immersive virtual environment to the participant, an electroencephalography (EEG) acquisition system, and a computer that delivers triggers and analyzes brain activity. The virtual environment, developed using *Unreal Engine*, features a traffic light that provides user task instructions (further details in section 4.1.2). Additionally, it includes a human-like hand that indicates the movement to be imagined: grasping a bottle of water. This familiar movement, commonly encountered in daily life activities, serves as the target for KMI. Once the system detects successful KMI, feedback is provided based on the user's performance. The feedback involves the hand pressing the bottle

and a jet of water emanating from it. Multiple levels are offered, enabling users to evaluate their progress and adjust their brain activity accordingly. The environment is displayed in figure 4.2.

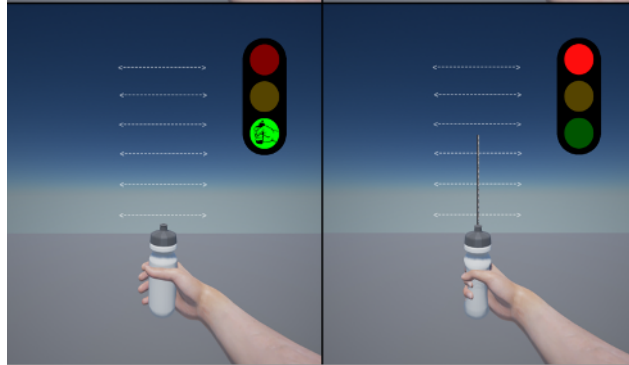


Figure 4.2: Virtual environment of GraspIt V1. A hand presses a bottle of water and a jet is displayed. A traffic light gives instructions to the user.

The EEG acquisition system is the Biosemi ActiveTwo, which consists of an acquisition module, an amplifier module, and a non-invasive 64-active-electrode cap following the 10-10 international system configuration. Lastly, the computer that controls the training session and analyzes the brain activity operates using the OpenViBE software [183].

4.1.2 Functioning of the BCI

After placing the electrode cap on the participant’s scalp, a short training phase is conducted for them to learn to perform KMI [184]. Subsequently, the calibration phase begins, during which the system learns to discriminate the participant’s brain activity associated with KMI and rest tasks. In this phase, the OpenViBE software records and labels the brain’s electrical activity during KMI and rest periods. The classification algorithm is then trained using the same software. A Common Spatial Filter (CSP) is applied to extract the most significant features, which are subsequently used to train a Linear Discriminant Analysis (LDA) algorithm for recognizing KMI and/or rest brain activity. Once the classifier is trained, the user can interact with the system and receive performance feedback.

The traffic light serves as an indicator to the user of the task to perform. A red light indicates rest, during which the user must remain still and refrain from speaking and moving. An orange light signifies preparation for KMI, while a green light indicates the user should perform the grasping KMI task.

The timing of the training is controlled through stimulation codes or triggers sent by OpenViBE using an LUA script. A Python script that interfaces with a Virtual-Reality Peripheral Network (VRPN) server facilitates communication to the Unreal Engine virtual interface. This arrangement enables the system to provide the necessary information to the user, such as changing the traffic light colors and animating the hand to press the bottle.

4.2 GraspIt V2: further gamification and integration of haptic feedback

The initial version of GraspIt served as the foundation for conducting studies with healthy individuals and post-stroke participants, allowing the evaluation and validation of the system’s functionality. Through these initial tests, areas for improvement were identified concerning the feedback and the duration of the training steps [182]. Therefore, this thesis first focused on addressing these challenges by implementing enhancements regarding the further gamification of the visual interface and the integration of three haptic feedback modalities. Based on the results of a large participatory design project involving caregivers and patients, as well as a pedagogical engineering phase carried out by the PErSEUs laboratory, this work required a major effort from a transdisciplinary team and several iterations to ensure the functionality of the system.

4.2.1 Adding movements and everyday life situations

For this second version of GraspIt, a new virtual environment was developed in *Unity*, replacing the previous environment in *Unreal Engine*. The decision was driven by the widespread adoption of Unity in both industry and academia. To facilitate this transition, the company *Octarina* assisted in developing the visual animations.

In this new version, four hand movements are proposed: grasping, release (hand opening), pinch, and wrist rotation. The operator, which is the experimenter or the physical therapist, may choose the movements shown in figure 4.3 according to the objective of the rehabilitation training. For each movement, three distinct scenes of everyday life situations are presented, called *games*. An example of the games corresponding to the grasping movement is displayed in figure 4.4. These scenes and animations aim to improve motivation and execution by projecting the subject into a useful task that is easy to understand and perform. It is important to note that selecting these movements and scenes was a separate endeavor, partially presented in [185].

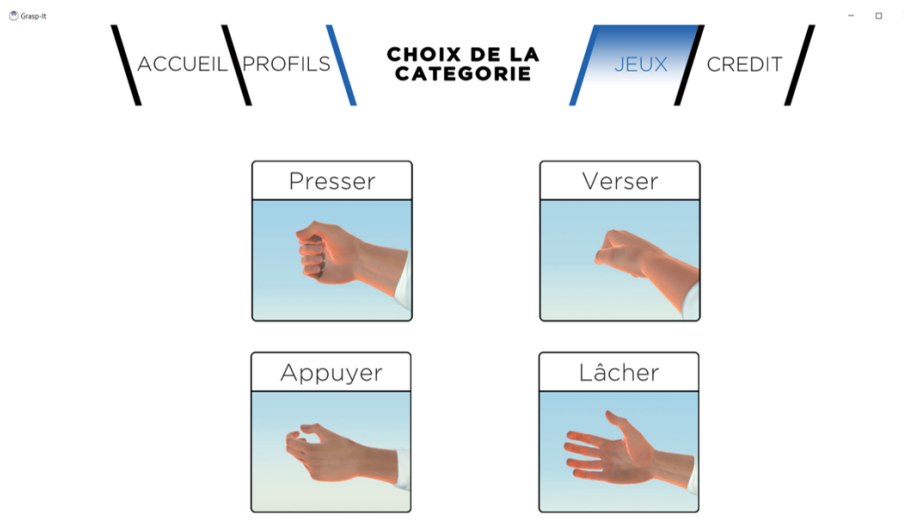


Figure 4.3: Four hand movements. From left to right, on the top row, grasping, and wrist rotation. On the bottom row, pinch and release.



Figure 4.4: Three grasping games, from left to right: Cupcake maker, hot dog, pressing a fruit.

4.2.1.1 Improvement and customization of the visual feedback

In addition to the hand animation, a performance gauge was introduced to enhance the precision of semi-gamified feedback. Each time the feedback score reached 100%, a visual animation resembling a ringing bell would be displayed, with no accompanying audio cue. Adjacent to the gauge, we included a display showcasing the participant's best score, serving as both a benchmark for their progress and a motivational tool to strive for higher scores. Additionally, a progress bar positioned at the bottom of the screen offered a clear indication of the ongoing trial and the total number of trials. The resulting visual feedback is shown in figure 4.5.

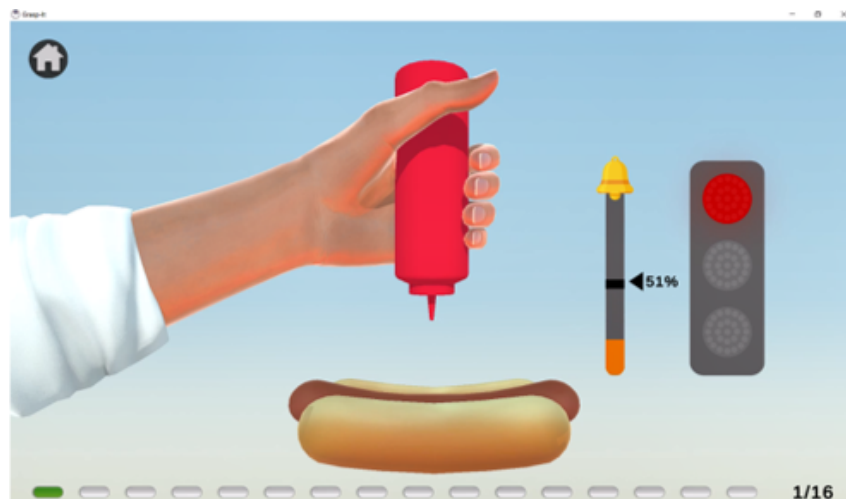


Figure 4.5: Grasping of a ketchup bottle. The visual feedback includes an animated hand and a gauge. A progress bar indicates the current trial.

It is important to note that the addition of the gauge and the progression bar is a result of the valuable input provided by post-stroke participants during the participatory design sessions, where they expressed a preference for the absence of auditory cues.

Furthermore, the option was implemented to allow the operator to select either the right or left arm, depending on the affected limb, choose the user's preferred skin color, and adjust the virtual arm's size, as shown in figure 4.6. This customization feature empowers users to select a virtual arm that closely resembles their own, fostering a more immersive and embodied experience.

The screenshot shows a web interface for creating a new user profile. At the top, there is a navigation bar with the following items: 'ACCUEIL', 'PROFILS', 'NOUVEAU PROFIL' (highlighted), 'JEUX', and 'CREDIT'. Below the navigation bar, the form contains the following elements:

- Nom :** A text input field containing 'ID-User|' and a small circular profile icon to its right.
- Taille du bras :** Two radio button options: 'Fort' (checked) and 'Fin'.
- Couleur de peau :** Three color swatches: a light skin tone (checked), a medium skin tone, and a dark skin tone.
- Main à rééduquer :** Two radio button options: 'Gauche' (checked) and 'Droit'.
- Sauvegarder**: A blue button with white text.

Figure 4.6: GraspIt User Parameters: User ID, arm size, skin color, left/right hand.

4.2.1.2 User training parameters

Two additional windows have been incorporated to enable the adjustment of user training parameters. These parameters must be tuned by the experimenter or the physical therapist, as they are responsible for determining the training to be followed by the user. Figure 4.7 illustrates the configurable parameters during the calibration phase of the BCI. During this phase, one can specify the number of trials and opt to display the virtual hand. The provision of a virtual hand may aid the user in identifying the movement to imagine. It is worth noting, however, that no feedback is provided during this phase, and the hand remains static.

Subsequently, figure 4.8 showcases the existing adjustable parameters for the feedback phase. In addition to the number of trials, users have the option to select from multiple feedback modalities. Regarding the visual feedback, choices include a fixed or animated hand and the possibility to display the gauge. Likewise, haptic feedback modalities can be chosen from three options: vibrotactile, tangible, or functional electrical stimulation. Users can opt for a single or multiple haptic feedback modes based on their preferred training approach. Importantly, it is viable to select no visual and/or haptic feedback at all, though the traffic light indicator is consistently present on the screen to guide the user.

Finally, the duration of the traffic light color transitions may be modified by accessing the advanced parameters, as shown in Figure 4.9. Within this interface, the operator may modify the duration (in seconds) of the rest, preparation, KMI, feedback, baseline phases, and the duration of random pauses between trials. This latter parameter is intended to prevent participant anticipation. Notably, setting a duration of zero seconds for a phase effectively eliminates it if needed. It is worth mentioning that since the calibration phase does not provide feedback, any duration specified for the feedback phase is disregarded.

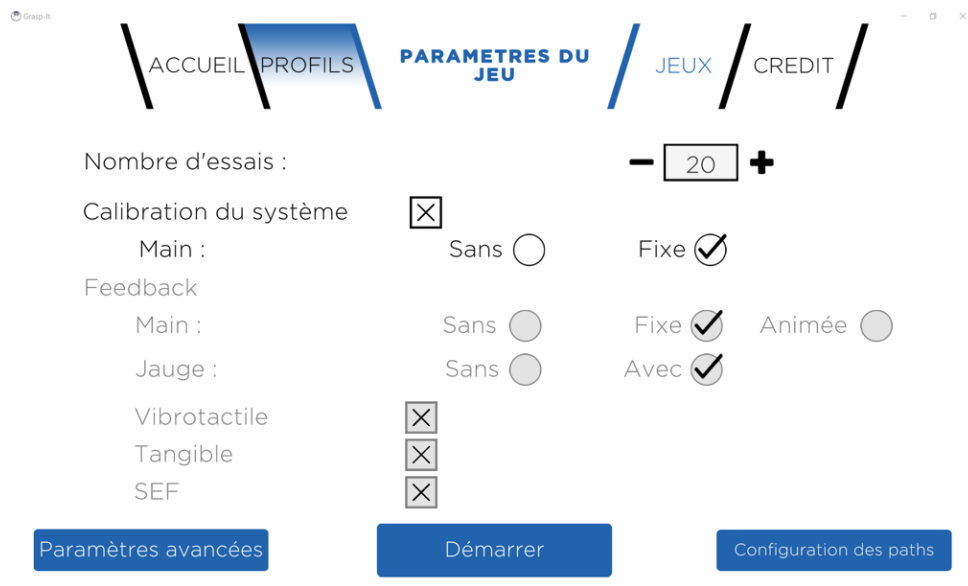


Figure 4.7: Calibration Parameters: number of trials, possibility to show a fixed hand or to not show anything.

4.2.2 OpenViBE communication and incorporation of haptic feedback

Numerous significant updates were imperative to enhance the efficacy of the OpenViBE scenarios in managing the user interface and achieving synchronization with EEG data and haptic feedback devices within the virtual environment. The initial focus of these updates was to guarantee the accurate transmission of stimulation codes to the VRPN server, which serves as the communication bridge between OpenViBE and Unity. This accurate transmission ensured that the virtual environment aligned precisely with the parameters indicated by the operator. These modifications concerned the integration of new stimulation codes into the LUA and Python scripts. These codes corresponded to the training hand, movement, game scene, calibration or feedback phases, and feedback modalities.

Moreover, the implementation of various haptic feedback solutions required additional modifications. In particular, three distinct feedback modalities were added: vibrotactile, tangible, and functional electrical stimulation. To support the use of vibrotactile and tangible modalities, a serial communication protocol via the Python script was established. This protocol facilitates seamless communication between the OpenViBE scenario and the respective hardware devices responsible for delivering the desired haptic feedback.

With these enhancements in place, the modified OpenViBE scenarios now offer precise control over the virtual environment while ensuring accurate synchronization with the EEG recordings and the delivery of feedback. This empowers operators and users with the flexibility to select their preferred haptic modality, whether it be vibrotactile, tangible, or functional electrical stimulation, based on their specific goals, research or rehabilitation objectives, needs, and preferences.

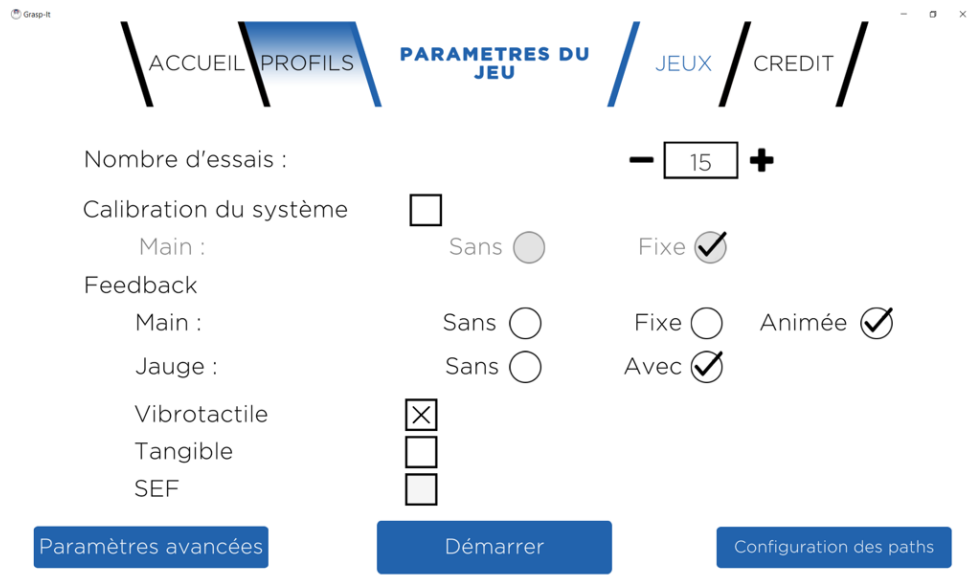


Figure 4.8: Feedback Parameters: number of trials and feedback modalities, visual (hand and/or gauge), vibrotactile, tangible, or functional electrical stimulation.

4.3 Conception and Building of a Novel Vibrotactile Device

The BCI GraspIt offers a gamified training of KMI. However, despite offering visual feedback, it does not address the challenge that KMI does not provide any tactile, kinesthetic, or proprioceptive feedback. Consequently, a novel vibrotactile feedback, that differs from the current haptic solutions (FES and exoskeletons), is proposed. The solution has the potential to be adapted to different user profiles and to answer the challenges posed by KMI-BCIs with haptic feedback.

The challenges addressed by the proposed haptic solution are the following:

1. Close the sensorimotor loop by offering tactile stimulation in addition to the visual feedback.
2. The stimulation must provide meaningful feedback.
3. The stimulation must have a rapid response to the user's mental state.
4. The device and stimulation must offer a pleasant user experience or not degrade the current state of the user.
5. The device must be adaptable to different morphologies. Ideally, a unique size that can be used for the right and left limbs.
6. The device must be wearable and portable, allowing the user to move freely if necessary (for example, for breaks during training).
7. Ideally, the device should be low-cost, so it can be easily and largely implemented in clinical practice and does not impact the already significant cost of BCI systems.

Before testing the efficiency of vibrotactile stimulation to support KMI, the device that will deliver the stimulation must be developed. In fact, commercial vibrotactile devices are available, but as they are meant for general use, they do not take into consideration the specific needs and

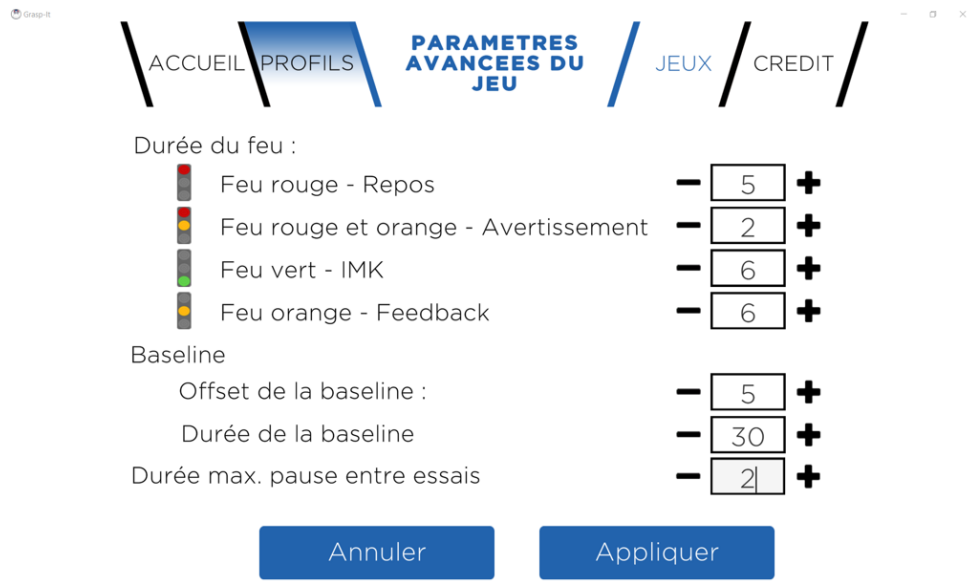


Figure 4.9: Advanced Parameters: rest, warning, KMI, feedback duration, baseline offset and duration, random pause between trials. Duration is expressed in seconds.

limitations of post-stroke patients. For instance, the MANUS Prime Haptic XR gloves⁴ offer vibrotactile feedback on the fingers and the hand, and are compatible with game engines, such as Unity. Nevertheless, multiple sizes are necessary to fit correctly all patients, and patients with severe spasticity may encounter difficulties putting on the gloves. Thus, a different solution that can be easily worn by different individuals is proposed in this section.

The conception and building of the device involved only the grasping movement. The idea was to focus on just one movement in order to develop a tailored solution, rather than a general one. Nevertheless, this device can be easily adjusted to any of the other movements proposed by GraspIt V2. By varying the stimulation, a different movement may be addressed, for example, activating only the hand for a pinching movement. Furthermore, we decided to focus on the Hot Dog game, where the hand presses a ketchup bottle to put sauce on a hot dog. In this way, all the validation tests concern the same visual environment and are directly comparable among them.

4.3.1 Components of the vibrotactile device

To deliver meaningful feedback to the user, we developed a novel vibrotactile device, that can be easily coupled with the visual BCI GraspIt.V2. The device comprises three 10-millimeter coin-type eccentric rotating mass (ERM) vibration motors (model B1034.FL45-00-015, Zhejiang Yuesui Electron Stock CO., LTD.). These motors operate at a rated speed of 13,000 +/- 3,000 revolutions per minute (rpm). Henceforth, all motor-related units will be expressed in rpm for simplicity. Notably, in the case of ERM motors, frequency and amplitude are coupled, thus, modifying one parameter will affect the other. Consequently, in this context, frequency and intensity are considered synonyms. However, frequency and amplitude are independent variables for other types of motors, such as linear resonance motors (LRA), making frequency and intensity distinct measures for LRA motors.

⁴<https://www.manus-meta.com/products/prime-3-haptic-xr>

Each motor is contained in dedicated 3D-printed cases and is secured to the forearm or hand by adjustable bracelets. In this way, the device can be easily adjusted to the left or right arm and different upper limb sizes according to the user's physical characteristics. In addition to being adaptable, the device is also easily portable, and due to its modest components, it is low-cost, being an ideal solution for the medical environment.

4.3.1.1 Controlling the vibration motors

The vibration intensity is controlled by an Arduino Uno, contained in a 3D-printed case, via pulse width modulation (PWM). PWM is a commonly used control technique to generate analog signals from digital devices, such as Arduino microcontrollers. It can be used to control light brightness and the speed of electric motors, among other applications. Using a digital controller, a square wave is generated and the duration of the ON/OFF time can be modulated as desired. The duration of the ON time is called pulse width and by modulating it, analog values are obtained. When the ON/OFF pattern is repeated fast enough, the result is a steady analog voltage between 0 and the output voltage of the microcontroller (VCC).

The duty cycle is the ratio of the ON time to the period of the signal. It is normally expressed in percentage, from 0% to 100%. Thus, a duty cycle of 100% means the square signal is always ON, a duty cycle of 50% means the signal is ON 50% of the time, and so on. To indicate this percentage using the Arduino Uno, one must indicate a value between 0 and 255, where 0 is 0% of the duty cycle and 255 indicates 100%. Finally, by varying these values, the intensity of each individual motor may be varied.

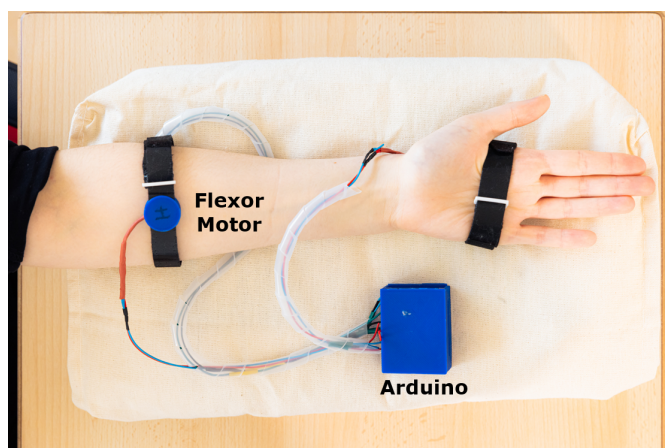
Furthermore, as each vibration motor is controlled independently, it is possible to alternate the activation and deactivation order of each motor. In this way, it is possible to study the impact of different vibration patterns while coupling them with the visual environment and find the one that is the most coherent and synchronized with the virtual animation, enhancing feedback embodiment.

4.3.2 Anatomical location of the motors

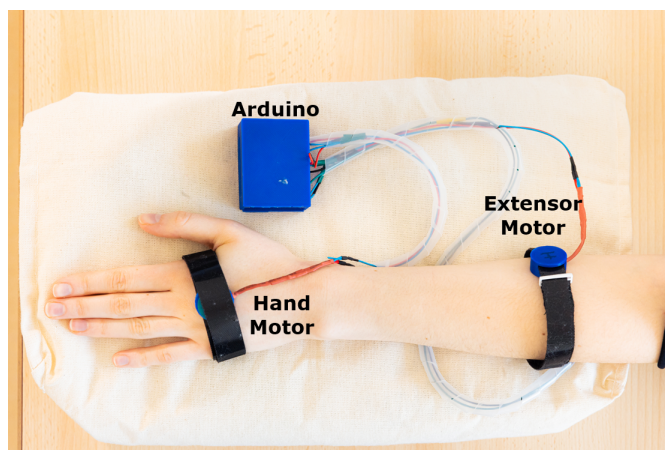
The vibration motors aim to stimulate the skin rather than other structures such as muscles, tendons, or bones. Consequently, the vibration stimulates the Pacinian and Meissner skin mechanoreceptors [186, 187]. As discussed in the previous Chapter 2, the stimulation may be delivered either on a congruent or a non-congruent anatomical location. As proposed in [179], a congruent location may result in better interaction with the system.

The principal objective in the choice of the anatomical location is for the vibration to be consistent with and representative of the imagined motor gesture. Accordingly, the motors are placed over the main muscles involved in grasping. Two motors are placed on the forearm, over the two largest superficial muscles present in grasping [188]: the flexor digitorum superficialis and the extensor digitorum. The flexor digitorum superficialis is present during the closing of the hand and holding an object. The extensor digitorum is activated when additional force is required to press an object held by the hand, for instance, a bottle. These two motors are then placed at least five centimeters from the head of the radius with the elbow at a 90° flexion, or where the muscle belly is located, depending on the anatomy of each individual.

A second bracelet holds the third motor placed on the top of the hand, aligned with the third metacarpal. Indeed, when holding and pressing an object, the hand, including the fingers,



(a) Anterior view



(b) Posterior view

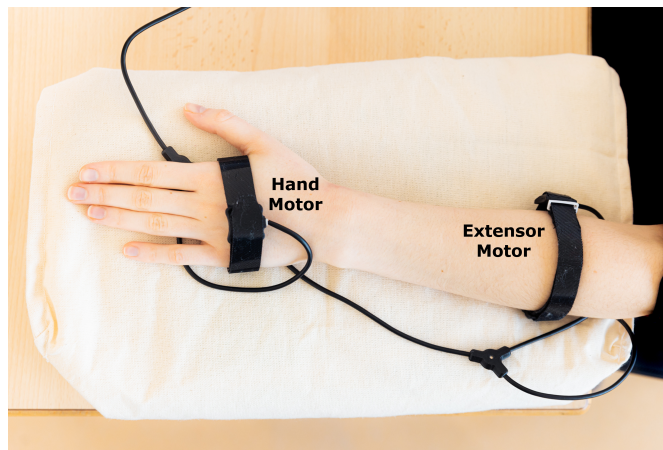
Figure 4.10: First version of the vibrotactile device.

exerts force on the object. It is important to note that stroke patients may present spasticity characterized by a closed hand, so placing motors inside of it may not be possible in these cases, hence the prioritization of motors on the dorsal part. Finally, the motors are simply named according to their placement: “hand”, “flexor”, and “extensor”. This intuitive naming helps experimenters and clinicians to know where to place the motors correctly. Figure 4.10 shows the first prototype resulting from this conception and building phase.

The experimental studies carried out in this thesis were performed with the first prototype. After the device and the stimulation were validated following the studies in chapters 5 and 6, a second prototype was developed with the industrial partner OpenEdge/Alchimies. The new prototype, displayed in figure 4.11, was more robust, preventing direct contact with cables and their breakage. The device could not be used in the studies because it was developed towards the end of the thesis due to a shortage of electronic components. It will be used for the upcoming studies involving post-stroke patients.



(a) Anterior view



(b) Posterior view

Figure 4.11: Second version of the vibrotactile device.

4.3.3 Summary of the challenges addressed by the vibrotactile device

The proposed novel vibrotactile device attempted to address different challenges concerning KMI-based BCIs with haptic feedback. The next table 4.1 provides a summary of the challenges and the manner in which the device addresses them.

Following the construction of the vibrotactile device, we proceeded to build the stimulation. The first step involved defining the minimum and uncomfortable sensory thresholds for the device, presented in Chapter 5. The aim of the study was to define sensorial thresholds that could be generalized for three groups of individuals belonging to similar age ranges. In this way, the stimulation intensity can be adapted to a group of individuals that share similar characteristics, prioritizing valuable time in the subsequent studies for training with the BCI.

After the sensorial thresholds proper to the vibrotactile device were identified, the next step was to design its activation patterns. An original activation and deactivation pattern was proposed, inspired by the forearm muscle activation during grasp and release movements. This innovative sequence was compared to a simultaneous activation pattern. Moreover, the number of motors was also varied and compared. The objective was to assess whether a more nuanced and detailed

Table 4.1: Challenges and solutions of the vibrotactile device

Challenges	Proposed Solutions
Closes the sensorimotor loop	The vibration triggers the skin mechanoreceptors in response to the KMI
Provides meaningful feedback	Vibration motors placed on congruent locations Activation patterns based on the natural muscular activation during grasping
Short latency stimulation (rapid response to mental state)	Vibration motors are easily and efficiently activated, providing immediate stimulation
Adaptable to different morphologies and left/right limbs	Bracelets are easily adjustable to limb side and size
Wearable and portable	Vibration motors are placed in cases and fixed to the limb with bracelets
Low cost	Accessible materials: commercial vibration motors, textile bracelets, Arduino UNO, 3D printed cases

stimulation could be perceived as more coherent and synchronized with the visual environment of GraspIt V2. This step is thoroughly developed in Chapter 6. Upon validating the vibrotactile stimulation, we proceeded to evaluate the new BCI system, FeelIt, which integrates visual and vibrotactile feedback.

4.3.4 FeelIt: a KMI-based BCI integrating visual and vibrotactile feedback

FeelIt is a KMI-based BCI that integrates visual and haptic feedback, intended for post-stroke motor rehabilitation of the upper limb. It combines vibrotactile feedback with the second version of GraspIt. The nomenclature "FeelIt" highlights the additional dimension of artificially *feeling* the activation and deactivation of grasping movements through vibrotactile stimulation. The development process of FeelIt encompassed the conception of the vibrotactile device, the formulation of stimulation techniques, their incorporation with the visual feedback, and ultimately the system's evaluation.

FeelIt has the key singularity of providing synchronized and congruent bimodal feedback for the KMI of grasping. The main hypothesis is that the bimodal feedback would enhance the efficiency of KMI execution by closing the sensorimotor loop more comprehensively than unimodal feedback. Moreover, it is expected that this bimodal feedback would foster user engagement and motivation during training sessions, ultimately offering a positive user experience and preserving emotional well-being.

To test these hypotheses, the FeelIt system was employed to conduct an initial study with healthy neurotypical users, elucidated in Chapter 7. Following the validation of the system, FeelIt will be used in the user evaluation with post-stroke patients, as described in Chapter 8.

4.4 Conclusion

In summary, this chapter has presented the technical platform, based on the initial GraspIt BCI, conceived to support the execution of KMI in post-stroke motor rehabilitation. A series of enhancements were implemented to the first version, transforming it into a more gamified and

immersive interface by incorporating more visual options and vibrotactile feedback.

The building process of the vibrotactile device was also detailed, shedding light on the choices of its component, anatomical placement, as well as the challenges it addresses. The upcoming chapters will delve deeper into the development of the vibrotactile stimulation and the evaluation of the resulting bimodal BCI system.

Part II

Design and Evaluation of Vibrotactile Feedback to Support Kinesthetic Motor Imagery of Grasping

Chapter 5

Identifying the Sensory Thresholds of a Vibrotactile Device for a KMI-Based BCI

Contents

5.1	Introduction	62
5.2	Material and Methods	63
5.2.1	Experimental protocol	63
5.2.2	Questionnaires	65
5.3	Results	65
5.3.1	Minimum Sensory Threshold	65
5.3.2	Uncomfortable Threshold	68
5.3.3	User Experience	69
5.4	Discussion	70
5.4.1	The minimum sensory threshold varies according to age and placement	71
5.4.2	Participants' tolerance toward high vibration intensities	72
5.4.3	A first user evaluation of the vibrotactile device	72
5.5	Conclusion	74

Related publications

- Herrera Altamira, G., Skiba, N., Lécuyer, A., Bougrain, L., & Fleck, S. (2023). "Multisensory neurofeedback design for KMI embodiment." *In SensoryX'23: Workshop on Multisensory Experiences, together with IMX 2023: ACM International Conference on Interactive Media Experiences*. June 12-15, 2023. Nantes, France ACM, New York, NY, USA, 3 pages. <https://doi.org/10.1145/3604321.3604352>
- Herrera Altamira, G., Bougrain, L., Lécuyer, A., & Fleck, S. "Design Process of an Upper-Limb Vibrotactile Stimulation for a KMI-based Brain-Computer Interface." *In preparation*.

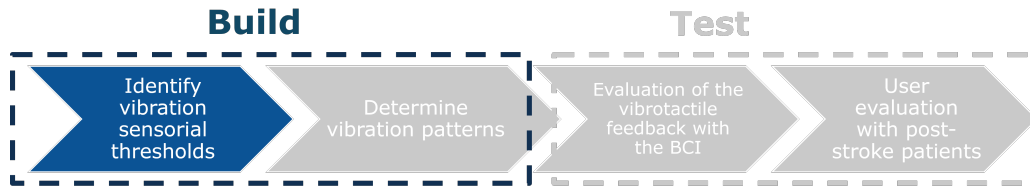


Figure 5.1: Methodology for the design and evaluation of vibrotactile feedback: Build phase - Identification of the vibrotactile sensorial thresholds.

5.1 Introduction

In Part I, we discussed the promising potential of kinesthetic motor imagery (KMI)- based brain-computer interfaces (BCI) for post-stroke motor rehabilitation [31, 30, 29, 28, 27, 26]. However, the lack of kinesthetic feedback presents a challenge to perform KMI [184]. To address this issue, providing feedback, including vibrotactile feedback, has been successful in other BCI paradigms such as P300 and Steady State Somatosensory Evoked Potentials [166, 189].

Nevertheless, the specific characteristics of the vibration for optimal execution of the KMI remain unclear. For instance, in some studies where a vibrotactile stimulation was used to improve motor imagery [40, 39], the applied frequency is not clearly justified. It is important to report whether participants were able to perceive the vibration or if it was too strong and potentially disturbing. Surprisingly, only a small percentage of studies screen the participant’s sensitivity to vibration, none of them involving motor imagery [189]. Vibration perception is known to depend on the Pacinian and Meissner receptors present on the skin, and this sensitivity tends to degrade with aging [190]. This means that older people may present sensory deficiencies, i.e., they may not be able to feel some vibration intensities that younger people can. Thus, in addition to a loss of sensitivity due to cortical damage, as almost 70% of post-stroke patients are older than 49 years [9], it is crucial to consider the possibility that they may have age-related sensory deficiencies and be unable to perceive certain vibration intensities. Consequently, adapting the vibration intensity by accounting for the effects of aging is important when designing devices for post-stroke patients.

Furthermore, the choice of anatomical location for providing feedback using vibrotactile stimulation is unclear. For example, some studies involving motor imagery of left and right hands delivered feedback on the upper back[38], while others apply it directly on the hand[156]. If the study aims to stimulate amputated individuals, then the choice of a different anatomical point is well-justified. However, if this is not the case, feedback on a different anatomical point may be perceived as difficult to interpret, strange, and inconsistent with the mental task and the visual feedback in case it is provided.

Therefore, to ensure the optimal and comfortable use of our novel vibrotactile device as feedback for KMI, we conducted a preliminary study with the main objective of defining two crucial thresholds proper to our device: the minimum sensory and uncomfortable thresholds (figure 5.1). The minimum sensory threshold (MST) refers to the minimal vibration intensity that users can perceive, while the uncomfortable threshold (UT) is the highest vibration intensity at which users still feel comfortable. Beyond this threshold, the vibration may become irritating or uncomfortable. Our primary interest lies in avoiding these intensities, not only to prevent discomfort but also to maintain user attention during KMI. Our focus was to identify these

thresholds at a general level for the population, considering factors such as age and physical characteristics. By doing so, we aim to make the interactions more efficient during the application of the BCI, avoiding the need for individualized tuning of vibration levels for each user and optimizing valuable time spent with them, especially when the user is a post-stroke patient.

We hypothesized that our vibrotactile device's threshold values would vary based on the position of the vibration motors. This expectation arises from the natural distribution of mechanoreceptors on the skin and physiological factors such as age and body composition. Specifically, we anticipated observing differences between the arm and the hand regarding these threshold values. Additionally, we aimed to investigate whether these threshold values are participant-dependent, requiring individual calibration for each new participant, or if they are participant-independent, allowing for generalization without the need for individual calibration. We also aimed to explore potential correlations between perceived vibration intensity and participants' age and/or body composition. By examining these relationships, we sought to gain insights into how these factors may influence the subjective experience of vibration intensity to adapt it to the different profiles of potential users.

Moreover, during this initial stage, we evaluated the usability and attractiveness of our device. This assessment provided valuable insights into the dimensions that require attention before employing the device in future studies.

5.2 Material and Methods

To determine the MST and the UT of three populations differing in age, we used the vibrotactile device presented in Section 4.3.1 and shown in Figure 4.10.

We recruited 40 subjects with no neurological disorders and with hand and arm sensibility, within three age groups:

- **Group 1:** 18–40 years old, 16 participants (7 females, 9 males, mean age= 25.5 years, s.d.= 3.6).
- **Group 2:** 40–60 years old, 12 participants (6 females, 6 males, mean age= 51.17 years, s.d.= 5.54).
- **Group 3:** older than 60 years, initially consisted of 12 participants, but one male participant was removed due to difficulties understanding the instructions and questionnaires, thus the final group consisted of 5 females and 6 males (mean age= 85.18 years, s.d.= 8.46).

To facilitate the recruitment of Group 3, we performed the tests at a nursing home. The youngest and oldest participants were 21 and 96 years old, respectively. All participants signed an informed consent approved by the local ethical committee of Inria (COERLE, approval number: 2022-07).

5.2.1 Experimental protocol

At the beginning of the session, we recorded the participant's age, gender, weight in kilograms, height in centimeters, and the following anthropomorphic measurements: forearm, neck, waist, and hip circumferences in centimeters. This data allowed us to study the relationship between the sensation of the vibration on the arm and the age and body composition of the participants.

Participants were comfortably seated on a chair and the vibrotactile device was placed on their non-dominant arm and hand. As the final device is intended for the impaired upper limb of stroke patients, performing the tests on the non-dominant limb may simulate this situation. We made sure the vibration motors were in contact with the skin by securing them with the bracelets while keeping a comfortable pressure. The upper limb was placed on top of a pillow so that the vibration would not propagate on a hard surface and generate undesired stimuli. On the other hand, participants held a button to indicate when they felt a vibration by pressing it.

The experiment was divided into two phases: first, we identified the MST, based on the protocol described in [191], and then the UT was determined. The protocol had to be shortened for Group 3 because they reported excessive fatigue and lack of attention while performing the experiment, and the first participants were not able to finish it.

5.2.1.1 Minimum Sensory Threshold

To identify the MST, the intensity of each of the three vibration motors was increased or decreased according to a randomly chosen condition. The increment or decrement of the intensity was tested in a discontinuous manner, divided into two conditions:

- Condition 1 - From high intensity to low intensity: the vibration started at 40% (102 PWM, 5,200 rpm approximately,) of its maximum value (255 PWM, 13000 rpm approximately) to avoid discomfort for the participant. The stimulus was applied for four seconds, followed by a pause of a random duration of two to four seconds to avoid anticipation before decreasing the intensity by 2%. For successive stimuli to be perceived as such, they must be separated by 5 milliseconds [192]. The participants indicated when they felt the vibration as soon as possible by pressing the button. The test finished once the participants did not feel the vibration. The last felt intensity was recorded as the “high-to-low” intensity [191]. This condition was repeated three times for groups 1 and 2, and the average intensity was called “Average-high-to-low” for each motor.
- Condition 2 - From low intensity to high intensity: the vibration started at 15% (38 PWM, 1950 rpm approximately) of its maximum value. The stimulus was applied for four seconds, followed by a pause of two to four seconds before increasing the intensity by 2%. The participants indicated as soon as they felt the vibration by pressing the button and the test finished. The reported intensity was called “low-to-high” [191]. This condition was repeated 3 times for groups 1 and 2, and the average intensity was called “Average-low-to-high” for each motor.

Finally, to determine the minimum sensory threshold, we compared the Average-high-to-low and Average-low-to-high intensities and chose the greatest of them to ensure participants are capable of feeling the vibration [191]. To avoid any bias due to the order of the conditions, half of the participants started with Condition 1, while the other half started with Condition 2. The order of the three motors was randomized. Participants from Group 3 performed the test only once instead of three times.

5.2.1.2 Uncomfortable Threshold

Once the minimum sensory threshold was defined for all three motors, we defined an uncomfortable threshold, i.e. a vibration intensity that may be either uncomfortable or annoying. This was necessary so that future participants will not suffer discomfort or unwanted disturbances

while performing kinesthetic motor imagery in our further studies. To find this threshold, all motors were activated simultaneously, starting at the previously defined MST for each of them. Then, a pause of two to four seconds took place, and next the intensity was increased every 4 seconds in steps of 5%. In this case, the participants indicated whenever the vibration was uncomfortable or annoying by pressing the button. If the maximum intensity was reached and the participants did not report discomfort, this was recorded as the uncomfortable threshold. This was repeated three times for groups 1 and 2, while group 3 performed it only once.

5.2.2 Questionnaires

At the beginning of the session, participants answered the following questionnaires:

- Medical Emotional Scale (MES) [193], to measure the emotional state at the beginning of the session.
- Four-Item Fatigue Screen (FIFS) [194] to evaluate the initial fatigue.

Then, at the end of the session, participants answered the following questionnaires:

- the MES, to compare the initial and final emotional state.
- the FIFS, to compare the initial and final fatigue level.
- a short version of the AttrakDiff questionnaire [195] to evaluate the perceived usability and the attractiveness of the vibrotactile device.

The objective of the MES questionnaires was to evaluate if the experimental session had an impact on the emotional state of the participants. It was essential to evaluate that the vibrotactile device did not provoke any negative emotions that might deteriorate the participant's emotional state. Moreover, it was also crucial to assess whether the vibrotactile stimulation could induce any important fatigue. By performing these evaluations during the first step of the design phase, we may identify potential aspects to be modified or to pay careful attention to.

During the first tests with the participants from group 3 we noticed fatigue and refusal to answer the MES at the end of the session. Consequently, the MES questionnaire was presented only at the beginning of the session to at least have an idea of their emotional state. This observation is relevant for future studies with post-stroke patients, as it is a potential indicator that the questionnaire is not adapted for patients with a limited attention span and that we must use a simplified version or another test.

5.3 Results

5.3.1 Minimum Sensory Threshold

The mean and standard deviation of the minimum sensory threshold for each motor and age group are shown in Table 5.1. Figure 5.2 shows the resulting MST group by location of the vibration motor (left) and by participant age (right).

5.3.1.1 Comparison among age groups

We first assessed if the age of participants influenced the MST of each motor individually. Regarding the extensor and flexor motors, the data followed a normal distribution (Shapiro-Wilk $p < 0.001$, $p = 0.03$, respectively), and had equal variances (Levene's $p < 0.001$, $p = 0.006$,

Table 5.1: Mean and standard deviation of the minimum sensory threshold for each motor and age group. Units are revolutions per minute (rpm).

Motor	Group 1			Group 2			Group 3		
	<i>Extensor</i>	<i>Flexor</i>	<i>Hand</i>	<i>Extensor</i>	<i>Flexor</i>	<i>Hand</i>	<i>Extensor</i>	<i>Flexor</i>	<i>Hand</i>
Mean	3,658	3,701	2,593	4,355	4,214	3,044	4,655	4,290	3,027
S.D.	327	305	362	424	232	608	687	587	633

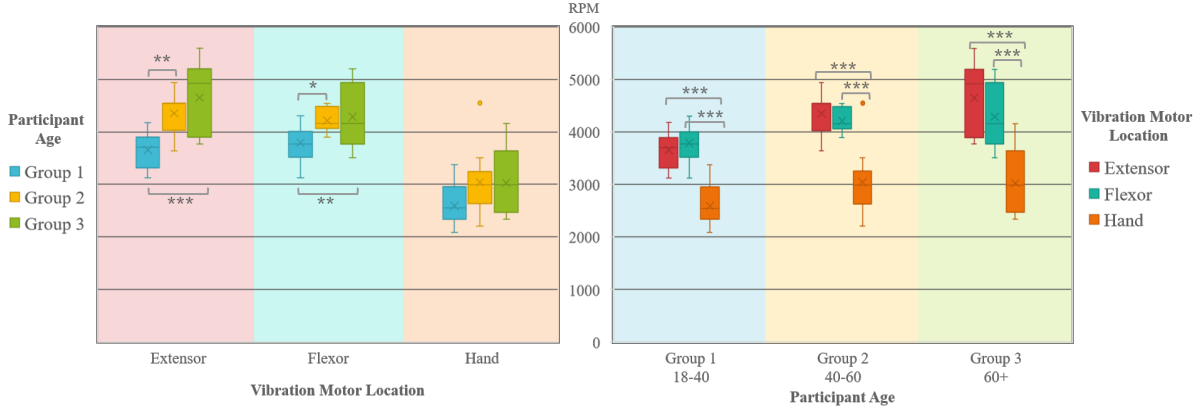


Figure 5.2: Box plots of the minimum sensory thresholds. To the left, the MST is grouped by vibration motor. To the right, MST is grouped by age group. RPM stands for revolutions per minute. (* $p < 0.05$, ** $p < 0.01$, *** $p < 0.001$).

respectively). We observed a statistically significant difference among age groups (one-way ANOVA $\alpha = 0.05$, $p < 0.001$ extensor motor, $p = 0.003$ flexor motor). Then, the Tukey posthoc test ($\alpha = 0.05$) on the extensor motor revealed a significant difference between Group 1 - Group 2 ($p = 0.02$, and Group 1 - Group 3 ($p < 0.001$), while no difference was observed between Group 2 and Group 3 ($p = 0.304$). Similarly, the Tukey posthoc test ($\alpha = 0.05$) on the flexor motor revealed a significant difference between Group 1 and both Groups 2 and 3 ($p = 0.019$, $p = 0.006$, respectively), and no difference was observed between Group 2 and Group 3 ($p = 0.887$). These results are observed in figure 5.2.

Concerning the hand motor, due to violation of normality (Shapiro-Wilk $p = 0.107$) and unequal variances (Levene’s $p = 0.225$), we performed a Welch’s ANOVA ($\alpha = 0.05$) which resulted in a slight difference ($p = 0.04$). However, the Games-Howell posthoc test did not reveal any statistically significant differences between the pair-wise comparisons (Group 1 and 2 $p = 0.086$, Group 1 and 3 $p = 0.134$, Group 2 and 3 $p = 0.998$).

In summary, Groups 2 and 3 presented a higher MST for the motors on the forearm than Group 1, while it was not significantly different between Groups 2 and 3. Additionally, all groups had a similar MST for the motor placed on the hand.

5.3.1.2 Comparison among the locations of the vibration motors

Once we observed the differences among age groups, we investigated whether there were differences among the motor locations, described in table 5.2. First, we grouped the data according to age group, as we saw that there were some differences among them (Figure 5.2). We then

Table 5.2: p-values corresponding to the comparison among the locations of the motors. Significant differences are marked in bold.

	Group 1	Group 2	Group 3
Extensor - Flexor	0.474	0.647	0.343
Extensor - Hand	<0.001	<0.001	<0.001
Flexor - Hand	<0.001	0.001	0.001

performed the Shapiro-Wilk and Levene's tests for each age group. Group 1 followed a normal distribution (Shapiro-Wilk's $p = 0.636$) but did not have equal variances (Levene's $p = 0.736$), Group 2 did not follow a normal distribution (Shapiro-Wilk's $p = 0.043$) but had equal variances (Levene's $p = 0.046$), same as Group 3 (Shapiro-Wilk's $p = 0.025$, Levene's $p = 0.527$).

The comparison among motors for Group 1 resulted in a statistically significant difference in the vibration intensity concerning the MST (Welch's ANOVA $\alpha = 0.05$, $p < 0.001$). The Games-Howell post hoc test ($\alpha = 0.05$) revealed high statistically significant differences between the extensor and the hand vibration motors ($p < 0.001$), as well as the flexor and hand motors ($p < 0.001$), but no difference between the extensor and flexor motors ($p = 0.474$).

For Group 2, the non-parametric Kruskal-Wallis test ($\alpha = 0.05$) revealed statistically significant differences ($p < 0.001$). The post hoc Dwass-Steel-Critchlow-Flinger (DSCF) test ($\alpha = 0.05$) showed differences between the extensor and the hand motors ($p < 0.001$) and between the flexor and hand motors ($p = 0.001$), but not between the extensor and flexor motors ($p = 0.647$).

Similarly, Group 3 presented statistically significant differences (Kruskal-Wallis, $\alpha = 0.05$, $p < 0.001$) between the extensor and the hand motors (DSCF $p < 0.001$) and between the flexor and hand motors (DSCF $p = 0.001$), but not between the extensor and flexor motors (DSCF $p = 0.343$).

5.3.1.3 Studying the correlation between participant characteristics and MST

Table 5.3: MST Pearson's correlation coefficient for each motor and participant's characteristics. BMI stands for body mass index. Significant correlations are marked in bold *** $p < 0.001$, * $p < 0.05$

Motor	Age	Forearm Circumference	Hand Size	BMI	Fat Percentage
Extensor	0.567***	0.089	-	0.059	0.126
Flexor	0.395*	-0.049	-	0.080	0.120
Hand	0.323*	-	0.068	0.035	-0.125

We computed Pearson's correlation coefficient to find the correlation between the MST and age, hand circumference, forearm circumference, body mass index, and body fat percentage, shown in Table 5.3. Concerning the hand circumference, finding the correlation with the hand motor was only coherent. Similarly, for the forearm circumference, finding the correlation between this measure and the extensor and flexor motors was only logical. Weak correlations were found between age and the MST of the flexor and extensor motors, while a moderate correlation was found between the age and the MST of the extensor motor. These results suggest that age has an impact on the minimal vibration intensity, with older participants requiring higher intensities to feel them. For the rest of the factors, no correlation was found.

5.3.2 Uncomfortable Threshold

The values in revolution per minute for the uncomfortable threshold are shown in Table 5.4. Most participants could test the highest vibration intensity (13,000 rpm approx.) without reporting any discomfort, resulting in a ceiling effect (figure 5.3).

Table 5.4: Mean and standard deviation of the uncomfortable threshold for each motor and age group individually. Units are revolutions per minute (rpm).

Motor	Group 1			Group 2			Group 3		
	<i>Extensor</i>	<i>Flexor</i>	<i>Hand</i>	<i>Extensor</i>	<i>Flexor</i>	<i>Hand</i>	<i>Extensor</i>	<i>Flexor</i>	<i>Hand</i>
Mean	12,045	12,061	11,806	12,049	12,054	11,625	10,313	10,828	11,059
S.D	1,839	1,834	2,213	1,683	1,737	2,201	3,746	3,108	2,928

First, we assessed whether there was a difference in the UT due to age. The normality Shapiro-Wilk test showed data did not follow a normal distribution ($\alpha = 0.05$, $p < 0.01$), possibly due to the ceiling effect. Therefore, we performed a Kruskal-Wallis test that revealed no significant difference among the three age groups ($p = 0.358$).

To assess potential differences among the placement of the three motors, we initially conducted a normality test (Shapiro-Wilk, $\alpha = 0.05$) for each age group. The results indicated that the data sets did not adhere to a normal distribution ($p < 0.01$ for all groups), possibly due to the ceiling effect. Consequently, we performed individual Kruskal-Wallis tests for each group. Interestingly, no significant differences were observed among the motor locations for any of the groups (Group 1 $p = 0.967$, Group 2 $p = 0.861$, Group 3 $p = 0.916$). Although there are no statistically significant differences among the three groups, it is clearly seen in figure 5.3 that Group 3, consisting of the oldest people, presents a large inter-participant variability. Some participants did not report any discomfort at the highest intensities, while others were uncomfortable at very low intensities.

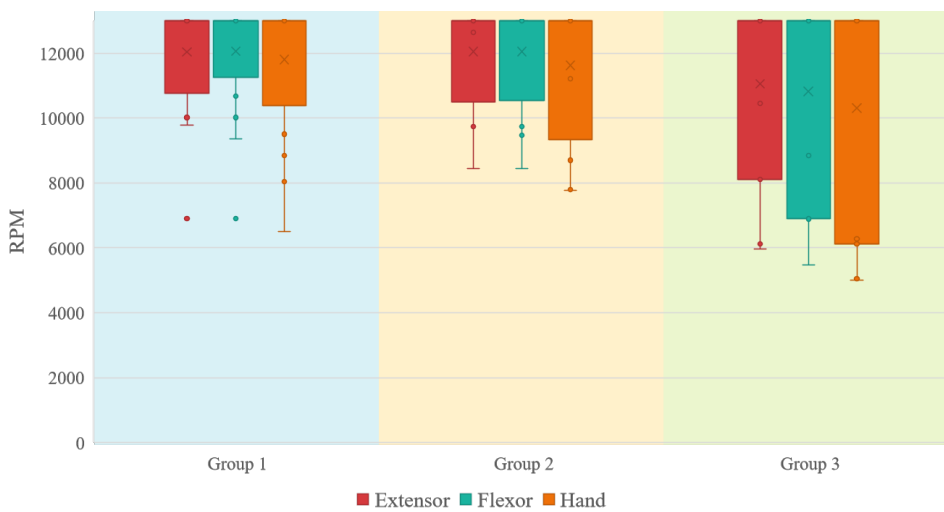


Figure 5.3: Box plots of the uncomfortable thresholds. RPM stands for revolutions per minute.

Table 5.5: UT Pearson’s correlation coefficient for each motor and participant’s characteristics. BMI stands for body mass index.

Motor	Age	Forearm Circumference	Hand Size	BMI	Fat Percentage
Extensor	-0.267	-0.028	-	0.089	0.058
Flexor	-0.209	-0.032	-	0.117	0.113
Hand	-0.128	-	-0.021	0.119	0.082

5.3.2.1 Studying the correlation between participant characteristics and UT

Similarly to the MST, we computed Pearson’s correlation coefficients to find the correlation between the UT and age, hand circumference, forearm circumference, body mass index, and body fat percentage (Table 5.5). Very weak negative correlations were found between age and the MST of all three motors. For the rest of the factors, no correlation was found.

5.3.3 User Experience

5.3.3.1 Evaluating the participant’s fatigue and emotional state

Surprisingly, most participants from Groups 2 and 3 were less tired at the end of the session than at the beginning (figure 5.4(a)). Still, none of these differences are significant (Wilcoxon’s W $p = 0.137$, t-test $p = 0.307$, respectively). Group 1 is slightly more tired than before the session, but the difference is not statistically significant (t-test $p = 0.633$). We hypothesized this could mean participants were more relaxed by the end of the session or presented an increase in activation emotions, either positive or negative. Therefore, we examined the responses from the MES questionnaire (figure 5.4(b)). However, as explained before, the third group answered this questionnaire only at the beginning of the session. Hence, we could only perform the analysis for Groups 1 and 2. The comparison of emotions before and after the session revealed a slightly significant decrease in the negative activation emotions (t-test $p = 0.044$) and a slightly significant increase in neutral emotions (t-test $p = 0.023$) for Group 1. On the other hand, for Group 2 no significant differences were observed for any emotions. Thus, the experimental session did not alter the participants’ emotional state and did not represent a significant change in the fatigue level.

5.3.3.2 Attractiveness of the vibrotactile device

We evaluated the attractiveness of the device via the AttrakDiff questionnaire. We first studied the questionnaire’s four dimensions: pragmatic quality (PQ), hedonic quality- identity (HQ-I), hedonic quality- stimulation (HQ-S), and attractiveness (ATT) (Figure 5.5(b)). Overall, the attractiveness score of the device was slightly negative (-0.17), which can be explained by the simplicity of the artifact but also by the passiveness generated by the task. In fact, in this study, participants were very inactive as the task involved just pressing a button in response to a vibration intensity. This task was very different from the final use of the device as feedback for a BCI. Hence, participants may not yet perceive the real value of the device, resulting in low attractiveness. This will be an important dimension to monitor during the following studies. Another possibility is that the population involved was not yet the target population, that is, the stroke patients. Therefore, they might not yet value and/or understand the solution’s potential. On the other hand, the PQ and the HQ-I resulted in positive mean values (1.76 and 1.30, respectively), and HQ-S in a neutral value (0.74), which means that the device accomplishes its

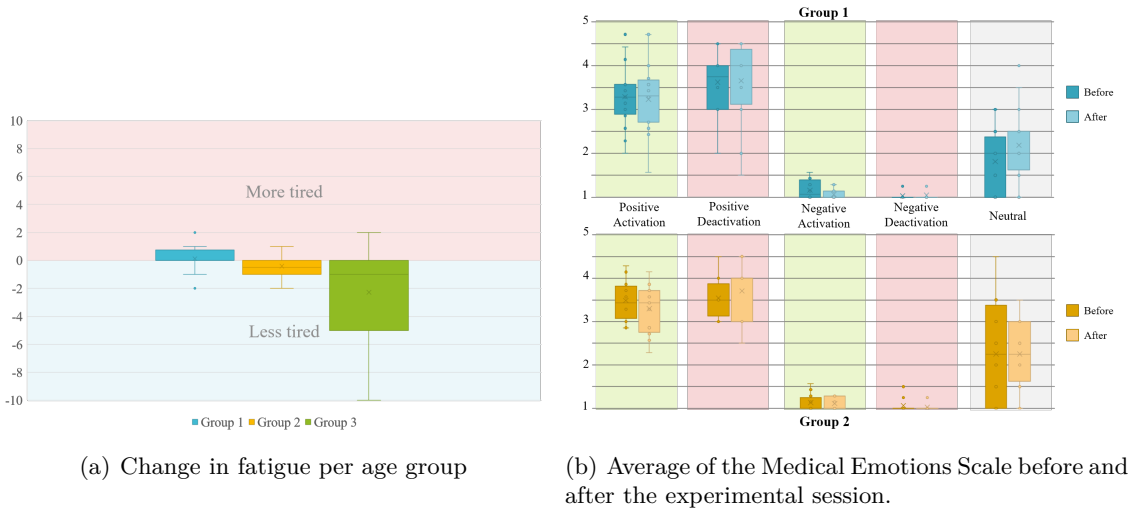


Figure 5.4: Participants' fatigue level and emotions.

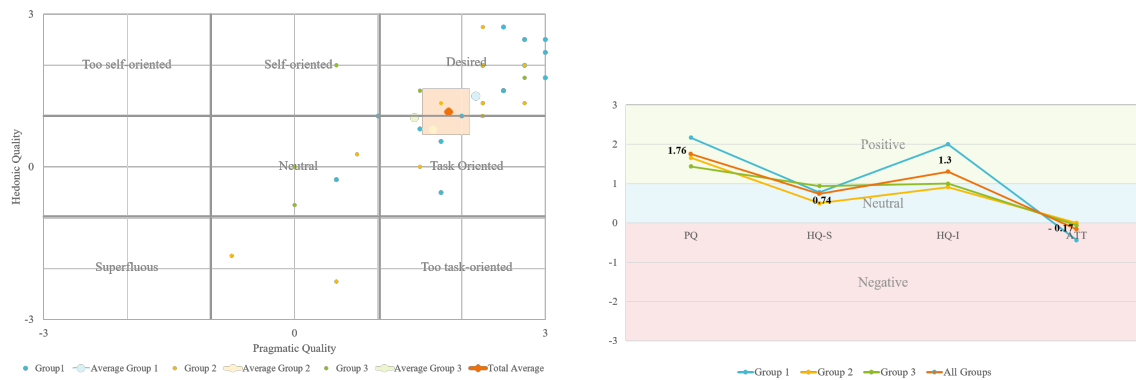
objective of stimulation without a negative impact, yet it can be improved. We expect these values to improve as the device is used for a more complex task, such as neurofeedback.

The AttrakDiff portfolio in Figure 5.5(a) revealed that, on average, participants perceived the vibrotactile device as *"desired"*, drifting to *"task-oriented"*. This was surprising because the test involved a simple task of detecting the vibration intensity. However, Group 2 in light blue, and Group 3 in light yellow perceived the device as *"task-oriented"*. Indeed, the confidence interval rectangle touches both zones, *"desired"* and *"task-oriented"*, indicating a significant variability in the user's evaluation.

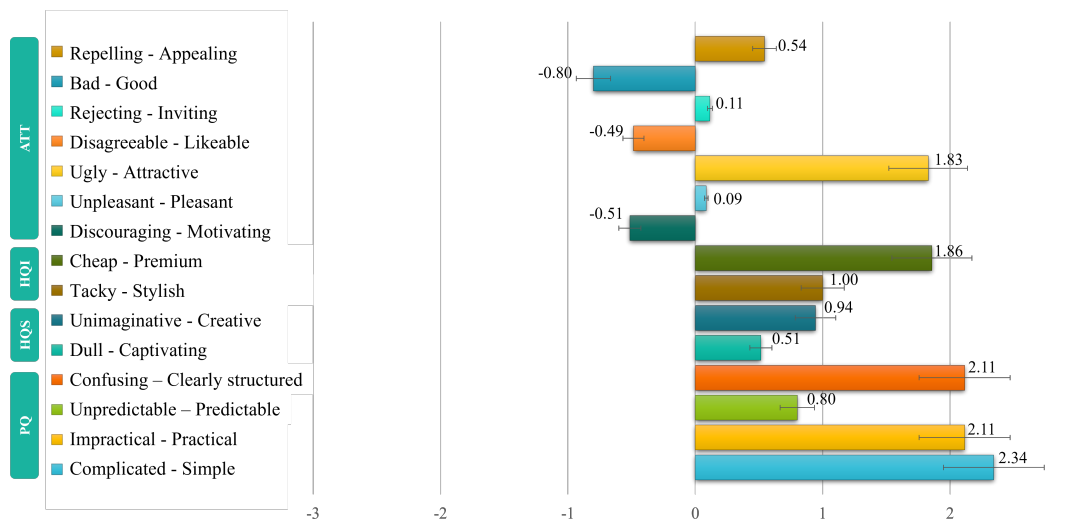
The word pairs diagram in Figure 5.5(c) allows us to explain in further detail the scores of each dimension. Due to the participant's passiveness during the tests, we were expecting low scores on the items regarding the attractiveness dimension. Indeed, three of them have negative values, but they are not critical as they are greater than -1. However, two of these items (*Disagreeable-Likeable* and *Discouraging-Motivating*) were expected as the test aimed to determine the uncomfortable vibration intensities. In particular, six items have critical scores under 1: *Rejecting-Inviting*, *Unpleasant-Pleasant*, *Unimaginative-Creative*, *Dull-Captivating*, *Unpredictable-Predictable*. These specific items must be taken carefully and they call for action to improve these aspects. These results motivated the development of a second version of the prototype, previously presented in chapter 4. Yet, participants still perceived the device as *premium*, *clearly structured*, and *practical*, which are relevant qualities for our further experiments.

5.4 Discussion

We identified the minimum and uncomfortable sensory thresholds of our vibrotactile device for three groups varying in age. The results will allow us to use the minimum and maximum vibration intensities as reference for our further experiments according to the age of the participants, ensuring they feel the stimulation while keeping it comfortable. Regardless of most participants being able to reach the maximum vibration intensity without reporting discomfort, we decided



(a) Attrakdiff Portfolio: Grand average in orange, and (b) Diagram of average values. Orange line: grand 95% confidence interval rectangle. The mean values average. Blue line: Group 1, yellow line: Group 2, of each group are shown in big circles: Group 1 in green line: Group 3. blue, Group 2 in yellow, and Group 3 in green. The individual scores are the small circles.



(c) Word pairs diagram - Grand average.

Figure 5.5: Results of the AttrakDiff questionnaire for the first experiment.

to set it at a lower intensity of approximately 11,471 rpm (225 PWM, 191 Hz) to avoid any unpleasant stimulation in future experiments.

5.4.1 The minimum sensory threshold varies according to age and placement

Our results showed differences among age groups regarding the MST of the two motors placed in the forearm. More specifically, the younger group, which involved people between 18 and 40 years old, could first notice the vibration on the forearm at lower intensities than the other two groups. These results suggest that whenever using the device with older populations, we must increase the minimum vibration for them to feel the stimulation. On the other hand, no statistically significant differences were observed between groups 2 and 3 on the forearm. Although this may suggest that using the same minimum vibration intensity for both groups is possible, we suggest using different intensities because the third group, involving the oldest

participants, presented greater variability than the second one. Hence, sharing the MST for both groups may result in some older participants not feeling the stimulation.

Previous studies on the fingertips demonstrated that age affects the perception of tactile vibration. The authors in [196] concluded that aging results in a decreased perception of vibratory stimuli intensity. This decline in vibration perception with age can be attributed to factors such as changes in mechanoreceptor structure and density, alterations in sensory processing in the nervous systems, and age-related changes in the biomechanical properties of the skin and underlying tissues [190]. Similarly, in [197], older adults exhibited difficulties localizing vibratory stimuli on their arms compared to young adults, which the authors attribute to age-related changes in the somatosensory system.

Surprisingly, no significant difference due to age was observed in the MST of the motor placed on the hand, suggesting all age groups might share the same threshold. This may be due to the number of mechanoreceptors found in the hand, which is larger than that of the forearm, leading to a higher sensitivity of the hand [186]. Nevertheless, as stated before, we recommend using different minimum vibration intensities for each group or at least applying a slightly higher intensity for groups 2 and 3 to ensure the individuals feel the vibration.

5.4.2 Participants' tolerance toward high vibration intensities

We did not observe any differences due to age in the uncomfortable threshold. Additionally, the UT was found to be remarkably consistent across all three motor locations, i.e. there was no difference in the vibration intensity between the forearm and the hand. However, it is worth noting that a ceiling effect was observed, where the majority of participants reached the maximum vibration intensity without experiencing any discomfort. This phenomenon can be attributed to the natural decline and deterioration of skin mechanoreceptors with age, leading to a decrease in sensitivity [190, 196]. Consequently, older participants are expected to exhibit higher tolerance towards vibration intensities, as they may have more difficulty perceiving them accurately.

We did not observe any influence for both sensory thresholds due to the participant's body composition or the size of the hand and arm. This confirms that response to stimuli on the skin depends on the mechanoreceptors rather than other physical characteristics. Thus, vibrotactile stimulation may be used regardless of the subject's physical characteristics. However, the size of our population is rather small. Studies on a larger population may confirm our observations. Moreover, the participants had never suffered a stroke, thus, the reported thresholds are most likely to change for this population.

While the process of identifying thresholds represents an additional step, it holds significant importance in ensuring optimal device functionality and a satisfying user experience. When designing tactile interfaces of this nature, we strongly recommend investing the time to identify the sensory thresholds, either on an individual basis or for groups of individuals sharing similar characteristics, such as age. This approach helps tailor the device's settings to an individual or specific user group, enhancing their overall satisfaction and usability.

5.4.3 A first user evaluation of the vibrotactile device

The reason for conducting a user evaluation was to complement the identification of minimum and uncomfortable sensory thresholds by assessing the usability and attractiveness of the vibro-

tactile device. Performing this evaluation during the early stages of device conception allows us to identify areas that require improvement before and/or during future experiments. However, it is important to acknowledge that the device was not used in its final environment with the BCI, which made it challenging for participants to provide a comprehensive evaluation.

We observed that the experimental session did not have a negative impact on the participants' emotional state, and the fatigue levels remained stable for Group 1. In contrast, Groups 2 and 3 experienced a slight reduction in fatigue. For Group 1, there was a slight decrease in negative activation emotions, indicating that the session benefited them. In the case of Group 3, verbal exchanges revealed their eagerness to participate in the session as it varied from their daily routine, which was particularly important as these participants lived in a medicalized nursing home where such experiences were uncommon. Their keen interest likely explains the decreased fatigue, as they actively engaged in the session.

According to the AttrakDiff scores related to pragmatic quality, the device exhibited high and positive usability for all three groups. Similarly, the hedonic quality-identity score was positive, indicating that participants, especially those in the younger Group 1, were appealed by the device. However, the device scored low in hedonic quality-stimulation, suggesting room for improvement in achieving its objective of providing stimulation, which is its main objective. Furthermore, the global attractiveness score was negative, highlighting the need for device enhancements. Specific attention should be given to the *Repelling-Appealing*, *Bad-Good*, *Rejecting-Inviting*, and *Discouraging-Motivating* items. This may be due to two reasons: first, the study was not well situated with a real problem for the participants as they were just required to press a button in response to a vibrotactile stimulation. This task differs greatly from the final intention of using the vibration as feedback for executing kinesthetic motor imagery. Consequently, participants might have had difficulties finding the real purpose of the device. As mentioned before, the second reason is that the participants were not post-stroke patients, which is the target population. Hence, they might have trouble placing themselves in a situation where the vibration benefits them. In fact, the participants presented overall good health, thus, it may be hard to project themselves as a stroke patient using a BCI with haptic feedback for motor rehabilitation.

One potential approach to improve these aspects could be using an improved prototype, as the current version had visible cables and was susceptible to breakage. Regarding the *Disagreeable-Likeable* and *Unpleasant-Pleasant* items, the scores align with the study's objective of determining uncomfortable vibration intensity, where the participants were exposed to potential disagreeable and unpleasant vibrations. Therefore, we anticipate improved scores when incorporating the virtual environment and brain-computer interface, enabling participants to have control over the vibration themselves.

An important limitation of this study could be that it was performed in a population of participants who have never suffered a stroke and presented normal sensitivity in the hand and the forearm. However, at this design stage, avoiding risking a problem with so-called vulnerable participants is an ethical necessity and requires the involvement of healthy participants. Moreover, this step was essential because neurotypical able-bodied participants may distinguish the different stimulation intensities in a better way, which is crucial for us to validate during the design phase. While post-stroke patients may initially struggle to differentiate these characteristics, their ability to do so may improve as they begin to regain lost functions. Therefore, it is important for us to anticipate this progression. However, it is worth noting that sensory thresholds may vary among post-stroke patients, as some may exhibit sensory deficits such as reduced

or heightened tactile sensitivity. Accordingly, it is essential to evaluate the sensory capabilities of post-stroke patients before implementing the vibrotactile device, as previously suggested by the authors in [198].

5.5 Conclusion

In conclusion, we have presented the methodology employed to determine the minimum and uncomfortable sensory thresholds of our vibrotactile device. By assessing the MST and UT for three distinct age groups, we have discovered that older participants require increased intensity of minimal vibrations to perceive them. Conversely, all groups exhibited tolerance towards the highest frequency without experiencing discomfort. However, due to significant variability in this measure, we recommend using a slightly lower vibration to prevent discomfort or distraction during participants' tasks. We will use this study's results for future studies of synchronizing the vibration with the virtual environment and using the brain-computer interface.

Furthermore, we conducted the first user evaluation of the device, marking its initial use and testing. The results obtained from the questionnaires serve as invaluable indicators for enhancing the device's performance. Most importantly, participants found the device user-friendly and could establish a connection with it. In our forthcoming study involving the brain-computer interface, the device will provide feedback to the participants, and we anticipate an improved user experience within this context. Given the heightened challenge of the task and the device's enhanced relevance, we expect notable improvements in user engagement and satisfaction.

Chapter 6

Design and Evaluation of the Vibrotactile Stimulation as Feedback for a KMI-Based BCI

Contents

6.1	Introduction	76
6.2	Design of the Vibrotactile Stimulation	78
6.2.1	Sequential Vibration Pattern	78
6.2.2	Simultaneous Vibration Pattern	80
6.3	Material and Methods	81
6.3.1	Experimental Setup	81
6.3.2	Questionnaires	83
6.3.3	Statistical Tests of the User Evaluation	84
6.3.4	EEG offline analysis	85
6.4	Results	85
6.4.1	User's subjective evaluation	85
6.4.2	Participants' emotional state, fatigue level, and mental workload	88
6.4.3	System's elicited emotions and attractiveness	89
6.4.4	Time-frequency analysis of EEG activity	91
6.4.5	Topographical analysis of EEG activity	96
6.4.6	Activity in delta and theta	100
6.5	Discussion	101
6.5.1	User preference for the three-motor sequential configuration	101
6.5.2	Positive user experience and system's attractiveness	101
6.5.3	EEG activity in the alpha, mu, and beta frequency bands	102
6.5.4	Activity in delta and theta: a potential indicator of attention and surprise	104
6.6	Limitations and Future Work	105
6.7	Conclusion	105

Related publications

- Herrera Altamira, G., Skiba, N., Lécuyer, A., Bougrain, L., & Fleck, S. (2023). "Multisensory neurofeedback design for KMI embodiment." *In SensoryX'23: Workshop on Multisensory Experiences, together with IMX 2023: ACM International Conference on Interactive Media Experiences*. June 12-15, 2023. Nantes, France ACM, New York, NY, USA, 3 pages. <https://doi.org/10.1145/3604321.3604352>
- Herrera Altamira, G., Fleck, S., Lécuyer, A., & Bougrain, L. (2023). "EEG Modulations Induced by a Visual and Vibrotactile Stimulation". *IEEE SMC 2023 - International IEEE Conference on Systems, Man, and Cybernetics 2023*. October 1-4, 2023. Oahu, Hawaii, USA.
- Herrera Altamira, G., Fleck, S., Lécuyer, A., & Bougrain, L. (2023). "User test and EEG insights of bimodal, visual and vibrotactile, stimuli." *Journées CORTICO 2023* May 9-10, 2023. Paris, France.
- Herrera Altamira, G., Bougrain, L., Lécuyer, A., & Fleck, S. "Design Process of an Upper-Limb Vibrotactile Stimulation for a KMI-based Brain-Computer Interface." *In preparation*.

In the previous chapter 5, the minimum sensory and uncomfortable threshold of the vibration for three age-related groups were identified. In this chapter, the second step of the design process (figure 6.1) are presented, involving 1) designing the activation and deactivation patterns of the vibrotactile stimulation and 2) incorporating the vibrotactile stimulation into the visual environment.

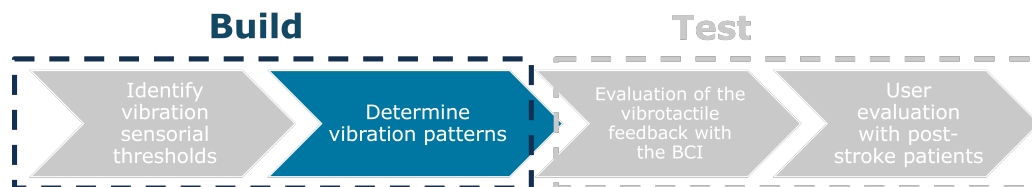


Figure 6.1: Methodology for the design and evaluation of vibrotactile feedback. Build phase - Design of the vibrotactile stimulation.

6.1 Introduction

BCIs hold promise for upper-limb motor rehabilitation in post-stroke patients [26, 27, 28, 29, 30, 31], with KMI being a suitable BCI-control method for individuals unable to physically move but capable of imagining the movement. Unlike visual motor imagery, KMI modulates sensorimotor cortical activity, potentially improving motor performance and aiding in primary motor cortex rehabilitation [199]. However, KMI lacks sensory and kinesthetic feedback, which poses challenges for BCI control and makes it difficult to learn and execute.

To address this limitation, various feedback modalities have been proposed such as functional electrical stimulation [200], tendon vibration, and tactile vibration [31, 71]. This study focuses on tactile vibration, which has shown promise in enhancing motor imagery BCIs [176, 201, 39, 40]. In this chapter, the building phase of the vibrotactile stimulation is presented.

Focal vibration therapy is a non-invasive therapeutic intervention for stroke rehabilitation that uses mechanical vibrations to decrease muscle spasticity [61, 62]. While commercial devices exist, they may be expensive and not wearable. Tendon vibration creating an illusion of movement without muscle contraction [68] has been explored for BCI performance improvement [150, 4] and post-stroke BCI-based rehabilitation [151]. However, the fixed duration and intensity of the vibration may limit its flexibility in BCI applications, where adaptive and dynamic feedback may be more beneficial.

Therefore, there is a need for affordable, wearable, and adjustable vibration devices. Moreover, tactile vibration, stimulating mechanoreceptors on the skin surface, emerges as a potential solution, yet remains unexplored in post-stroke stimulation despite its simplicity. This type of vibration offers short latency, quick response to user performance, and the potential for different levels of stimulation, making it suitable for BCI applications based on motor imagery.

Tactile vibration has been explored as a feedback modality in motor imagery-based BCIs. Design considerations include spatial location, vibration patterns, and variable intensities, each crucial for optimizing effectiveness in post-stroke rehabilitation.

Various spatial locations have been explored for vibrotactile stimulation, ranging from congruent sites with MI like the hand [42, 39, 156, 202], arm [176, 170], wrist and ankles [177], and fingers [40], to less congruent areas such as the back [38], neck [7, 203], and forearm and neck [204]. While congruent feedback yields better results [179], non-congruent locations may be justified for specific cases, such as limb amputation or severe sensory deficiencies post-spinal cord injury. Considering the potential benefits of vibration on post-stroke spasticity, applying vibrotactile feedback on the affected limb remains relevant and necessary.

Activation and deactivation patterns of multiple vibration motors are crucial considerations. For instance, all motors may be activated and deactivated simultaneously [42, 156], or sequentially. A study by Leeb et al. [7] applied vibration starting from the center and moving to the left or right based on the imagined hand, yet it involved a non-congruent location. Sequential vibration patterns on congruent locations, such as the forearm and hand, could be considered as a better alternative.

Varying vibration intensity provides different feedback levels, potentially aiding users in modulating their activity, but their impact on EEG modulations is unclear. An fMRI study indicated that vibration can impact brain activity, particularly event-related desynchronization (ERD) and synchronization (ERS) [180]. ERD and ERS patterns on the mu frequency band reflect sensorimotor decrease or increase of power, respectively [32, 205]. Studies in somatosensory evoked potentials have demonstrated that the brain activity in response to a vibrotactile stimulus is observed in the same frequencies as the vibration frequency [166]. However, in MI-based BCIs the frequencies of interest are found in the alpha and beta bands [108], hence it is important to determine the impact that the vibration can have on these specific frequency bands.

In some studies, simultaneous delivery of vibration while practicing motor imagery has improved MI classification [176, 201, 39, 40]. However, differentiating brain activity due to motor imagery from vibration poses a challenge. In post-stroke rehabilitation, this could lead to over-reliance on vibrotactile stimulation rather than proper motor imagery. The aim of the vibrotactile feedback is to aid patients in recalling sensations to perform KMI accurately by improving awareness of the affected limb [66]. Efforts to differentiate these brain activities have been made [206], suggesting that vibrotactile feedback increases ERD lateralization, potentially improving BCI

decoding accuracy. Understanding the effect of vibrotactile stimulation on the frequency bands related to MI is crucial before using it as feedback in BCIs.

Carefully justifying and considering spatial location, vibration patterns, and intensities in tactile feedback for MI-based BCIs can enhance their potential in post-stroke motor rehabilitation, improving patient interaction and therapy outcomes.

In summary, the reasons behind the design choices of vibrotactile feedback for MI-based BCIs are not clearly justified. Specifically, it is unclear why some studies involved a simultaneous vibration and others involved a sequential one, as it seems that none of them compared their effects. Additionally, the choice of the spatial location is not justified either. In this study, **the aim was to design the vibration patterns that provide detailed feedback about the activation and deactivation of a grasping movement.** The objectives included achieving successful time synchronization of the vibrotactile stimulation with the virtual environment and assessing the coherence between visual and tactile feedback modalities. Simultaneous and sequential vibration patterns were explored, with either two or three vibration motors. The hypothesis was that a sequential vibration consisting of three motors delivered additional details that may correspond better to the visual animation of a grasping hand.

Additionally, an analysis was conducted on the effects of bimodal stimulation (combining visual and tactile vibration feedback) on EEG signals in the alpha and beta frequency bands associated with motor imagery. Specifically, differences between sequential and simultaneous patterns were investigated, as well as the impact of different vibration intensities on EEG signals.

By successfully integrating tactile vibration with the visual environment and identifying optimal vibration patterns and intensities, we can use this bimodal stimulation as feedback for KMI-based BCIs in post-stroke motor rehabilitation. This step is crucial for the effective functioning of the BCI and may improve patient interaction and therapy outcomes.

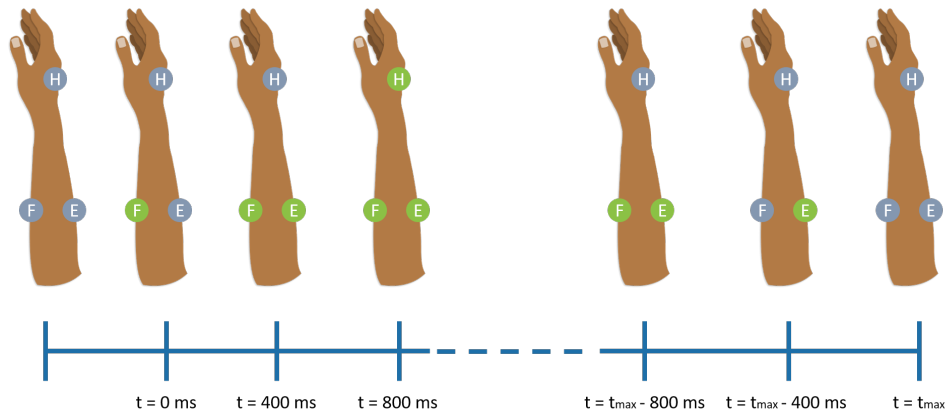
6.2 Design of the Vibrotactile Stimulation

Before testing the vibrotactile stimulation, a building phase was necessary. Two vibration patterns resulted from this build phase: a sequential pattern and a simultaneous pattern. These patterns differ in the activation and deactivation order of the motors, which directly correlates with the number of motors involved. Both vibration patterns were designed to function with a three-motor or a two-motor configuration, as detailed in the following two subsections. Note that both vibration patterns are also dependent on the intensity. The visual interface provides four visual levels of feedback: *None*, *Low*, *Medium*, and *High*. Therefore, the vibration involved the same four levels, where *None* implied no vibration at all. Consequently, three vibration intensities were proposed: *Low*, *Medium*, and *High*. As these values are age-dependent, more details are provided in the upcoming sections.

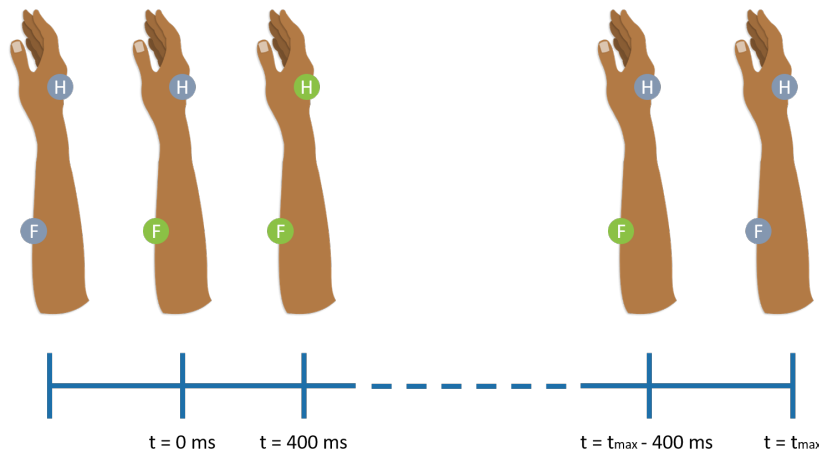
6.2.1 Sequential Vibration Pattern

The first pattern, called the *sequential* pattern, drew inspiration from the natural activation timing of the main muscles involved in grasping as described in [188]. The flexor digitorum superficialis is present during the closing of the hand and holding an object. The extensor digitorum is activated when additional force is required to press an object held by the hand. Moreover, the sequence aimed to mimic the progression of vibration from the forearm to the hand during a grasping movement, as proposed in the study that involved the control of a hand

prosthesis [207]. Figure 6.2 illustrates the sequential activation pattern, which started with the *Flexor* motor, followed by the *Extensor* motor (only active in the three-motor configuration), and finally the *Hand* motor. A 400-millisecond delay separated the activation of each motor. In this way, the sequential pattern mimics the natural activation of the flexor and extensor muscles and finalizes with the hand muscles. The vibration is maintained, simulating the exerting force of holding and pressing a bottle with the hand.



(a) Three motors



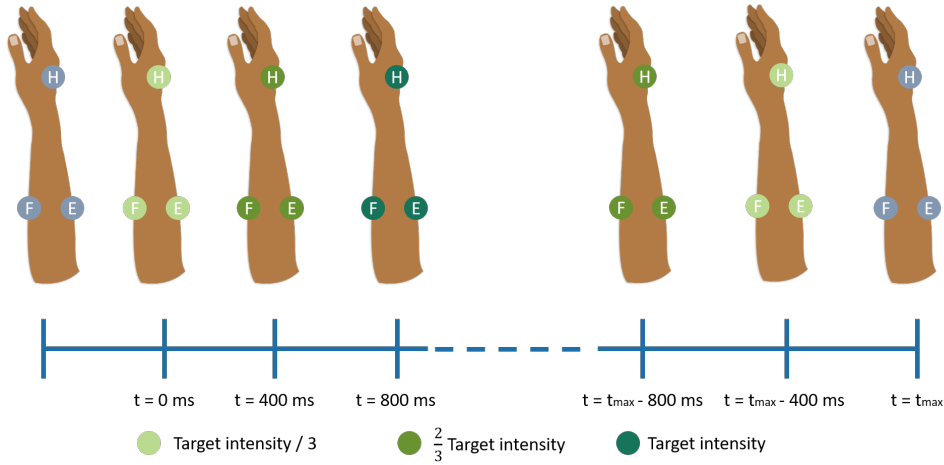
(b) Two motors

Figure 6.2: Sequential vibration patterns. The circles represent the vibration motors: H is the *hand* motor, F is the *Flexor* motor and E is the *Extensor* motor. The gray color depicts motors that are not active. The green color depicts motors that are turned on. t_{max} is the maximum duration of the stimulation which depends on the intensity.

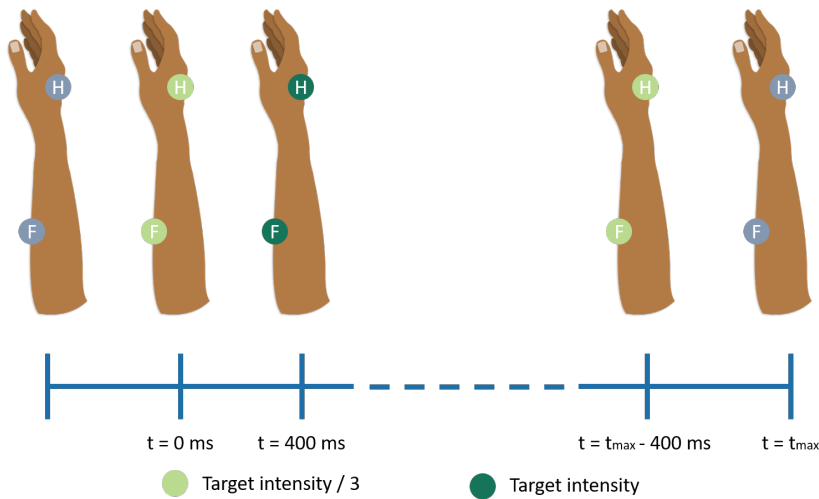
For deactivation, the *Hand* motor was the first to be turned off, followed by the *Flexor* motor, and lastly the *Extensor* motor. The *Extensor* motor was the last one to be deactivated based on the understanding that a small activation of the extensor muscles might occur during object release (opening of the hand). Similar to the activation sequence, there was a 400-millisecond delay between deactivating each motor. Hence, the second-last motor, *Hand* for the two-motor configuration and *Flexor* for the three-motor configuration, was deactivated 400 ms before the maximum duration of the stimulation (two, four, or six seconds, depending on the intensity).

Consequently, the duration during which all motors were activated simultaneously depends on the final intensity level (*Low, Medium, High*).

6.2.2 Simultaneous Vibration Pattern



(a) Three motors



(b) Two motors

Figure 6.3: Simultaneous vibration patterns. The circles represent the vibration motors: H is the *hand* motor, F is the *Flexor* motor and E is the *Extensor* motor. The color gray depicts motors that are not active. The green color depicts motors that are turned on. The shades of green indicate the intensity of the vibration. t_{max} is the maximum duration of the stimulation.

The second pattern, named the *simultaneous* pattern, involved activating and deactivating all two or three motors at the same time (fig.6.3). To ensure the consistency between the sequential and simultaneous patterns, the simultaneous pattern adopted the same number of activation and deactivation steps as the sequential one. In fact, the stimulation of one single motor (as that from the sequential pattern) may be perceived as weaker than the stimulation of three motors activated simultaneously, as previously observed in [42]. Consequently, a simultaneous pattern was designed, which was perceived equally than the sequential one.

Firstly, for the *Medium* or *High* intensity conditions, the target intensity was divided by two or three, depending on the number of motors involved. A 400-millisecond delay separated each step of the progressive activation and deactivation, illustrated by the shades of green in figure 6.3. For the *Low* intensity condition, the intensity was already very low, thus it was not possible to lower it any further. In summary, all motors would be activated at the same time. Then, the vibration intensity would increase gradually, in two or three steps depending on the number of motors, until it reached the target value. This vibration intensity would be maintained for a few milliseconds (depending on the target value), and finally, it would attenuate in two or three steps until it turned off completely. This simultaneous pattern was then consistent with the sequential pattern.

6.3 Material and Methods

In order to determine the vibration pattern that better corresponded to a virtual grasping movement, we performed an experiment where participants tested and compared four different vibration patterns. All participants signed an informed consent approved by the local ethical committee of Inria (COERLE, approval number: 2022-17).

For this study, 18 participants were recruited, above 18 years old, the mean age was 25.94 years, and the standard deviation was 3.7. Nine subjects were female and none of them reported any neurological disorders or sensibility issues of the arm and hand.

6.3.1 Experimental Setup

Participants were seated on a chair and the vibrotactile device was placed on their non-dominant arm and hand, as explained previously in section 4.3.1. Participants also held a bottle with their non-dominant hand, and the virtual hand that was presented was also the non-dominant one. The final device is intended for the impaired upper limb of stroke subjects, thus, performing the tests on the non-dominant limb may simulate this situation since recalling sensations is more difficult. As all participants were right-handed, all tests involved the left upper limb. The participant's arm was placed on a pillow so that the vibration would not propagate on a hard surface and generate undesired stimuli.

Additionally, to study the effects of the vibration on the electroencephalographic signals, we recorded them with the OpenViBE software platform [183] and a Biosemi Active Two 64-channel EEG system in accordance with the international 10-10 system and a sampling rate of 2048 Hz. A screen was placed in front of the participants to show the visual environment consisting of a hand grasping a ketchup bottle, a traffic light, and a vertical bar. The final setup is shown in figure 6.4.

The visual environment was the same as presented in chapter 4. The visual animation consisted of a hand pressing a bottle of ketchup. The hand's size and skin color were modified to resemble the participant's upper limb. There were four levels of ketchup quantity that usually depended on the performance of the BCI. Nevertheless, the ketchup quantity was pseudo-randomized for this study to present each level four times to participants. The vibration intensity was proportional to the visual animation, matching four stimulation levels: no vibration-no ketchup, low vibration-small ketchup quantity, medium vibration-medium ketchup quantity, and high vibration – large ketchup quantity. Each level was presented four times, resulting in one run of 16 trials, as depicted in table 6.1.



Figure 6.4: The participant is comfortably seated on a chair, holding a bottle with the non-dominant hand. The vibrotactile device is placed on the non-dominant limb and a cushion is placed underneath to avoid dispersing the vibration on the table. The screen displays the visual animation and the brain activity is recorded with a 64-electrode EEG cap and a Biosemi Active Two system.

The timeline of one trial was the following: first, the traffic light was red for 30 seconds where the participants were resting, giving them some time to prepare for the test. Then, the light turned red and orange to warn the participant that the stimulation was about to start. After two seconds, the light turned orange and the visual+vibrotactile stimulation was presented. Lastly, the light turned red for a random duration between five and seven seconds to indicate the resting phase. Hence, one trial consisted of warning (2s), stimulation (2-6s), and rest (5-7s) phases. Note the duration of the simulation phase was variable because it depended on the level of stimulation (see table 6.1). The reasoning behind this choice is the inherent need for a longer time when a larger quantity of sauce is involved. Therefore, a lengthier visual animation contributes to enhancing the realism of the animation. The run was repeated four times, each one with a different device configuration. Participants were indicated not to move or talk during the whole run, and they had a short pause in between runs according to their fatigue level.

6.3.1.1 Vibration Intensities

The vibration intensity was controlled by an Arduino Nano using Pulse Width Modulation (PWM), which is a value between 0 and 255. In order to report the intensity in a more familiar manner, we include in table 6.2 the approximated equivalent values in revolutions per minute and frequency in hertz. According to the results presented in Chapter 5, we should modify the intensity of the vibration according to the participant's age. For this study, all participants were under 40 years old. Thus, they belonged to Group 1 and we used the vibration intensities accordingly. The intensity of the vibration and the visual display were equivalent, that is, the higher the quantity of displayed sauce, the stronger the vibration was. This was to keep both





Trials	Duration [seconds]	Vibration Intensity	Visual Animation
4	2	None	
4	2	Low	
4	4	Medium	
4	6	High	

Table 6.1: Number of trials and duration of the bimodal stimulation intensities

stimuli congruent, as it may help with KMI execution and BCI performance [179].

Vibration Intensity	PWM	RPM	Hz
None	0	0	0
Low	75	3,823	64
Medium	150	7,647	127
High	225	11,471	191

Table 6.2: Vibration intensity approximate equivalencies: pulse width modulation (PWM), revolutions per minute (RPM), and hertz (Hz).

6.3.1.2 Device configurations and vibration patterns

Participants evaluated four device configurations that differed in the number of vibration motors (two or three) and the activation/deactivation patterns. The three-motor configuration included the *Hand* motor, the *Flexor* motor, and the *Extensor* motor. The two-motor configuration involved the *Hand* and *Flexor* motors because flexor muscles are more involved during grasping than extensor motors.

The four device configurations were as follows: 3-motor sequential, 3-motor simultaneous, 2-motor sequential, and 2-motor simultaneous. Half of the participants started with the 2-motor configuration to avoid bias due to the presentation order, while the other half started with the 3-motor configuration. Both vibration patterns (sequential and simultaneous) were presented before switching the number of motors and the presentation order of the vibration patterns was also varied among participants. Specifically, half of the participants first evaluated the simultaneous activation pattern, while the other half started with the sequential pattern. This approach ensured a balanced evaluation and reduced potential bias in the results.

6.3.2 Questionnaires

While the experimenter was placing the EEG cap, participants answered the following questionnaires:

- Medical Emotional Scale (MES) [193], to measure the participants' emotional state at the beginning of the session.

- Four-Item Fatigue Screen (FIFS) [194], to evaluate the participants' initial fatigue.

At the end of the session, participants answered the following questionnaires

- MES, to compare the participants' emotional state before and after the session.
- FIFS, to compare the change in fatigue.
- NASA-TLX, to evaluate the mental workload [208].
- a short version of the AttrakDiff questionnaire [195] to evaluate the system's usability and attractiveness.
- the module II of the meCUE questionnaire [209], to evaluate the emotional experience elicited by the interaction with the system.

It is important to note that the *system* was defined as the vibrotactile device, the screen with the virtual environment, and the EEG cap.

6.3.2.1 Participant Evaluation and Qualitative Feedback of the Vibrotactile Stimulation

After trying each configuration, i.e. at the end of each run, participants performed an evaluation through a series of written questionnaires. First, they were given a sheet of paper with an arm on it and they were instructed to draw where and how they felt the vibration. Then, they indicated if they felt different intensities, as well as the quantity. Next, participants evaluated the configuration across 5 items using a 7-point Likert scale: 1) proportionality between the vibration and the sauce quantity, 2) synchronization between the vibration and visual stimuli, 3) comfort of the vibration, 4) discomfort of the vibration, and 5) realism. For the latter item, realism meant if the vibration was close or reminded participants about the sensations of a grasping movement, such as muscular contraction and/or nervous activation.

After testing the simultaneous and the sequential vibration patterns with either two or three motors, participants chose the one they preferred in terms of 1) synchronization with the virtual hand and 2) with the ketchup, 3) coherence between the intensity of the vibration and the amount of displayed ketchup, and 4) overall comfort. Once they tried the 2 and 3-motor configurations, participants chose the one they preferred in the same terms as before. In this way, we did not have only the Likert-based scores but participants were also obliged to choose their preferred configuration so that we could choose the best one for the BCI. Questionnaires can be found in Annex A for more details. Participants were asked to read the questionnaires at the beginning of the session, before testing the first device configuration, so they could anticipate the elements to be assessed and direct their attention accordingly. In this way, we prevented bias during the evaluation of the first configuration since in the following conditions participants would have already answered the questionnaire and would know what to evaluate.

6.3.3 Statistical Tests of the User Evaluation

We performed a repeated measures ANOVA ($\alpha = 0.05$) using *jamovi* to evaluate if there was a difference in the means of the Likert-based evaluation among the four device configurations for each of the five items. To identify if there was a preference when choosing the three or the two-motor configuration and the vibration pattern, we computed the percentage of participants that preferred each option.

6.3.4 EEG offline analysis

In addition to the subjective evaluation, we studied the effect of the visual and vibrotactile stimulation on the EEG signals to understand how it may influence the BCI performance. More specifically, we looked for differences among

1. the vibrotactile device configurations, expecting to observe a more important brain activity with the 3-motor configuration
2. the four stimulation intensities, expecting a larger brain activity in higher intensities.

We performed the offline analysis of the EEG signals with EEGLab v2022.1 [210] toolbox in Matlab R2021b. One participant had to be excluded from the study due to errors during data acquisition, more specifically, the EEG files were not saved correctly, resulting in data being wrongly labeled. Nevertheless, the questionnaires were applied in the correct order, so we kept this participant for the user's subjective evaluation. For each participant, there were four files, each one corresponding to one device configuration. Each file followed the next processing and analysis.

First, the raw EEG data were re-referenced using the Common Average Reference method. Next, data was high-pass filtered at 1 Hz and a 50 Hz notch filter was applied. Then, data were downsampled to 512 Hz after applying an antialiasing low-pass filter at 256 Hz. We needed to have a high sampling rate to follow the recommendation of $20 \times (\text{number of channels})^2$ data points to perform an independent component analysis (ICA). The ICA allowed us to remove eye and muscle artifacts using the IClab tool.

After completing the preprocessing stage, we extracted epochs that encompassed 4.1 seconds before the onset of the stimuli and 10 seconds afterward. We defined a baseline of 2 seconds, occurring 4 seconds before the stimuli onset. This decision was based on the fact that participants were given a 2-second window to prepare for the upcoming stimulation, which could potentially elicit EEG activity during this anticipation period. Subsequently, each epoch was labeled according to the corresponding level of vibration intensity.

For each epoch, we performed a time-frequency grand average analysis to observe the Event-Related Spectrum Perturbations (ERSPs). In this case, the baseline was defined at 500 ms before stimuli onset. The average was performed among participants ($n=17$) and the four vibration patterns. This analysis allowed us to identify the frequency bands with the most activity during the stimulation. Finally, we used these results to obtain topographies corresponding to the average duration of the stimulation to study the EEG activity over the cortex. We used the EEGLab statistics study tool to perform parametric statistics with FDR correction and a statistical threshold $p = 0.05$ for the time-frequency ERSPs and 0.01 for the topographical analyses.

6.4 Results

6.4.1 User's subjective evaluation

6.4.1.1 Qualitative feedback of hand and arm sensations

Figure 6.5 presents a visual summary of the sensations reported by the participants through their drawings. Consistently, all participants indicated feeling the vibration precisely at the location of the motors, marked by the green circle, with its intensity gradually diffusing outwards the motor

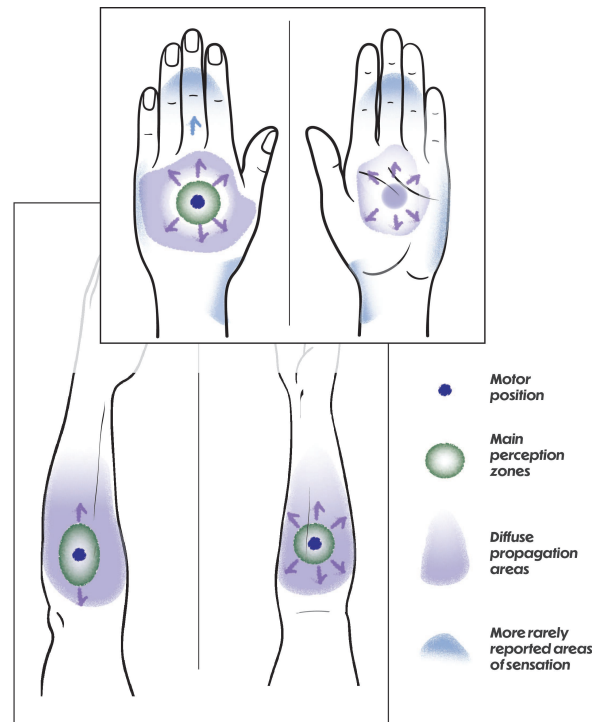


Figure 6.5: Participant's description of the vibrotactile stimulation on the hand and forearm.

placement (indicated by the purple diffused area). Additionally, a subset of participants reported perceiving the vibration spreading from the hand to the fingers, and a few also experienced sensations extending to the wrist (depicted by the blue diffused areas). Hence, the vibrotactile stimulation elicited consistent sensations among the participants.

6.4.1.2 Participant evaluation of the device configurations

In the experiment, all participants, except for one, were able to perceive at least three levels of vibration intensities across all device configurations. The participant who did not discern different vibration intensities reported this only during the evaluation of the 2-motor simultaneous configuration. For the remaining configurations, this participant could differentiate between various vibration intensities. As this observation was limited to just one participant and one configuration, it is likely attributed to a momentary lack of attention rather than a fundamental issue with the perception of different intensities.

Regarding the Likert evaluation of the five items (fig.6.6), no statistically significant differences were observed among the four configurations for any of the assessed items (repeated measures ANOVA, Proportional to sauce quantity $p = 0.094$, Synchronization with hand movement $p = 0.156$, Comfortable $p = 0.238$, Disturbing $p = 0.752$, Realistic $p = 0.778$). Nevertheless, it is worth noting that the vibration was consistently perceived as highly proportional to the sauce quantity displayed on the screen (fig.6.6(a)) and highly synchronized with the virtual hand movement (fig.6.6(b)) across all device configurations. Furthermore, participants rated the vibration as highly comfortable (fig.6.6(c)) for all configurations as well. As for the item related to realism, average scores were consistently high, with all device configurations receiving more than 4 Likert points (fig.6.6(e)).

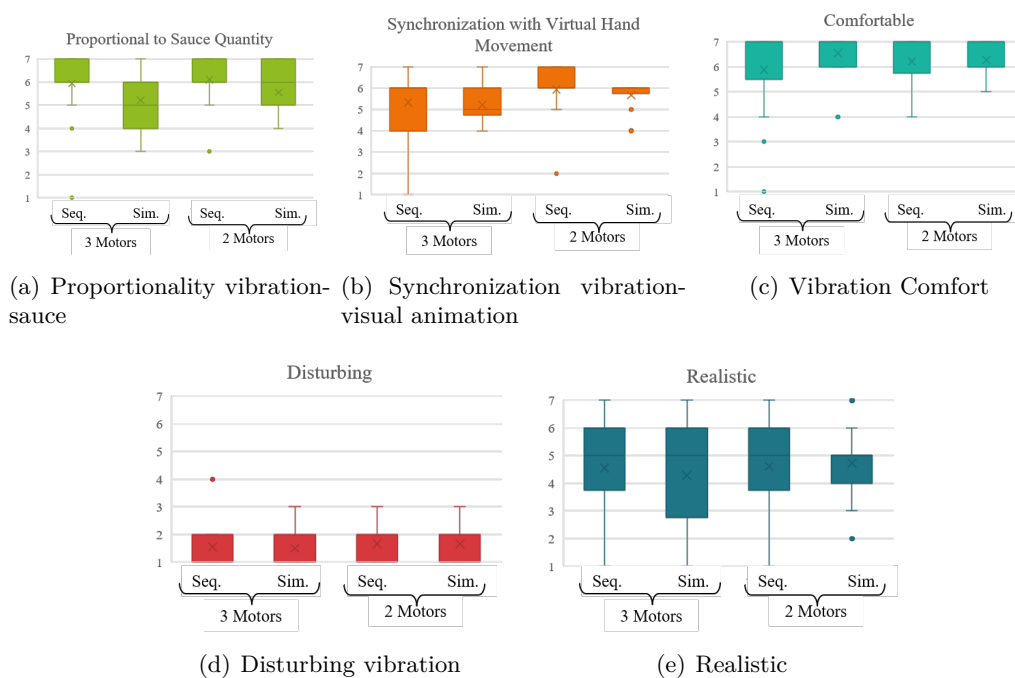


Figure 6.6: Box plots of the Likert evaluation of the four vibration configurations

While the results of the Likert evaluation were consistently positive, they did not provide a clear choice for the best configuration among the tested options. To address this, participants were asked to make a forced choice between the 3 and 2-motor configurations (figure 6.7). Interestingly, the majority of participants (11 out of 18) preferred the 3-motor configuration in terms of hand synchronization, sauce synchronization, and coherence between the vibration intensity and the visual animation. Regarding overall comfort, two participants had no particular preference, while half of the remaining participants favored the 3-motor configuration. Consequently, the 3-motor configuration emerges as the overall preferred choice among participants.

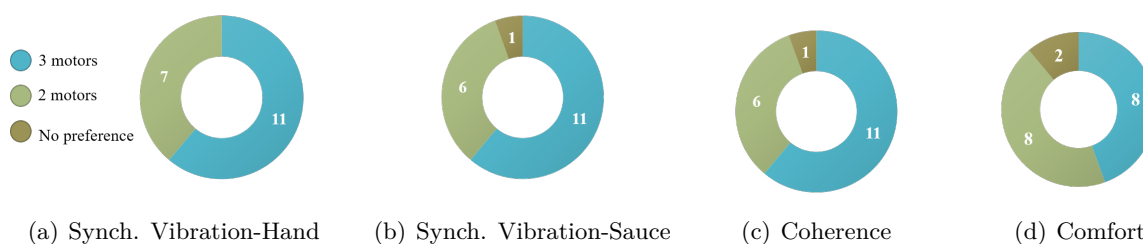


Figure 6.7: Participants forced choice: three versus two motors

When evaluating the 3-motor configuration and asked to choose between the sequential and simultaneous patterns (figure 6.8), participants reported a small preference for the sequential one for comfort (9 participants, 2 no preference), synchronization with the hand and the sauce animations (11 participants for each item). On the other side, there was a slight preference for the simultaneous pattern regarding coherence (9 participants, 2 no preference).

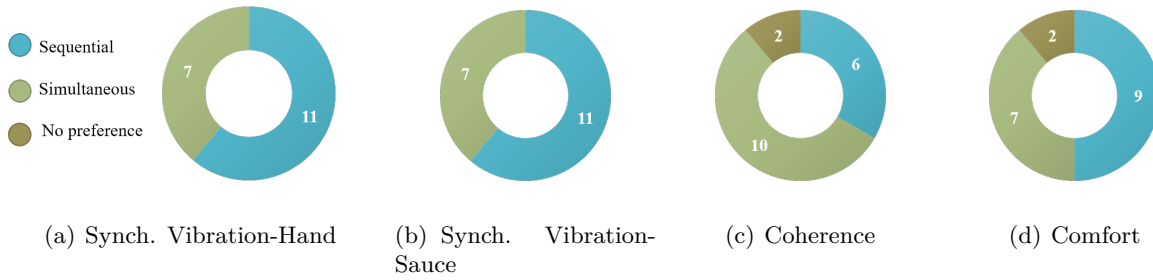


Figure 6.8: Participants forced choice: three motors, sequential versus simultaneous

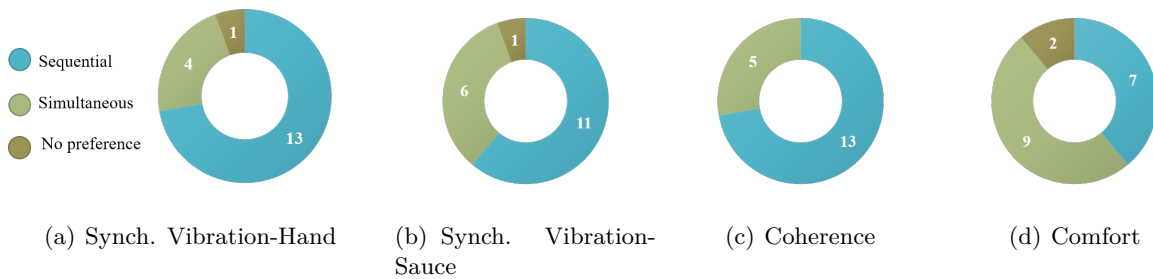


Figure 6.9: Participants forced choice: two motors, sequential versus simultaneous

Regarding the 2-motor configuration (figure 6.9), 13 participants preferred the sequential pattern concerning coherence and sauce synchronization. Regarding hand synchronization, 13 participants preferred the sequential pattern and one had no preference. Contrarily, regarding comfort, 9 participants preferred the simultaneous pattern and 2 had no preference. Consequently, regardless of the number of motors, the sequential pattern was perceived as more synchronized than the simultaneous pattern.

6.4.2 Participants' emotional state, fatigue level, and mental workload

We observed participants were more tired by the end of the session (T-test $p < 0.001$, figure 6.10(a)). Notably, there was a significant decrease in the positive activation emotions (T-test $p = 0.034$, $\alpha = 0.05$) and negative activation emotions (T-test $p = 0.021$, $\alpha = 0.05$), indicating that participants felt less active as the session progressed (figure 6.10(c)). However, we did not observe an increase in deactivating and neutral emotions.

Moreover, participants' mental workload, as assessed by the NASA-TLX questionnaire, was somewhat high (mean value= 30.56, s.d.=12.30, figure 6.10(b)). Despite this, there was only a weak, non-significant correlation between the mental workload and the final fatigue level (Kendall's $\tau-b=0.122$, $p = 0.508$).

Overall, the experimental session did not negatively impact the emotional state of the participants. While the session demanded considerable effort from the participants, the mental workload remained within reasonable limits, and the fatigue level was not excessive. This suggests that the experimental protocol was well-tolerated by the participants and did not result in emotional stress or overwhelming mental demands, reinforcing the validity of the results.

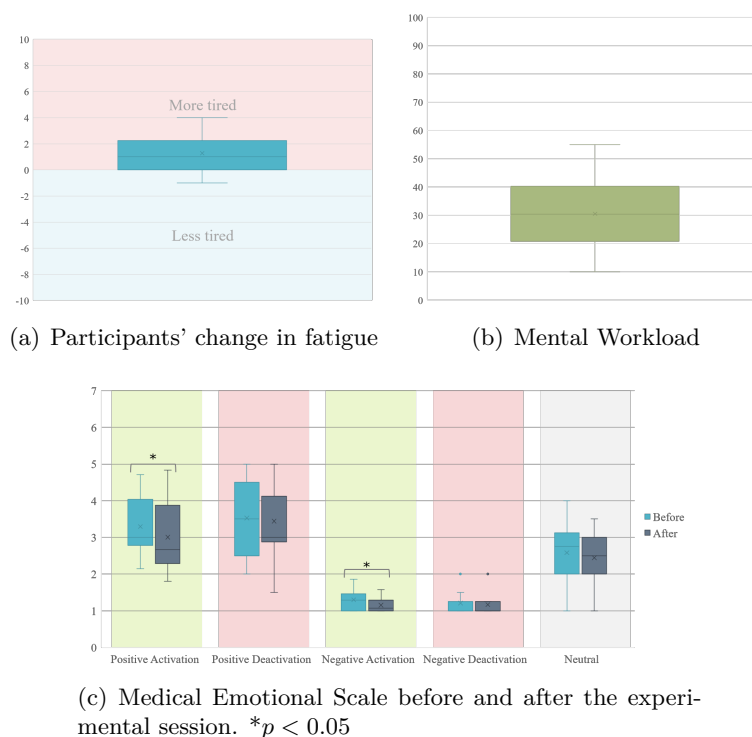


Figure 6.10: Participant's fatigue, mental workload, and emotions during the session.

6.4.3 System's elicited emotions and attractiveness

The meCUE questionnaire's module II allows for the assessment of emotions elicited during the interaction with the system. It is essential not to confuse this with the MES questionnaire, which evaluates emotions experienced during the session. Regarding positive emotions, 72% of the participants agreed with the statement *The system exhilarates me* (fig.6.11(a)). However, only 22% reported feeling cheerful while using the system and 72% remained neutral (fig.6.11(b)). Additionally, 67% of participants stated that the system relaxed them (fig.6.11(c)), and 56% indicated a sense of calmness (fig.6.11(d)). These scores are consistent with the observations from the MES questionnaire, where a decrease in activation emotions was noted, thereby eliciting relaxation and calmness among participants.

Concerning negative emotions, we anticipated participants to disagree with the affirmations, as they all represent negative aspects. Indeed, none of the participants reported feelings of anger (fig.6.12(a)) or frustration (fig.6.12(b)) during the interaction with the system. However, 33% of the participants mentioned feeling tired (fig.6.12(c)), which is consistent with the previously reported change in fatigue, as depicted in figure 6.10(a). Surprisingly, the majority (72%) disagreed with the statement *The system makes me feel passive*, despite not having control over either the vibration or the visual animation. This may indicate that the stimulation elicits some form of intellectual activation rather than a physical one. In fact, a few participants reported that the vibration "woke them up" whenever they felt tired or were at risk of losing focus.

These observations shed light on the diverse emotional responses elicited by the system. While positive emotions such as exhilaration, relaxation, and calmness were evident in many participants, the absence of anger and frustration further emphasizes the system's positive impact on

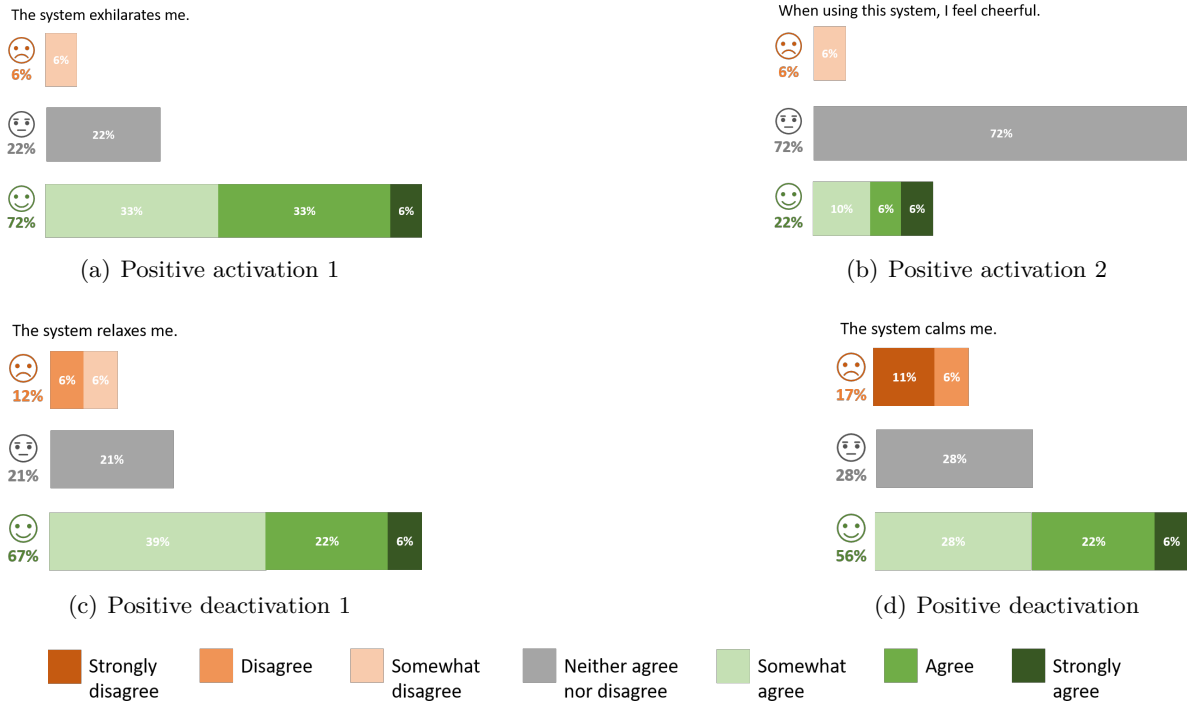


Figure 6.11: meCUE's positive emotions

emotions. The surprising activation response elicited by the system, even in a passive setting, highlights its potential to influence participant engagement and attention during the interaction.

To assess the attractiveness of the system, involving the vibrotactile device, visual environment, and EEG helmet, we used the AttrakDiff questionnaire. Mean values for each dimension of the AttrakDiff questionnaire are presented in figure 6.13(a), and all of them were slightly positive. Specifically the pragmatic quality scored an average of 1.32, hedonic quality Stimulation 1.08 and Identity 1.06, with an overall attractiveness of 1.08.

As shown in figure 6.13(b), the average value of the pragmatic (mean= 1.32, 95% confidence interval= 0.86, 1.78) and hedonic (mean= 1.07, 95% confidence interval= 0.65, 1.49) qualities from AttrakDiff questionnaire indicate that the system was perceived as desirable. However, when examining the individual participants' responses (represented by the blue small circles), half of them found the system either self or task-oriented, with one person expressing a neutral opinion.

Furthermore, the grand average (n=18) word pairs of each item (Figure 6.13(c)) reveals that all items received positive values, indicating an improvement from the results in the previous chapter 5. Particularly, the *Confusing - Clearly Structured* item scored the highest (mean= 2.39), followed by *Bad - Good* (mean= 1.94). This suggests that participants understood the bimodal stimulation very well, while also finding it good for themselves. On the other hand, the lowest value was observed for the *Ugly - Attractive* item (mean= 0.33). Additionally, although all items were scored positively, careful attention must be drawn to the six items that scored less than 1: *Repealing - Appealing*, *Rejecting - Inviting*, *Unimaginative - Creative*, *Impractical*

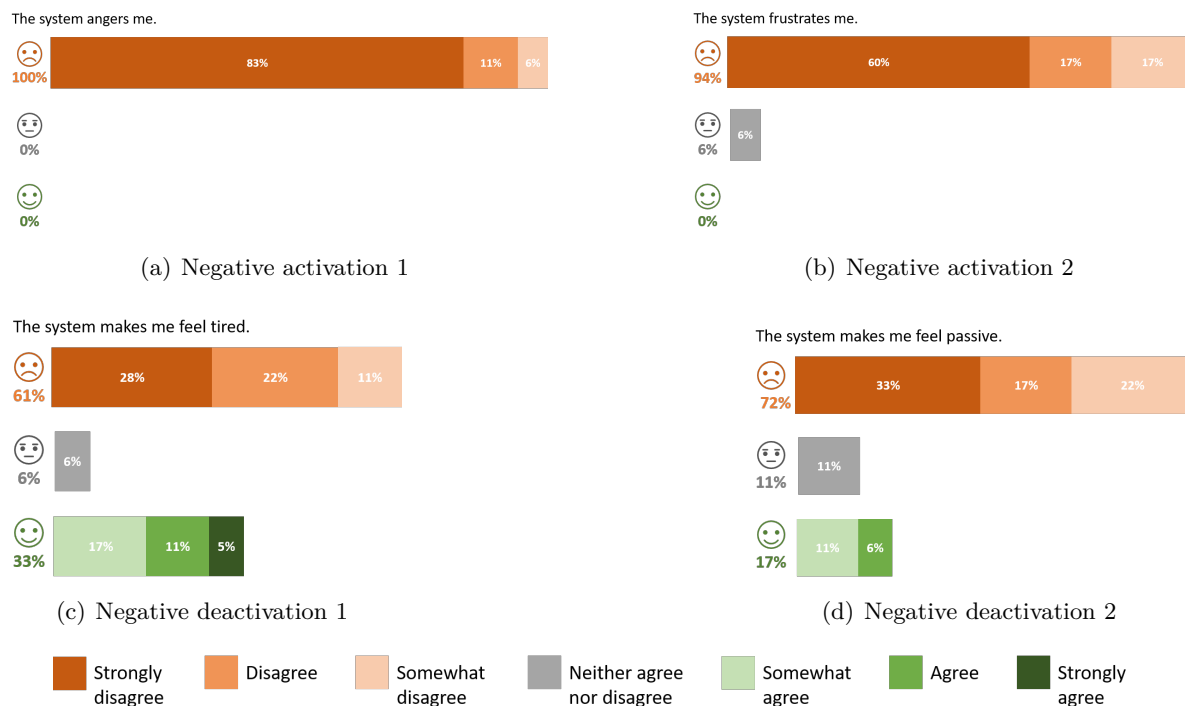


Figure 6.12: meCUE's negative emotions

- *Practical*, and *Complicated - Simple*.

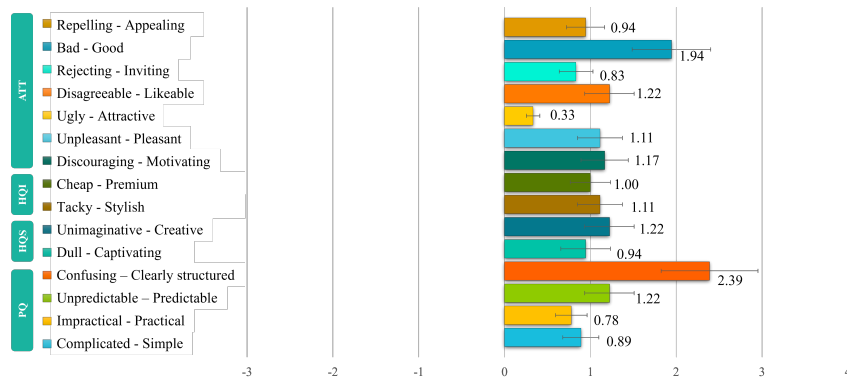
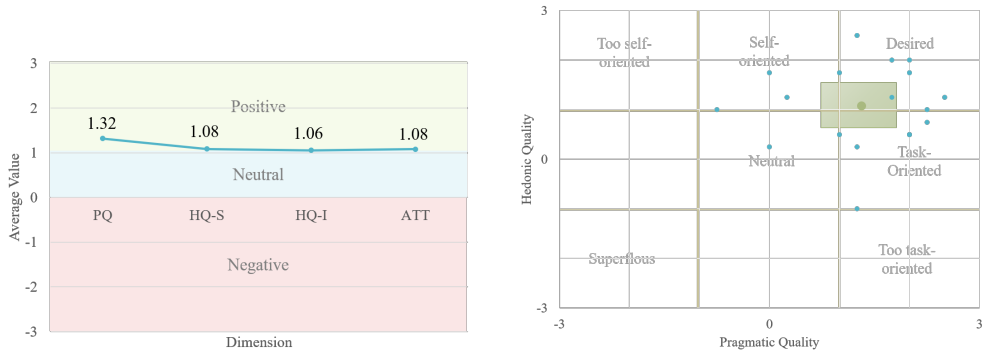
Overall, the findings from the AttrakDiff questionnaire suggest that the system was positively perceived by the participants displaying favorable scores for pragmatic, hedonic, and identity qualities. These results indicate that the system is well-received and holds potential for effective use in the context of motor-imagery-based BCIs.

6.4.4 Time-frequency analysis of EEG activity

We present the results of time-frequency analyses for the four stimulation intensities, as previously introduced in 6.2, involving visual and vibrotactile stimuli. For this study, the ERSPs for the different device configurations, where 2 or 3 vibration motors were activated simultaneously or sequentially, were averaged. Subsequently, we grouped the ERSPs based on stimulation intensity: *None*, *Low*, *Medium*, *High*.

In figure 6.14, we present the time-frequency analysis results for two electrodes placed over the central gyrus, namely C_3 , C_4 in the 10-10 system. These electrodes report activity in both the motor and sensory primary cortex ([211]). Additionally, we analyzed two electrodes on the somatosensory cortex (CP_3 , CP_4). As the stimulation involves a visual animation, we also performed the analysis for electrodes O_1 and O_2 (fig.6.15) located on the occipital lobe, as it involves the visual cortex [212]. The onset of the stimulation is depicted by a green dotted line at $t=0$ ms, while the stimulation offset is shown by a red dotted line at $t=2000$ ms for the *None* and *Low* intensity conditions, $t=4000$ ms for the *Medium* intensity, and $t=6000$ ms for the *High* intensity. A 3-second-resting period was included after each stimulation offset.

The last column, titled "*Statistics*" in both figures 6.14 and 6.15, shows the statistically signif-



(c) Word pairs diagram - Grand average.

Figure 6.13: Results of the AttrakDiff questionnaire for the second experiment.

icant differences among stimulation intensities using a Repeated measures ANOVA with FDR correction ($p < 0.05$). It is important to note that the stimulation intensities vary in duration. Therefore, for this last column, we compared only the first two seconds of stimulation. After this time period, any comparison would involve the rest period of the *None* and *Low* intensity conditions with the stimulation period of the *Medium* and *High* intensity conditions.

6.4.4.1 Comparing right and left hemispheres

Regarding the analysis of brain activity in the motor and somatosensory cortices (figure 6.14), we observed activity in both brain hemispheres, namely the ipsilateral (left) and contralateral (right) to the upper limb being stimulated. This activity was predominantly present in two frequency bands: first, between 8 and 14 hertz, which corresponds to a combination of mu and low-beta frequency bands, and second, between 17 and 26 hertz, which corresponds to the high-beta frequency band. Notably, this high-beta activity was mainly observed during the intensities where vibration was present (*Low*, *Medium*, and *High*). While both hemispheres showed activity, differences were observed between them.

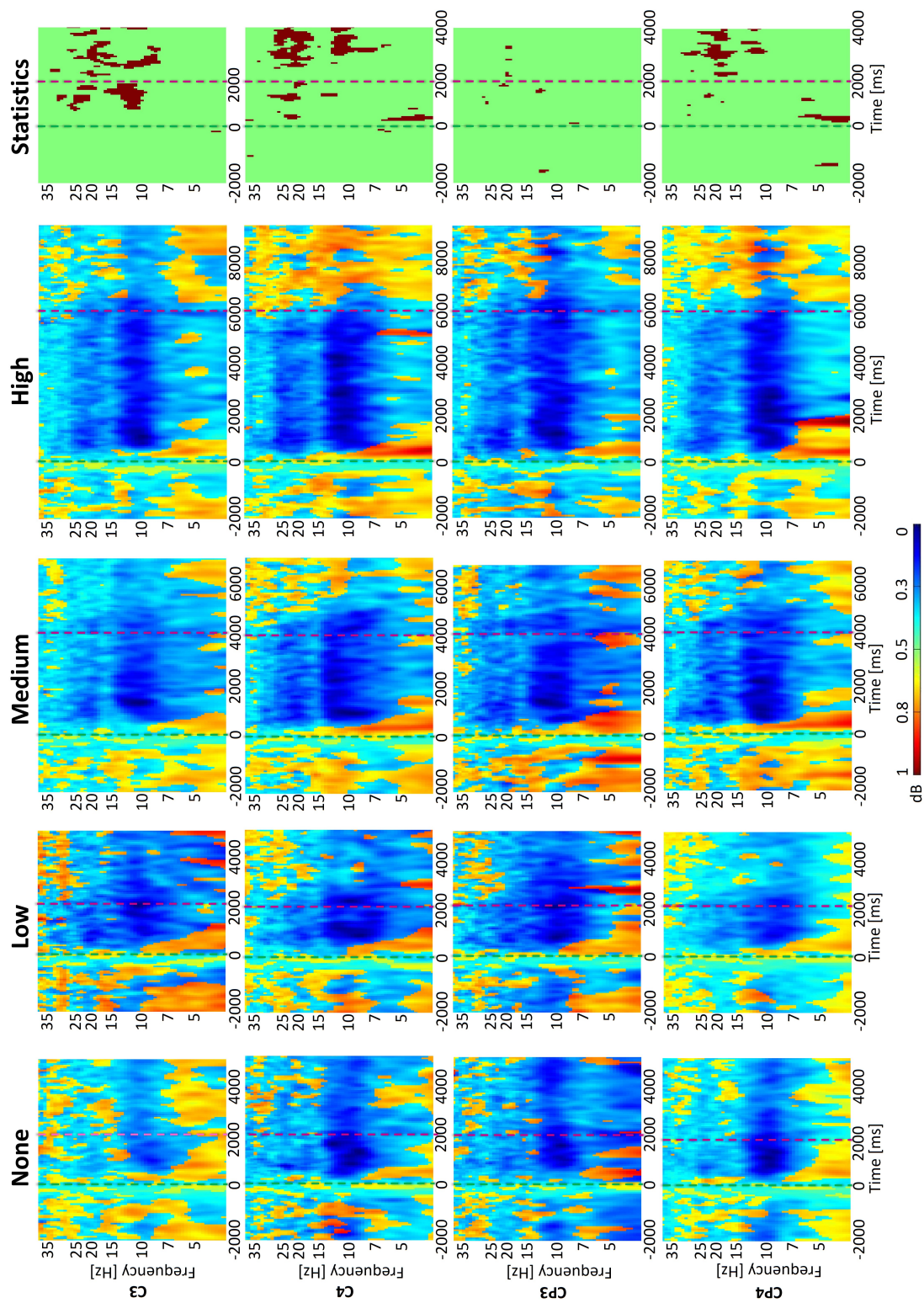


Figure 6.14: ERSPs grand average time-frequency analysis ($n=17$) for electrodes C_3 , C_4 , CP_3 , CP_4 . In columns, the stimulation intensity (*None*, *Low*, *Medium*, *High*), the last column indicates the statistically significant differences ($p < 0.05$) in ERSP values among conditions. The green dotted line indicates the stimulation onset, while the red dotted line indicates the stimulation offset.

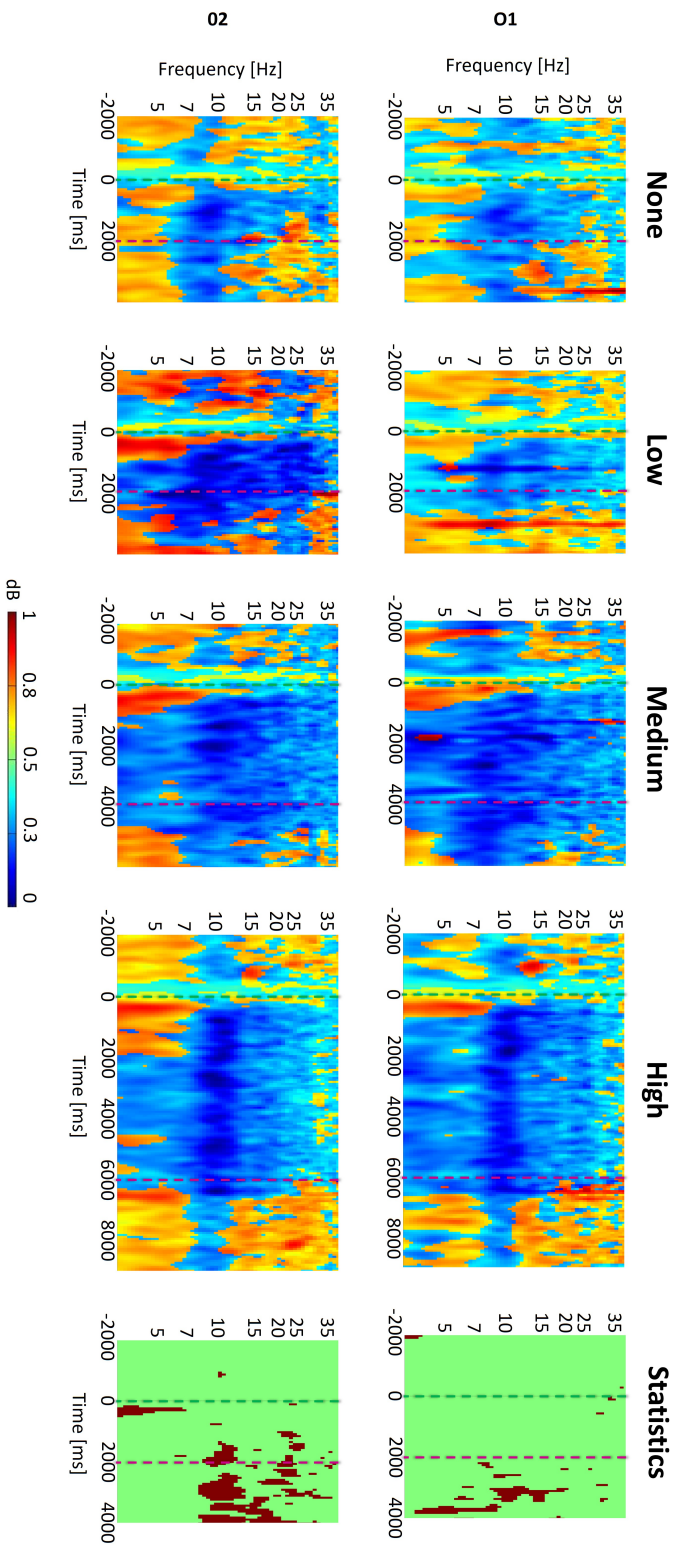


Figure 6.15: ERSPs grand average time-frequency analysis ($n=17$) for electrodes O_1 and O_3 . In columns, the stimulation intensity (*None*, *Low*, *Medium*, *High*), the last column indicates the statistically significant differences ($p < 0.05$) in ERSP values among conditions. The green dotted line indicates the stimulation onset, while the red dotted line indicates the stimulation offset.

6.4.4.1.1 Ipsilateral hemisphere In electrodes C_3 and CP_3 , an ERD was observed during the stimulation period, persisting even one to two seconds after the stimulation offset. Surprisingly, we did not observe an ERS once the stimulation ended for either of these two electrodes. A short rebound was noticed only for the *High* intensity condition around 11-14 Hz, with a more pronounced effect in CP_3 compared to C_3 . Moreover, in CP_3 , a transient ERS was observed around 3-7 Hz during the first 500 ms of the stimulation among all conditions, whereas in C_3 , this event was mainly observed during the *Low* condition and minimally for the others.

6.4.4.1.2 Contralateral hemisphere Similar to the observations on the ipsilateral hemisphere, an ERD was observed in electrodes C_4 and CP_4 during the stimulation period. However, in this case, the ERD was attenuated once the *None* and *Low* intensity conditions concluded. For the *Medium* condition, a weak, short-lived ERS was visible around 5500 ms at 11-14 Hz. The ERS became more important during the *High* condition in C_4 , where it was observed almost 1 second after stimulation offset at 7-10 Hz, and a few milliseconds after offset at 10-14 Hz. Similarly, in CP_4 , the ERS of the *High* condition was mainly observed at 10-14 Hz around 500 ms after stimulation offset.

In summary, while both hemispheres displayed mu and beta-related ERDs for all intensities, these responses are slightly stronger in the contralateral hemisphere. Moreover, post-stimulation ERS was more evident in the contralateral hemisphere. These findings highlight the patterns of brain activity in response to the visual and vibrotactile stimulation and provide valuable insights into the hemispheric differences during this bimodal stimulation.

6.4.4.2 Activity in the occipital lobe

The time-frequency analysis results for the two electrodes (O_1 and O_2) on the occipital lobe are presented in figure 6.15. As expected, both electrodes exhibited an ERD at 8-14 hertz, corresponding to the alpha band, throughout the entire duration of the stimulation. Additionally, a weaker ERD was also observed around 15 hertz for all stimulation intensity conditions, except for the *Medium* condition. Notably, the ERD was attenuated after stimulation offset for the *None* and *High* conditions of both electrodes. However, this attenuation was not observed for the *Medium* condition of O_1 , nor for the *Low* and *Medium* conditions of the O_2 electrode.

Furthermore, a transient ERS was observed at the beginning of the stimulation around 3-7 hertz in both electrodes, primarily during the *Low*, *Medium*, and *High* intensity conditions where vibration was present.

6.4.4.3 Comparing stimulation intensities

The repeated measures ANOVA ($p = 0.05$) did not reveal any statistically significant differences among intensity conditions in CP_3 and O_1 during the stimulation period (figures 6.14 and 6.15, respectively). However, in C_3 significant differences were observed around 10-15 hertz, and 20-25 hertz approximately 500ms after the stimulation onset until its offset. Additionally, significant differences were observed in O_3 at 3-7 hertz at the beginning of the stimulation, and around 9-13 hz and 20-25 hz during the last second of the stimulation. Regarding the contralateral hemisphere, C_4 and CP_4 exhibited a significant difference around 3-7 hz at the beginning of the stimulation, likely related to the transient ERS mentioned earlier. No other significant differences were observed during the first two seconds of the stimulation period.

6.4.5 Topographical analysis of EEG activity

The time-frequency analysis provided insights into the frequency-specific responses of the brain during bimodal stimulation. We proceeded to do a topographical analysis of the identified frequencies at specific moments in time to have a better understanding of the EEG oscillations due to the stimulation.

6.4.5.1 Comparing the device configurations

Figure 6.16 displays the brain activity during the initial two seconds of stimulation for the four device configurations, focusing on the alpha and low beta (8 - 15 hertz) frequency bands. We chose this time window to ensure that the stimulation is consistently present, given the variations in stimulation duration across intensities. Contralateral ERD patterns are noticeable in all conditions, particularly around C_4 extending to FC_4 , and in posterior and occipital contralateral regions, with the 2-motor simultaneous configuration showing a more pronounced ERD. However, no statistically significant differences were found among the device configurations (repeated measure ANOVA, FDR correction, $p < 0.01$), suggesting a constant ERD response regardless of the device configuration.

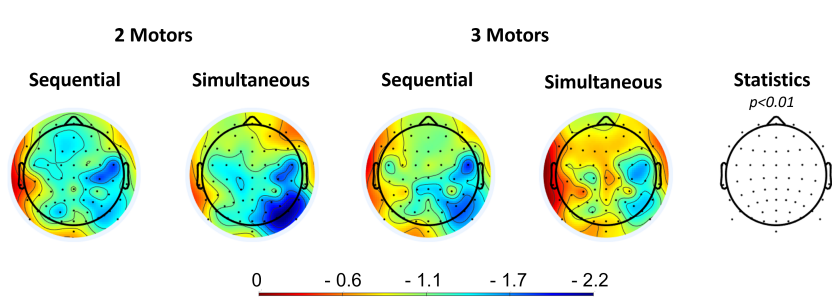


Figure 6.16: Topographies of the average of the first 2 seconds of the stimulation in the alpha + low beta (8-15hz) frequency band. Each column corresponds to one of the four device configurations. The last column indicates the statistically significant differences ($p < 0.01$) among device configurations.

In figure 6.17, brain activity in high beta (15-25 hertz) is presented. A contralateral ERD is observed around C_4 and FC_4 , although weaker than that found in alpha + low beta. Notably, the response to the stimulation was similar across all four intensity conditions, with no statistically significant differences observed (repeated measure ANOVA, FDR correction, $p < 0.01$). Consequently, for both frequency bands, the bimodal stimulation elicits a consistent ERD regardless of the device configuration.

6.4.5.2 Comparing stimulation intensities

As no statistically significant differences were observed due to the device configuration, we grouped the EEG activity by stimulation intensity and generated the respective topographies for alpha+low beta and high beta frequency bands.

In figure 6.18, the topographies corresponding to the alpha+low beta (8-15 hertz) frequency bands are presented. For the initial two seconds of stimulation of the *None* and *Low* intensities, a predominantly contralateral ERD was observed around C_4 , C_6 , and FC_4 , extending to the posterior contralateral area. As the intensity increased to *Medium*, the ERD became bilateral,

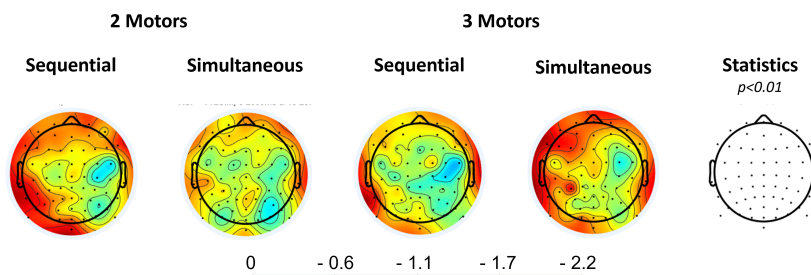


Figure 6.17: Topographies of the average of the first 2 seconds of the stimulation in the high beta (15-25hz) frequency band. Each column corresponds to one of the four device configurations. The last column indicates the statistically significant differences ($p < 0.01$) among device configurations.

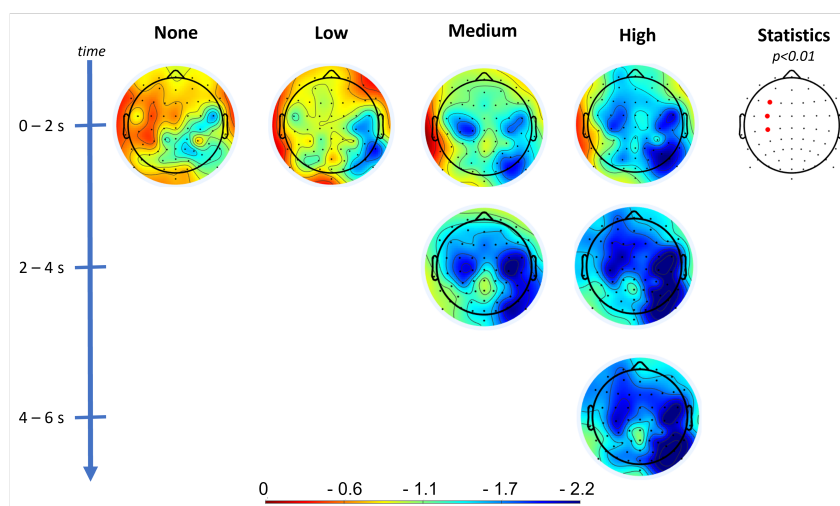


Figure 6.18: Topographies of the 2-second average of the stimulation in the alpha + low beta (8-15hz) frequency band, from $t=0$ until $t=6$ seconds. Each column corresponds to one of the four stimulation intensities. The last column indicates the statistically significant differences ($p < 0.01$) among intensity, valid only for the first 2 seconds of the stimulation.

observed around C_1 and C_3 , and extended towards posterior areas (P_6 , P_8). Similarly, a bilateral ERD was present during the *High* intensity, with a similar location to the *Medium* intensity but extending further. Statistically significant differences from the repeated measures ANOVA with FDR correction were observed in three ipsilateral electrodes: F_3 , FC_3 , and C_3 . For these electrodes, we performed pairwise Tukey comparisons in *jamovi* [213] which revealed significant differences in C_3 between the *High* and *None* conditions ($p = 0.018$), and *Medium* and *None* ($p = 0.011$).

Subsequently, we computed the 2-second average during two to four seconds of the *Medium* and *High* intensity conditions, and four to six seconds of the *High* condition, remaining constant with the duration of the stimulation. We observed that as the duration increased, the initial ERD extended to broader areas of the brain. During the last two seconds of the *High* condition, the ERD encompassed almost the entire brain cortex.

In the high beta (15-25 hertz) frequency band (fig. 6.19), we observed a weak ERD for the *Low*

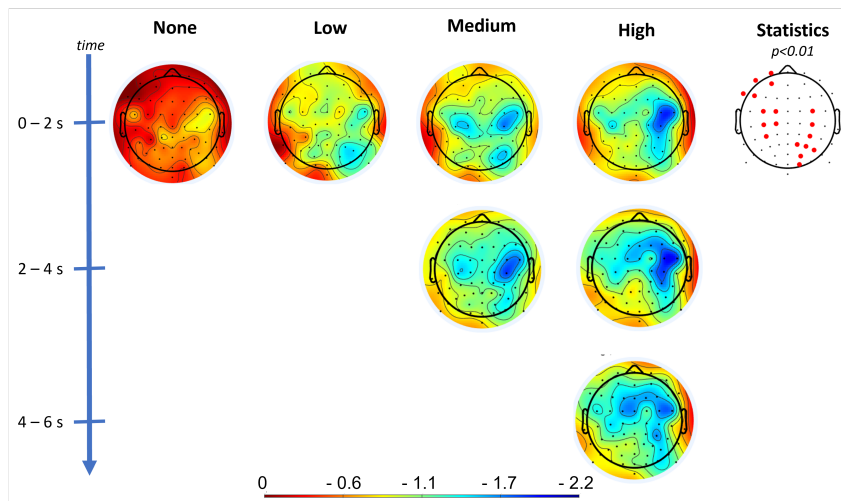


Figure 6.19: Topographies of the 2-second average of the stimulation in the high beta (15-25hz) frequency band, from $t=0$ until $t=6$ seconds. Each column corresponds to one of the four stimulation intensities. The last column indicates the statistically significant differences ($p < 0.01$) among intensity, valid only for the first 2 seconds of the stimulation.

intensity during the initial two seconds. The ERD became stronger and bilateral for the *Medium* and *High* intensity conditions. Statistically significant differences were observed across intensity conditions in the frontal ipsilateral region (Fp_1 , Af_3 , Af_7 , F_5 , F_7 , FC_1 , FC_3), the ipsilateral sensorimotor region (C_1 , C_3 , CP_3), and the contralateral sensorimotor (C_3 , CP_3), posterior (P_1 , P_3 , P_5 , PO_3), and occipital (O_2) regions. We then performed pairwise Tukey comparisons in C_3 , which indicated significant differences in C_3 between: *High* and *Low*, and *Medium* and *Low* both with $p < 0.05$, *High* and *None* ($p < 0.01$), and *Medium* and *None* ($p < 0.001$). No statistically significant differences were observed between the *High* and *Medium* intensities.

Similarly to the alpha + low beta responses, the magnitude of the ERD increased with the stimulation duration. In the *High* intensity, the ERD extended to frontal regions but it did not cover a vast area as in the alpha + low beta band. Moreover, the ERD appeared weaker in this frequency band than in the alpha + low beta band.

6.4.5.2.1 Post-stimulation topographies In continuation with the time-frequency analysis (section 6.4.4), where we did not observe synchronization (ERS) after the stimulation ended, we generated the topographies representing the average from zero to one-second post-stimulation and one to two seconds post-stimulation for both the alpha + low beta and high beta frequency bands.

In the alpha + low beta (8-15 hertz) frequency band (fig. 6.20, consistent with the time-frequency observations, one second after the stimulation, the ERD was still present for the *None*, *Low*, and *Medium* intensities. In contrast, the *High* intensity showed a slight synchronization around C_4 during this period. One second later, the ERD had largely dissipated, and the synchronization became more prominent for the *High* intensity condition. Regarding the high beta (15-25 hertz) frequency band, an ERS was present during the first second of the stimulation, persisting one to two seconds post-stimulation for all intensity conditions except for the *Medium* intensity, where, surprisingly, a slight ERD is visible.

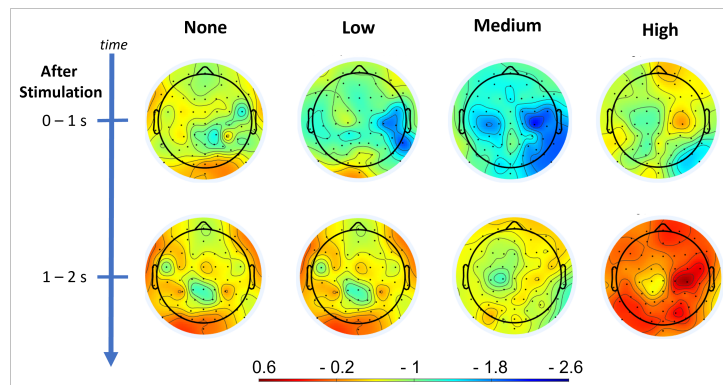


Figure 6.20: Brain activity post-stimulation in the alpha + low beta (8-15 Hz) frequency band. The first row corresponds to the average of zero to one second post-stimulation, and the second row corresponds to the average of one to two seconds post-stimulation. In columns, the stimulation intensity *None*, *Low*, *Medium*, and *High*

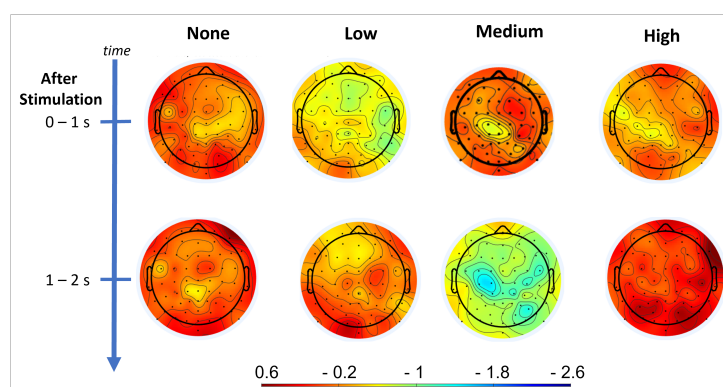


Figure 6.21: Brain activity post-stimulation in the high beta (15-25 Hz) frequency band. The first row corresponds to the average of the zero to one second post-stimulation, and the second row corresponds to the average of one to two seconds post-stimulation. In columns, the stimulation intensity *None*, *Low*, *Medium*, and *High*

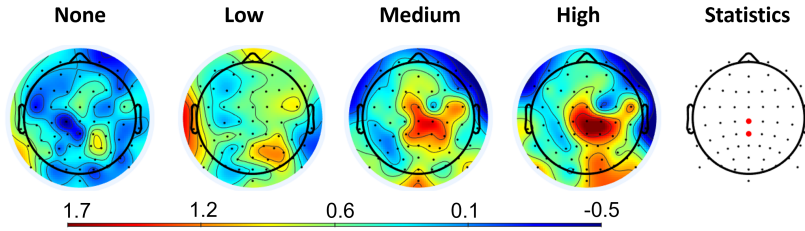


Figure 6.22: One-second average topographies in the delta (1-4hz) frequency band, corresponding to the first second of the stimulation. Each column corresponds to one of the four stimulation intensities. The last column indicates the statistically significant differences ($p < 0.01$) among intensities.

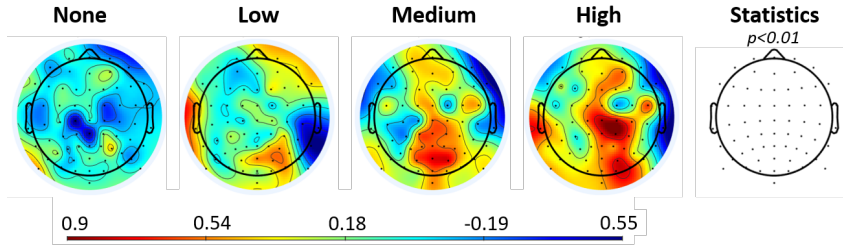


Figure 6.23: One-second average topographies in the theta (4-8hz) frequency band, corresponding to the first second of the stimulation. Each column corresponds to one of the four stimulation intensities. The last column indicates the statistically significant differences ($p < 0.01$) among intensities.

6.4.6 Activity in delta and theta

The time-frequency analysis revealed a low-frequency transient ERS at the beginning of the stimulation, primarily during the *Medium* and *High* intensity conditions. We aimed to further investigate this phenomenon by computing the topographies for the delta and beta bands during the first second of the stimulation.

Figure 6.22) displays the average of the first second of the stimulation for delta (1-4 hertz). The power increase is present only for the *High* and *Medium* intensity conditions, primarily around C_z , CP_z , C_2 , CP_2 , and extending slightly towards C_1 , C_4 , CP_1 , CP_4 , and FC_z . Notably, statistically significant differences from a repeated measure ANOVA with FDR correction ($p < 0.01$) were observed for the electrodes C_z and CP_z .

A similar analysis for theta (4-8 hertz) in figure 6.23, revealed similar results, with a power increase during the *High* and *Medium* intensity conditions. While this activity was observed mainly in central brain areas including C_z , CP_z , C_2 , CP_2 , the power increase extended to posterior areas (P_z , PO_z , PO_1 , PO_2) in the *Medium* and *High* intensity conditions, and even to frontal areas (F_z , AF_4) in the *High* intensity. Despite this evident activity, no statistically significant differences were observed (repeated measures ANOVA, FDR correction, $p < 0.01$)

6.5 Discussion

Our findings provide valuable insights into the effectiveness of the vibrotactile stimulation used in the study. The participant's ability to perceive the vibration precisely at the targeted motor locations demonstrates the successful application of the vibrotactile stimulation. Additionally, participants did not report any vibration on the bracelet holding the motors on the forearm, which confirms the successful specific-location stimulation. Moreover, the varying diffusion patterns experienced by different participants indicates the potential for individualized responses to the stimulation. Overall, the reported sensations confirm the suitability of the designed vibrotactile stimulation and its potential as a feedback modality in kinesthetic motor imagery-based BCIs, particularly for enhancing post-stroke rehabilitation. Nevertheless, further investigation and user feedback may be necessary to optimize the stimulation parameters and ensure its effectiveness and acceptability among post-stroke patients.

6.5.1 User preference for the three-motor sequential configuration

The Likert scores did not reveal statistically significant differences among the various device configurations for any of the evaluated items (Section 6.4.1.2). However, rather than viewing this outcome as a limitation, it actually indicates the successful integration of the vibrotactile stimulation with the visual environment. These results suggest that the multiple vibrotactile device configurations can effectively complement the visual animation of the grasping hand. A forced-choice evaluation was conducted to establish a definitive preference among the configurations. Remarkably, the 3-motor configuration emerged as the clear favorite among participants. Notably, one participant, who practiced weight training at a gym, reported that this particular configuration provided more vivid details about the grasping movement and even evoked sensations reminiscent of the effort involved in grasping during upper limb workouts.

Further analysis of the activation patterns during the 3-motor configuration revealed that participants favored the sequential pattern in three out of four items (comfort, synchronization with the hand animation, and synchronization with the sauce animation). However, the simultaneous pattern was perceived as more coherent with the visual animation. An in-depth examination of the Likert scales for the item "Proportional to Sauce Quantity", indicated a slight preference for the sequential pattern. Taking these factors into account, the decision was made to adopt the sequential pattern for our future studies involving the BCI.

These results demonstrate that the vibrotactile stimulation was successfully synchronized and proportional to the visual animation, regardless of the configuration. Yet, the findings demonstrate the subtle superiority of the three-motor sequential configuration in terms of user preference and highlight the importance of selecting an appropriate activation pattern to enhance the coherence and immersion between the vibrotactile and visual elements of the system. Additionally, the stimulation was perceived as highly comfortable, synchronized, and realistic, highlighting the successful integration of the vibrotactile stimulation with the virtual environment. These findings affirm the feasibility of employing vibrotactile and visual stimulation as a valuable feedback modality for KMI-based BCIs.

6.5.2 Positive user experience and system's attractiveness

We studied the participants' emotional state, fatigue level, and mental workload during the test of the different device configurations. Participants reported feeling more tired towards the

end of the session, with a significant decrease in positive and negative activation emotions. Indeed, the meCUE questionnaire revealed that the majority of participants experience positive deactivation emotions such as relaxation and calmness as well as positive activation such as exhilaration. Negative emotions such as anger and frustration were notably absent. Surprisingly, the system's passive use elicited activation in many participants, suggesting that the stimulation contributed to heightened engagement and attention. Despite the demanding mental workload, the participants coped well, and there was no significant correlation between mental workload and final fatigue levels.

The attractiveness of the system was evaluated through the AttrakDiff questionnaire. Overall, participants found the system desirable, with positive scores for both pragmatic and hedonic qualities and the system's attractiveness. Particularly, the system was perceived as clearly structured, suggesting users found it easy to comprehend and use, despite the stimulation being independent of their brain activity in this study. Additionally, the users considered the system was good for them, which is confirmed by the positive emotions reported through the meCUE questionnaire. However, some variability was observed in the individual response, with participants perceiving the system as either self or task-oriented. This aspect deserves attention in further experiments with BCI and post-stroke patients. Furthermore, we observed an improvement in all negative scores compared to the previous chapter's results, where the vibrotactile device was used alone (see section 5.3.3.2). This improvement suggests two key points:

- The successful integration of the virtual and visual environment contributed to a more positive perception, making the system more likable and pleasant than before.
- The context in which the vibrotactile device is used might significantly impact its attractiveness.

Although progress has been made, certain scores, such as those related to *Inviting* and *Likable* still have room for improvement. One potential approach to address this is by using a "cleaner" prototype of the vibrotactile device, like the second version introduced in section 4.3.1, which was developed towards the end of this thesis. It would be insightful to investigate the results when the system is employed in the BCI context, where the stimulation corresponds to feedback during the execution of KMI, and compare them to the present findings. This further exploration could provide valuable insights to enhance the system's attractiveness and refine its application in practical settings.

6.5.3 EEG activity in the alpha, mu, and beta frequency bands

In this study, we explored the electroencephalographic modulations of brain activity during a bimodal stimulation comprising synchronized visual and vibrotactile stimuli on the non-dominant hand and the forearm. The stimulation involved four device configurations, varying in the number of motors and vibration patterns. We also studied brain activity during four distinct stimulation intensities.

6.5.3.1 ERDs presence in all stimulation configurations and are intensity-dependent

The EEG time-frequency and topographical analyses revealed consistent bilateral ERDs in the motor and somatosensory cortices across two frequency bands: alpha + low beta (8 to 15 hertz), and low beta, (15 to 25 hertz). This activity was observed across all four device configurations, indicating successful stimulation of the contralateral motor and somatosensory cortices. Addi-

tionally, brain activity was observed in the parietal and occipital lobes mainly in the alpha + low beta band, suggesting cognitive processing and visual processing, respectively [214]. The activity in the sensorimotor area was observed regardless of the device configuration, thus, the choice of the optimal vibrotactile device configuration is based mainly on the results from the subjective evaluation of the participants.

The alpha-related activity in the motor and somatosensory cortices might as well correspond to the mu rhythm due to its location [215, 216]. Mu-related activity is present during motor and neurocognitive activities [34] and often mixed with central beta [215]. ERDs act as an electrophysiological representation of cortical network activity when processing sensorimotor information, indicating heightened excitability of cortical neurons during this cognitive process [32, 33, 34]. As the stimulation involves a visual component, which is the virtual hand grasping a bottle, the observed mu-desynchronization corresponds as well to the activation of mirror neurons in response to the observed grasping [217]. These results suggest that the bimodal stimulation leads to enhanced excitability of contralateral cortical neurons in the motor and somatosensory cortices, similar to motor execution, motor imagery, and motor observation [33, 108, 218, 217]. Moreover, we observe that both the ERD location and magnitude vary with the intensity of stimulation (see figures 6.18 and 6.19), where more areas were recruited during the *High* condition. This is consistent with the observations made during an fMRI study, where variations in the somatosensory cortex were observed due to the changes in the vibration frequency applied on the biceps[180].

The ERD observed in the high-beta frequency bands also reflects the activity of somatosensory and motor cortices associated with the bimodal stimulation[219, 205]. Furthermore, the absence of an ERD in the high-beta band for the *None* condition, where vibration was not present, suggests that vibration stimulus elicits EEG modulations in this frequency band rather than visual stimulus.

In summary, our findings indicate the following:

- The bimodal stimulation leads to enhanced excitability of contralateral cortical neurons in the motor and somatosensory cortices, in alpha and beta frequency bands, including the mu rhythm as well.
- The ERDs are independent of the vibrotactile device configuration, i.e. all configurations successfully elicited ERDs on the motor and somatosensory cortices.
- The ERDs seem to be intensity-dependent, with stronger stimulation leading to more prominent ERDs.

6.5.3.2 The ipsilateral ERD relies on the intensity and duration of the stimulation

Surprisingly, we observed an ipsilateral ERD primarily during the *Medium* and *High* intensity conditions in the alpha + low beta frequency band. This observation is consistent with similar findings during focal vibration on the biceps at 75 hertz [220]. The statistically significant differences observed in figure 6.18 are likely due to the ipsilateral ERD present only in *Medium* and *High* conditions, while the contralateral ERD remained constant across all conditions. Thus, our results suggest:

- The ipsilateral ERD is elicited by the vibrotactile component of the stimulation rather than the visual component.

- The ipsilateral ERD is presumably dependent on the intensity, most likely the frequency of the stimulation.

Further studies involving vibrotactile stimulation only without the visual component, as well as vice versa, are necessary to confirm our observations.

6.5.3.3 The post-stimulation ERS may depend on the stimulation intensity

As previously stated, a contralateral ERD was present during all conditions, thus we were expecting an ERS once the stimulation was finished, similarly to the one observed during action observation ([221, 222]). For the alpha + beta band, the ERS was not present during the first second after the stimulation, but it became visible 2 seconds post-stimulation. More specifically, we did not observe an ERS once the *None* intensity stimulation was finished. One possible explanation for this phenomenon is that the virtual hand reopens when the resting phase starts at 2000 ms. This may be interpreted as a second movement that elicits another ERD, suppressing the ERS corresponding to the first movement. It is important to note that the absence of vibration in this condition rules out vibration stimulus as a cause of the missing ERS. On the other hand, during the *Low* and *Medium* conditions, the ERD attenuates at stimuli offset, and an ERS becomes visible in the *High* condition. Additionally, we were expecting a post-stimulation ERS in the high-beta frequency band (15-25 hertz) [219]. The ERS was observed as soon as one second after the stimulation for all intensity conditions, and remained present two seconds afterward, except for the *Medium* intensity condition where it was less visible. **Our observations suggest that the appearance of the ERS is more prominent in the high-beta band and it is dependent on the vibration intensity.**

6.5.4 Activity in delta and theta: a potential indicator of attention and surprise

We observed a significant transient ERS at the beginning of the stimulation in the delta and theta frequency bands (fig. 6.14). Traditionally, delta activity has been related to states of diminished consciousness [223]. Furthermore, it has been suggested that delta oscillations are synchronized with visual cues timing [224] and decision-making in frontal and parietal cortical areas [225]. Yet, we only observed delta activity in the *Medium* and *High* conditions, and the visual cues were deliberately varied to prevent participant anticipation. Therefore, we cannot conclude that delta activity resulted solely from the visual cues. Activity in the delta band has been previously reported during continuous-attention tasks [226] and during vibrotactile stimulation of the biceps during an eyes-opened condition suggesting it increased attention [206]. Given that we observed delta activity only in the *Medium* and *High* conditions, it is plausible that attention is proportionally dependent on the vibration intensity, where stronger vibration attracts more attention from the user, reflected as a larger delta synchronization. Further studies on attention and vibrotactile stimulation are needed to substantiate this hypothesis.

Similarly, the theta band displayed an ERS during the first second of the stimulation. Theta EEG oscillations have a role in attentive visual exploration of space [123, 122] Indeed, the visual stimulation involves various elements: the hand movement, the ketchup flowing, and the moving gauge. Thus, attention may be separated to process the different visual stimuli and modulated at theta, as described in [122]. Furthermore, an increase of medio-frontal theta power has been observed when participants are presented with a novel stimulus [227] and in frontal areas during surprise [228]. Indeed, the *Medium* and *High* intensity conditions may cause surprise as

they encompass stronger, yet comfortable, vibrations. However, during intensity conditions, the increase in theta power was more important in central electrodes than in frontal ones, which are correlated with decision-making and recognition memory [229]. This may suggest that participants were indeed comparing the different stimulation they were receiving by recalling previous ones.

6.6 Limitations and Future Work

The study presented in this chapter presents the following limitations. Firstly, we conducted the study on neurotypical volunteers who had no sensory impairments of the upper limb. This step was essential because this particular group is more adept at describing and discerning changes in stimulation, such as different intensities and sequential versus simultaneous activation. It was crucial for us to validate these distinctions during the design phase. While individuals who have experienced a stroke may initially struggle to differentiate these characteristics, as they begin to regain lost functions, their ability to do so may improve. Therefore, it is prudent for us to anticipate this progression. However, it is worth noting that sensory thresholds may vary among stroke survivors, as some patients may exhibit sensory deficits such as reduced or heightened tactile sensitivity. Consequently, it is vital to evaluate the somatosensory sensory capabilities of post-stroke patients before implementing the proposed device [198].

Furthermore, it was impossible to differentiate the brain activity resulting from the visual component of the stimulation and the one from the vibrotactile one because they were synchronized. To gain further insights and isolate the effects of each stimulus at different intensities, it would be valuable to perform a study comparing different stimulation modalities. Such research could enhance our understanding of how the brain processes vibrotactile information on the forearm and hand. Further investigations and experiments will help establish the precise mechanisms underlying these EEG modulations and their implications for BCI applications.

In the upcoming chapter, we will present the incorporation of our proposed bimodal stimulation into the functional KMI-based BCI GraspIT to assess its impact on BCI performance and user experience. In this context, the stimulation will depend on the brain activity during KMI, hence it will be used as feedback. As demonstrated in this article, visual and vibrotactile stimulation enhances neuronal activity in the motor and somatosensory cortices. This may be beneficial when the objective is to improve the detection of motor imagery or motor attempts by dedicated algorithms. However, overlapping of the brain activity due to the KMI and the stimulation may occur. In this case, there is the risk of giving feedback based on the stimulation rather than on the user's activity. In the context of post-stroke motor rehabilitation, this is concerning because our aim is that the patients learn to modulate their brain activity to promote recovery. Thus, giving feedback based on other activities rather than their own is useless and nonsense. Therefore, in our protocol, the feedback will be provided once the KMI task concludes to avoid overlapping of the brain activity. Furthermore, we will compare the bimodal feedback to visual-only and vibrotactile-only feedback, expecting variation in EEG oscillations during the feedback phase due to the distinct sensory modalities.

6.7 Conclusion

In this study, we compared four distinct configurations of a novel vibrotactile device to determine the most suitable option for synchronizing with the animation of a virtual hand grasping a bottle.

All four configurations were successfully synchronized and coherent with the visual environment. Nevertheless, the three-motor configuration emerged as the clear preference based on a forced-choice evaluation.

The user evaluation during the session showed that it was well-tolerated by participants, producing positive emotional responses and demonstrating an overall attractiveness for the system. The findings from this study provide valuable insights into the system's positive impact on participants' emotional states and its potential for enhancing engagement in the context of KMI-based BCIs. The positive perception of the system encourages its further research and development, not only in the BCI-related field but also for further applications in assistive technologies, rehabilitation, and immersive virtual experiences.

In addition, our study delved into the EEG modulations elicited by the bimodal stimulation. The different configurations of the vibrotactile device led to an increased excitability of sensorimotor areas, characterized by of alpha and beta desynchronization. Moreover, this activity revealed variations depending on the stimulation intensity. Interestingly, this activity was not limited to central regions but also pre/postcentral, posterior, and occipital brain regions. Contrary to our expectations, bilateral central brain activity was observed, varying with the stimulation intensity, with the contralateral hemisphere showing stronger activity. Furthermore, the stimulation induced an increase in synchronized delta and theta power, particularly during the strongest stimulation intensities, suggesting their potential role in attention.

Overall, our findings provide valuable insights for refining the design of a BCI paradigm employing the proposed bimodal stimulation as feedback for KMI of the upper limb. They also offer useful information regarding the brain responses associated with different stimulation intensities, paving the way for improved BCI implementation. As we continue to explore and optimize the system, these insights will be beneficial in maximizing its efficacy and usability, further advancing the BCI field and potential application in other domains.

Chapter 7

Evaluation of a KMI-Based BCI Integrating Visual and Vibrotactile Feedback

Contents

7.1	Introduction	108
7.2	Material and Methods	109
7.2.1	Participants	109
7.2.2	Experimental Setup	110
7.2.3	Questionnaires	110
7.2.4	Experimental Procedure	111
7.2.5	Online Classification	115
7.2.6	EEG Offline Analysis	116
7.2.7	Statistical Analyses of Behavioral Data and BCI Performance	117
7.3	Results	117
7.3.1	BCI Performance Across Feedback Modalities	117
7.3.2	Participants' Subjective Assessment of the Bimodal BCI	121
7.3.3	Evaluation of the Participants' Well-Being	125
7.3.4	Influence of Participant's Characteristics on BCI Performance	131
7.3.5	System's Elicited Emotions and Attractiveness	135
7.3.6	EEG Analysis	139
7.4	Discussion	146
7.4.1	BCI performance is comparable in all feedback modalities	146
7.4.2	Participants' preference for the bimodal feedback	146
7.4.3	Factors influencing the performance	147
7.4.4	The bimodal BCI offers a positive user experience	149
7.4.5	EEG activity	150
7.5	Conclusion	151

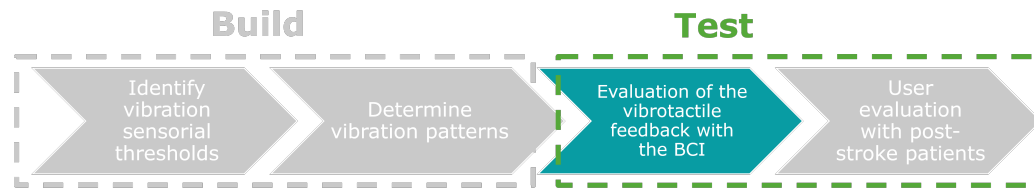


Figure 7.1: Methodology for designing and evaluating vibrotactile feedback: Test phase - Evaluation of the feedback.

Related publication

- Herrera Altamira, G., Fleck, S., Lécuyer, A., & Bougrain, L. "Visuo-Vibrotactile Feedback to Support Kinesthetic Motor Imagery of Grasping" *In preparation*.

7.1 Introduction

In the chapters 5 and 5 the design process of the vibrotactile stimulation was presented. The vibrotactile device's intensities were tailored according to the participant's age, and the vibration pattern that best matched the visual animation of a virtual hand grasping a bottle was selected. In this chapter, the carefully designed stimulation is used and evaluated as a feedback modality within our KMI-based BCI, FeelIt. This chapter corresponds to the third step of the methodology depicted in figure 7.1.

As discussed in chapter 2, KMI-based BCIs are a promising technology for post-stroke rehabilitation. However, KMI is a challenging task to perform due to the absence of kinesthetic and proprioceptive feedback. This issue may be addressed by providing artificial feedback, either visually or haptically. Visual feedback can take various forms, such as a bar that extends to a specific direction if the task is executed correctly [230]. However, enhancing the sense of embodiment through realistic feedback is essential for improving motor imagery learning [231]. Visual feedback, while valuable, still lacks kinesthetic and proprioceptive components and may not be the optimal solution to enhance KMI.

Haptic modalities can then offer an alternative solution to close the sensorimotor loop by stimulating the tactile and kinesthetic senses. Functional electrical stimulation, exoskeletons, and robots have been proposed as solutions to induce movement that indicate changes in brain activity during motor imagery. While these technologies offer therapeutic benefits [31], 40% of post-stroke patients struggle to achieve an acceptable BCI accuracy of 70% [232], hindering their potential to benefit from BCI training. Moreover, patients with limited limb movement may find these feedback modalities uncomfortable, calling for the development of an alternative feedback approach.

Vibrotactile stimulation has been employed in post-stroke rehabilitation (see chapter 1) and in MI-based BCIs, but its potential in BCIs for post-stroke motor rehabilitation remains underexplored. Furthermore, multimodal feedback can offer a more comprehensive experience [152], and be more effective than unimodal feedback [233], especially for inexperienced subjects [234]. However, designing multimodal feedback requires careful consideration to ensure it re-

mains understandable and does not overly tax users already engaged in the challenging KMI task [235, 230]

In this chapter, a study is presented in which two feedback modalities are combined: 1) gamified visual feedback consisting of a hand pressing a bottle and 2) the carefully designed vibrotactile feedback that delivers information about the KMI of a grasping movement. The integration of these feedback modalities is accomplished through the BCI FeelIt, introduced in chapter 4. The primary objective was to compare three feedback modalities within a KMI-based BCI and determine whether the bimodal feedback modality could enhance grasping KMI compared to unimodal alternatives, all while ensuring a positive user experience.

Based on previous observations in the literature, it is expected the BCI performance to increase or at least remain similar during bimodal feedback compared to unimodal visual or vibrotactile feedback. Additionally, the unimodal vibrotactile feedback may free the visual channel, resulting in comparable or increased BCI accuracy to the visual feedback [38, 7, 203, 42].

Regarding EEG oscillations, we anticipate observing contralateral ERD in mu and beta frequency bands, which are typically associated with motor imagery [33, 137], in all feedback modalities, with a more significant effect during the bimodal feedback. Furthermore, ERD in the sensorimotor cortex should be more pronounced in the contralateral hemisphere to the stimulation, increasing during the bimodal feedback compared to the unimodal visual or vibrotactile feedback [39, 40, 206].

Personality traits and participants' characteristics have been shown to influence BCI performance [236, 141]. Therefore, an assessment was conducted to determine whether manual activities, sports, and meditation practices may influence BCI performance.

In summary, this study aims to demonstrate that the BCI FeelIt, integrating carefully designed visual and vibrotactile feedback, supports the execution of KMI of grasping and has the potential to be used in post-stroke motor rehabilitation of the upper limb.

7.2 Material and Methods

To study the different feedback modalities and determine the most effective one for enhancing KMI of grasping, we conducted a study where participants were exposed to three feedback modalities: visual-only, vibrotactile-only, and bimodal, consisting of the coupled visual and vibrotactile modalities. All participants signed an informed consent approved by the local ethical committee of Inria (COERLE, approval number: 2022-32).

7.2.1 Participants

A cohort of 39 healthy and neurotypical participants was recruited, spanning ages 18 to 60 years, with an average age of 38.18 years and a standard deviation of 10.89. One male participant was removed from the experiment because the BCI performance was always 100%. Thus, the system did not work correctly for this person, and the answers to the questionnaires may not be considered valid. The resulting gender distribution included 18 female and 20 male participants. Furthermore, 35 participants were right-handed, while three were left-handed. None of the participants presented depression, epilepsy, stroke, diabetes, chronic fatigue, or any other neurological disease. Additionally, no skin disorders affecting the arms and hands were reported, and none were undergoing anxiolytic treatments or any other medical interventions that might

interfere with the experimental sessions. Importantly, none of the participants indicated the consumption of drugs.

7.2.2 Experimental Setup

The participants sat comfortably on a chair. EEG signals were recorded with a BioSemi Active Two 64-channel EEG system following the international 10-10 system and a sampling rate of 2048 Hz. A screen was placed in front of the participants to display the non-immersive virtual environment, featuring a hand grasping a ketchup bottle, a traffic light, and a vertical gauge.

The experimental procedure commenced with properly placing the EEG cap and installing the vibrotactile device on the forearm and hand of the participant's non-dominant limb. The final device is intended for stroke victims with upper limb hemiparesis. Consequently, participants should perform the tests on the non-dominant limb to get closer to this situation, as recall of sensations is usually more complicated. The participant's arm was placed on a pillow so the vibration would not propagate on a hard surface and generate undesired stimuli. The participants held a bottle with the same hand that participants perform KMI of, as previous research suggested that mu rhythm is increased by the presence of an object during the observation of an action [237].

7.2.3 Questionnaires

While the experimenter was placing the EEG cap, participants answered the following questionnaires:

- Medical Emotional Scale (MES) [193], to measure the participants' emotional state at the beginning of the session.
- Four-Item Fatigue Screen (FIFS) [194], to evaluate the participants' initial fatigue.
- New Self-efficiency general scale (NGSE) [238], to measure the participants' self-perceived efficiency.
- Freiburg Mindfulness Inventory (FMI) [239] to assess mindfulness abilities.
- a dedicated questionnaire to identify manual, sport, and meditation habits (available in Annex B).

After the calibration and each feedback modality condition (visual, vibrotactile, and bimodal), participants answered the following questionnaires:

- FIFS, to evaluate the fatigue evolution.
- NASA-TLX, to evaluate the subjective cognitive workload [208].
- NEXT-Q, to evaluate cognitive states during the training session [240].

At the end of the session, participants answered the following questionnaires:

- a dedicated questionnaire to rank feedback modalities by order of preference (available in Annex C).
- a dedicated questionnaire to evaluate the influence of feedback modalities in the execution of KMI (available in Annex C).

- MES, to compare the participants' emotional state before and after the session.
- a short version of the AttrakDiff questionnaire [195] to evaluate the system's usability and attractiveness.
- the module II of the meCUE questionnaire [209], to evaluate the emotions elicited by the interaction with the system.

It is important to note that the *system* was defined as the vibrotactile device, the screen with the virtual environment, and the EEG cap.

7.2.4 Experimental Procedure

Once participants were equipped with the EEG cap and the vibrotactile device, they started the KMI training with the BCI. The experimental session consisted of three consecutive stages: 1) learning to perform KMI, 2) calibration, and 3) feedback.

7.2.4.1 Learning to Perform KMI

Before using the BCI, we ensured the participants understood how to perform the KMI of a grasping movement. We followed the training proposed in [184] to avoid highly variable performances due to the difficulty of performing KMI [241]. This training consisted of four main stages:

1. *Feel the movement*: The experimenter described all the sensations (muscular contraction, skin stretching, pressure, temperature) that participants should actively perceive or attend to while executing a grasping movement. Subsequently, participants executed the movement for a brief interval to gain awareness of these sensations.
2. *Feel the KMI*: In this stage, the participants performed micromovements while holding in their awareness the sensations discerned in the preceding phase. Gradually, this process facilitated the seamless transition into KMI.
3. *Perform the KMI*: Participants performed the KMI without any physical movement for a few minutes, focusing on the sensations they identified previously.
4. *Implement the KMI*: The participants executed five trials with the visual interface to learn to perform the KMI following the instructions given by a traffic light, as explained in sections 7.2.4.2 and 7.2.4.3.

Notably, between steps one and two, participants engaged in a brief dialogue with the experimenter, facilitating the articulation of the sensations identified during actual movements. This procedure, in turn, enabled the experimenter to validate the correctness of the executed movements and the congruence of focused sensations. Furthermore, participants were reassured they were performing the correct mental task.

7.2.4.2 Calibration

Once the participants learned to perform the KMI, they performed it following the instructions of the visual environment without feedback to train the classifier. This calibration phase encompassed two runs, each comprising 20 trials to furnish the classifier with an ample dataset for its training.

The participants were presented with visual cues manifested through a traffic light delineating the KMI/rest phases, as depicted in figure 7.2. The chronological sequence of one calibration trial unfolded as follows: initially, the traffic light was red for 30 seconds when the participants were in a resting state, i.e., no movement or motor imagery was needed. This interval allowed participants to prepare and establish a baseline of their EEG activity. Subsequently, the light transitioned to red and orange (warning phase) for a span of two seconds, during which the participant prepared to perform a KMI. Once the light turned green, the participants engaged in the KMI task for a duration of four seconds. Finally, the light turned red for a random interval between five and seven seconds, marking a resting phase where the participants did not move nor perform KMI. The trial concluded once the resting phase was finished and the red and orange lights resumed (warning phase), initiating a new trial. Throughout the entire run, participants were presented with the virtual hand holding the ketchup bottle; however, it remained stationary, abstaining from any form of feedback. Participants had a two-minute pause between runs.

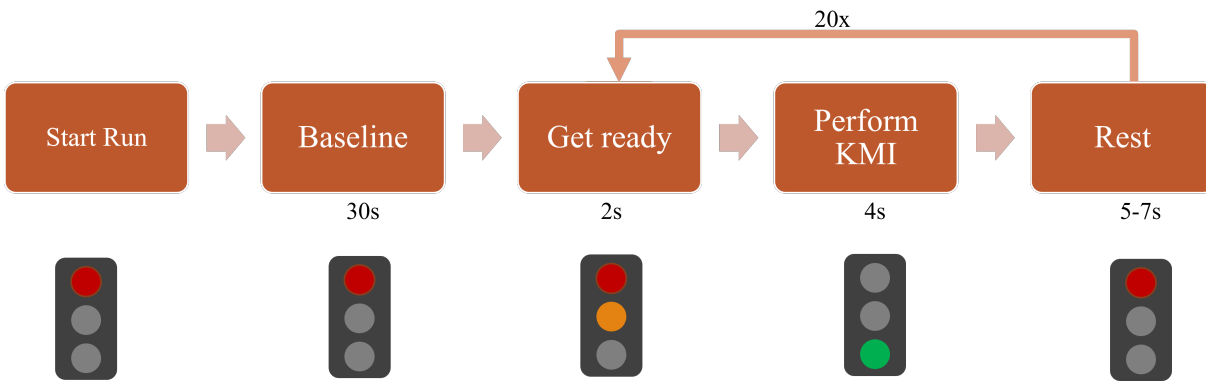


Figure 7.2: Calibration run consisting of 20 trials. Participants performed KMI without any feedback during the calibration. *s* stands for seconds.

7.2.4.3 Feedback

When testing the different types of feedback, the participants underwent a series of two runs, encompassing 15 trials each for every given condition. This procedure was very similar to the calibration phase, with a notable modification: upon executing the KMI (indicated by the green light), participants received feedback was given to the participant, during which an orange light was displayed. The feedback modality was either visual, vibrotactile, or bimodal. It is important to note that the feedback was presented after the participant completed the KMI. This strategic timing ensured participants could concentrate on either performing the KMI or the assimilation of the feedback, unfettered by concurrent cognitive demands. Lastly, the light turned red for a random duration between five and seven seconds to indicate a resting phase where the participant did not move, nor performed KMI. The trial was completed after the resting phase was over and the red and orange lights turned on again (warning phase), starting a new trial, as shown in figure 7.3. Participants tested all three feedback modalities in a pseudo-randomized order. Each of the feedback modalities is explained in the following sections.

7.2.4.3.1 Visual Feedback Modality During this feedback modality, the participants were presented with an animation of a virtual hand performing a grasping movement of a ketchup

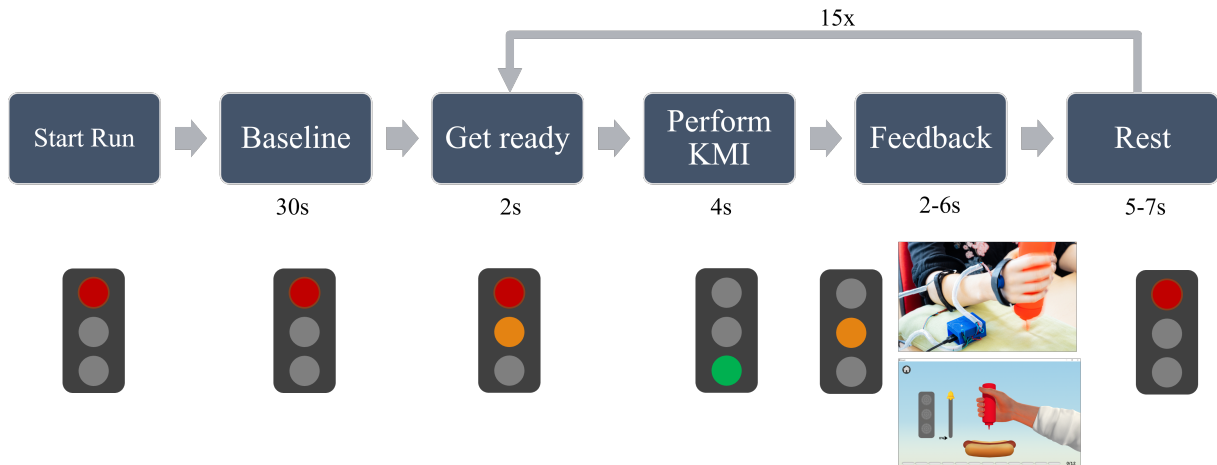


Figure 7.3: Feedback run consisting of 15 trials. Participants performed KMI and received visual, vibrotactile, or bimodal feedback. *s* stands for seconds.

bottle to put the sauce on a hot dog for a variable time duration. The quantity of ketchup displayed corresponds to four different levels: no ketchup, small, medium, and large sauce quantity, corresponding to the participants' performance as detailed in table 7.1. Additionally, next to the hand, a gauge presented the level of performance, and the participant's best performance of the run was displayed next to it. If the participant achieved a score of 100%, the bell on top of the gauge vibrated as if it was ringing, without producing any sound.





Performance	Duration [s]	Sauce Quantity	Visual Feedback
0% - 25%	2	No ketchup	
25% - 50%	2	Small ketchup quantity	
50% - 75%	4	Medium ketchup quantity	
75% - 100%	6	Large ketchup quantity	

Table 7.1: Four levels of visual feedback corresponding to the participant's performance

7.2.4.3.2 Vibrotactile Feedback Modality In this condition, the virtual hand was not presented on the screen, but the traffic light remained to give the indications to the participant, as shown in figure 7.4. The vibration was activated only when the light was orange after KMI. Similar to the visual feedback condition, vibrotactile feedback consisted of four levels: no vibration, low, medium, and high vibration intensities, as shown in table 7.2. The vibration intensities depended on the participant's age, thus, they were modified according to the results we presented in chapter 5. The activation and deactivation of the vibration were sequential, according to the results obtained from the previous chapter 6.

Performance	Duration [s]	Vibration Intensity
0% - 25%	2	None
25% - 50%	2	Low
50% - 75%	4	Medium
75% - 100%	6	High

Table 7.2: Four levels of vibrotactile feedback corresponding to the participant’s performance

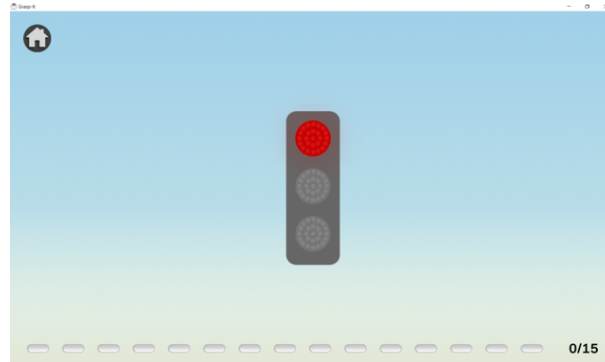


Figure 7.4: Traffic light provides instructions for the participants when visual feedback is inactive.

7.2.4.3.3 Bimodal Feedback Modality The bimodal feedback consisted of synchronized visual and vibrotactile modalities presented after the KMI phase. The vibration was activated and deactivated sequentially, as described in the previous chapter 6. Similarly to the unimodal feedback modalities, the bimodal feedback was proportional to the KMI performance, as explained in table 7.3.





Performance	Duration [s]	Vibration Intensity	Visual Feedback
0% - 25%	2	None	
25% - 50%	2	Low	
50% - 75%	4	Medium	
75% - 100%	6	High	

Table 7.3: Four levels of bimodal feedback corresponding to the participant’s performance

7.2.4.3.4 Order of presentation of feedback modalities The presentation order of the feedback conditions was pseudo-randomized to avoid any biases and ensuring the same number of participants for each group in the following way:

1. All participants started with the calibration phase, with no feedback.

2. The feedback modality was presented in one of the next order combinations:

- (a) Group A: Visual \rightarrow Vibrotactile \rightarrow Bimodal
- (b) Group B: Visual \rightarrow Bimodal \rightarrow Vibrotactile
- (c) Group C: Vibrotactile \rightarrow Visual \rightarrow Bimodal
- (d) Group D: Vibrotactile \rightarrow Bimodal \rightarrow Visual
- (e) Group E: Bimodal \rightarrow Visual \rightarrow Vibrotactile
- (f) Group F: Bimodal \rightarrow Vibrotactile \rightarrow Visual

7.2.5 Online Classification

7.2.5.1 Training of the classification algorithm

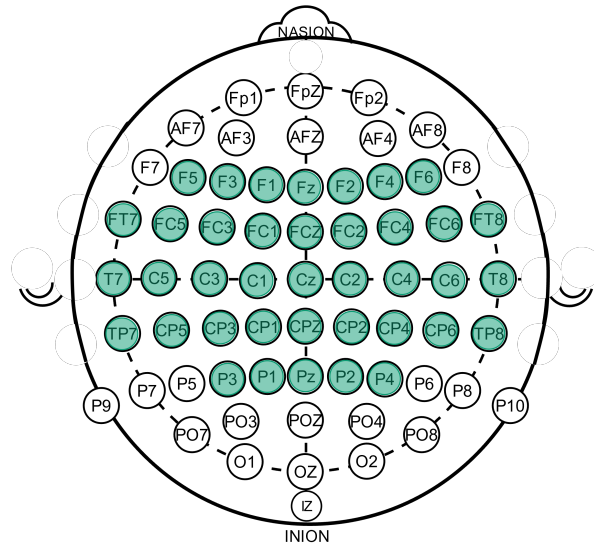


Figure 7.5: 39 electrodes (in green) selected from the original 64-electrode setup.

The software OpenViBE 3.3.0 [183] was used to train the classification algorithm. First, for each calibration run, a subset of 39 electrodes was selected out of the original 64, as visually depicted by the green markers in figure 7.5. Next, the two calibration runs were concatenated, followed by applying a bandpass filter between 8 and 30 hertz. The filtered EEG was then segmented into epochs lasting 2.5 seconds each, aligning with the KMI/rest phases. An epoch offset of one second was applied for the KMI phase and two seconds for the rest phase. These extracted epochs served as the basis for training a Common Spatial Patterns (CSP) filter. Additionally, time-based sub-epochs of one-second duration, with a sliding window of 0.0625 seconds, were extracted from each KMI/rest epoch. the log-transformed average epoch power was computed employing the formula:

$$\log(1 + \overline{X}) \quad (7.1)$$

where \overline{X} is defined as:

$$\overline{X} = \frac{1}{n} \sum_{t=1}^n x_t^2 \quad (7.2)$$

In the latter equation, t represents a specific time point, while n signifies the total number of time points within the epoch. The resultant values were aggregated in a feature vector, which was used to train a Linear Discriminant Analysis (LDA) algorithm to classify KMI and rest epochs. This process was executed on an individual participant basis.

7.2.5.2 Test of the classification algorithm: feedback scores

The online classification was performed using the previously trained CSP+LDA algorithm based on epochs with a one-second duration and a sliding window of 0.0625 seconds. This configuration yielded a total of 40 epochs for each KMI/rest phase, translating to 40 classification labels produced by the classifier. The feedback score was computed based solely on the recall of the KMI class, which is the number of correct classification outputs. This score was quantified by employing the following equation:

$$score = \frac{\text{true positives}}{\text{true positives} + \text{false negatives}} * 100\% = \frac{\text{true positives}}{40} * 100\% \quad (7.3)$$

Consequently, in this context, BCI performance refers to the feedback score based on the recall presented in the previous equation.

7.2.6 EEG Offline Analysis

The offline analysis of EEG signals was performed with EEGLab v2023.0 [210] toolbox in Matlab R2021b. First, the raw EEG data were re-referenced using the Common Average Reference (CAR) method. Next, data was high-pass filtered at 1 Hz and a 50 Hz notch filter was applied to remove line noise. Then, data were downsampled to 128 Hz after applying an antialiasing low-pass filter at 64 Hz. A high sampling rate was needed to follow the recommendation of $20 \times (\text{number of channels})^2$ data points to perform an independent component analysis (ICA). A visual inspection was performed to eliminate channels that presented artifacts even after the mentioned preprocessing filters. From this inspection, we observed the last three seconds of all EEG files presented extreme EEG values that polluted the ICA decomposition. Therefore, the last three seconds of each run were eliminated from all files. Moreover, eight participants had files that exhibited extremely noisy signals and thus were excluded from the EEG study. One more participant was excluded because their feedback score was consistently 100% during the whole training session, indicating the BCI did not work successfully for this particular participant. After removing the noisy channels, CAR was applied again to the signals because it is based on the mean value of all electrodes.

Subsequently, the ICA analysis was performed using the toolbox in EEGLab. All the files concerning one participant were concatenated, as they were all recorded during the same session. In this way, ICA results in a more robust decomposition as the number of samples is increased. The resulting components were automatically labeled using the IClab tool. Finally, the components labeled as muscle, eye, heart, or line noise were removed.

After the preprocessing stage, the epochs corresponding to the KMI were extracted. The beginning of the epoch was considered two seconds before the start of the KMI, and the end of the epoch was set to nine seconds after the start of the KMI. Thus, the total duration of one KMI epoch was 11 seconds. As a reminder, the duration of the KMI was four seconds. During the calibration phase, the KMI was followed by a rest phase of five to seven seconds, while during the feedback phase, the KMI was followed by a feedback phase of two to four seconds. Each epoch

was labeled according to the calibration phase or the feedback modality (visual, vibrotactile, or bimodal).

Finally, the Event-Related Spectrum Perturbations (ERSPs) were computed to perform a time-frequency analysis and study the variations in frequency across time. The baseline for this analysis was defined at 1000 ms before KMI onset. The average was computed among right-handed ($n=27$) and left-handed participants ($n=3$). Finally, these results served to obtain topographies corresponding to the average EEG power during KMI for mu and beta frequency bands over the brain cortex and compare it across feedback modalities and calibration. The EEGlab statistics study tool was used to compare ERSPs across the calibration phase and feedback conditions. Repeated measures ANOVA was performed, with permutation and FDR correction for multiple comparisons.

7.2.7 Statistical Analyses of Behavioral Data and BCI Performance

A series of comprehensive statistical analyses were performed with the jamovi software [213] aligned with the objective of the evaluation. In an initial step, all data, including responses to the different questionnaires and the BCI performances, were tested for normality using the Shapiro-Wilk test with a significance level $\alpha = 0.05$ and complemented with the visual inspection of the Q-Q plots. Subsequently, when comparing feedback modalities or presentation order, both involving multiple groups, a repeated measures ANOVA analysis was conducted with a significance level of $\alpha = 0.05$. When a significant difference emerged, post hoc Tukey pairwise tests were administered, maintaining the significance level at $\alpha = 0.05$. Alternatively, when the data distribution was different from a normal distribution, Friedman's repeated measures ANOVA analysis was performed at a significance level of $\alpha = 0.05$. Afterward, pairwise comparisons were analyzed via the Durbin-Conover test with a significance level $\alpha = 0.05$.

Exploring correlations between two variables, for instance, BCI performance and a behavioral measurement (such as fatigue, emotions, mental workload, system attractiveness, etc.), involved computing the Pearson's r correlation coefficient at $\alpha = 0.05$. Alternatively, when data distribution deviated from normality, Spearman's rho coefficient was calculated also at $\alpha = 0.05$. These correlations allowed to study the influence of the behavioral measurement on BCI performance.

Additionally, when contrasting fatigue or emotional states at the session's beginning with those at the end, a student t-test was employed at $\alpha = 0.05$. For data displaying a non-normal distribution, a Wilcoxon rank test was performed again at a significance level at $\alpha = 0.05$. This comparison was performed to control the participants' well-being during the study. Detailed information regarding the tests performed and their respective outcomes is provided in the Results section.

7.3 Results

7.3.1 BCI Performance Across Feedback Modalities

In this section, the BCI performances are presented in the form of average feedback scores described in section 7.2.5.2. The mean scores regarding each feedback modality across trials were computed for each participant.

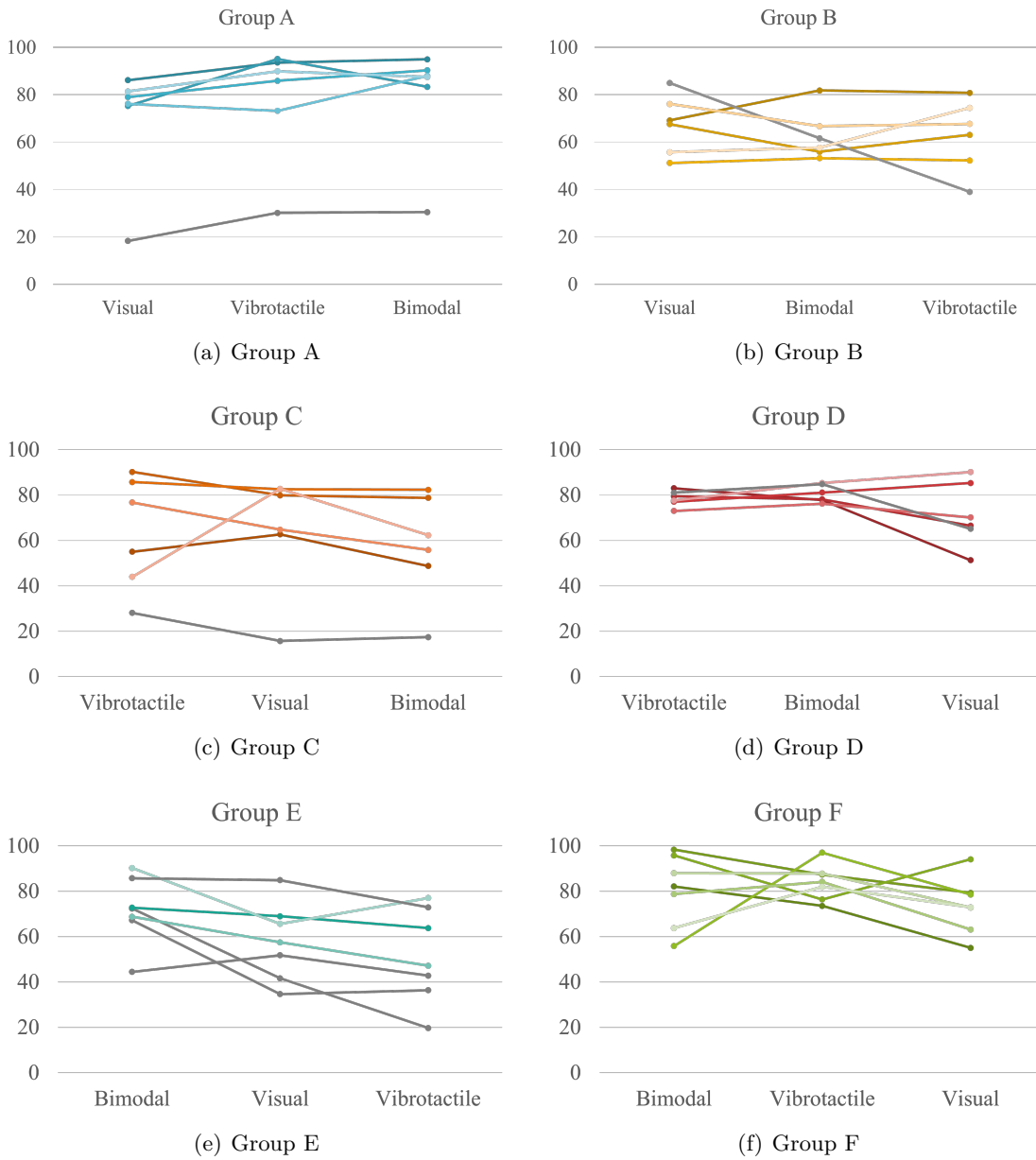


Figure 7.6: Individual BCI performance represented as the feedback scores [%] across the three feedback modalities and grouped by presentation order. Each subfigure depicts a distinct group, with individual participants' data illustrated as lines. The dashed line indicates the chance level of classification (50%).

7.3.1.1 Individual mean feedback scores

First, the average feedback scores were examined for each participant individually, presented in figure 7.6, according to the group of the order of presentation. This figure facilitated a first visual inspection to identify the participants who exhibited average performance levels below chance (50%) across all three feedback modalities. These five participants did not manage to control the BCI for a variety of reasons.

These participants were distributed across groups A, C, and E. Notably, the participant in group A (fig.7.6(a)) encountered considerable ambient noise within the experimental setting, possibly exerting an adverse effect on their concentration during the session. Furthermore, within group E (fig.7.6(e)), one participant exhibited a drop in performance probably due to problems during the acquisition where the system stopped working abruptly. Two more participants presented a considerable amount of artifacts on the EEG signals, probably explaining their low performances. These distinct cases warrant special attention in the subsequent sections as we attempt to determine the factors contributing to their diminished performance. Moreover, one participant in group B (fig.7.6(b)) presented a drop in performance due to a disconnected electrode. Two participants in groups D (fig.7.6(d)) and E also presented EEG signals with a considerable amount of artifacts, resulting in high performances. All of these participants are marked in gray in their respective graphs in figure 7.6.

7.3.1.2 Feedback scores by feedback modality and presentation order

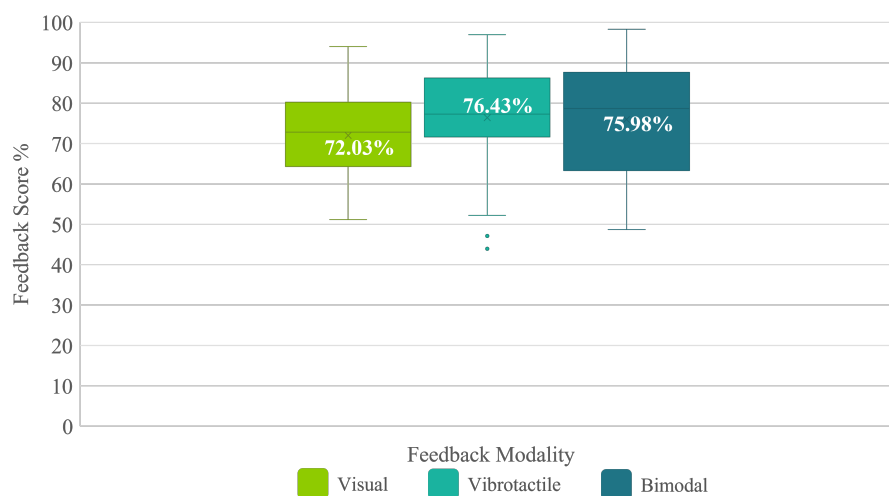


Figure 7.7: BCI performance represented as the feedback scores [%] across the three feedback modalities. The average across participants is displayed in the white numbers.

To assess the influence of feedback modality and presentation order on the feedback scores, it was necessary to remove some participants. This choice was due to some EEG being polluted or recorded incorrectly, for instance, electrodes that were disconnected during the session. These issues lead to either very low or high performances that do not rely on the participant's brain activity. Therefore, their interaction with the BCI cannot be considered valid, and the feedback scores are not correlated correctly with the mental task. Thus, the cohort of participants used for this section consisted of 30 participants, and three of them were left-handed. The average age was 31.65 years old s.d. 10.89, and 14 of them were female.

The first step involved comparing the performance scores across feedback modalities. The mean performances are presented in figure 7.7, grouped by feedback modality. The vibrotactile modality exhibited the highest mean feedback score 76.43%, closely followed by the bimodal modality with 75.98%, and the visual modality scored the lowest with a mean of 72.03%. The repeated measures ANOVA indicated that there were no statistically significant differences due to the feedback modality ($p = 0.183$). All three modalities exhibited a score greater than 70%, considered a standard for the good functioning of a BCI [242]. Thus, the BCI is reliable for any of the three employed modalities. A summary of the average feedback scores and the standard deviation is provided in table 7.4.

Table 7.4: Mean feedback scores and standard deviation for the three feedback modalities.

	Visual	Vibrotactile	Bimodal
Mean	72.03%	76.43%	75.98%
S.D.	11.32%	13.68%	13.99%

Subsequently, it was not possible to test the differences due to each presentation order group (from A to F), because after removing participants, the groups did not have the same number of participants. In fact, group E consisted finally of only three individuals, while other groups, such as group F, consisted of seven participants. This group imbalance did not allow for comparative analysis.

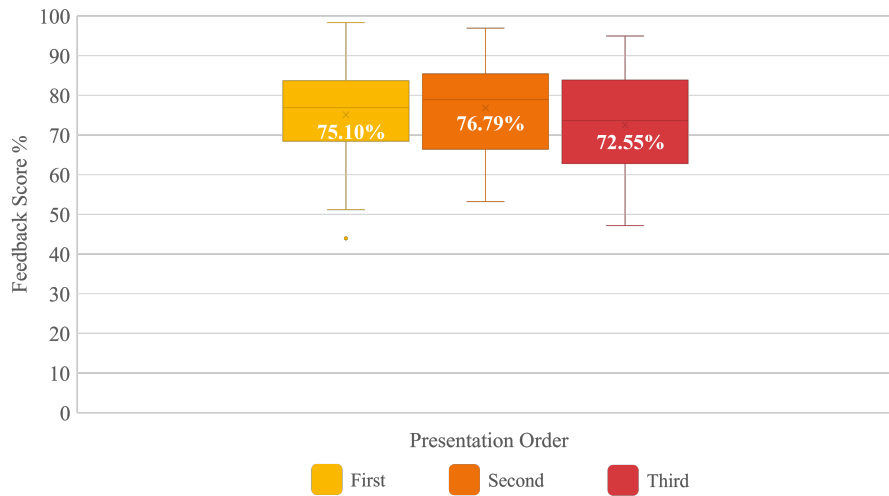


Figure 7.8: BCI performance represented as the feedback scores [%] grouped by order of presentation, regardless of feedback modality. The average across participants is displayed in white numbers.

Therefore, to assess the effect of presentation order on the performance score, the average scores were grouped by first, second, and third presentation order, regardless of the feedback modality. The results are depicted in figure 7.8. A small decrease was observed in the third condition (72.55%) compared to the first (75.10%) and second (76.79%) conditions. Nevertheless, this difference was not statistically significant, as demonstrated by repeated measures ANOVA ($p = 0.0.238$). A summary of the feedback scores by order presentation and the standard deviation is presented in table 7.5. In future research, it will be important to verify that this reduction is not greater during longer experimental sessions.

Table 7.5: Mean performance scores and standard deviation by order of presentation.

	First	Second	Third
Mean	75.10%	76.79%	72.55%
S.D.	13.13%	11.99%	14.06%

7.3.2 Participants' Subjective Assessment of the Bimodal BCI

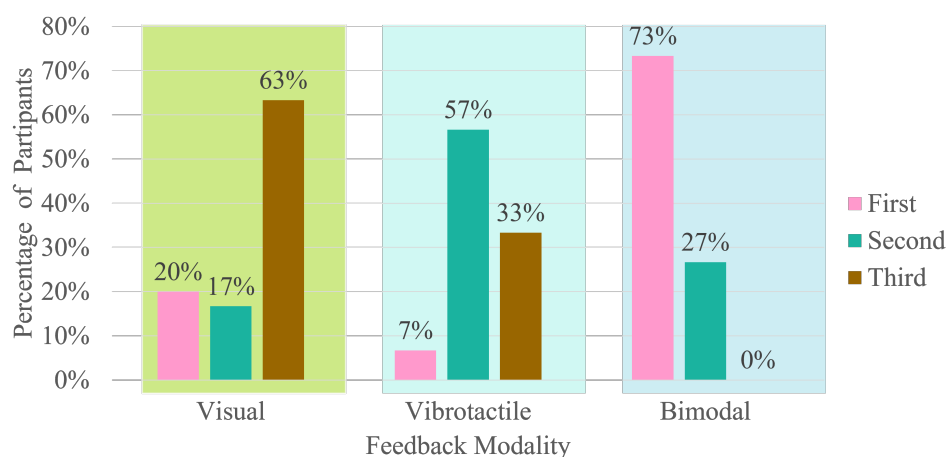


Figure 7.9: Ranking of feedback modalities: each modality (visual, vibrotactile, bimodal) was ordered as the first, second, or third preference. The results are shown as the percentage of participants that preferred each modality.

Participants performed a subjective assessment concerning their preferred feedback modality. Thus, for this assessment, the cohort of 30 participants was involved, as the correct interaction with the BCI may influence their preferences. For instance, participants with incorrectly high scores, polluted by wrong EEG acquisition, may be biased towards a modality, hence the importance of removing them from the analysis.

Based on subjective assessments, as illustrated in figure 7.9, a significant majority of 73% of participants expressed a pronounced preference for the bimodal feedback modality. In contrast, only 20% and 7% selected the visual and vibrotactile modalities as the first preferred choices, respectively. Ranking the modalities by order of preference allowed for a comprehensive analysis of the second and third choices. Surprisingly, the vibrotactile feedback emerged as the second most favored option with 57% of participants selecting it, while the visual modality was the third preferred option for 63% of the participants. Notably, the bimodal option was never ranked as the third choice, reinforcing its unequivocal distinction and preference over unimodal feedback.

To gain deeper insights into the participants' preferences, an analysis of five additional items was conducted. Firstly, figure 7.10 clearly shows that 60% of the participants indicated that the bimodal feedback helped them to perform the KMI. Only 23% and 17% of the participants selected the visual and vibrotactile modalities as the ones that helped the most, respectively.

Similarly, figure 7.11 points out that the bimodal feedback was perceived as the most entertaining (63%), followed by the visual (27%) and vibrotactile (10%) modalities. Furthermore, the bimodal feedback was perceived as the most realistic by 53% of the participants. Interestingly, one participant indicated the No Feedback condition (the calibration phase) as the most realistic

The feedback modality that helped me to imagine the movement better:

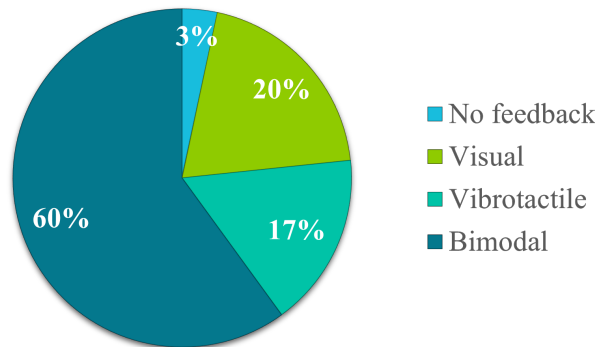


Figure 7.10: Chart depicting the users' perception of the feedback modality that helped the most to imagine the movement.

The most entertaining feedback modality:

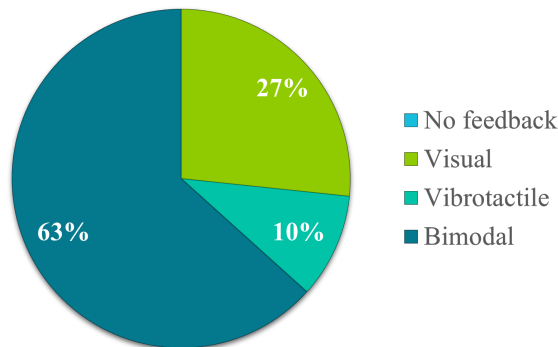


Figure 7.11: Chart depicting the users' preference of the most entertaining feedback.

one. However, this particular individual also selected the bimodal feedback as their preferred overall modality. Moreover, this person indicated that the vibration *"allows [me] to imagine the movement where the [muscle] contraction should be"*. Although these answers may seem contradictory, a possible explanation is that, for this individual, the stimulation helps to imagine the movement, but they do not consider it realistic. This could be confirmed with further discussion with the participants after the experiment.

In terms of ease of comprehension, the visual modality was the easiest to understand, as indicated by 47% of the participants. This modality was closely followed by the bimodal modality selected by 40% of the participants, as depicted in figure 7.13. This suggests that the bimodal feedback did not impose additional cognitive effort for these participants to understand it, despite integrating the visual and haptic senses. Interestingly, one person indicated that the No feedback modality was the easiest to understand. This individual indicated in their written feedback that for them *"it is better, in my case; to not have feedback but to have the [virtual] hand in front, to imagine [the movement] easier"*. This comment highlights the importance of having visual support that guides the user on how to perform the KMI.

The feedback modality that felt most realistic:

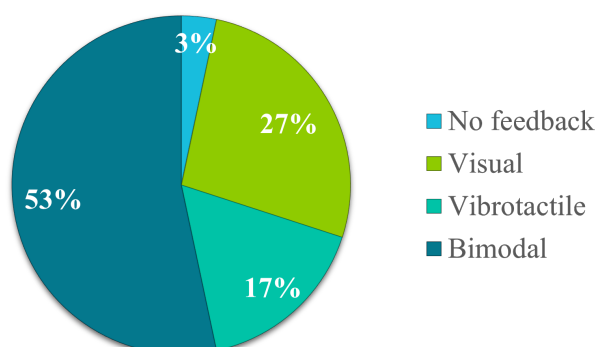


Figure 7.12: Chart depicting the users' preference of the most realistic feedback.

The easiest feedback modality to understand:

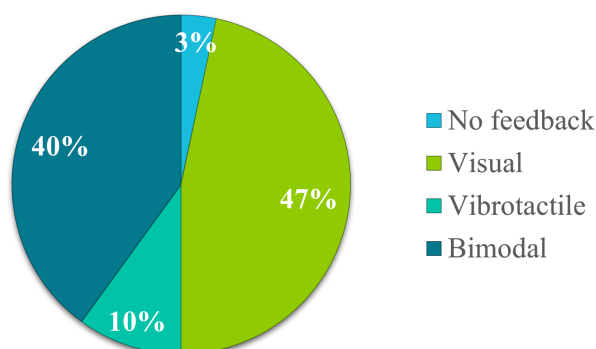


Figure 7.13: Users' perception on the easiest feedback modality to understand.

Finally, figure 7.14, showcases the modalities that users perceived the hardest to understand. The absence of feedback, corresponding to the calibration phase, posed the greatest challenge in terms of understanding for 77% of the participants. Given that this phase was the first one presented to the participants, it is plausible that this context influenced the comprehension difficulty. Furthermore, the visual and vibrotactile modalities were also considered the hardest to understand by 6% and 17% of the participants, respectively. Strikingly, the bimodal modality was never considered the most challenging to understand, even though it integrated two sensory modalities.

These results demonstrate the undoubted preference for bimodal feedback among BCI users, attributed to its facilitation of KMI performance, user-friendly comprehension, engaging nature, and perception of heightened realism. Indeed, participants' written feedback accentuated that bimodal feedback helped them to visualize their performance results through the hand animations and to quantify it via the gauge, but also to experience tangibly through the vibrations, offering a more comprehensive and immersive feedback experience. A few examples of the participants' written feedback that prefer bimodal feedback are provided in the following list, each phrase corresponds to a different participant:

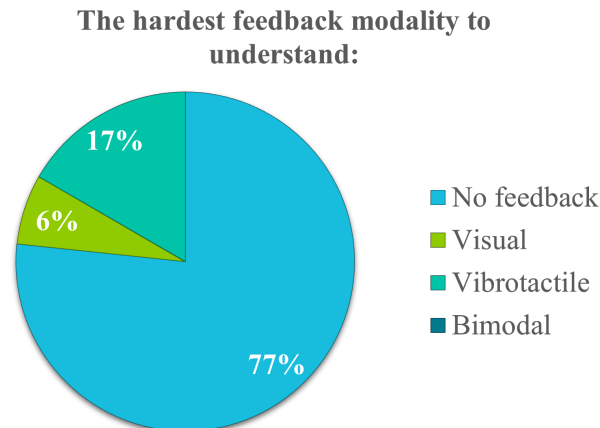


Figure 7.14: Users' perception on the hardest feedback modality to understand.

- *“Having feedback allows to better understand how to get a response/perform the [KMI] exercise correctly. The vibrotactile feedback allows to ‘wake-up’ the hand and to focus at each repetition. The vibrotactile feedback combined with the visual allowed me to have a satisfying feedback (visual) and to concentrate (vibrotactile).”* Participant S52.
- *“The visual feedback is very encouraging, but can also be sometimes frustrating when it does not correspond to our internal feeling. For this reason, the visual + vibrotactile [feedback] was at the same time encouraging and more gratifying. In any case, I found the vibrotactile feedback more gratifying.”* Participant S50.
- *“The vibrotactile feedback helps with the awareness of the muscles, so this help[s] to imagine the movements and maintain a good performance. The visual feedback help[ed] me with a detailed performance review and a motivation to focus. The combination of both is the best option.”* Participant S32.
- *“The visual and vibrotactile feedback provide a more complete reference about the performance: the vibrotactile feedback mimics (despite its limits) the vibration sensation inside the arm that I feel when imagining de movement; and the visual feedback provides a rather satisfying reward. Having both [feedback modalities] is more interesting.”* Participant S26.
- *... The vibrotactile allied to the visual [feedback] gives a maximum of signals that reassure, they are references, and allow to re-focalize many things to improve [the KMI], we get more self-confident more rapidly. The vibrotactile leaves an impression of ‘tingling’ in the hand that allow to be more conscious about own’s touch and facilitates the imagination of sensation. Each vibration ‘creates’ a new memory to focus on to imagine the next one ... The [visual] gauge is more motivating.* Participant S47
- *"With the vibrotactile, I can know if a trial was better than another one, but I do not know if it was good or not. The visual gauge allows answering this question, plus having the same effect of the vibrotactile."*

7.3.3 Evaluation of the Participants' Well-Being

In this experiment, the participants' well-being throughout the session was monitored. This included surveying the fatigue level during the session (section 7.3.3.1) and the positive, negative, and neutral emotions at the session's beginning and end (section 7.3.3.2). As these controls did not consider the feedback scores, we evaluated the fatigue and emotions among 38 participants, including those with low BCI performance.

7.3.3.1 Fatigue level during the session

The assessment of fatigue level over the course of the session revealed a notable increase in participants' tiredness by the session's end compared to the beginning (paired-samples student t-test, $p = 0.004$), as presented in figure 7.15. A significant increase in fatigue was also observed from the second feedback condition to the third feedback condition (Wilcoxon signed rank test $W < 0.001$), occurring at a moment approximately three-fourths into the session duration.

We attempted to determine any existing correlation between BCI performance and fatigue levels. However, no discernible correlation was evident between BCI performance in condition 1 and its corresponding fatigue level (Spearman's rho: 0.073, $p = 0.665$), nor for conditions 2 (Spearman's rho: -0.237, $p = 0.152$) and 3 (Spearman's rho: -0.219, $p = 0.186$). These outcomes suggest that the BCI performance remained unaffected by the participant's fatigue level. It is important to note that, as displayed in table 7.6, the standard deviation across each evaluated fatigue time point was considerable, indicating substantial variability among subjects. Indeed, eight participants reported no discernible fatigue change, while six noted a decrease, and 19 indicated an increase of 1 to 3 points.

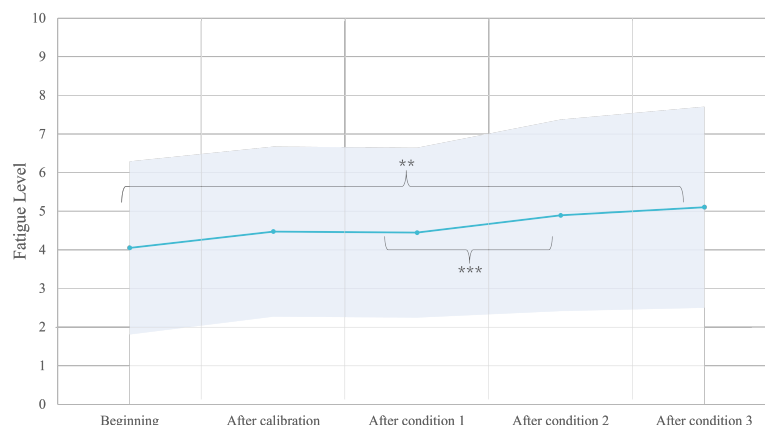


Figure 7.15: Temporal evolution of the mean fatigue levels across the session: The graph illustrates the overall average progression of fatigue levels during the session. The shaded blue area represents the standard deviation. *** $p < 0.01$, *** $p < 0.001$

	Beginning	Calibration	Condition 1	Condition 2	Condition 3
Mean	4.05	4.47	4.45	4.89	5.11
s.d.	2.24	2.20	2.20	2.48	2.60

Table 7.6: Average and standard deviation of the temporal evolution of fatigue levels across the session.

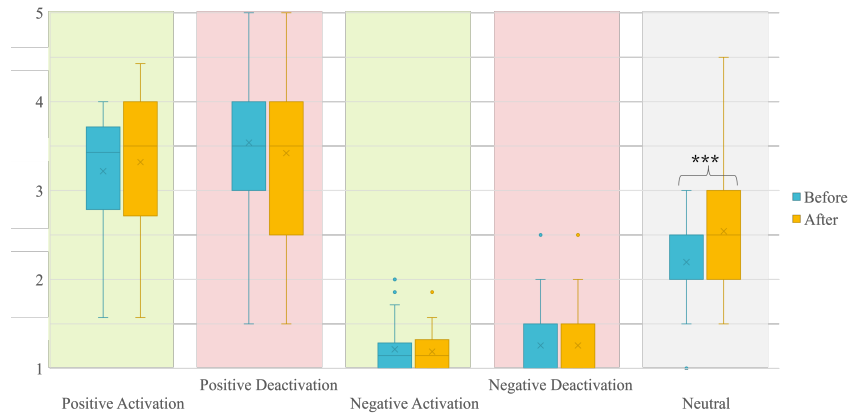


Figure 7.16: Emotional states of participants before and after the session. *** $p < 0.001$

7.3.3.2 Emotional states before and after the session

The results of the participants' emotional states pre- and post-session are displayed in figure 7.16. A noteworthy statistically significant difference emerged specifically within the domain of neutral emotions (Wilcoxon rank, $p < 0.001$). To further understand this difference, we compared the initial and final states of the two components that make up this emotion: neutral and surprise. Remarkably, only the surprise component exhibited a statistically significant increase after the experimental session (Wilcoxon rank, $p < 0.001$). Indeed, surprise has been suggested as one of the factors that indicate engagement in learning [243, 244]. Collectively, these findings strongly indicate that the experimental session not only refrained from degrading participants' emotional states but also contributed to an overall pleasant experience.

7.3.3.3 Mental workload during the training

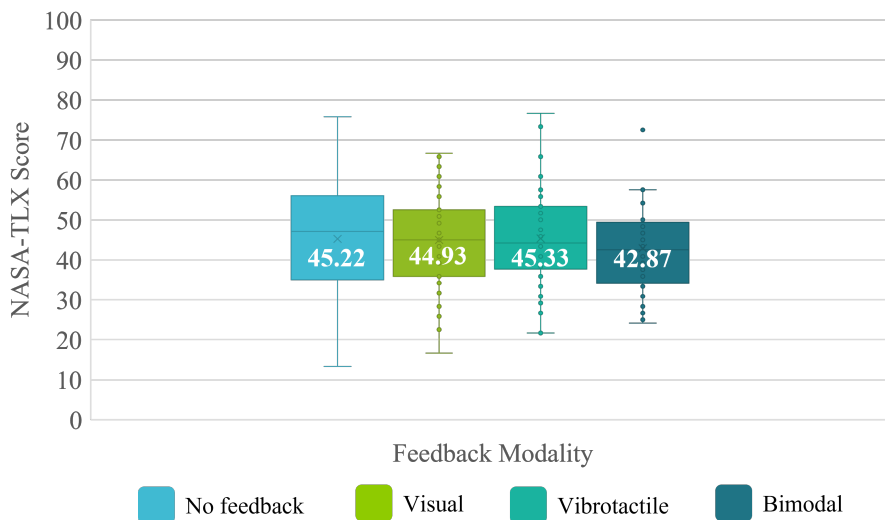


Figure 7.17: Raw mental workload score of the NASA-TLX questionnaire for each feedback modality. The grand average is displayed in white.

The subjective mental workload was assessed throughout the session with the NASA-TLX ques-

tionnaire. A summary of the scores is provided in table 7.7. The raw average mental workload scores were assessed across the three feedback modalities and visually depicted in figure 7.17. All test conditions, including calibration and the three feedback modalities, exhibited a similar somewhat high mental workload as revealed by a repeated measures ANOVA analysis ($p = 0.531$), thus the feedback modality did not impact the mental workload. Moreover, the participants who had notably noisy EEG signals, potentially influencing the feedback scores, did not deviate from the average mental workload. This suggests that even though the feedback was lowly reliable, the mental workload was not impacted either negatively or positively.

To gain a more comprehensive understanding of the average NASA-TLX score, an exploration of the individual items assessed by this questionnaire was undertaken. Figure 7.18 summarizes the scores of each item for every modality, and their respective values are presented in Table 7.7. Notably, the mental effort was consistently high across all modalities, with no significant difference observed (repeated measures ANOVA - Friedman $p = 0.512$). Conversely, physical effort was generally moderate, except for vibrotactile feedback which exhibited a high score. However, this difference was not statistically significant (repeated measures ANOVA - Friedman $p = 0.113$).

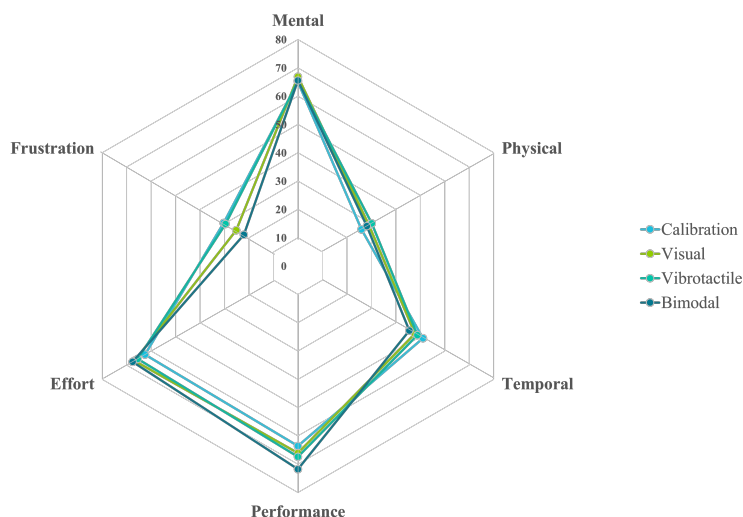


Figure 7.18: Scores of each item of the NASA-TLX questionnaire for the calibration and feedback modalities.

The temporal effort was high for all feedback modalities and somewhat high for the calibration, but without statistical significance (repeated measures ANOVA - Friedman $p = 0.279$). Strikingly, participants perceived their performance was high across modalities, including calibration, with the bimodal modality exhibiting the highest score. Yet, these differences lacked statistical significance (repeated measures ANOVA - Friedman $p = 0.468$). Interestingly, frustration was more pronounced during calibration than during any feedback modality, although the difference did not reach significance (repeated measures ANOVA - Friedman $p = 0.100$).

The lack of statistically significant differences in all these five items suggests that participants perceived similar mental workload for all modalities, including the calibration. However, it is essential to note that all items exhibit a large standard deviation. This indicates substantial variability in the data, reflecting a diverse range in the study's participant population.

Lastly, the overall effort was high across all modalities, with significant differences observed

(repeated measures ANOVA - Friedman $p = 0.045$). Pair-wise comparisons revealed that effort was higher for visual and bimodal feedback compared to calibration (Durbin test $p = 0.015$, for both). The increased effort could be attributed to participants processing more information when presented with feedback. Moreover, they received more details about their performance, and they could change their strategy to have better results, requiring additional effort. This contrasts with situations with no feedback, where the same strategy might persist even if it is suboptimal.

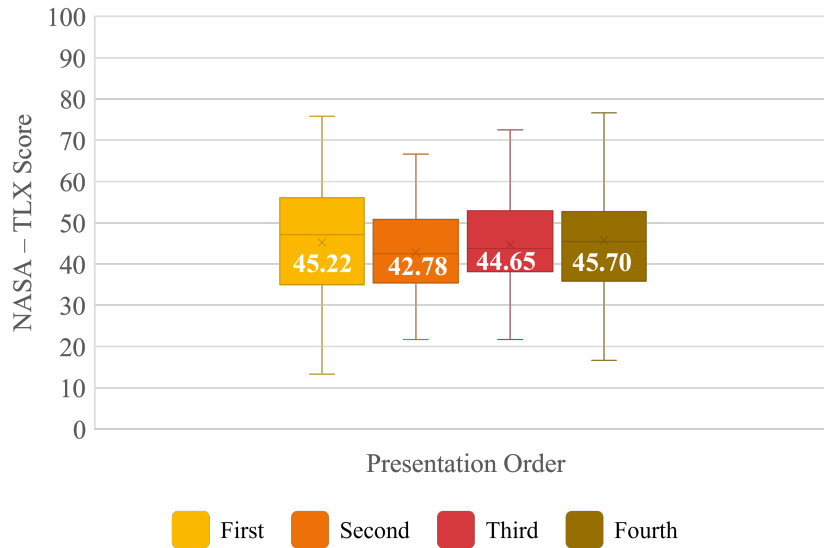


Figure 7.19: Mental workload score of the NASA-TLX questionnaire by presentation order. The grand average is displayed in white.

The influence of the presentation order on the mental workload was also assessed, displayed in figure 7.19. No statistically significant differences were observed due to the presentation order (repeated measures ANOVA $p = 0.231$), neither in the interaction of feedback modality and order ($p = 0.247$). Nevertheless, two participants, who presented issues with EEG acquisition, exhibited an important increase in mental workload by the end of the session. More specifically, an electrode was disconnected for one of the participants, leading to a drop in the feedback score. These incorrect scores might have troubled the participant to the point where the mental workload was affected negatively by increasing.

The impact of the average mental workload on the BCI scores corresponding to each feedback modality was assessed. We did not find any correlation between the mental workload and scores from the visual (Spearman's $\rho = -0.198$, $p = 0.234$), vibrotactile (Spearman's $\rho = -0.089$, $p = 0.596$), and bimodal (Spearman's $\rho = -0.251$, $p = 0.128$) feedback modalities.

7.3.3.4 Cognitive states associated with feedback modality

The cognitive states were evaluated via the NEXT-Q questionnaire applied after each of the feedback modalities. The questionnaire evaluates the following dimensions: *Mood*, *Mindfulness*, *Motivation*, *Cognitive Load*, and *Agency* after neurofeedback training. From the cohort of 38 participants, two came out as clear outliers, exhibiting lower or higher scores for each dimension. These two participants actually experienced EEG acquisition issues, where for one of them, one electrode was disconnected, leading to a drop in the feedback scores. Regarding the other

Table 7.7: Raw scores of the NASA-TLX questionnaire across feedback modalities.

Item		Calibration	Visual	Vibrotactile	Bimodal
<i>Average Score</i>	Mean	45.22	44.93	45.33	42.87
	S.D.	14.36	11.87	13.80	11.34
<i>Mental</i>	Mean	65.00	66.84	65.26	65.53
	S.D.	22.51	19.95	22.96	17.51
<i>Physical</i>	Mean	25.92	28.95	30.13	28.16
	S.D.	21.51	21.06	23.72	21.70
<i>Temporal</i>	Mean	51.05	47.76	48.82	45.53
	S.D.	21.22	19.06	19.22	17.23
<i>Performance</i>	Mean	63.55	66.05	67.37	71.71
	S.D.	23.96	19.77	19.34	17.98
<i>Effort</i>	Mean	62.50	66.84	65.53	67.63
	S.D.	23.53	20.08	21.17	19.27
<i>Frustration</i>	Mean	30.39	25.26	29.61	22.11
	S.D.	21.85	20.33	21.88	16.91

participant, the system stopped working abruptly, also leading to low feedback scores. Thus, these two participants were removed from the analysis as their responses for the NEXT-Q questionnaire are associated with the false feedback (i.e. not related to the mental state) they received. This observation indicates that false feedback will affect the questionnaire's evaluation.

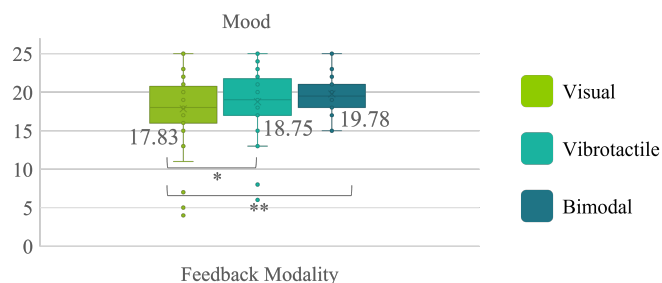


Figure 7.20: NEXT-Q: Score for the *Mood* dimension per feedback modality. The average for each modality is shown in gray. * $p < 0.05$, ** $p < 0.01$

The *Mood* score of the participants was rather high, and it tended to increase with the bimodal feedback, displayed in figure 7.20. A statistically significant difference was observed in this dimension due to the feedback modality (repeated measures ANOVA - Friedman $p = 0.012$). More specifically, a higher score was exhibited during the vibrotactile than in the visual modality (Durbin-Conover $p = 0.013$), and during the bimodal modality rather than in the visual one (Durbin-Conover $p = 0.006$). These outcomes suggest that the bimodal modality and the vibration produced a better mood among participants than visual feedback. No difference was observed between the vibrotactile and bimodal modalities, suggesting these two were similar.

Similarly, the score concerning *Motivation*, was rather high, especially for the bimodal modality, as presented in figure 7.21. A statistically significant difference emerged among the feedback modalities (repeated measures ANOVA - Friedman $p = 0.008$). More specifically, the visual

and bimodal feedback presented a significant difference (Durbin-Conover pairwise comparisons $p = 0.002$), as well as the vibrotactile and bimodal modalities (Durbin-Conover $p = 0.04$). No significant difference was observed between the visual and vibrotactile modalities (Durbin-Conover $p = 0.226$). Overall, the bimodal modality was considered more motivating than the two unimodal modalities, probably due to the integration of both visual and tactile senses.

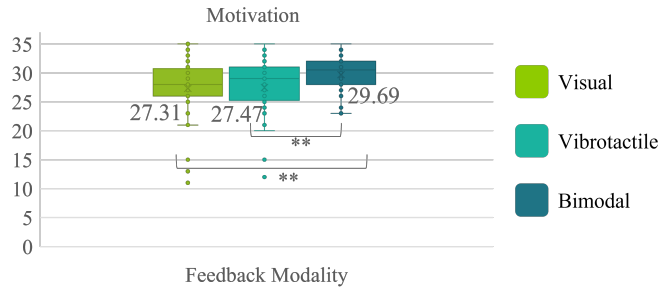


Figure 7.21: NEXT-Q: Score for the *Motivation* dimension per feedback modality. The average for each modality is shown in gray. ** $p < 0.01$

Concerning *Mindfulness*, depicted in figure 7.22, the visual and vibrotactile modalities had very similar scores. The bimodal modality presented a slightly higher score, nevertheless, this difference was not statistically significant (repeated measures ANOVA - Friedman $p = 0.155$). These results suggest that mindfulness throughout the session was not impacted by the feedback modality.

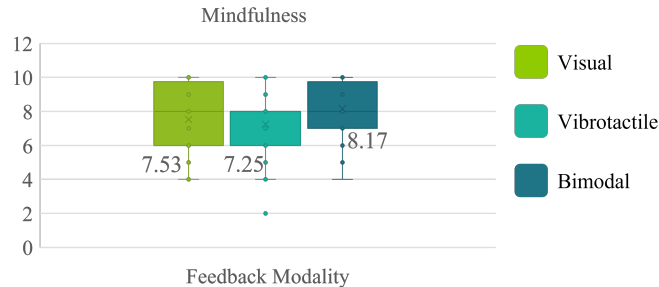


Figure 7.22: NEXT-Q: Score for the *Mindfulness* dimension per feedback modality. The average for each modality is shown in gray.

Likewise, all three feedback modalities presented a comparable *Cognitive Load* (fig.7.23), confirmed by Friedman's repeated measures ANOVA with $p = 0.368$. These observations suggest all modalities represented similar cognitive load and that the bimodal feedback modality did not demand additional cognitive effort from the participants, despite integrating two sensory modalities.

Finally, another relevant dimension of the feedback evaluation is *Agency*, depicted in figure 7.24. An increase in agency was observed for the bimodal feedback. This was confirmed by repeated measures ANOVA, which revealed a statistically significant difference among feedback modalities ($p = 0.022$). Concerning the pair-wise comparisons, no differences were observed between the visual and vibrotactile modalities (Tukey $p = 0.992$), nor between the vibrotactile and bimodal modalities (Tukey $p = 0.090$). Furthermore, the bimodal feedback presented a significantly higher score than the visual one (Tukey $p = 0.008$). This outcome suggests that

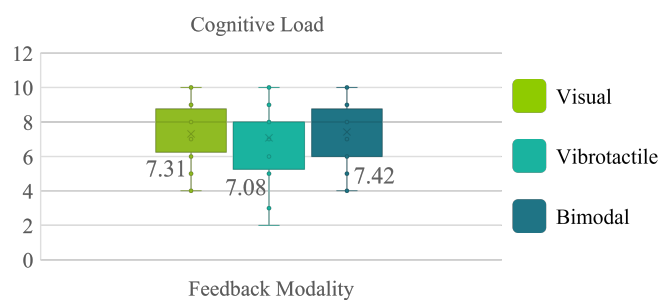


Figure 7.23: NEXT-Q: Score for the *Cognitive Load* dimension per feedback modality. The average for each modality is shown in gray.

merging the two unimodal modalities resulted in a successful increase of agency, indicating participants sensed control over their neural activity.

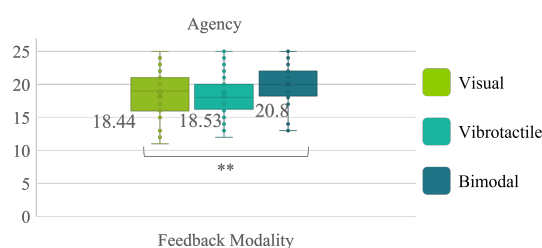


Figure 7.24: NEXT-Q: Score for the *Agency* dimension per feedback modality. The average for each modality is shown in gray. ** $p < 0.01$

7.3.4 Influence of Participant's Characteristics on BCI Performance

An exploratory analysis was conducted to discern intra-participant factors influencing KMI execution and BCI performance. Given the inherent association of KMI with motor activity, individuals engaged in frequent manual activities may demonstrate greater ease in performing the mental task, as previously observed in [236]. Additionally, the learning process may be influenced by the individuals' perceived self-value. Lastly, considering KMI's connection with mindfulness, individuals who commonly practice mindfulness activities, such as meditation, may exhibit better performances [245]. Therefore, these elements were evaluated to determine their influence on BCI performance.

7.3.4.1 Impact of participant manual activity habits on BCI performance

To assess the influence of the participants' profiles on overall feedback score, regardless of the feedback modality, a linear model was constructed, considering the following key characteristics:

- Practice of manual activities:
 - Playing a musical instrument
 - Cooking
 - Painting/drawing skills

- Video game-playing habits
- Knitting/sewing habits
- Sport practice
- Meditation practice

In fact, previous studies have suggested that manual activities may influence BCI performance [236]. Moreover, mindfulness and meditation practices have been suggested to improve the BCI performance and accuracy [246, 245]. Therefore, a linear model of the present participant cohort may aid in supporting previous studies. The linear model was computed using R [247]. All the characteristics consisted of *Yes* or *No* questions, thus the answers were converted to dummy variables, taking values of 0 for *No* and 1 for *Yes*. The resulting equation was the following:

$$feedbackScore = 66.51 + 2.38MI + 8.41C - 1.39P + 9.80V - 8.60K + 1.17S - 9.25MP \quad (7.4)$$

Where:

- MI: practice of a musical instrument
- C: cooking
- P: painting and/or drawing
- V: playing video games
- K: knitting and/or sewing
- S: sport practice
- MP: meditation or mindfulness practice

The model described in the equation 7.4, indicates that users who do not perform any of the activities will, more likely, present a feedback score of 66.51% +/- 4.15. Nevertheless, the model's adjusted r-square is 0.3101, which implies that the model explains only 31.01% of the variation in the training data. Therefore, the statistically significant results, presented in table 7.8, must be taken carefully and only as potential indicators of elements that may influence KMI execution.

Notably, a positive statistically significant association was found with activities such as cooking ($p = 0.029$) and playing video games ($p = 0.009$). These findings suggest that individuals who regularly engage in cooking and/or playing video games tend to receive higher feedback scores. Conversely, a statistically significant negative correlation was observed with meditation practice ($p = 0.035$), indicating that participants who practiced meditation tended to have lower feedback scores. The rest of the characteristics did not exhibit any statistically significant influence on overall BCI performance.

To gain a deeper understanding of the impact of meditation, a closer exploratory examination of the responses related to meditation practice was conducted. Out of the thirty participants, six reported engaging in meditation. Three participants reported practicing meditation at least five times per week for less than 30 minutes and achieved an overall feedback score exceeding 70%. In contrast, one individual achieved an overall feedback score of 52.20% while meditating once per week for less than 30 minutes. Therefore, it is important to exercise caution when interpreting this data, as this particular participant may be considered an outlier. Given the limited number of participants who practiced meditation, drawing definitive conclusions is difficult.

Table 7.8: Linear model: coefficients, standard error, and p-values associated with the participant’s characteristics. Significant values are in bold.

Activity	Coefficient	Std. Error	<i>p-value</i>
Practice of a musical instrument	2.38	3.93	0.551
Cooking	8.41	3.60	0.029
Painting and/or drawing	-1.39	3.61	0.703
Playing video games	9.80	3.46	0.009
Knitting and/or sewing	-8.60	4.57	0.073
Sport practice	1.17	3.92	0.767
Meditation or mindfulness practice	-9.25	4.11	0.035

7.3.4.2 Impact of self-efficiency and mindfulness in BCI performance

7.3.4.2.1 Perceived self-efficiency and BCI performance The average perceived self-efficiency among all participants in the study was fairly high with 3.66 out of 5 points, s.d= 0.59, as depicted in figure 7.25. Only two participants reported scores lower than 2.5, meaning that the majority of the participants reported medium to high self-efficiency.

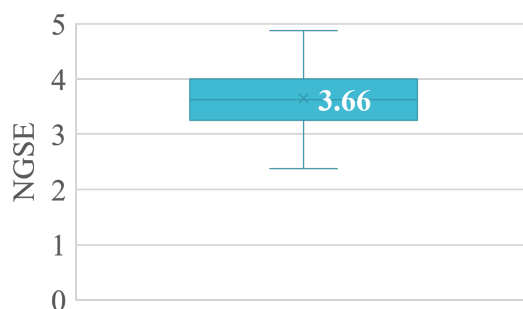


Figure 7.25: Grand average of self-efficiency score.

To determine if perceived self-efficiency had an impact on BCI performance, we attempted to determine the correlation between the results from the NGSE scale and the feedback scores. No correlation between self-efficiency and the session’s average feedback score was found (Spearman’s $\rho = 0.177$, $p = 0.342$). Strikingly, as observed by the red circles in figure 7.26, two participants that exhibited low-self-efficiency performed equally or better than the two participants with the highest self-efficiency scores, reinforcing the non-correlation between the NGSE score and performance. Furthermore, there was no correlation between the NGSE score and the feedback scores corresponding to the visual (Spearman’s $\rho = 0.025$, $p = 0.895$), vibrotactile (Spearman’s $\rho = -0.049$, $p = 0.795$), and bimodal (Spearman’s $\rho = 0.343$, $p = 0.059$) modalities. These results suggest that the feedback score was independent of the user’s perceived self-efficiency in this study.

7.3.4.2.2 Mindfulness and BCI performance At the beginning of the session, the participant’s mindfulness ability was assessed through the FMI questionnaire, which results in two dimensions: *Presence* and *Acceptance*. It is important to note that this assessment differs from the two previous evaluations of mindfulness. In section 7.3.4.1, participants indicated the frequency of their meditation and/or meditation practices. In fact, individuals may not perform

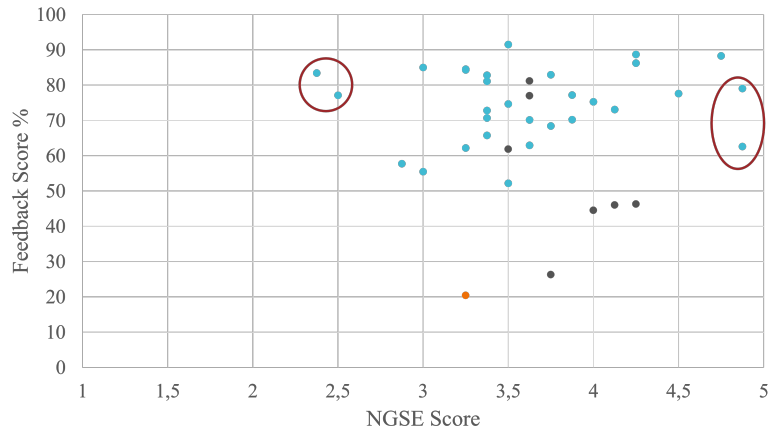
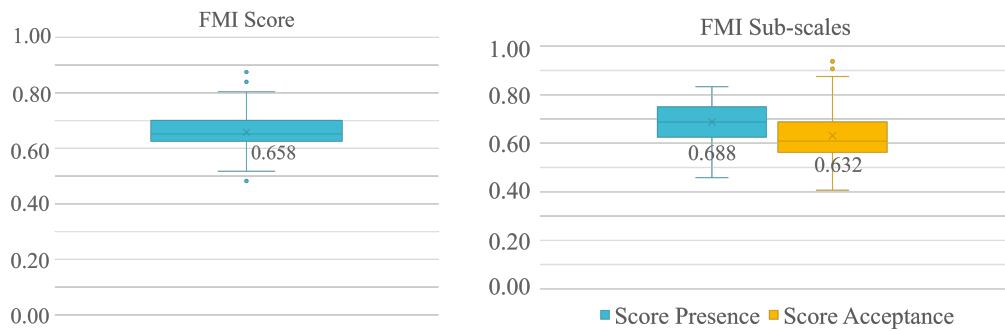


Figure 7.26: Correlation between self-efficiency and average feedback score. The participants with the lowest and the highest NGSE scores are encircled in red. The participants who presented EEG acquisition issues are depicted in gray. One participant with very low performance and no acquisition problems is depicted in orange.

any meditation or mindfulness activity but still have some ability, as revealed by the FMI questionnaire.

Overall, the participants reported a relatively high FMI score, as depicted in figure 7.27(a), as well as *Presence* and *Acceptance* scores in figure 7.27(b). The effect of mindfulness on the average feedback score, and for each feedback modality, was assessed through correlations. However, the corresponding Spearman’s rho coefficients did not reveal any correlation between the mindfulness scores and any of the feedback scores, as shown in table 7.9. These results suggest mindfulness ability, as assessed by the FMI questionnaires, does not affect KMI performance in this study.



(a) FMI Score. The mean is depicted in gray. (b) FMI Subscales score. Mean values are depicted in grey.

Figure 7.27: Results from the Freiburg Mindfulness Inventory.

		FMI Score	Presence	Acceptance
Average	Spearman's rho	0.011	0.086	0.078
	p-value	0.953	0.645	0.677
Visual	Spearman's rho	0.081	0.154	0.159
	p-value	0.666	0.409	0.392
Vibrotactile	Spearman's rho	-0.006	0.128	-0.014
	p-value	0.976	0.491	0.939
Bimodal	Spearman's rho	0.026	-0.081	0.127
	p-value	0.891	0.666	0.495

Table 7.9: Correlation between mindfulness (FMI) and BCI performance: Spearman's r coefficient and p-value (significance level $\alpha = 0.05$)

7.3.5 System's Elicited Emotions and Attractiveness

7.3.5.1 Emotions elicited by the interaction with the Bimodal BCI

The emotions elicited by the interaction with the BCI were assessed using the second module of the meCUE questionnaire. The results concerning the positive emotions are presented in figure 7.28. Regarding positive emotions, 92% of the participants agreed with the statement *The system exhilarates me* (fig.7.28(a)), and 59% reported feeling cheerful (fig.7.28(b)) while using the system. Nevertheless, 18% of the participants either did not feel cheerful while using the system and 23% were neutral about it, summing up to 41%. Although this does not necessarily represent a bad score, it is a point of attention for future studies, where the target population may experience different emotions due to the system fulfilling their necessities concerning motor rehabilitation.

On the other hand, 44% of participants sensed the system calmed them (fig.7.28(c)), while the rest 56% were either in disagreement (26%) or neutral (30%) about this aspect. Concerning relaxation, the scores were equally divided among agreeing, disagreeing, or being neutral about it (fig.7.28(d)), suggesting the system did not play an active role in relaxation. This dimension is of great importance because the system represents a training technique that requires effort. Although the objective is to deliver a good user experience, calming and relaxing in excess could potentially distract the user from performing the KMI.

Furthermore, 92% of the participants did not agree with feeling anger due to their interaction with the system (fig.7.29(a)). Only 18% of the participants reported frustration while interacting with the BCI (fig.7.29(b)), which could probably associated with a low sense of competence.

Additionally, 16% reported feeling tired due to the system (fig.7.29(c)), which is in line with the fatigue levels reported in section 7.3.3.1. Finally, no participant reported feeling passive while using the BCI (fig.7.29(d)).

Altogether, the interaction with the BCI yielded positive and activating emotions such as exhilaration and cheerfulness. Moreover, the absence of negative emotions highlights the overall good experience while interacting with the system. Naturally, six participants felt tired while using the system, which is plausible considering KMI is a task that requires high attention. Notably, none of the participants felt passive while using the system, suggesting they all knew they had to perform an action to receive feedback, and they perceived the system was responding to their own KMI.

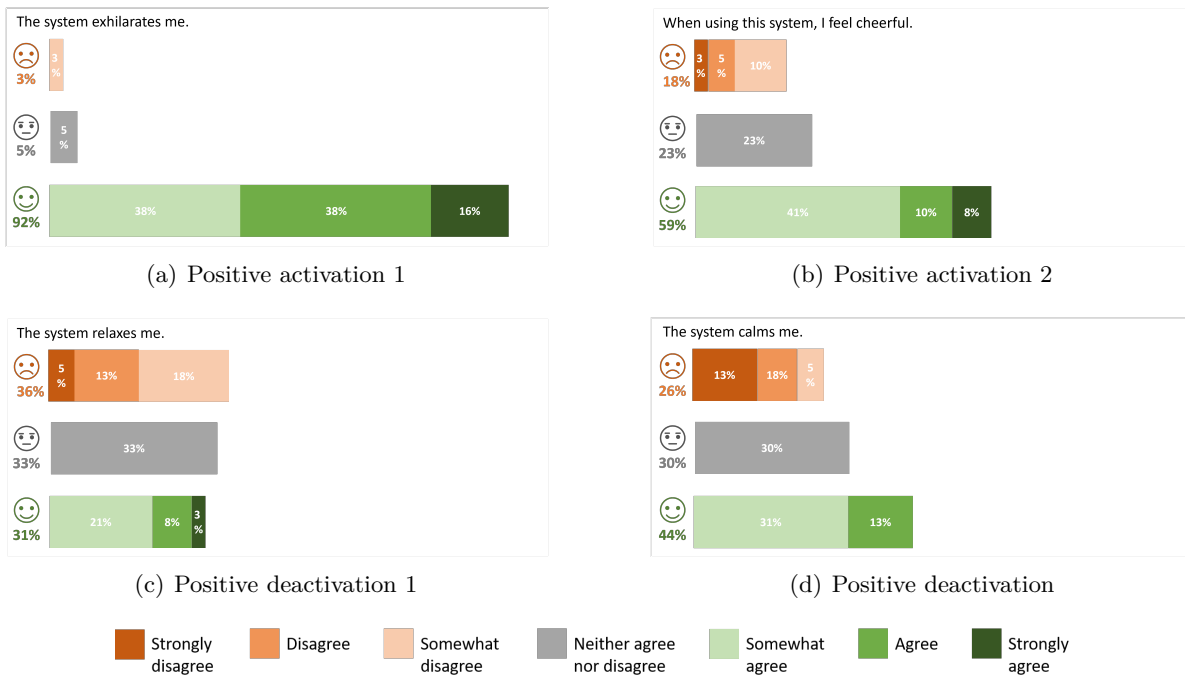


Figure 7.28: Visualization of meCUE's positive emotional responses during the third experiment.



Figure 7.29: Visualization of meCUE's negative emotional responses during the third experiment

7.3.5.2 Attractiveness of the bimodal BCI

The system successfully fulfilled its pragmatic and hedonic qualities of stimulation and identity, demonstrated by the positive scores of these dimensions resulting from the evaluation with the AttrakDiff questionnaire (figure 7.30). Furthermore, the system had a positive general attractiveness score. However, the evaluation was performed with a population different from the target post-stroke patients. Therefore, the scores are expected to increase during the evaluation with individuals who actually need the interface for their recovery.

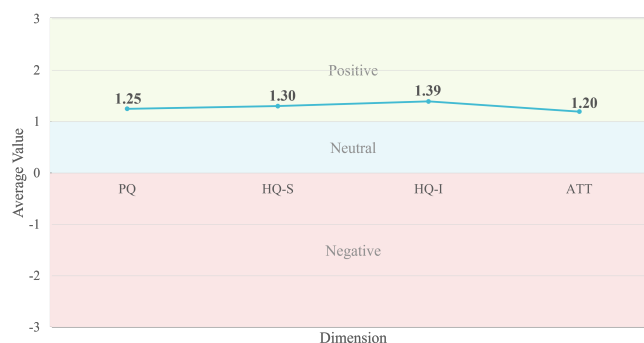


Figure 7.30: AttrakDiff for the third experiment: Diagram of average values of each dimension. PQ: Pragmatic quality, HQ-S: Hedonic identity - stimulation, HQ-S: Hedonic quality - identity, ATT: attractiveness.

Although the evaluation was performed with a non-target population, the system was perceived as *desired*, as shown by the orange circle in the AttrakDiff portfolio in figure 7.31. The participant who exhibited low feedback scores and no acquisition issues was neutral about the interface. This highlights the potential influence of feelings of success or performance on judgments of interface quality. Moreover, it was observed that five participants who had biased feedback scores due to acquisition issues (green and gray in figure 7.31), still perceived the system as *desired*. This suggests that the participants may not have perceived the problems or that they have not affected their judgment.

To have a better understanding of the overall scores, an examination of the items evaluated by the questionnaire was performed, and is displayed in figure 7.32. Unlike the two previous building phases, all the items presented a positive score. However, items with a score lower than one have the potential to be improved. These items include: *Disagreeable-Likeable*, *Ugly-Attractive*, *Unpredictable-Predictable*. This last item may be related to the user's facility to interact with the BCI.

Furthermore, the *Ugly-Attractive* item may improve by using the second version of the vibrotactile device (presented in chapter 4), as for this study, the first prototype was employed. On the other hand, the highest score was for item *Clearly structured*, suggesting that participants undoubtedly understood the instructions and how to interact with the system. Additionally, it was also considered as *Motivating*, which is a relevant item for motor rehabilitation and in line with the results from the NEXT-Q questionnaire.

Finally, the correlation between the AttrakDiff dimensions and the mean user performance was studied through a Spearman correlation test with $\alpha = 0.05$. A medium significant correlation was observed between the average feedback score and the pragmatic quality (Spearman's rho:

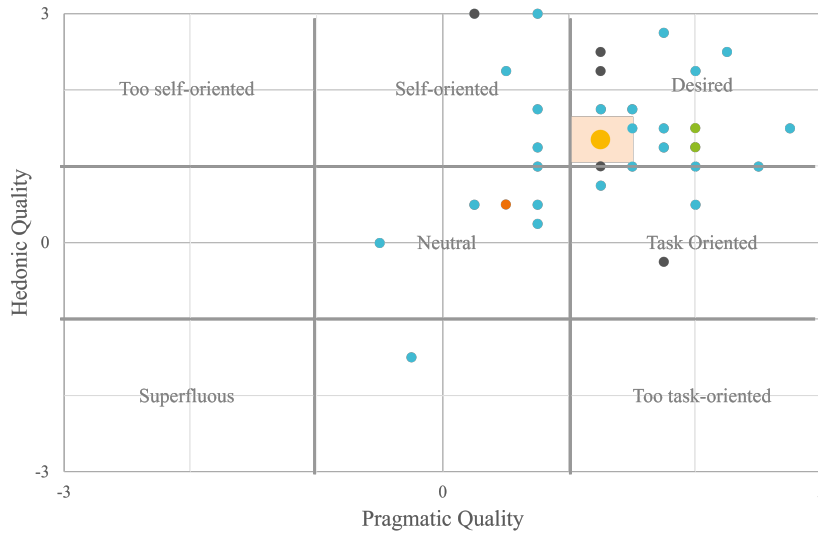


Figure 7.31: AttrakDiff Portfolio. Grand average is in orange. The rectangle corresponds to the 95% confidence interval. The individual participants' scores are small blue circles. Gray circles correspond to participants with biased low performances, while green ones correspond to biased high performances.

0.330, $p = 0.043$), yet no correlation was found with the hedonic qualities, stimulation and identity, nor with attractiveness.

The same correlation analysis was performed with the feedback scores of each feedback modality individually. Regarding the bimodal feedback, a correlation was observed with the pragmatic quality (Spearman's rho: 0.356, $p = 0.028$), but no correlations were found with the other dimensions. Concerning the visual and vibrotactile modalities, no correlation was found between their feedback scores and any of the AttrakDiff dimensions. A summary of the correlation coefficients and p values is provided in table 7.10. These results indicate that the performances impacted the perceived usability and easiness of the interface, mostly influenced by the bimodal feedback modality. Furthermore, the attractiveness and hedonic qualities were successfully met, independently of the feedback scores.

Table 7.10: Spearman correlation coefficients and p-values between the feedback scores and the AttrakDiff dimensions.

		PQ	HQ-S	HQ-I	ATT
Average	Spearman's rho	0.330	0.198	0.125	0.062
	p-value	0.043	0.233	0.455	0.688
Visual	Spearman's rho	0.212	0.212	0.261	0.144
	p-value	0.201	0.201	0.114	0.390
Vibrotactile	Spearman's rho	0.239	0.299	0.120	0.185
	p-value	0.148	0.068	0.473	0.266
Bimodal	Spearman's rho	0.356	0.037	-0.022	-0.091
	p-value	0.028	0.827	0.894	0.586

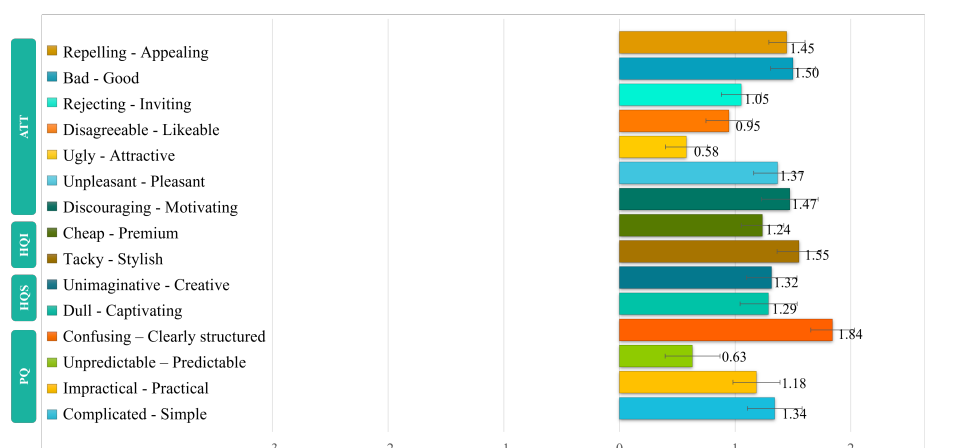


Figure 7.32: AttrakDiff word pairs diagram. The mean is displayed in black numbers, and the standard error is displayed in lines on top of each bar.

7.3.6 EEG Analysis

In this section, the results of the EEG analysis are presented. First, the time-frequency analysis results are presented. Subsequently, the topographies corresponding to the KMI and the feedback phases are presented.

7.3.6.1 Time-frequency analysis

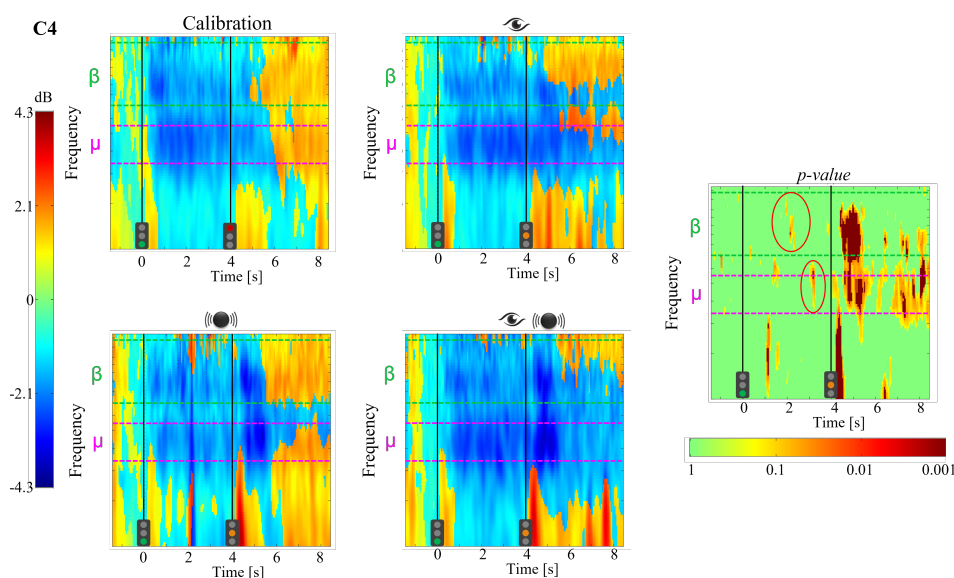


Figure 7.33: Time-Frequency Analysis (ERSP) of left-hand MI ($n=28$) at electrode C_4 during calibration and three feedback conditions. Feedback modalities include eye-visual, vibrating motor-vibrotactile, and both-bimodal. Red represents increased power, blue decreased power. Frequency bands: β (15-30 Hz), μ (8-12 Hz). p-values obtained through permutation analysis with FDR correction. Significant differences are encircled in red.

The first step of the EEG offline analysis consisted of verifying the recruitment of the sensori-

motor cortex corresponding to the left or right hand during the KMI phase. This corresponds to electrode C_3 for left-hand MI and C_4 for right-hand motor imagery. Additionally, the calibration phase and the three feedback modality conditions were compared to determine significant differences due to feedback.

Time-frequency analysis on electrodes C_3 and C_4 allowed us to observe the changes in power across time, as displayed in figures 7.34 and 7.33 for left-hand MI and figure 7.36 and 7.35 for right-hand MI. The KMI started at $t=0s$, indicated by a green light. During the calibration phase, the KMI ended at $t=4s$, indicated by a red light and followed by a resting phase, whereas during the feedback phases, the end of the KMI was indicated by an orange light, and it was followed by the feedback.

7.3.6.1.1 Left hand KMI As a reminder, participants were asked to imagine a KMI for their non-dominant hand. The majority of participants were right-handed, then left-handed KMIs were the most common.

In the context of left-hand MI ($n=28$), the time-frequency analysis of brain activity in both hemispheres using electrodes C_3 and C_4 (as shown in figure 7.34 and figure 7.33, respectively). This analysis presented the well-known ERD in both electrodes while executing KMI [33]. This power decrease indicates that participants engaged their sensorimotor areas throughout the four-second duration of KMI.

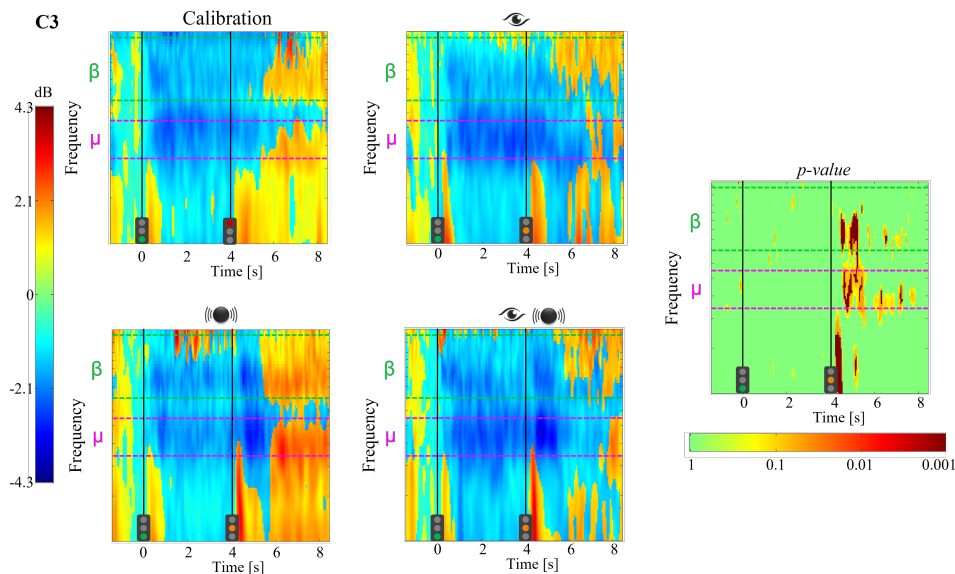


Figure 7.34: Time-Frequency Analysis (ERSP) of left-hand MI($n=28$) at electrode C_3 during calibration and three feedback conditions. Feedback modalities include eye-visual, vibrating motor-vibrotactile, and both-bimodal. Red represents increased power, blue decreased power. Frequency bands: β (15-30 Hz), μ (8-12 Hz). p-values obtained through permutation analysis with FDR correction.

The contralateral electrode C_4 exhibited an ERD in the beta and mu frequency bands during KMI. Similarly, the decrease in power seemed greater during the bimodal feedback. Few statistically significant differences were identified in the beta and mu frequency bands during KMI execution, encircled in red within the p-value graph in figure 7.33. Furthermore, at approxi-

mately $t=1s$, a statistically significant difference emerged at frequencies around 1-7 Hz, more likely due to an increase in power observed during the vibrotactile feedback condition.

For the ipsilateral electrode C_3 (depicted in figure 7.34), the ERD was observed in the beta (15-30 Hz) and mu (8-12 Hz) frequency bands, starting at the onset of KMI ($t=0s$) and persisting until its finale at $t=4s$. Notably, the ERD appeared more pronounced, denoted by a darker shade of blue, during the bimodal feedback condition. However, no statistically significant differences emerged in C_3 during KMI execution, as shown by the right-most p-value graph. This suggests that participants performed equally well in all four conditions.

During the feedback phase at $t=4s$, a statistically significant difference was observed only during the initial second of the feedback, specifically at frequencies 1-7 Hz for both electrodes C_3 and C_4 . This observation may be associated with the transient increase in power at the beginning of the feedback stimulation. This phenomenon was more pronounced during the vibrotactile and bimodal feedback conditions, similar to the earlier findings during the bimodal stimulation discussed in chapter 6. It is important to note that at $t=4s$, the resting phase of the calibration started, whereas, for the three feedback conditions, this time point marked the onset of the feedback phase. Therefore, the statistical differences after the KMI ($t=4s$) correspond the differences between the calibration's rest and the period corresponding to the feedback stimulation.

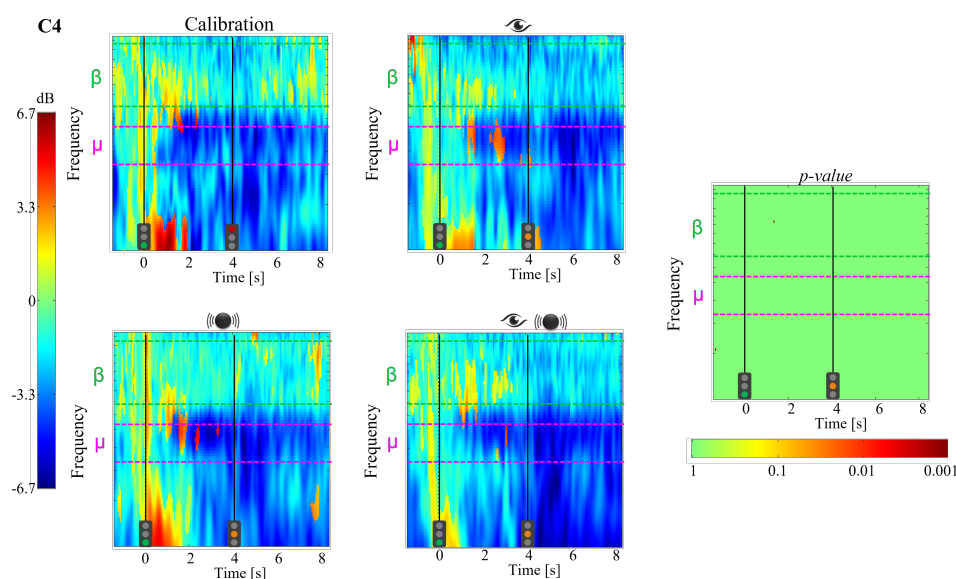


Figure 7.35: Time-Frequency Analysis (ERSP) of right-hand MI ($n=3$) at electrode C_4 during calibration and three feedback conditions. Feedback modalities include eye-visual, vibrating motor-vibrotactile, and both-bimodal. Red represents increased power, blue decreased power. Frequency bands: β (15-30 Hz), μ (8-12 Hz). p-values obtained through permutation analysis with FDR correction.

7.3.6.1.2 Right hand KMI In this study, only three participants were left-handed, thus they performed right-hand MI. Due to the limited number of individuals, the results presented here are of an exploratory and observational nature, with a larger dataset being required to establish definitive conclusions. Nonetheless, these initial observations shed light on the system's adaptability, as users with varying hand preferences are effectively accommodated by it. This

adaptability is particularly relevant when considering post-stroke patients, whose affected limb may differ.

Only three participants were left-handed, thus, they executed right-hand KMI of the right hand. The time-frequency analysis of the ipsilateral electrode C_4 in figure 7.35 revealed a sustained ERD in the mu frequency band during KMI, extending across the calibration and all feedback conditions. Indeed, no statistically significant differences were observed among the four conditions, as shown by the p-values in the rightmost graph. Interestingly, an ERS was observed during calibration and vibrotactile feedback, while it was attenuated for the visual and bimodal feedback conditions.

During the feedback phase, starting at $t=4s$, the ERD was observed for frequencies below 15 Hz. Moreover, this ERD was present in the rest phase of the calibration, leading to no statistically significant differences after KMI completion.

Moving to the contralateral electrode C_3 depicted in figure 7.36, a consistent ERD was also observed for the mu frequency band throughout the entire KMI task during calibration. The ERD started around $t=1s$ during the visual and bimodal feedback conditions, exhibiting components in mu and in frequencies spanning 1-7 Hz. In the visual condition, the ERD appeared in mu and around 12-15 Hz, commencing around $t=2s$, preceded by a brief ERS in the same frequencies. Despite these observations, no statistically significant differences were detected among conditions, probably due to the very limited number of participants. Additionally, the ERD was present during the feedback phase at $t=4$, primarily in the mu band and lower frequencies, indicating the processing of the feedback stimulation.

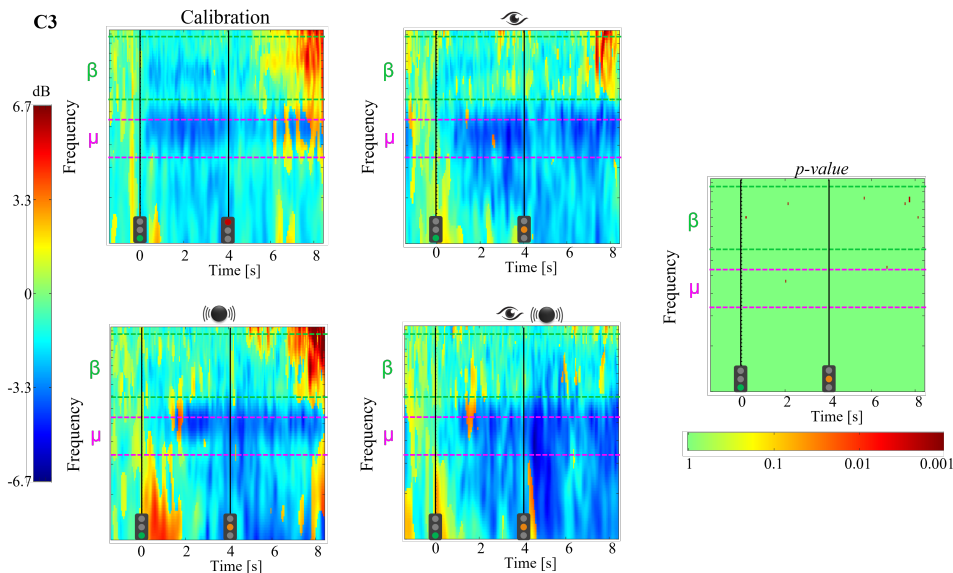


Figure 7.36: Time-Frequency Analysis (ERSP) of right-hand MI ($n=3$) at electrode C_3 during calibration and three feedback conditions. Feedback modalities include eye-visual, vibrating motor-vibrotactile, and both-bimodal. Red represents increased power, blue decreased power. Frequency bands: β (15-30 Hz), μ (8-12 Hz). p-values obtained through permutation analysis with FDR correction.

7.3.6.2 Scalp topographies of the KMI phase

Following the EEG offline analysis, the topographies corresponding to the KMI phase were obtained. In this way, observing the average power during the four seconds of KMI for the 64 electrodes is possible, obtaining an image covering most of the top scalp.

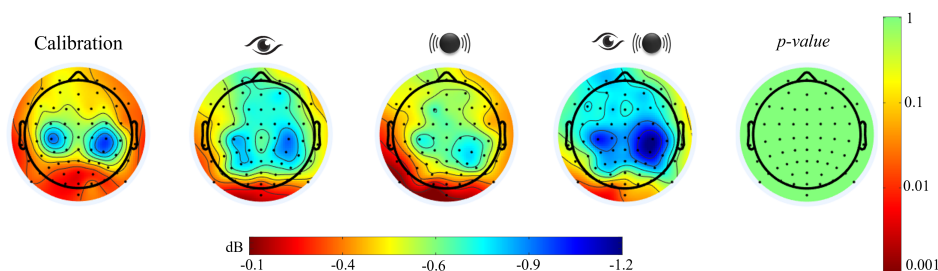


Figure 7.37: Scalp topographies of the average of left-hand KMI ($t=0-4s$) for the 8-30 Hz frequency band for the calibration and feedback phases ($n=28$). Feedback modalities include eye-visual, vibrating motor-vibrotactile, and both-bimodal. Red represents increased power, blue decreased power. Frequency bands: β (15-30 Hz), μ (8-12 Hz). p-values obtained through permutation analysis with FDR correction.

7.3.6.2.1 Left hand KMI Figure 7.37 displays the topographies corresponding to the average power during KMI ($t=0-4s$) for the combined mu and beta frequencies (8 to 30 Hz), corresponding to the frequency band used for the online classification. A bilateral ERD was observed during calibration and feedback phases, mainly in C_3 and C_4 , but it also extended to CP_4 . In all four conditions, the ERD seemed more pronounced in the contralateral hemisphere to the imagined limb, depicted by C_4 .

The ERD was more pronounced during the bimodal feedback (depicted by an eye and a vibrating motor), where more electrodes surrounding C_4 and C_3 also presented an ERD. These results suggest that the bimodal feedback leads to higher desynchronization of the sensorimotor areas corresponding to hand movement. Interestingly, the ERDs observed in the unimodal feedback conditions (visual, vibrotactile) seemed weaker than the one in the calibration. Despite these observations, no statistically significant difference was observed among the four conditions, as shown by the rightmost p-value topography in the same figure. These results may suggest that participants engaged the sensorimotor cortex successfully throughout the entirety of the experimental session.

As both mu and beta contain information related to KMI, the topographies for each of these frequencies were obtained as well. First, the ERDs present in the beta frequency bands (fig. 7.38(a)) were weaker than those in mu (fig. 7.38(b)), as noted by the smaller scale corresponding to the beta band. The ERD present in this band was very localized bilaterally during the calibration phase, while for the three feedback modalities, it occupied most of the sensorimotor areas, ranging from the row corresponding to Fc electrodes to the row comprising CP electrodes. Furthermore, during the bimodal feedback condition, the ERD extended to frontal areas. Nevertheless, no statistically significant differences were observed among the different calibration and feedback conditions.

Concerning the mu frequency band, the ERD during the calibration was clearly bilateral, depicted by C_3 , C_4 , and CP_4 in figure 7.38(b). The ERD was more prominent on the contralateral

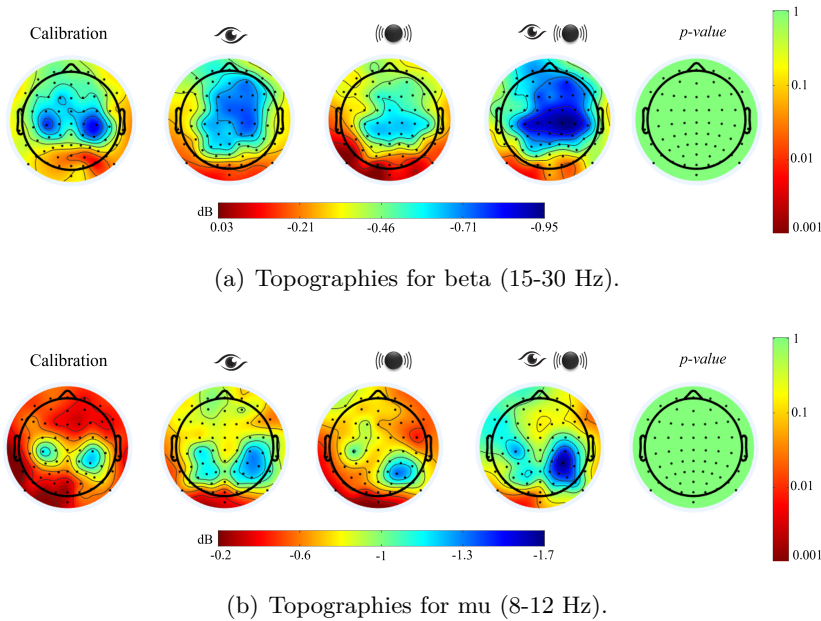


Figure 7.38: Scalp topographies of the average of left-hand KMI ($t=0-4s$) for a) mu and b) beta frequency bands for the calibration and feedback phases ($n=28$). Feedback modalities include eye-visual, vibrating motor-vibrotactile, and both-bimodal. Red represents increased power, blue decreased power. Frequency bands: β (15-30 Hz), μ (8-12 Hz). p-values obtained through permutation analysis with FDR correction.

side during bimodal feedback, corresponding to electrodes C_4 , CP_4 , and P_4 , extending to neighbor electrodes. Interestingly, during the vibrotactile feedback modality, the ERD was present mainly on the posterior contralateral electrodes P_4 and P_6 . No statistically significant difference was observed among the four conditions for the mu frequency band, suggesting participants executed similar KMI throughout the session.

7.3.6.2.2 Right hand KMI The scalp topographies corresponding to the KMI of the right hand by the three left-handed individuals are displayed in figure 7.39. An ERD is visible in the electrode C_3 , contralateral to the KMI during the calibration phase. However, for the three feedback conditions, the ERD is almost non-existent. Remarkably, a bilateral ERS was observed in posterior electrodes. This is in line with the observation of the study in [248], where an ERS was observed in posterior electrodes during visual MI of the right hand by left-handed individuals. Nevertheless, the small number of left-handed individuals ($n=3$) does not allow us to formulate definitive conclusions. Instead, these results are merely observational and exploratory.

7.3.6.3 Scalp topographies of the feedback phase

In the preceding study presented in chapter 6, brain activity was examined during the bimodal stimulation of the left upper limb. However, this analysis lacked a comparative dimension between modalities as it did not allow for a direct assessment of brain activity associated with visual-only and vibrotactile-only stimulation. In the current study, it was possible to address this gap, as the three modalities were presented. One notable limitation, however, was the inherent imbalance in the four stimulation levels (None, Low, Medium, High) owing to the dependence

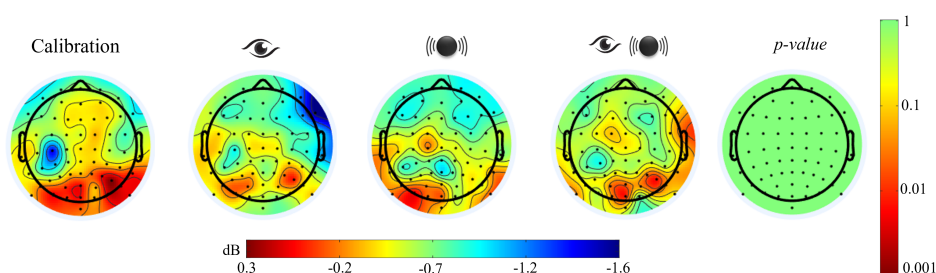


Figure 7.39: Scalp topographies of the average of right-hand KMI ($t=0-4s$) for the 8-30 Hz frequency band for the calibration and feedback phases ($n=3$). Feedback modalities include eye-visual, vibrating motor-vibrotactile, and both-bimodal. Red represents increased power, blue decreased power. Frequency bands: β (15-30 Hz), μ (8-12 Hz). p-values obtained through permutation analysis with FDR correction.

of the stimulation intensity based on the brain activity during KMI. To mitigate this imbalance, the scalp topographies were obtained for the first two seconds of the feedback, which are common to all four stimulation levels.

The brain activity elicited by the feedback stimulus is presented in figure 7.40. Consistent with the observation in the previous chapter, the ERD corresponding to the bimodal stimulation displayed a bilateral pattern, with a more pronounced effect on the contralateral side of the stimulation. However, in this study, it was present mainly in electrodes C_4 , CP_6 , and P_6 , and it extended to neighboring electrodes, such as C_6 and CP_6 . Additionally, the ipsilateral posterior electrodes P_1 , P_3 , and P_5 exhibited an ERD in response to the bimodal feedback.

In contrast, the visual-only feedback, as shown in the leftmost topography, exhibited ERDs primarily in posterior electrodes, suggesting a focus on the visual processing related to the hand animation. On the other hand, the vibrotactile feedback generated ERDs concentrated on the contralateral hemisphere around electrodes C_4 , C_6 , CP_4 , and CP_6 . These discernible differences were confirmed by the statistical permutation tests, where significant differences were exhibited. The main differences were in the contralateral hemisphere as well as in all posterior electrodes. These results highlight that bimodal feedback was indeed the integration of two senses: visual and tactile.

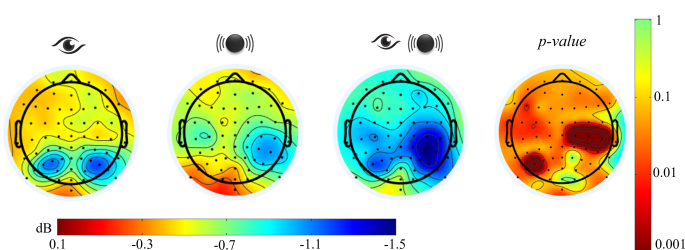


Figure 7.40: Scalp topographies of the average of the feedback phase ($t=4-6s$) for the 8-30 Hz frequency band ($n=28$). Feedback modalities include eye-visual, vibrating motor-vibrotactile, and both-bimodal. Red represents increased power, blue decreased power. Frequency bands: β (15-30 Hz), μ (8-12 Hz). p-values obtained through permutation analysis with FDR correction.

7.4 Discussion

7.4.1 BCI performance is comparable in all feedback modalities

In this study, participants tested three feedback modalities: visual, vibrotactile, and bimodal. The experimental session aimed to evaluate their KMI execution of grasping a bottle throughout the feedback modalities, where the performance scores corresponded to the recall. The results demonstrated that the mean performance in all three modalities exceeded the commonly accepted 70% threshold often used in BCIs to determine successful control [242]. This suggests that participants were able to effectively control the BCI irrespective of the feedback modality employed.

Furthermore, the order of presentation did not significantly impact the performance scores. Although a slight decrease in scores was observed during the last condition, this difference did not reach statistical significance. It is worth noting that longer training sessions may lead to more pronounced decreases in performance impacted by fatigue. In this study, the fatigue level increased significantly at the end of the session. No effect was observed on the performance scores due to fatigue. However, this might change in longer sessions. Therefore, for future studies involving post-stroke patients, the recommendation is to maintain a training duration of a similar or shorter length.

Several factors could account for this successful interaction. First, all participants followed a brief training session to familiarize themselves with the KMI task, which likely enhanced their task comprehension and contributed to the relatively high-performance levels observed. Second, the fact that participants held a physical bottle in their hands, similar to the one displayed on the screen, likely helped them to execute the grasping KMI, as previously demonstrated in [249]. Thirdly, the visual feedback incorporated gamified elements while maintaining a realistic hand animation. On the other hand, the vibrotactile feedback was meticulously designed, as detailed in chapter 6, drawing inspiration from the muscle activation during grasping. The realism and fidelity of the feedback to the real movement likely contributed to the high levels of performance observed.

Given that the three feedback modalities yielded similar levels of performance, it is possible to conclude that any of these modalities may be employed to support KMI. Therefore, the choice of feedback modality may be made mainly based on user's preferences. Most importantly, in the context of post-stroke motor rehabilitation, the selection of feedback modality may be tailored to the patient's capabilities and needs. For instance, a patient with visual deficiencies, such as hemineglect, may benefit from the vibrotactile modality to follow the BCI training. Conversely, hypersensitive patients who may find vibrations uncomfortable or painful could opt for the visual modality. Hemiparetic patients without visual or sensory impairments could benefit from the bimodal modality. In summary, the designed BCI system can be adapted to individual patient requirements while maintaining comparable performance levels.

7.4.2 Participants' preference for the bimodal feedback

The majority of the participants expressed a distinct preference for the bimodal feedback modality, which combined visual and haptic sensory inputs. Numerous participants noted in their written comments that the bimodal feedback provided them with a valuable combination of visual and tactile cues, enhancing their ability to mentally imagine the sensations required for the KMI rather than its visualization.

The participants' ranking of feedback modalities revealed that the bimodal modality was consistently favored and was never ranked as the least preferred option, highlighting its superiority over the other two modalities. Conversely, the visual modality was consistently ranked as the least preferred modality. Surprisingly, the vibrotactile feedback ranked second place despite lacking a visual component. Participants reported that the vibration helped them to concentrate on the sensory aspects necessary for KMI without the distraction of visual motor imagery. Nevertheless, it is important to note that one participant who preferred visual feedback found the vibration distracting from the mental task. Interestingly, this participant exhibited the lowest performance during the vibrotactile modality. While this is an isolated case, it emphasizes the potential impact of user preference on performance, highlighting the importance of an adaptable BCI system like the one used in this study.

In addition to the ranking of feedback modalities, five more items were evaluated. The results revealed a strong preference for the bimodal feedback in terms of supporting movement imagination, realism of the feedback, and entertainment value. Strikingly, the visual and the bimodal modalities were considered equivalent regarding comprehensibility. This indicates that, despite requiring the integration of two sensory modalities (visual and tactile), the bimodal feedback was easily understood. This finding aligns with the acceptable mental workload measured using the NASA-TLX and the cognitive load with the NEXT-Q. Therefore, it is possible to conclude that the bimodal feedback is understandable and not too complex, fulfilling the suggestions of comprehensible feedback in [230].

7.4.3 Factors influencing the performance

To identify the factors that influence BCI performance, we conducted an examination of potential manual activities that may influence KMI execution. To this end, a linear model was constructed to assess the effect of different manual activities on the average KMI performance. The resulting model explains only around 31% of the variation in the data, thus, the results must be taken carefully.

The results of the model indicate that playing video games and cooking practice have a positive influence on KMI performance. This positive effect of gaming aligns with the previous findings by Vourvopoulos et al. [250], which suggested that a strong gaming profile is associated with improved BCI training. Moreover, the gaming experience has been linked to enhanced learning and improving motor imagery skills over time [251].

Similarly, cooking practice exhibited a positive effect on KMI performance. This could be attributed to the fine motor skills and the visuo-motor coordination involved in cooking. In fact, visuo-motor coordination abilities have been suggested as potential predictors of BCI performance [252].

Conversely, no significant impact was found due to other manual activities, such as painting/-drawing and knitting/sewing. The practice of a musical instrument, despite its modulation of mu rhythm in BCI control [253], did not yield a significant effect on BCI performance scores. This finding is consistent with the results reported in [236] and [254]. The latter study attributed this lack of impact to the number of participants engaged in music practice. However, in the present study, the music players accounted for 36.67% of the participants. Therefore, the relationship between music practice and performance warrants further exploration in future studies.

Furthermore, although regular physical practice has been suggested to improve motor imagery

[236], our study found that sports practice did not significantly affect performance scores, in line with the results from [254]. The contrasting findings underscore the need for further research into the relationship between sports practice and motor imagery abilities.

Mindfulness has been suggested to enhance BCI performance [246, 245]. Surprisingly, a negative effect on performance scores was observed due to meditation and/or meditation practices. As detailed in the results section, this anomaly may be attributed to the presence of an outlier participant who reported practicing mindfulness/meditation activities but exhibited very low performance. This outlier's influence on the sample may have led to the negative effect. Additionally, the impact of mindfulness was evaluated using the FMI questionnaire and no correlation was found between mindfulness ability and the performance score, corroborating the observations from our linear model. The limited number of participants engaging in mindfulness activities may explain the lack of impact on performance. Consequently, mindfulness ability may not be a prerequisite for post-stroke patients to successfully interact with the BCI.

Finally, no correlation was detected between the performance scores and participant's perceived self-efficiency. It is noteworthy that participants reported consistently high self-efficiency scores, and even those with the lowest self-efficiency scores achieved high-performance levels. Although self-efficiency did not emerge as a performance predictor, it is indicative that future patients do not need high perceived self-efficiency to interact effectively with the BCI. Post-stroke patients, for instance, may encounter depression or diminished emotional states due to their condition, having a negative impact on their perceived self-efficiency. As our study involved a neurotypical population, future studies with patients should consider measuring self-efficiency to assess its potential impact on BCI performance.

It is important to emphasize that while certain factors may serve as predictors of BCI performance, they should not be misconstrued as exclusionary criteria. For example, instead of excluding patients who do not engage in video gaming on the presumption that they cannot control the BCI, a more constructive approach would involve adapting the BCI training to meet their specific needs. This might entail increasing the frequency of practice sessions or dedicating additional time to facilitate the learning and comprehension of KMI.

Given the contrasting results observed among studies for various factors, such as musical practice, sports, and mindfulness, it would be unwise to consider them as definitive elements in predicting performance in MI-based BCIs.

7.4.3.1 Further exploring low performances

Further exploratory investigation was conducted to delve deeper into the performance of four participants whose overall BCI scores fell below 60% and exhibited no discernible EEG artifacts. The primary objective was to gain a more profound understanding and potential indicators of the factors contributing to their remarkably low BCI performance.

It's essential to highlight that two of these participants did not engage in any meditation or mindfulness activities. The remaining two participants who did engage in such practices did so infrequently, meditating only once a week for less than 30 minutes. Additionally, two out of the four participants did not report participating in any of the manual activities suggested, and none of them played video games. Furthermore, one participant, who exhibited an average feedback score of 55.46%, did not report practicing any of the proposed activities, nor practiced any sports or meditation practice.

The absence of regular engagement in manual activities could potentially be an indicator of low BCI performance, as it might signify a lack of body awareness, which could influence KMI performance. Interestingly, one participant with an average score of 52.50% reported practicing four of the suggested manual activities, except for playing video games, and also engaged in sports and meditation. These findings raise intriguing questions about the relationship between manual activities, body awareness, and BCI performance. However, it is important to note that further studies are required to validate this hypothesis and establish a more comprehensive understanding of these dynamics.

7.4.4 The bimodal BCI offers a positive user experience

The results obtained from the MES questionnaire revealed that the BCI training session had no adverse impact on the participants' emotional well-being. In fact, participants reported feelings of surprise at the end of the session. Given that all participants were novices at BCI training, this surprise may be attributed to the novelty of interacting with this type of system for the first time. For future long-term studies, it would be relevant to investigate whether this initial surprise persists or attenuates as participants become more familiar with the BCI interface. Indeed, the first stages of learning a motor task require focalized attention [255]. Therefore, future research should consider the evaluation of dimensions associated with learning.

Additionally, the interaction with the BCI elicited positive emotions, such as exhilaration and cheerfulness, while negative emotions, including anger and frustration, were notably absent, according to the results from the meCUE questionnaire. These findings align with the high score on the *Mood* dimension of the NEXT-Q questionnaire. Moreover, this dimension was enhanced by the bimodal feedback, indicating the positive impact of this modality on the participants' emotional states.

Regarding motivation, results from the NEXT-Q questionnaires reveal a positive effect of the bimodal feedback, outperforming the unimodal visual and vibrotactile feedback. This could be attributed to more comprehensive feedback provided by the bimodal system, as confirmed by participants' written feedback and their preference for this modality. The positive impact was also observed in the AttrakDiff questionnaire, where motivation received a positive score. Furthermore, participants indicated the system did not render them passive, suggesting they were actively motivated to engage in the KMI task. Indeed, as indicated by prior research, motivating feedback is crucial for effective learning [256]. In this study, both the NEXT-Q and the AttrakDiff questionnaires demonstrate that bimodal feedback significantly enhances motivation, which in turn, is expected to benefit the learning of KMI tasks, favoring bimodal feedback over unimodal modalities.

According to the AttrakDiff questionnaire, only the performance scores during the bimodal feedback revealed an effect on the pragmatic quality dimension. This highlights the utility of bimodal feedback in facilitating the correct execution of KMI. Notably, participants perceived the bimodal BCI as desirable, even though this study did not involve the target post-stroke population. This positive perception likely arises from the participants' impression that the bimodal BCI can assist in the performance of KMI tasks, which aligns with its ultimate goal of aiding post-stroke motor recovery. The favorable AttrakDiff scores provide robust evidence of the system's overall attractiveness and usability, laying a solid foundation for an upcoming study with post-stroke patients. In this new study, improvements in the physical appearance and comfort of the device are expected, as an enhanced second version of the vibrotactile device

as well as fewer EEG electrodes will be employed.

Lastly, the sense of agency was higher during the bimodal feedback than the visual modality. However, it was similar between the vibrotactile and the bimodal feedback. These findings suggest that bimodal feedback is clearly superior in enhancing the sense of control over the BCI, and haptic feedback may be sufficient for increasing agency. This aligns with prior studies that have indicated that haptic feedback can enhance the sense of agency [257]. The present study demonstrates that combined visual and vibrotactile feedback effectively stimulates the skin mechanoreceptors and enhances agency without requiring limb movement. This finding is particularly relevant for post-stroke patients who may experience discomfort when moving the affected upper limb, rendering them unable to benefit from feedback using exoskeletons or robots. Thus, the proposed novel bimodal feedback is a potential alternative for them.

In summary, the BCI FeelIt, which provides bimodal feedback to support grasping KMI, offers a positive user experience. The emotional well-being of participants remained intact, with predominantly positive emotions observed during interactions with the system. Furthermore, the bimodal feedback enhances mood, motivation, and agency while effectively supporting the execution of the KMI task.

7.4.5 EEG activity

The EEG activity was analyzed across the three feedback modalities and the calibration. ERD was observed in both the mu and beta frequency bands, which are commonly associated with motor imager-related brain activity, during all four conditions. Interestingly, the ERD observed during the calibration did not differ from the ERD seen during the feedback modalities. This observation suggests that the brief training for performing KMI just before using the BCI was effective, and participants clearly understood how to perform the KMI task. Moreover, the bimodal feedback generated a notably stronger ERD in sensorimotor areas compared to the two other two feedback modalities and calibration (refer to figure 7.37). However, it is worth noting that this difference did not reach statistical significance. Therefore, all feedback modalities succeeded in supporting KMI similarly.

The ERD was observed in both brain hemispheres but was more pronounced in the contralateral hemisphere. This is in contrast to previous research, where the motor imagery of the upper limb elicited ERDs primarily in the contralateral hemisphere [108, 258]. However, studies involving EEG and fMRI analysis of motor imagery of the non-dominant hand have shown bilateral ERD activity [259, 260, 261]. This bilaterality has been present even in cases of long-term KMI execution of the dominant hand [262]. Motor imagery is influenced by how people normally perform actions [263], as in a dominant or nondominant manner. This bilateral activation may suggest that participants expended greater effort to perform non-dominant KMI due to their lack of familiarity with the action, resulting in a larger mobilization of the sensorimotor area. This aligns with the findings in [258], where complex motor imagery tasks lead to less pronounced ERD lateralization, supporting the presence of bilateral ERD during non-dominant KMI. Furthermore, bilateral ERD activity has been documented in post-stroke patients during motor imagery of the affected limb [261]. Thus, employing the non-dominant hand for KMI in neurotypical participants can effectively simulate the conditions of post-stroke patients.

During the feedback phase, the ERD was observed in regions corresponding to each modality. Posterior electrodes exhibited bilateral ERDs during the visual feedback phase, indicating the visual processing of the hand animation, in line with the findings from the literature [264,

34]. In contrast, vibrotactile feedback displayed activity on the central-parietal contralateral electrodes, as previously observed in [206]. Lastly, bimodal feedback induced a bilateral ERD, which was more pronounced on the contralateral side, primarily in the central and central-posterior electrodes, suggesting effective integration of visual and tactile senses. This integration is further confirmed by the statistically significant differences, indicating that bimodal feedback produced oscillations more prominently compared to the two unimodal feedback.

7.5 Conclusion

In this chapter, an evaluation of the BCI FeelIt, integrating visual and vibrotactile feedback, was conducted. Three feedback modalities were compared: visual, vibrotactile, and bimodal (visual and vibrotactile) regarding BCI performance and overall user experience. The primary objective was to determine whether the bimodal feedback modality could enhance grasping KMI compared to unimodal alternatives, all while ensuring a positive user experience.

While the BCI performance remained consistent and acceptable across all three feedback modalities, the participants strongly favored the bimodal feedback approach. Additionally, the bimodal modality yielded superior results in influencing mood, motivation, and agency, which are critical factors for successful BCI control, as well as KMI execution and learning. It is worth noting that the bimodal feedback also elicited brain activity during KMI in the form of event-related desynchronization in the sensorimotor cortex, similar to unimodal feedback. Moreover, during the feedback stimulation phase, it exhibited a more substantial desynchronization on the sensorimotor cortex than unimodal feedback.

In summary, this study demonstrates that the innovative bimodal feedback significantly enhances the user experience during BCI interaction and effectively supports KMI execution. The similar BCI performances in the three feedback modalities emphasize the potential for tailoring the system to accommodate patient-specific limitations, preferences, and rehabilitation goals. While the study involved a neurotypical population, the promising outcomes lay a robust foundation for advancing our research to include post-stroke patients.

Chapter 8

Toward a Post-Stroke Evaluation of a KMI-Based BCI Integrating Visual and Vibrotactile Feedback: Experimental Protocol

Contents

8.1	Introduction	154
8.2	Objectives	155
8.2.1	Primary Objective	155
8.2.2	Secondary Objectives	156
8.3	Participants	157
8.3.1	Inclusion and Non-Inclusion Criteria	157
8.3.2	Pseudo-Anonymization	158
8.4	Study Procedure	158
8.4.1	Experimental Setup	158
8.4.2	Procedure	158
8.4.3	Study Duration	164
8.5	Statistical Tests	164
8.6	Benefits and Risks	165
8.7	Withdrawal	165
8.8	Management of Adverse Events	165
8.8.1	Evaluation and report of adverse events	165
8.9	Data Archiving and Access to Documents	166
8.10	Conclusion and Study Limitations	166

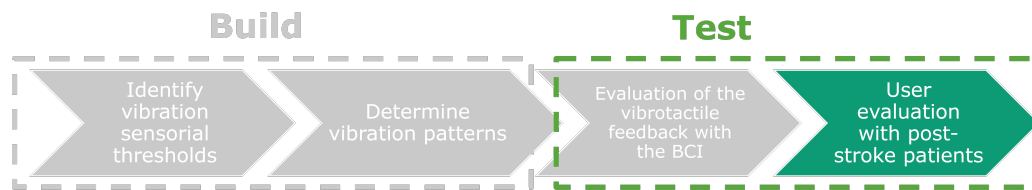


Figure 8.1: Methodology for designing and evaluating vibrotactile feedback: Test phase - User evaluation with post-stroke patients.

8.1 Introduction

In this chapter, we present a proposition of the experimental protocol to evaluate the usability and attractiveness of Feellt, which is the second test step of the DBR methodology in figure 8.1.

The ANR project Grasp-IT aims to recover upper limb control by improving the performance of kinesthetic motor imagery of post-stroke patients using a tangible and haptic interface within a gamified BCI training environment. Within the project, three haptic modalities are developed by different partners:

- Functional electrical stimulation (FES) feedback, developed by the Inria team project Camin,
- Tangible feedback, developed by the PERSEUs team from the Université de Lorraine, the company Alchimies/OpenEdge, and the Neurorhythms team at LORIA.
- Vibrotactile feedback, developed by Neurorhythms team at LORIA, the PERSEUs team and the Inria team Hybrid and presented in this thesis.

The protocol with post-stroke participants is divided into two phases:

- The first phase aims to ensure the system is reliable, pleasant, and effective in helping the patient perform the KMI. It aims to assess the potential of the three haptic modalities to support a positive user experience (including effective and efficient execution of KMI), and to determine the feasibility of using the system for a clinical study.
- The second phase comprises a clinical study that will evaluate the therapeutic effects of the previously validated solutions on motor recovery due to the BCI training.

Both phases involve a multi-center protocol, where all centers will have the same visual feedback, but the haptic feedback modality will be different for each center, as follows:

- FES - University Hospital Center (CHU) in Toulouse.
- Tangible - Institut Régional de Réadaptation (IRR) - Rehabilitation Center of Lay-Saint-Christophe.
- Vibrotactile - University Hospital Center (CHU) Rennes.

At the time of writing this thesis, the FES and tangible modalities are undergoing design and feasibility tests. Consequently, the protocol presented in this chapter, corresponding to the first phase of the clinical protocol, involves only the vibrotactile feedback modality. Therefore, this protocol proposition is a single-center single-blinded, non-interventional user study. The study

will be submitted for approval by a Committee for Personal Protection (Comité de Protection des Personnes - CPP), which is responsible for issuing a decision on the validity of any research concerning the human body, as outlined in article L 1123-7 of the French Public Health Code (Code de la Santé Public - CSP) ⁵. Participants will be recruited at the rehabilitation service of the University Hospital Center of Rennes, France, where the research will take place. This proposition will serve as the basis for the multi-center protocol, facilitating the integration of the other feedback modalities.

8.2 Objectives

In the previous chapters, we presented our design process of the vibrotactile feedback and proved its potential to improve the execution of KMI, as well as to confirm the reliability of the BCI Feellt. The positive overall results allow us to perform an initial non-interventional user test among the post-stroke population.

8.2.1 Primary Objective

The primary objective of this protocol is to estimate the potential of three feedback modalities, visual, vibrotactile, and bimodal (visual and vibrotactile), to support post-stroke patients in the effective and efficient execution of a KMI grasping movement and a good-quality BCI experience for patients.

To provide post-stroke participants with support in KMI-based rehabilitation sessions, the device must first meet the following dimensions:

- Usefulness;
- Usability;
- Desirability.

The participants will evaluate the three dimensions for each feedback modality according to the following criteria.

8.2.1.1 Usefulness Criteria

This dimension assesses the degree to which the BCI fulfills its intended purpose, in this case, to activate the sensorimotor cortex corresponding to the upper limb. Additionally, it should allow participants to keep a constant execution of the KMI throughout the session and to help them maintain or increase their performance. The evaluation criteria are the following:

1. Score > 50% of the BCI performance (the score's computation is explained in section 7.2.5.2).
2. Constant BCI performance score across trials, or score improvement throughout the session.
3. Greater ERDs observed during the feedback modalities vs. the without feedback modality in the electrodes corresponding to the sensorimotor areas.

⁵<https://www.iledefrance.ars.sante.fr/comites-de-protection-des-personnes-cpp>

4. Greater ERDs observed during the bimodal feedback modality than the unimodal modalities in the electrodes corresponding to the sensorimotor areas.

8.2.1.2 Usability Criteria

This dimension evaluates the system's ease of comprehension and use. The evaluation criteria and their corresponding scores are outlined below:

1. Score > 1 for the pragmatic qualities of the AttrakDiff questionnaire [195].
2. Score $> 50\%$ of the BCI performance (the score's computation is explained in section 7.2.5.2). This criterion is similar to criterion 1 above.
3. Emotional states from MES questionnaire [193]: decrease or stability of scores related to the negative emotions, increase or stability of scores related to the positive emotions.
4. Stable fatigue level throughout the session, or low increase (less than 3 points in the FIFS scale [194]).
5. Score > 12 in the agency dimension of the NExT-Q questionnaire [240].
6. Score > 5 in the mindfulness dimension of the NExT-Q questionnaire.

8.2.1.3 Desirability Criteria

For the system to achieve long-term adoption and acceptance, it needs to possess an appealing and motivating quality while minimizing the mental and cognitive effort required. The corresponding evaluation criteria and their associated scores are as follows:

1. Score > 1 for the hedonic qualities and attractiveness dimension of the AttrakDiff questionnaire.
2. Score > 1 for the ratio of the mean score of hedonic and pragmatic qualities dimensions of the AttrakDiff questionnaire.
3. Score < 50 on the mental workload measured by the NASA-TLX questionnaire [208].
4. Score > 17 in the motivation dimension of the NExT-Q questionnaire.
5. Score > 12 in the mood dimension of the NExT-Q questionnaire.
6. Score < 8 in the cognitive load dimension of the NExT-Q questionnaire and stable across feedback modalities.

8.2.2 Secondary Objectives

The first secondary objective is to evaluate the potential of the BCI to be integrated into clinical rehabilitation services. In this case, the BCI must also be usable, useful, and desirable for the physical therapists. Thus, the evaluation criteria are as follows:

1. Score > 1 concerning the pragmatic, hedonic, and attractiveness dimensions of the AttrakDiff questionnaire;
2. Scores < 4 of the first three modules of the meCUE questionnaire;
3. Score > 2.5 of the fourth module of the meCUE questionnaire.

The second secondary objective is to evaluate the impact of different feedback modalities on the execution of KMI and prove the superiority of the bimodal modality. Consequently, we will compare the results of the NExT-Q and NASA-TLX questionnaires across the three feedback modalities. Furthermore, we will compare the ERDs/ERSs generated during the KMI tasks corresponding to each feedback modality.

8.3 Participants

8.3.1 Inclusion and Non-Inclusion Criteria

For this study, we will recruit 24 post-stroke participants. The inclusion criteria for participants are the following:

- The individual must be between 18 and 80 years old.
- First episode of unilateral ischemic or hemorrhagic stroke (supratentorial) of less than six months and more than three months after the event (late sub-acute phase [52]), confirmed by MRI or CT scan.
- The individual must have received full information on the organization of the research study and must have signed an informed consent form.

The non-inclusion criteria are the following:

- Presence of cognitive (CASP < 22 [265]) or/and sensory disorders hindering understanding of instructions and/or use of the device (assessment by an investigating physician).
- Impaired verbal comprehension (Boston Aphasia Quotient < 4 [266]).
- Presence of an unstable or infectious cardiovascular condition (assessed by the principal investigating physician).
- Severe spasticity (modified Ashworth score > 3 [267] for upper limb flexors).
- Presence of an implanted pacemaker (cardiac, deep-brain stimulation).
- Presence of a craniotomy, likely to modify the EEG response.
- Individuals unable to feel the vibrotactile stimulation, verified in 8.4.2.2
- Individuals covered by articles L. 1121-5 to L. 1121-8, L1122-2, and L. 1122-1-2 of the French Public Health Code:
 - Pregnant women, parturients, or nursing mothers;
 - Individuals deprived of liberty by judicial or administrative decision;
 - Individuals under psychiatric care;
 - Individuals admitted to a health or social establishment for purposes other than research;
 - Minors (not emancipated)
 - Adults under legal protection (guardianship, curatorship, safeguard of justice);
 - Individuals in emergency situations;

- Individuals of full age who is unable to give consent and who is not under legal protection.

8.3.2 Pseudo-Anonymization

To maintain the pseudo-anonymization of the participants and keep a record of the collected data (electrophysiological signals, questionnaires), the participants will be assigned the following ID: **VTBCI_PX**, where:

- VTBCI is the ID of the experiment - vibrotactile brain-computer interface;
- PX refers to the participant and X corresponds to a random number between 1 and 100 assigned to the participant, for example, P54.

The files with the EEG signals will be named **VTBCI_PX_Condition_Session_Run**, where:

- VTBCI is the ID of the experiment - vibrotactile brain-computer interface;
- PX refers to the participant and X corresponds to a random number between 1 and 100 assigned to the participant;
- Condition corresponds to Calibration, Visual, Vibrotactile, Bimodal;
- Session is S, plus a number from 1 to 4 corresponding to the session (for example, S3);
- Run is R, plus a number from 1 to 4 (1 or 2 for the calibration) corresponding to the run (for example, R2).

Under no circumstances personal data such as first and/or last names, age, gender, or address will be encoded in the ID.

8.4 Study Procedure

8.4.1 Experimental Setup

In this study, we will use the BCI FeelIT, presented in section 7.2.2 of chapter 7. The participants will be equipped with a BioSemi Active 2 EEG system. Unlike previous tests, a configuration involving only 39 electrodes will be employed (refer to figure 7.5 for specifics). Notably, during tests with neurotypical participants (see chapter 7) the classification algorithm was trained with 39 electrodes, underscoring its practicality. This approach reduces the participant's preparation time, ultimately leading to a more efficient procedure by allocating more time to BCI training. Furthermore, the vibrotactile device (shown in figure 4.11) will be positioned on the affected upper limb, with the virtual hand correspondingly aligned with the same limb. Lastly, electromyography (EMG) electrodes (recorded as external electrodes of the Biosemi system) will be placed on the flexor digitorum superficialis to ensure participants do not contract the muscle while practicing KMI.

8.4.2 Procedure

The study involves one pre-inclusion visit with the physician and five sessions, as shown in figure 8.2. A period of at least 48 hours is estimated between sessions to allow sufficient resting period between sessions. The study plan and evaluations are summarized and presented in table 8.1.

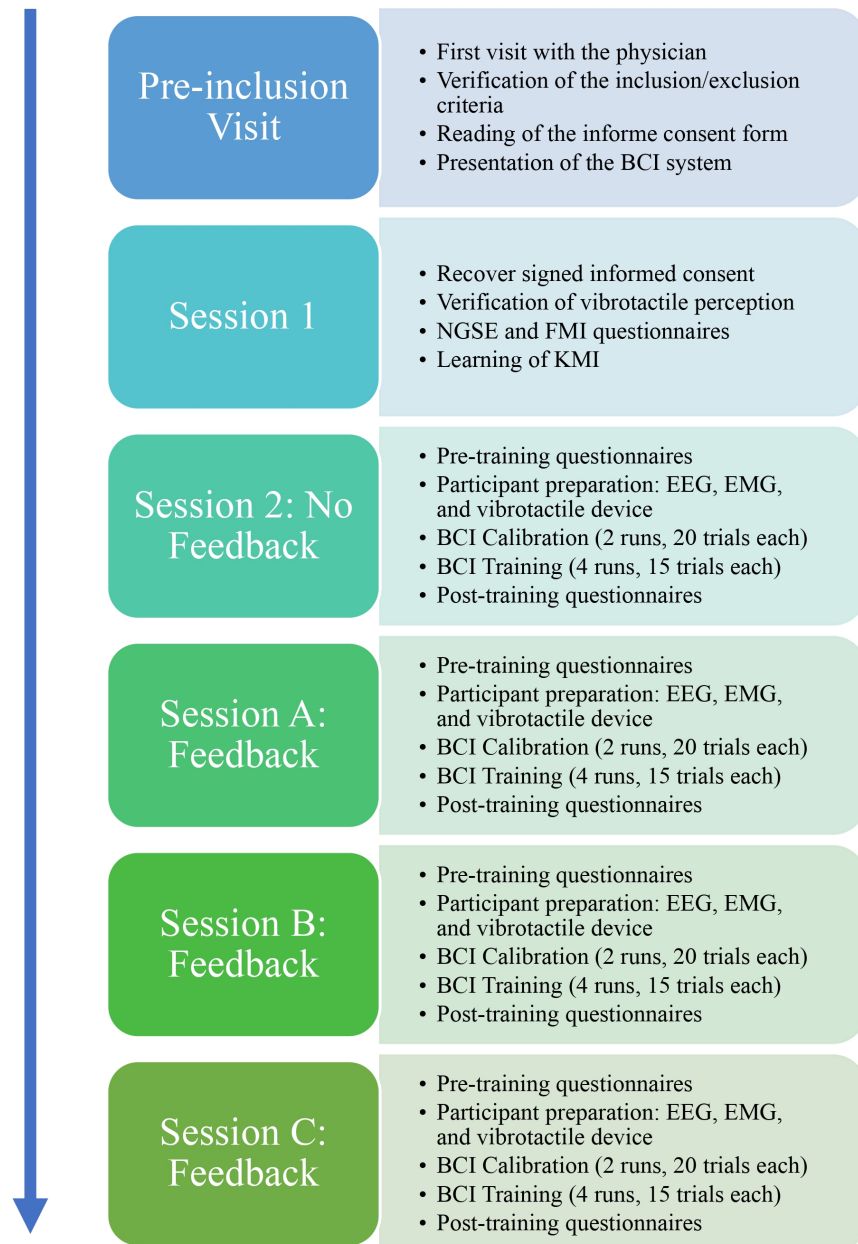


Figure 8.2: Study Design: Pre-inclusion visit and BCI training sessions.

	Pre-Inclusion Visit	Session 1	Session 2	Session A	Session B	Session C
Inclusion/Exclusion Criteria	X					
Signed Informed Consent Form		X				
Verification of vibrotactile perception		X				
Learning KMI		X				
BCI Training			X	X	X	X
User profile questionnaire (FMI, NGSE)	X					
Daily status questionnaire (MES, FIFS)			X	X	X	X
Feedback procedure assessment (NExT-Q)				X	X	X
Mental workload assessment (NASA-TLX)			X	X	X	X
AttrakDiff						X
meCUE						X
Ranking feedback modalities						X

Table 8.1: Study plan and outcome measures

8.4.2.1 Pre-Inclusion Visit

In the Pre-inclusion visit, potential participants will meet with the principal investigator who will clearly explain the experimental procedure, objectives, and any related risks. After reviewing the inclusion and exclusion criteria, two copies of the informed consent form will be given to the participants. A reflection period of at least one week will take place before the next session. The participants will be introduced to the BCI system, including the EEG acquisition system, the vibrotactile device, and the visual interface. They will not use it, rather they will just get visually familiar with it.

8.4.2.2 First Session: Verification of Vibrotactile Perception and System Presentation

At the beginning of the session, the voluntary participants will test the lowest vibration intensity of the vibrotactile device at least three times. The vibration intensity will be chosen according to their age, as observed in the results from chapter 5. The intensities are summarized in table 8.2. If participants cannot feel the lowest vibration at least two times out of three, we will increase the intensity by 10% until they can feel it. If participants cannot feel at least 75% of the maximum vibration (i.e. 191 PWM), they will not be included in the study. This step is crucial to ensure participants feel the vibration during feedback. The investigator will register the vibration intensity corresponding to each participant retained.

	Extensor		Flexor		Hand	
	<i>RPM</i>	<i>PWM</i>	<i>RPM</i>	<i>PWM</i>	<i>RPM</i>	<i>PWM</i>
Group 1	3,658	72	3,701	74	2,593	51
Group 2	4,355	85	4,214	83	3,044	60
Group 3	4,655	93	4,290	85	3,027	60

Table 8.2: Lowest vibration intensities to test with participants. PWM: pulse width modulation, RPM: revolutions per minute.

The informed consent form should be completed and signed by the participating patients. The investigator will countersign the document, and the session will start.

Participants will start by filling out the following two questionnaires:

- the NGSE questionnaire [238], to evaluate the influence of perceived self-esteem on the

performance;

- FMI questionnaires [239], to evaluate the influence of mindfulness on the performance.

Subsequently, participants will undergo initial training in KMI following an instructional video⁶ and receiving guidance from the experimenter. Next, they will discover how to perform the KMI following the instructions provided by the visual interface, akin to a calibration run, detailed in the next section. The EEG system will remain inactive during this session, hence, no feedback will be given to the participants. This session will allow participants to familiarize themselves with the task and the visual interface before their active engagement in the subsequent sessions.

8.4.2.3 Second Session: BCI Training Without Feedback

During this session, participants will use the BCI without any feedback. This will allow us to have a control condition without any supporting interface. They will start by filling out MES [193] and FIFS [194] questionnaires to evaluate their emotional and fatigue initial status, respectively. At the same time, the experimenter will start placing the EEG electrodes, and they will visually verify the filtered EEG signals (artifacts, blink presence, face muscular contraction) and electrode offset via the Biosemi ActiveView software (ideally between -10 and 10 μV , but a variation of $\pm 40 \mu\text{V}$ is accepted according to the manufacturer [268]). The EMG electrodes and the vibrotactile device will be placed on the forearm.

Initially, participants will perform five familiarization trials with the interface. The objective of these trials is that participants may remember how to interact with the interface, when to perform the KMI, and prepare to perform the calibration. This way, we ensure participants are ready to start the BCI training.

The calibration phase will start, consisting of two runs of 20 trials each run, summing up to 40 trial in total. The participants will be presented with visual cues through a traffic light indicating the KMI/rest phases, and they will hold a plastic bottle similar to a ketchup one with the affected limb. The chronological sequence of one calibration trial is as follows (see figure 8.3): Initially, the traffic light will be red for 30 seconds, indicating a resting state. This interval allows participants to relax and prepare, as well as to establish a baseline of their EEG activity. Subsequently, the light will transition to red and orange (warning phase) for two seconds, during which the participant prepares to perform a KMI. Once the light turns green, the participants will engage in the KMI task of mentally imagining squeezing a bottle of ketchup really hard for six seconds. Finally, the light will turn red for a random interval spanning between five and seven seconds, marking a resting phase where the participants will rest, and should not move or perform KMI. The trial will conclude once the resting phase is finished. Throughout the entire run, participants will be presented with the virtual hand holding the ketchup bottle (see figure 8.4, so they have a visual representation of the movement. However, it will remain stationary, abstaining from any form of feedback.

Once the calibration is done, participants will interact with the BCI without receiving any feedback. This phase consists of four runs of 15 trials, similar to the calibration phase, following the same timeline. Participants will have a two-minute pause between runs. At the end of each of the four runs, the participants will indicate their fatigue level using the FIFS 10-point scale. At the end of the session, participants will fill out the NASA-TLX [208] and MES questionnaires.

⁶Video available at: https://youtu.be/aQwr7-_REiU

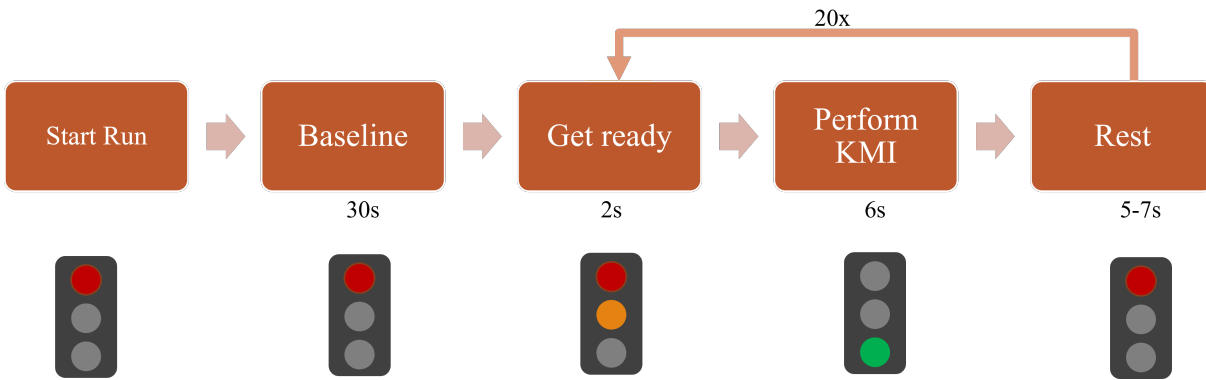


Figure 8.3: Calibration run timeline for study among post-stroke participants.

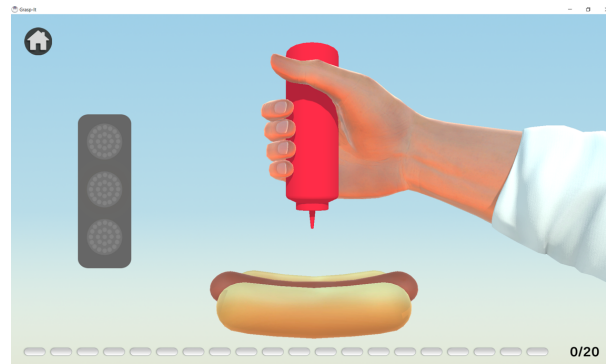


Figure 8.4: Image depicting the screen participants will see during the calibration. The virtual arm will match the participant's affected limb.

Furthermore, during this session, participants will be assigned to an experimental group. The presentation order will vary, and all participants will be presented with the three feedback modalities. The order of presentation of each modality will be pseudo-randomized ensuring even distribution of participants in the groups. Participants will belong to one of the six groups:

- **Group A:** Session A - Visual → Session B - Vibrotactile → Session C - Bimodal
- **Group B:** Session A - Visual → Session B - Bimodal → Session C - Vibrotactile
- **Group C:** Session A - Vibrotactile → Session B - Visual → Session C - Bimodal
- **Group D:** Session A - Vibrotactile → Session B - Bimodal → Session C - Visual
- **Group E:** Session A - Bimodal → Session B - Visual → Session C - Vibrotactile
- **Group F:** Session A - Bimodal → Session B - Vibrotactile → Session C - Visual

Participants will be assigned to one of the groups during the pre-inclusion visit. Only the experimenter will know to which group the participants belong, resulting in a single-blind experiment. Nevertheless, participants will know at the beginning of the session the feedback modality they will be presented with.

8.4.2.4 Third, Fourth, and Fifth Sessions: BCI Training with Different Feedback Modalities

Participants will test the three feedback modalities visual, vibrotactile, and bimodal, in each session, depending on the group they have been assigned to.

At the beginning of the session, participants will fill out questionnaires to evaluate their emotional and fatigue initial status. At the same time, the experimenter will start placing the EEG electrodes and they will verify the EEG signals via the ActiveView software. The EMG electrodes and the vibrotactile device will be placed on the forearm as well, regardless of the feedback modality. In this manner, we may eliminate any bias due to the vibrotactile device being present. Additionally, at the beginning of Session A, participants will read or will be read the NExT-Q [240] questionnaire so they know beforehand the elements to be evaluated.

Similarly to Session 2, participants will start with five familiarization trials. The calibration phase will be performed as explained in the previous section.

Subsequently, the feedback phase will start, following the next procedure (see figure 8.5 for details). First, participants will start with a 30-second rest period, during which the traffic light will be red. Then, a two-second warning phase starts when the traffic light is red and orange. The traffic light will then turn green for six seconds to indicate the KMI phase. Next, the traffic light will turn orange only and feedback will be provided to the participants either under a visual, vibrotactile, or bimodal modality. Note that during the vibrotactile modality, only the traffic light is displayed on the screen. Once the feedback is over, the traffic light will turn red for a period of 5 to 7 seconds, marking the end of a trial. Participants will perform four runs of 15 trials to complete the training. They will have a two-minute pause between runs. At the end of each run, they will indicate their fatigue level using the FIFS 10-point scale.

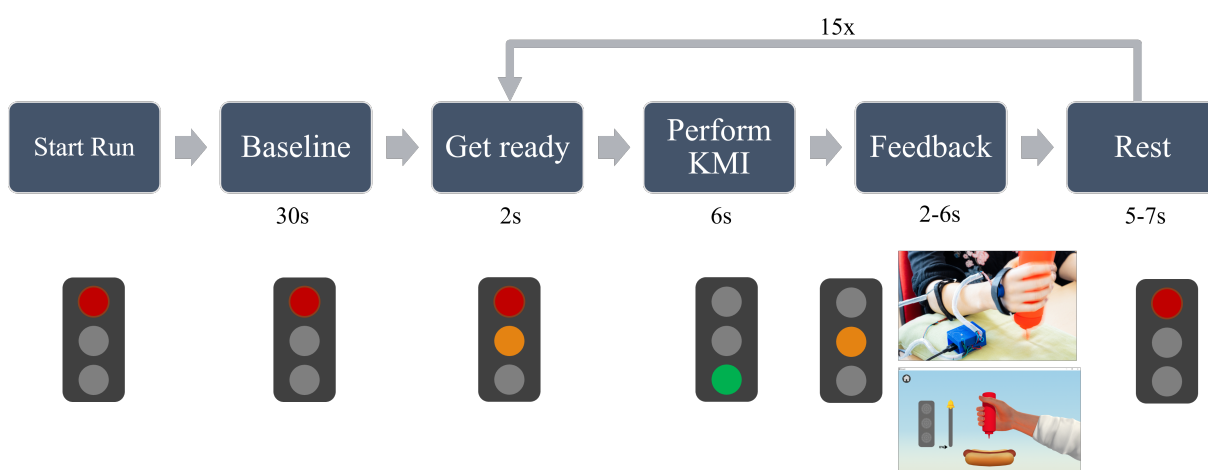


Figure 8.5: Feedback run timeline for study among post-stroke participants.

At the end of the session, participants will fill out the NExT-Q, NASA-TLX, and MES questionnaires. Furthermore, at the end of the fifth and last session, participants will rank the three feedback modalities by order of preference, and they will complete the short version of the AttrakDiff and module 2 of the meCUE questionnaire.

		Day 1	Day 2	Day 3	Day 4	Day 5
Week 1	Session 1	Participant 1	Participant 2	Participant 3	Participant 4	Participant 5
		Participant 6	Participant 7	Participant 8		
Week 2	Session 2	Participant 1	Participant 2	Participant 3	Participant 4	Participant 5
		Participant 6	Participant 7	Participant 8		
Week 3	Session A	Participant 1	Participant 2	Participant 3	Participant 4	Participant 5
		Participant 6	Participant 7	Participant 8		
Week 4	Session B	Participant 1	Participant 2	Participant 3	Participant 4	Participant 5
		Participant 6	Participant 7	Participant 8		
Week 5	Session C	Participant 1	Participant 2	Participant 3	Participant 4	Participant 5
		Participant 6	Participant 7	Participant 8		

Figure 8.6: Schedule of the study sessions for eight post-stroke participants.

8.4.3 Study Duration

The anticipated study duration for one participant is estimated to not exceed five weeks. A time period of one week (seven days) has been allocated between successive sessions to allow participants to disengage from the prior session, minimizing any carryover effects. Consequently, the overall study timeline is expected to encompass fifteen weeks, accommodating a minimum enrollment of eight participants per week. An example of the schedule corresponding to the first eight participants is depicted in figure 8.6.

8.5 Statistical Tests

In an initial step, all data, including responses to the different questionnaires and the BCI performances, will be tested for normality using the Shapiro-Wilk test with a significance level $\alpha = 0.05$ and complemented with the visual inspection of the Q-Q plots. Subsequently, to compare feedback modalities or presentation order, a repeated measures ANOVA analysis will be conducted with a significance level of $\alpha = 0.05$. In instances where a significant difference emerges, post hoc Tukey pairwise tests will be administered, maintaining the significance level at $\alpha = 0.05$. Alternatively, when the data distribution is different from a normal distribution, Friedman's repeated measures ANOVA analysis will be performed at a significance level of $\alpha = 0.05$. Afterward, pairwise comparisons will be analyzed via the Durbin-Conover test with a significance level $\alpha = 0.05$.

Exploring correlations between two variables, for instance, BCI performance and a self-perception measurement (such as fatigue, emotions, mental workload, system attractiveness, etc.), will be performed to assess the influence of these measures on the performance. Correlations of data following a normal distribution will be studied by computing Pearson's r correlation coefficient at $\alpha = 0.05$. Alternatively, when data distribution deviates from normality, Spearman's ρ coefficient will be calculated also at $\alpha = 0.05$). Additionally, when contrasting fatigue or emotional states at the session's beginning with those at the end, a paired-sample student t-test will be employed at $\alpha = 0.05$. For data displaying a non-normal distribution, a Wilcoxon rank test will be performed at a significance level at $\alpha = 0.05$.

In the case of qualitative data, such as participants' preferred feedback modality, we will deter-

mine the percentage of participants favoring one modality over the other.

8.6 Benefits and Risks

The potential risks for the participants involved in the study are deemed not only acceptable but also negligible. While the study does not represent an immediate benefit for the participants, its primary goal is to advance our understanding of BCIs in the context of upper limb rehabilitation post-stroke. This new knowledge will pave the way for the development of an efficient interface for motor rehabilitation. As a result, the collective benefit derived from this research will transcend the individual level, resulting in enhanced post-stroke rehabilitation practices.

Regarding the potential risks, the study primarily represents a time and concentration commitment for the participants. The session may induce fatigue in the participants; Installing the system and its use is estimated to take approximately one hour and 15 minutes. Aside from this time-related aspect, no other risks or constraints are associated with participation in the study.

8.7 Withdrawal

Participants may be withdrawn from the study after inclusion in the presence of any of the following conditions:

- participant's withdrawal of the informed consent form (no justification will be required);
- participant's refusal to attend the sessions;
- hospitalization;
- appearance of a serious illness;
- death;
- Average BCI performance of less than 50% in at least two of the feedback sessions.

8.8 Management of Adverse Events

According to the French Public Health Law (Article R1123-46), an adverse event is any harmful event occurring in a person participating in research involving human subjects, whether this event is related to the study of the product under investigation. An adverse effect is an adverse event occurring in an individual participating in research involving human subjects, when this event is related to the study or product under investigation. A serious adverse event or effect is any event or undesirable effect that results in death, endangers the participant's life, requires hospitalization or its prolongation, causes significant or lasting incapacity or disability, or results in congenital anomaly or malformation.

8.8.1 Evaluation and report of adverse events

The investigator will record any adverse events occurring during the study, they will evaluate the severity and the causal link with the device under investigation, and will send the assessment to the sponsor. The sponsor will also evaluate the severity and the causal link of the adverse event. All adverse events must be monitored until they are completely resolved. The investigator will

notify the sponsor of any additional information concerning the evolution of the event. In turn, the sponsor will declare the new facts to the relevant authorities.

Finally, the sponsor will write an annual safety report throughout the whole duration of the study. This report will include a list of all the adverse events related to the research and will be shared with the competent authority.

8.9 Data Archiving and Access to Documents

At the end of the study, all documents related to it (including copies of observation notebooks) will be archived at the study site or in a centralized archive provided by the Université de Lorraine, PETA. Particular attention will be given to the list identifying the participants and their informed consent forms, as they are the most important documents to be archived by the principal investigator. Additionally, the investigator will keep the protocol and its amendments, the source files of the participants, including electrophysiological recordings and questionnaires, and all other documents related to the study. Any document destruction or removal must be consulted with and agreed upon by the sponsor. All study-related documents will be kept for 15 years after the end of the study. At the end of this period, the sponsor will inform the investigators of the end of the archiving.

8.10 Conclusion and Study Limitations

In this chapter, a single-center, single-blinded, non-interventional user study of a KMI-based BCI integrating visual and vibrotactile feedback is proposed. The principal aim of this study is to assess the potential of three feedback modalities - visual, vibrotactile, and bimodal (visual and vibrotactile)- to support the effective and efficient execution of KMI for a grasping movement, and the reliability of the program. By evaluating the dimensions of utility, usefulness, and desirability, our goal is to establish that the bimodal BCI not only supports KMI execution but can also be employed in a subsequent protocol aimed at assessing the therapeutic impacts of the BCI.

Nonetheless, it is important to acknowledge the limitations of the present protocol. To start with, individuals vary in their ability to self-regulate brain activity. It is estimated that around 10% to 50% of potential participants may lack the ability to control BCIs [269], so we must consider the potential that some participants may struggle with BCI control. This can, however, be examined by analyzing the participant's EEG activity during offline analysis. Moreover, stroke participants might exhibit sensory deficits, rendering some unable to participate due to an inability to perceive vibrations. To mitigate this constraint, we plan to evaluate the vibrotactile device during the first session and adapt the vibration intensity accordingly. To account for these two limitations, it will be necessary to consider a larger number of participants than the final 24 that will complete the study.

Furthermore, each participant will only experience each feedback modality in a single session. As a result, assessing the therapeutic effects of BCI training is impossible. However, this will be evaluated in a subsequent therapeutic study where participants will undergo a larger number of sessions.

Lastly, the vibrotactile feedback modality employed in this protocol could be easily replaced with any of the two other haptic modalities, tangible or FES, to study the devices developed by

the project partners. The evaluation criteria will remain consistent, ensuring the comparability of results across all three feedback modalities. Once the remaining two haptic modalities have terminated their ongoing tests, we will include them in the present protocol and update it to a multi-center study.

This experimental protocol is expected to be implemented at the University Hospital Center (CHU) in Rennes, France during the course of the year 2024.

Chapter 9

General Discussion and Perspectives

Contents

9.1	General Summary	169
9.2	Future Work	172
9.3	Primary Takeaways	173
9.3.1	The importance of a user-centered design	173
9.3.2	The importance of adapting the BCI to the patient	173

In this thesis, a user-centered and design-based approach was used in the design and evaluation of vibrotactile feedback within the context of a KMI-based BCI for post-stroke motor rehabilitation. This framework aims to shift the paradigm towards a more holistic understanding of user specificities, needs, preferences, and experiences.

In this final chapter, a reflective general discussion is engaged. It begins with an overall summary encompassing the principal contributions, findings, and insights throughout the research. Next, the perspectives associated with this work are explored, highlighting the broader implications and potential directions for future research in this domain.

9.1 General Summary

In chapter Brain-Computer Interfaces for Post-Stroke Rehabilitation of the Upper Limb, a narrative review was conducted to examine the current approaches in MI-BCIs for post-stroke upper limb rehabilitation. The chapter delves into the prevalent mental tasks to control the BCI, the signal processing methodologies commonly employed, and the feedback modalities used. While studies commonly report the mental task, few explained the strategy employed among those concerning motor imagery of the upper limb. Thus, low BCI performances may arise from implementing different strategies and difficulties while performing the task. Although KMI mobilized the sensorimotor cortex [37], making it suitable for motor recovery, scarce attention has been given to its learning aspect. Given its inherent complexity, it is crucial to ensure patients understand correctly how to perform it to maximize its advantages.

To facilitate both patients and therapists in assessing KMI execution, feedback is often provided through various modalities. Haptic feedback has predominantly focused on facilitating

movement, resulting in better results than visual feedback. Notably, alternative options like vibrotactile feedback remain underexplored. Unfortunately, existing feedback systems often prioritize the technological aspects over user-centered considerations, sometimes overlooking users' individual needs and preferences beyond their physical recovery.

Consequently, we explored applications of vibrotactile feedback in MI-based paradigms, recognizing its potential to yield similar BCI performance compared with visual feedback. An additional advantage justifying this choice lies in the liberation of the visual channel, allowing users to redirect their focus to tasks rather than processing visual feedback. Nevertheless, the design choices of the vibrotactile stimulation often need more clarity, leading to important questions, for instance, on the activation sequence of devices involving multiple actuators and the appropriate vibration intensities. Therefore, a user-centered approach was proposed in the design of the vibrotactile stimulation. The resulting stimulation can then be integrated with visual animations to create a more comprehensive bimodal feedback, which can be tested as a feedback modality for a KMI-based BCI.

The principal objective of this thesis was to design and evaluate a novel vibrotactile feedback to support the execution of KMI to interact with a BCI intended for post-stroke motor rehabilitation. In chapter 3, a design-based research methodology was presented to achieve this objective. This methodology merges scientific and design methods to create technological solutions that generate knowledge. Following this methodology, a novel, carefully designed solution was introduced, specifically addressing the needs of post-stroke patients. The initial focus involved constructing the vibrotactile device and stimulation following a user-centered approach. Subsequently, the test phase implicated the evaluation of the device and stimulation first with a neurotypical population and then with the post-stroke patients.

Chapter 4 introduced the technological platform used in this thesis. Initially, the first version of the BCI GraspIt was introduced, aimed to enhance KMI execution of grasping movements through visual affording feedback. This version served as the scientific and technical foundation for the second version developed and used in this thesis. The second version integrated improvements based on the preliminary tests with GraspIt V1, including customizable visual feedback and additional movements for a more comprehensive training experience. These visual enhancements required significant software modifications to incorporate haptic feedback in vibrotactile, tangible, and FES forms.

This chapter also detailed the development of the vibrotactile device. Three vibration motors were strategically located based on the main active muscles during grasping, ensuring congruence with the physical movement. The motors were attached with adjustable bracelets, facilitating interchangeability between left and right limbs. The vibrotactile device was seamlessly integrated into the GraspIt V2 interface, resulting in a new BCI named FeelIt. FeelIt refers to the KMI-based BCI that integrates visual and vibrotactile feedback to support KMI execution. Before testing the bimodal feedback's usability, the vibrotactile stimulation had to be built and synchronized with the visual environment, as detailed in the following two chapters.

The first experimental contribution, presented in chapter 5, involved identifying the vibration sensorial thresholds based on age for our vibrotactile device. Participants were grouped by age, and they indicated the lowest and the highest yet comfortable vibration intensities. The main findings revealed age-related variations in the minimum sensory threshold, enabling generalization to groups for faster device setup. The maximum vibration threshold did not significantly differ across age groups, suggesting the safety and comfort of the highest vibration level. Nev-

ertheless, caution is advised against using the maximal value to prevent potential undesirable effects, especially in post-stroke individuals. The identified threshold values highlight tactile sensory differences based on age and underscore the importance of adjusting the stimulation intensity for recognition of the stimulation and comfort without compromising the BCI's feedback goal of providing information about the mental task performance.

Chapter 6 introduced the second experimental contribution, aimed at comparing four vibration patterns to identify the most suitable one to complement the visual animation of a hand pressing a bottle. The goal was to create a meaningful vibrotactile stimulation that conveyed tactile information corresponding to the displayed image. The challenge involved comparing patterns and ensuring their congruence and synchronization with the visual animation of a grasping hand. Inspired by the natural activation of the main muscles during grasping, a novel vibration pattern was designed to align with real grasping movements. Testing involved two and three vibration motors, believed to offer more detail and congruence with the visual animation. The resulting bimodal stimulation, incorporating visual and vibrotactile elements across four intensity levels, was positively evaluated by users. The sequential vibration pattern with three motors was perceived as more coherent and synchronized with the virtual environment, providing a comfortable and positive experience.

Additionally, EEG activity during the stimulation was studied in the alpha, mu, and beta frequency bands. Event-related desynchronizations (ERDs) observed over sensorimotor brain areas during the bimodal stimulation in all vibration patterns suggested successful stimulation of the sensorimotor cortex, relevant for promoting neuroplasticity in post-stroke motor rehabilitation. Significant differences among the four intensity levels of the stimulation were observed in the EEG, with the highest level inducing larger ERDs.

The study confirmed that a sequential pattern resembling the actual movement is perceived as congruent and synchronized with a visual hand animation. When designing tactile stimulation, considering the task can provide more meaningful information to users. The positive user experience underscores the stimulation's potential as a feedback signal for BCIs. While EEG oscillations indicate its capacity to enhance BCI detection of specific mental tasks, caution is necessary for motor imagery BCIs. Simultaneous stimulation and execution of the mental task can also result in the superposition of EEG activities, complicating the accurate detection of MI. Although this might be beneficial to detect MI for certain applications, it might not be the case in motor neurorehabilitation, emphasizing the need to encourage the patient to perform motor imagery tasks to stimulate the sensorimotor cortex effectively.

Chapter 7 presented the third experimental study, focusing on the assessment of the bimodal BCI *FeelIt* among a neurotypical population. The evaluation involved three feedback modalities, visual, vibrotactile, and bimodal, to understand their impact in facilitating KMI of grasping. Results indicated similar BCI performance across the three feedback modalities, suggesting modality selection should consider other aspects that align with the user's capabilities, goals, needs, and preferences. EEG oscillations revealed consistent sensorimotor cortex activity for all modalities. This highlights the possibility of adapting the BCI to the user's limitation, e.g., using visual-only feedback for users with sensory deficits. Furthermore, participants indicated a strong preference for the bimodal feedback, as they considered it more comprehensive. Furthermore, the bimodal feedback demonstrated greater positive effects on mood, motivation, and agency. These aspects are particularly important for stroke rehabilitation, which is long and tedious. This suggests the efficiency of the bimodal feedback to support KMI. A holistic evaluation considering user perspectives is crucial, supplementing techno-centered assessments and facilitating clearer

and well-justified feedback choices. The positive user experience and system attractiveness are encouraging for the upcoming study with post-stroke patients.

Chapter 8 outlined the experimental protocol for the initial user evaluation of the KMI-based BCI integrating visual and vibrotactile feedback. Set to take place at the University Hospital at Rennes, France, in 2024, the study aims to assess three feedback modalities (visual, vibrotactile, and bimodal) in facilitating the effective and efficient KMI execution of grasping movements among the post-stroke population. This study will assess the utility, usefulness, and desirability of the BCI within the target population, a necessary step before a longitudinal study. The protocol's flexibility allows easy substitution of the vibrotactile modality with the tangible or the FES feedback developed by the partners of the GraspIt project. This adaptability enables a comprehensive comparative analysis across various haptic feedback modalities using the same experimental protocol.

9.2 Future Work

The immediate future work involves the user evaluation of the bimodal BCI with post-stroke patients. Successful validation of the BCI will pave the way for a subsequent study investigating the therapeutic impact of BCI training on post-stroke motor rehabilitation. This follow-up investigation represents a crucial step in understanding the potential contributions of the BCI in improving the therapy and lives of individuals recovering from stroke-related motor impairments.

While the current exploration focused on vibrotactile feedback aligned with KMI associated with grasping movements in the GraspIt interface, it is important to remember that this platform offers the possibility to train three additional movements: hand opening, pinch, and arm rotation. Therefore, future endeavors should involve developing vibrotactile simulations tailored to these specific movements. While leveraging the same vibrotactile device and sensory thresholds, it is possible that distinct vibration patterns need to be designed, given that the existing one was specifically crafted for grasping movements.

Moreover, the established paradigm linking vibration intensity to performance inspires consideration of an alternative approach. An inversely proportional paradigm, wherein better KMI execution reflected as better BCI performance corresponds to reduced vibration, could be explored. This approach envisions strong vibrations alerting users with lower performance levels to focus on the intended sensations for KMI. However, potential incongruities with visual feedback need to be carefully addressed, making it an area for future investigation.

The visual feedback used in the present work consisted of a semi-immersive virtual environment that could potentially be transferred to a fully immersive experience through a head-mounted virtual reality device. The pilot study in [144] demonstrated the feasibility of a BCI with immersive VR for post-stroke rehabilitation. Following this line, future research may explore implementing the visual environment from this work into a head-mounted display VR device. This adaptation could offer a heightened immersive experience and introduce vibrotactile feedback to enhance overall sensory engagement.

9.3 Primary Takeaways

9.3.1 The importance of a user-centered design

While BCIs for rehabilitation have been studied for several years, their widespread adoption in clinical practice is minimal. Examples like the recoveriX system have begun to emerge. However, ensuring a useful and coherent system for both patients and therapists requires continuous control of the user experience with a BCI. User satisfaction may play a crucial role in successfully deploying these technologies. Unfortunately, many studies have primarily focused on technology development, deferring the user evaluation to the latter testing stages. Placing this assessment at the late stages can impede the early detection of design errors, potentially leading to a final device that users perceive negatively, impacting its use and therapeutic outcomes.

In this thesis, user well-being was constantly controlled throughout the design process, with their feedback considered before advancing to subsequent phases. The positive impact of this approach is reflected in the BCI evaluation in chapter 7. Indeed, the BCI performance was acceptable for most participants, and the system's acceptability, usability scores, and emotions improved compared to the initial design stages. Therefore, it is strongly recommended that researchers integrate a user-centered approach to mitigate the risk of testing phase failures due to design flaws that could have been identified earlier.

It is essential to mention that user experience extends beyond measuring the fatigue or comfort associated with the BCI. It encompasses elements related to usability such as the device's ease of use, utility i.e., if the device accomplishes its objective, and perceived attractiveness. Assessing these dimensions provides valuable insights into the improvements necessary for BCIs for motor rehabilitation for broader clinical use. Furthermore, the majority of the standardized questionnaires lack adaptation to the target public and BCI technologies. Consequently, a critical necessity exists to develop questionnaires specifically tailored for assessing the user experience within the domain of BCIs, with a heightened emphasis on the application in post-stroke rehabilitation contexts.

9.3.2 The importance of adapting the BCI to the patient

A significant heterogeneity exists across the studies involving EEG-based BCIs for post-stroke upper limb rehabilitation. Differences in training characteristics, such as the number of sessions, session and study duration, feedback modalities, and mental tasks are observed. Moreover, heterogeneity among patients, including stroke type, lesion extent, time since the event, affected limb, and comorbidities complicates comparison within and among studies. Given the diverse rehabilitation goals, personal preferences, and needs of individual patients, BCIs for rehabilitation cannot be considered a one-size-fits-all solution. However, personalizing each element of the BCI requires more research effort to understand the underlying mechanisms in stroke recovery and how they influence BCI training. In the meantime, adapting the BCI to groups of stroke patients with similar characteristics is a practical step.

While techniques involving passive limb movements like FES or robotic therapies, may offer more favorable clinical outcomes [28, 29, 31], some patients may be unable to benefit from them due to reported unbearable pain when moving paralyzed limbs. Others may struggle with understanding how to perform KMI, rendering them unable to use the system effectively.

Rather than proposing the novel vibrotactile and/or bimodal (visual and vibrotactile) feedback as replacements for BCIs using FES or robotic orthoses, they could serve as valuable additional

pre-training feedback. For post-stroke patients with severely limited mobility and/or trouble understanding the mental task, starting BCI training with the bimodal feedback may allow them to get familiar with the system, learn its usage, and present initial benefits. As their mobility gradually improves, transitioning to an FES modality could be considered. Notably, the FES modality is currently under development within the Grasp-IT ANR project. Therefore, both vibrotactile and FES modalities share the same technological platform, facilitating comparison.

By offering a progressive BCI training approach that adapts to individual patient needs, abilities, and limitations, the aim is to provide a better-tailored therapy experience and potentially improve rehabilitation outcomes. The ultimate goal would be to personalize the therapy as much as possible to meet the individual patient's needs, characteristics, and desires.

This new approach requires further research, as numerous aspects are yet to be delineated. These include the number of sessions for each feedback modality, identifying the relevant patient characteristics for feedback selection, specifying the appropriate duration of the training, and deciding the selection criteria for the number of feedback modalities to be incorporated. The potential advantages offered by a progressive approach underscore the importance of dedicating research efforts to its exploration.

Appendix A

Questionnaires for the user evaluation of the vibration patterns

This annex includes the questionnaires used to evaluate the four vibrotactile device configurations described in Chapter 6.

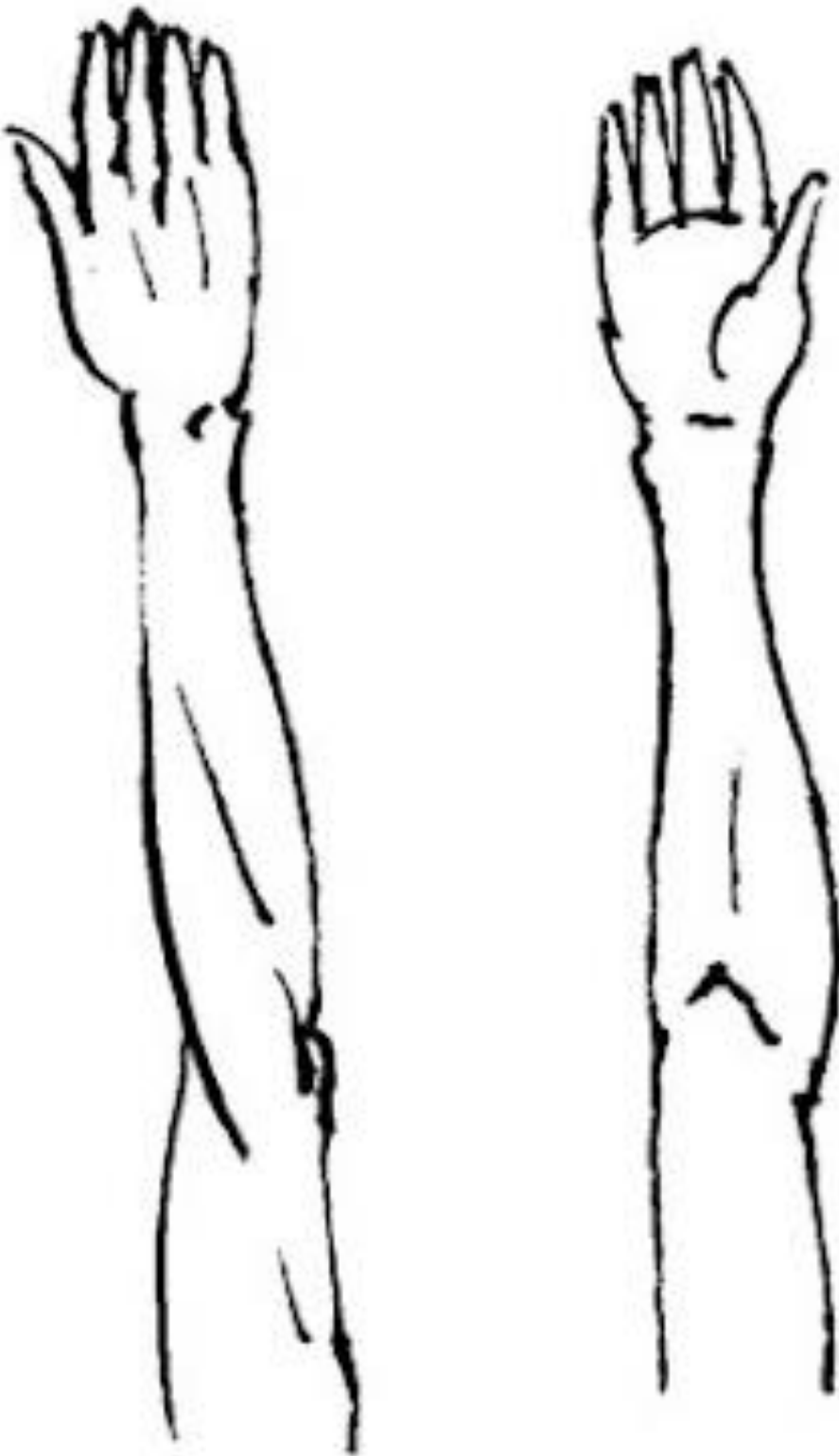
VISUAL + VIBROTACTILE QUESTIONNAIRE 1

ID Participant _____

Condition _____

Regarding the vibration that you have just experienced:

- 1) Draw how you perceived the vibration



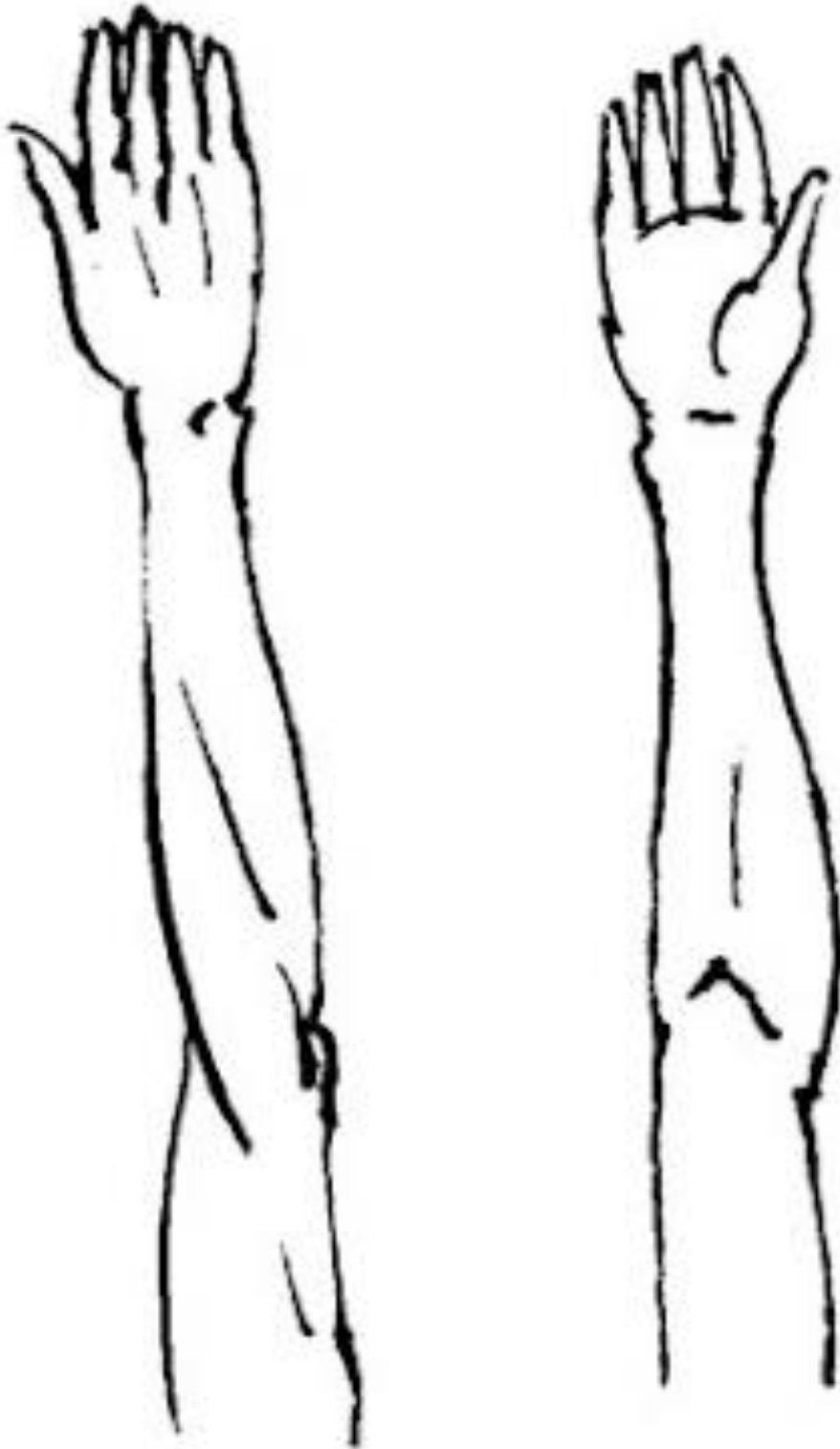
VISUAL + VIBROTACTILE QUESTIONNAIRE 2

ID Participant _____

Condition _____

Regarding the vibration that you have just experienced:

- 1) Draw how you perceived the vibration



2) Did you perceive different intensities?

Yes

No

c. If yes, how many intensities were you able to identify? (Including no vibration)

2 3 4 More than 4

d. If yes, were they related to the amount of ketchup displayed on the screen?

never *almost never* *rarely* *half of the time* *often* *most of the time* *always*

Please select your level of agreement with the following statements:

“During the experiment, there were moments in which...

3) the vibration was synchronized with the movement of the virtual hand”

never *almost never* *rarely* *half of the time* *often* *most of the time* *always*

4) the vibration was comfortable.”

never *almost never* *rarely* *half of the time* *often* *most of the time* *always*

5) the vibration was painful or disturbing.”

never *almost never* *rarely* *half of the time* *often* *most of the time* *Always*

6) I felt a realistic sensation in my body when I felt the vibration.”

never *almost never* *rarely* *half of the time* *often* *most of the time* *always*

Activation of the vibration motors

Regarding the two vibration activation patterns that you have just experienced, indicate the pattern that you prefer in terms of:

	Pattern 1	Pattern 2
Comfort		
Synchronization with the virtual hand movement		
Synchronization with the sauce		
Coherence with the sauce quantity		

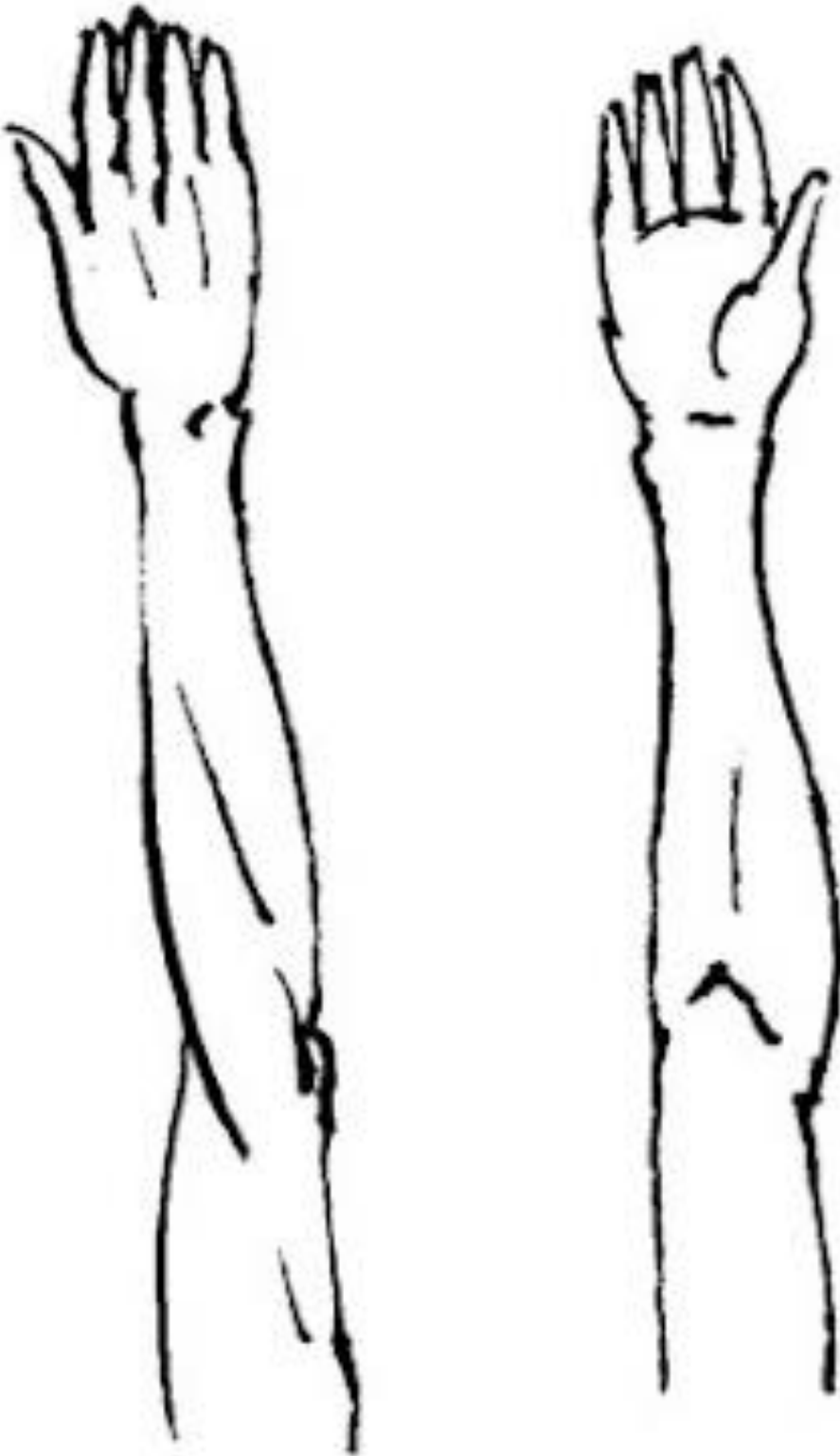
VISUAL + VIBROTACTILE QUESTIONNAIRE 3

ID Participant _____

Condition _____

Regarding the vibration that you have just experienced:

- 1) Draw how you perceived the vibration



2) Did you perceive different intensities?

Yes

No

e. If yes, how many intensities were you able to identify? (Including no vibration)

2 3 4 More than 4

f. If yes, were they related to the amount of ketchup displayed on the screen?

never

almost never

rarely

*half of the
time*

often

*most of the
time*

always

Please select your level of agreement with the following statements:

“During the experiment, there were moments in which...

3) the vibration was synchronized with the movement of the virtual hand”

never

almost never

rarely

*half of the
time*

often

*most of the
time*

always

4) the vibration was comfortable.”

never

almost never

rarely

*half of the
time*

often

*most of the
time*

always

5) the vibration was painful or disturbing.”

never

almost never

rarely

*half of the
time*

often

*most of the
time*

Always

6) I felt a realistic sensation in my body when I felt the vibration.”

never

almost never

rarely

*half of the
time*

often

*most of the
time*

always

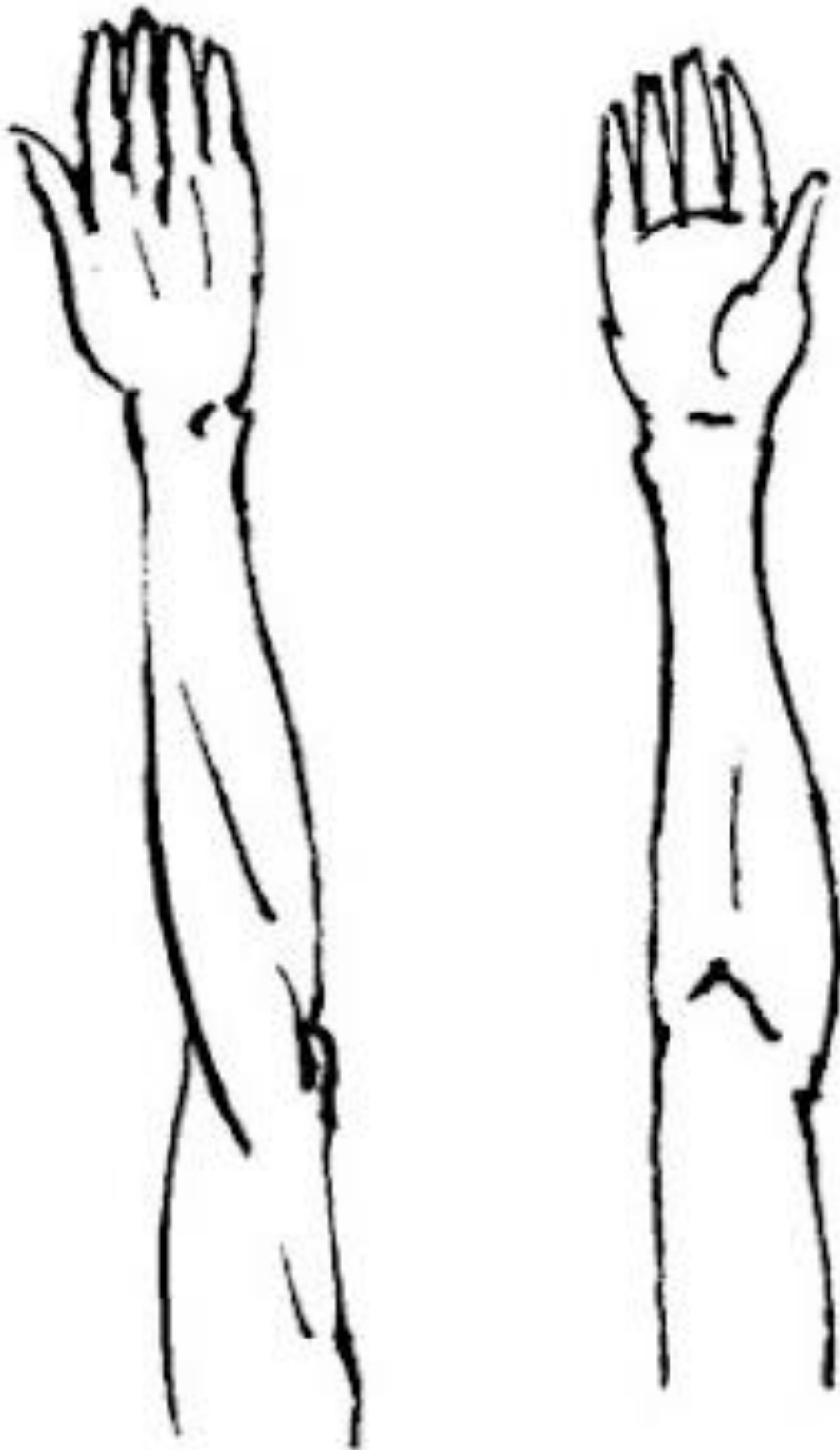
VISUAL + VIBROTACTILE QUESTIONNAIRE 4

ID Participant _____

Condition _____

Regarding the vibration that you have just experienced:

- 1) Draw how you perceived the vibration



7) Did you perceive different intensities?

Yes No

g. If yes, how many intensities were you able to identify? (Including no vibration)

2 3 4 More than 4

h. If yes, were they related to the amount of ketchup displayed on the screen?

never *almost never* *rarely* *half of the time* *often* *most of the time* *always*

Please select your level of agreement with the following statements:

“During the experiment, there were moments in which...

8) the vibration was synchronized with the movement of the virtual hand”

never *almost never* *rarely* *half of the time* *often* *most of the time* *always*

9) the vibration was comfortable.”

never *almost never* *rarely* *half of the time* *often* *most of the time* *always*

10)the vibration was painful or disturbing.”

never *almost never* *rarely* *half of the time* *often* *most of the time* *Always*

11)I felt a realistic sensation in my body when I felt the vibration.”

never *almost never* *rarely* *half of the time* *often* *most of the time* *always*

Activation of the vibration motors

Regarding the two vibration activation patterns that you have just experienced, indicate the pattern that you prefer in terms of:

	Pattern 1	Pattern 2
Comfort		
Synchronization with the virtual hand movement		
Synchronization with the sauce		
Coherence with the sauce quantity		

Quantity of Motors

Regarding the quantity of the motors (3 or 2), indicate the one you prefer in terms of:

	3 Motors	2 Motors
Comfort		
Synchronization with the virtual hand movement		
Synchronization with the sauce		
Coherence with the sauce quantity		

Appendix B

Questionnaire Participants' Characteristics

This annex includes the questionnaire used to record participants' characteristics during the experiment described in Chapter7.

Pre-experiment Questionnaires 3

ID Participant VTBCI_S

GENERAL INFORMATION

Sex Female Male

Age _____

Handedness: Left-handed Right-handed

Last level of education: _____

ACTIVITIES

Do you practice one or more of the following manual activities

- Music (playing an instrument) Cooking Paint / drawing Videogames Sewing/ knitting

Other (please indicate):

How often (times per week) ?

Do you practice any sports? Yes No

If yes, which ones?

How often do you practice sports ?

One time per week

2 to 4 times per week

At least 5 times per week

How long are your sport sessions?

Less than 30 minutes

Between 30 minutes and one hour

More than one hour

Do you practice any meditation and/or mindfulness? Yes No

How often do you practice meditation and/or mindfulness?

One time per week

2 to 4 times per week

At least 5 times per week

Pre-experiment Questionnaires 3

How long are your meditation and/or mindfulness sessions?

Less than 30 minutes

Between 30 minutes and one hour

More than one hour

Appendix C

Questionnaire for the user evaluation of the feedback modalities

This annex includes the questionnaire to rank the feedback modalities by order of preference during the experiment described in Chapter7.

Post-experiment Questionnaires 3

ID Participant VTBCI_S

Feedback Rating

Please rate the feedback modalities by order of preference, from 1 to 4, 1 being your most preferred and 4 being your least preferred:

Feedback Modality	Order of preference (from 1 to 4)
No feedback	
Visual only	
Vibrotactile only	
Visual and Vibrotactile	

Please explain your choice. Be as detailed as possible.

The feedback modality that helped me to imagine the movement better:

- No feedback
- Visual Only
- Vibrotactile Only
- Visual and Vibrotactile

The most entertaining feedback modality:

- No feedback
- Visual Only
- Vibrotactile Only
- Visual and Vibrotactile

The feedback modality that felt most realistic:

- No feedback
- Visual Only
- Vibrotactile Only
- Visual and Vibrotactile

Post-experiment Questionnaires 3

The easiest feedback modality to understand:

- No feedback
- Visual Only
- Vibrotactile Only
- Visual and Vibrotactile

The hardest feedback modality to understand:

- No feedback
- Visual Only
- Vibrotactile Only
- Visual and Vibrotactile

Appendix D

Questionnaires for the user evaluation with post-stroke patients

This annex includes all the questionnaires for the user evaluation with post-stroke patients. As the population will more likely involve mainly french-speaking individuals, the questionnaires are presented in their french version.

Pre-Inclusion Visit

Questionnaire F-FMI, version française du Freiburg Mindfulness Inventory (Trousselard et al., 2010)

Le but de ce test est de décrire comment vous avez vécu ces derniers mois qui viennent de s'écouler. Répondez de votre mieux à chaque énoncé, aussi franchement et spontanément que possible. Il n'y a pas de réponses justes ou fausses, bonnes ou mauvaises. Ce qui est important est votre expérience personnelle.

	Rarement	Occasionnellement	Assez souvent	Presque toujours
Je suis ouvert(e) à vivre le moment présent	<input type="radio"/>	<input type="radio"/>	<input type="radio"/>	<input type="radio"/>
Je ressens mon corps, par exemple en mangeant, en cuisinant, en nettoyant ou en parlant.	<input type="radio"/>	<input type="radio"/>	<input type="radio"/>	<input type="radio"/>
Quand je remarque que mon esprit est absent, je reviens doucement à l'expérience ici et maintenant	<input type="radio"/>	<input type="radio"/>	<input type="radio"/>	<input type="radio"/>
Je suis capable de m'apprécier	<input type="radio"/>	<input type="radio"/>	<input type="radio"/>	<input type="radio"/>
Je fais attention à ce qui se cache derrière mes actions	<input type="radio"/>	<input type="radio"/>	<input type="radio"/>	<input type="radio"/>
Je perçois mes erreurs et mes difficultés sans porter de jugement dessus	<input type="radio"/>	<input type="radio"/>	<input type="radio"/>	<input type="radio"/>
Je me sens connecté(e) à mon expérience ici et maintenant	<input type="radio"/>	<input type="radio"/>	<input type="radio"/>	<input type="radio"/>
J'accepte les expériences déplaisantes	<input type="radio"/>	<input type="radio"/>	<input type="radio"/>	<input type="radio"/>
Je suis un(e) ami(e) pour moi-même lorsque les choses vont mal	<input type="radio"/>	<input type="radio"/>	<input type="radio"/>	<input type="radio"/>
Je regarde mes sentiments sans m'y perdre	<input type="radio"/>	<input type="radio"/>	<input type="radio"/>	<input type="radio"/>
Face à une situation difficile, je sais me poser sans réagir immédiatement	<input type="radio"/>	<input type="radio"/>	<input type="radio"/>	<input type="radio"/>
Je connais des moments de paix et de bien-être intérieur, même quand les choses sont agitées et stressantes	<input type="radio"/>	<input type="radio"/>	<input type="radio"/>	<input type="radio"/>
Je suis impatient(e) avec moi-même et les autres	<input type="radio"/>	<input type="radio"/>	<input type="radio"/>	<input type="radio"/>
Je suis capable de sourire lorsque je remarque que la vie est parfois difficile.	<input type="radio"/>	<input type="radio"/>	<input type="radio"/>	<input type="radio"/>

Questionnaire NGSE estimation du sentiment général d'efficacité personnelle (Chen et al., 2001)

D'une manière générale, je peux dire de moi que ...

	Totalement faux	Plutôt Faux	Cela dépend	Plutôt vrai	Totalement vrai
Je suis en mesure d'atteindre la plupart des objectifs que je me suis fixés	<input type="radio"/>	<input type="radio"/>	<input type="radio"/>	<input type="radio"/>	<input type="radio"/>
Lorsque je suis confronté à des tâches difficiles, je suis certain que je les accomplirai	<input type="radio"/>	<input type="radio"/>	<input type="radio"/>	<input type="radio"/>	<input type="radio"/>
En général, je pense que je peux obtenir des résultats qui sont importants pour moi	<input type="radio"/>	<input type="radio"/>	<input type="radio"/>	<input type="radio"/>	<input type="radio"/>
Je pense que je peux réussir au maximum toutes les entreprises auxquelles je pense	<input type="radio"/>	<input type="radio"/>	<input type="radio"/>	<input type="radio"/>	<input type="radio"/>
Je serai capable de surmonter avec succès de nombreux défis	<input type="radio"/>	<input type="radio"/>	<input type="radio"/>	<input type="radio"/>	<input type="radio"/>
Je suis convaincu que je peux accomplir efficacement de nombreuses tâches différentes	<input type="radio"/>	<input type="radio"/>	<input type="radio"/>	<input type="radio"/>	<input type="radio"/>
Par rapport à d'autres personnes, je peux très bien accomplir la plupart des tâches	<input type="radio"/>	<input type="radio"/>	<input type="radio"/>	<input type="radio"/>	<input type="radio"/>
Même lorsque les choses sont difficiles, je peux être assez performant	<input type="radio"/>	<input type="radio"/>	<input type="radio"/>	<input type="radio"/>	<input type="radio"/>

Session 2

Questionnaire subjectif MES (Medical Emotion Scale) (Duffy et al., 2020)

À l'aide de l'échelle ci-dessous, indiquez comment vous vous sentez actuellement en gardant à l'esprit l'activité que vous êtes sur le point de commencer. Pour chaque émotion, veuillez indiquer la force de cette émotion en sélectionnant le chiffre qui décrit le mieux l'intensité de votre émotion.

	Pas du tout	Un peu	Moyennement	Fortement	Totalement
Confus	<input type="radio"/>	<input type="radio"/>	<input type="radio"/>	<input type="radio"/>	<input type="radio"/>
Optimiste	<input type="radio"/>	<input type="radio"/>	<input type="radio"/>	<input type="radio"/>	<input type="radio"/>
Désintéressé	<input type="radio"/>	<input type="radio"/>	<input type="radio"/>	<input type="radio"/>	<input type="radio"/>
Fier	<input type="radio"/>	<input type="radio"/>	<input type="radio"/>	<input type="radio"/>	<input type="radio"/>
Triste	<input type="radio"/>	<input type="radio"/>	<input type="radio"/>	<input type="radio"/>	<input type="radio"/>
Anxieux	<input type="radio"/>	<input type="radio"/>	<input type="radio"/>	<input type="radio"/>	<input type="radio"/>
Heureux	<input type="radio"/>	<input type="radio"/>	<input type="radio"/>	<input type="radio"/>	<input type="radio"/>
Frustré	<input type="radio"/>	<input type="radio"/>	<input type="radio"/>	<input type="radio"/>	<input type="radio"/>
Désespéré	<input type="radio"/>	<input type="radio"/>	<input type="radio"/>	<input type="radio"/>	<input type="radio"/>
Joyeux	<input type="radio"/>	<input type="radio"/>	<input type="radio"/>	<input type="radio"/>	<input type="radio"/>
Honteux	<input type="radio"/>	<input type="radio"/>	<input type="radio"/>	<input type="radio"/>	<input type="radio"/>
Neutre	<input type="radio"/>	<input type="radio"/>	<input type="radio"/>	<input type="radio"/>	<input type="radio"/>
Compatissant	<input type="radio"/>	<input type="radio"/>	<input type="radio"/>	<input type="radio"/>	<input type="radio"/>
Surpris	<input type="radio"/>	<input type="radio"/>	<input type="radio"/>	<input type="radio"/>	<input type="radio"/>
Curieux	<input type="radio"/>	<input type="radio"/>	<input type="radio"/>	<input type="radio"/>	<input type="radio"/>
Effrayé	<input type="radio"/>	<input type="radio"/>	<input type="radio"/>	<input type="radio"/>	<input type="radio"/>
Reconnaissant	<input type="radio"/>	<input type="radio"/>	<input type="radio"/>	<input type="radio"/>	<input type="radio"/>
Déçu	<input type="radio"/>	<input type="radio"/>	<input type="radio"/>	<input type="radio"/>	<input type="radio"/>
	Pas du tout	Un peu	Moyennement	Fortement	Totalement
Rassuré	<input type="radio"/>	<input type="radio"/>	<input type="radio"/>	<input type="radio"/>	<input type="radio"/>

En colère	<input type="radio"/>	<input type="radio"/>	<input type="radio"/>	<input type="radio"/>	<input type="radio"/>
Relaxé	<input type="radio"/>	<input type="radio"/>	<input type="radio"/>	<input type="radio"/>	<input type="radio"/>
Dégouté	<input type="radio"/>	<input type="radio"/>	<input type="radio"/>	<input type="radio"/>	<input type="radio"/>

Questionnaire FIFS (Davis et al., 2013)

1. A quelle fréquence ressentez-vous de la fatigue ?

Jamais Parfois Habituellement Toujours

2. Sur une échelle de 0 à 10 (0 correspondant à une absence de fatigue et 10 à une forte fatigue), comment évaluez-vous votre fatigue en ce moment ?

0	1	2	3	4	5	6	7	8	9	10
<input type="radio"/>	<input type="radio"/>	<input type="radio"/>	<input type="radio"/>	<input type="radio"/>	<input type="radio"/>	<input type="radio"/>	<input type="radio"/>	<input type="radio"/>	<input type="radio"/>	<input type="radio"/>

3. Quel est le niveau de votre fatigue aujourd'hui ?

Aucune Légère Modérée Sévère

4. Votre fatigue est-elle aujourd'hui meilleure, pire, la même qu'hier ?

Meilleure Pire Même

NASA Task Load Index – Auto-évaluation de la charge mentale (Hart & Staveland, 1988)

La méthode TLX (Task Load Index) de Hart et Staveland évalue la charge de travail sur cinq échelles à 7 points. Des incréments d'estimations élevées, moyennes et faibles pour chaque point donnent lieu à 21 gradations sur les échelles.

Dans quelle mesure, la tâche était-elle mentalement exigeante ?

Très faiblement Modérément Très fortement

Dans quelle mesure, la tâche était-elle physiquement exigeante ?

Très faiblement Modérément Très fortement

Dans quelle mesure, le rythme de la tâche était-il rapide ou précipité ?

Très faiblement Modérément Très fortement

Sessions A, B, and C

Questionnaire subjectif MES (Medical Emotion Scale) (Duffy et al., 2020)

À l'aide de l'échelle ci-dessous, indiquez comment vous vous sentez actuellement en gardant à l'esprit l'activité que vous êtes sur le point de commencer. Pour chaque émotion, veuillez indiquer la force de cette émotion en sélectionnant le chiffre qui décrit le mieux l'intensité de votre émotion.

	Pas du tout	Un peu	Moyennement	Fortement	Totalement
Confus	<input type="radio"/>	<input type="radio"/>	<input type="radio"/>	<input type="radio"/>	<input type="radio"/>
Optimiste	<input type="radio"/>	<input type="radio"/>	<input type="radio"/>	<input type="radio"/>	<input type="radio"/>
Désintéressé	<input type="radio"/>	<input type="radio"/>	<input type="radio"/>	<input type="radio"/>	<input type="radio"/>
Fier	<input type="radio"/>	<input type="radio"/>	<input type="radio"/>	<input type="radio"/>	<input type="radio"/>
Triste	<input type="radio"/>	<input type="radio"/>	<input type="radio"/>	<input type="radio"/>	<input type="radio"/>
Anxieux	<input type="radio"/>	<input type="radio"/>	<input type="radio"/>	<input type="radio"/>	<input type="radio"/>
Heureux	<input type="radio"/>	<input type="radio"/>	<input type="radio"/>	<input type="radio"/>	<input type="radio"/>
Frustré	<input type="radio"/>	<input type="radio"/>	<input type="radio"/>	<input type="radio"/>	<input type="radio"/>
Désespéré	<input type="radio"/>	<input type="radio"/>	<input type="radio"/>	<input type="radio"/>	<input type="radio"/>
Joyeux	<input type="radio"/>	<input type="radio"/>	<input type="radio"/>	<input type="radio"/>	<input type="radio"/>
Honteux	<input type="radio"/>	<input type="radio"/>	<input type="radio"/>	<input type="radio"/>	<input type="radio"/>
Neutre	<input type="radio"/>	<input type="radio"/>	<input type="radio"/>	<input type="radio"/>	<input type="radio"/>
Compatissant	<input type="radio"/>	<input type="radio"/>	<input type="radio"/>	<input type="radio"/>	<input type="radio"/>
Surpris	<input type="radio"/>	<input type="radio"/>	<input type="radio"/>	<input type="radio"/>	<input type="radio"/>
Curieux	<input type="radio"/>	<input type="radio"/>	<input type="radio"/>	<input type="radio"/>	<input type="radio"/>
Effrayé	<input type="radio"/>	<input type="radio"/>	<input type="radio"/>	<input type="radio"/>	<input type="radio"/>
Reconnaissant	<input type="radio"/>	<input type="radio"/>	<input type="radio"/>	<input type="radio"/>	<input type="radio"/>
Déçu	<input type="radio"/>	<input type="radio"/>	<input type="radio"/>	<input type="radio"/>	<input type="radio"/>
	Pas du tout	Un peu	Moyennement	Fortement	Totalement
Rassuré	<input type="radio"/>	<input type="radio"/>	<input type="radio"/>	<input type="radio"/>	<input type="radio"/>

En colère	<input type="radio"/>	<input type="radio"/>	<input type="radio"/>	<input type="radio"/>	<input type="radio"/>
Relaxé	<input type="radio"/>	<input type="radio"/>	<input type="radio"/>	<input type="radio"/>	<input type="radio"/>
Dégouté	<input type="radio"/>	<input type="radio"/>	<input type="radio"/>	<input type="radio"/>	<input type="radio"/>

Questionnaire FIFS (Davis et al., 2013)

5. A quelle fréquence ressentez-vous de la fatigue ?

Jamais Parfois Habituellement Toujours

6. Sur une échelle de 0 à 10 (0 correspondant à une absence de fatigue et 10 à une forte fatigue), comment évaluez-vous votre fatigue en ce moment ?

0	1	2	3	4	5	6	7	8	9	10
<input type="radio"/>	<input type="radio"/>	<input type="radio"/>	<input type="radio"/>	<input type="radio"/>	<input type="radio"/>	<input type="radio"/>	<input type="radio"/>	<input type="radio"/>	<input type="radio"/>	<input type="radio"/>

7. Quel est le niveau de votre fatigue aujourd'hui ?

Aucune Légère Modérée Sévère

8. Votre fatigue est-elle aujourd'hui meilleure, pire, la même qu'hier ?

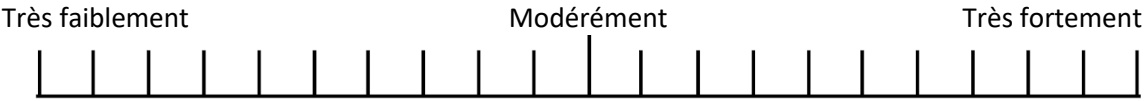
Meilleure Pire Même

NeXT-Q (Bismuth et al., 2019)

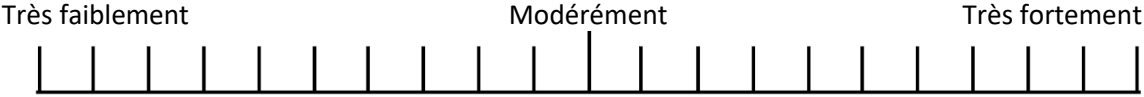
Pour chacune des propositions suivantes, indiquez la réponse qui correspond le plus à ce que vous éprouvez en ce moment entre les deux options proposées. Il n'y a pas de bonne ou de mauvaise réponse. Pendant cette session :

Le temps me semblait s'écouler	rapidement	<input type="radio"/>	<input type="radio"/>	<input type="radio"/>	<input type="radio"/>	<input type="radio"/>	lentement
Je me sentais	calme	<input type="radio"/>	<input type="radio"/>	<input type="radio"/>	<input type="radio"/>	<input type="radio"/>	nerveux(se)
Mon esprit avait tendance spontanément à	s'évader	<input type="radio"/>	<input type="radio"/>	<input type="radio"/>	<input type="radio"/>	<input type="radio"/>	rester dans la tâche
Mon implication dans la tâche était	légère	<input type="radio"/>	<input type="radio"/>	<input type="radio"/>	<input type="radio"/>	<input type="radio"/>	résolue
Le signal de feedback me semblait	déroutant	<input type="radio"/>	<input type="radio"/>	<input type="radio"/>	<input type="radio"/>	<input type="radio"/>	prévisible
Mon niveau de confort pendant la tâche était	élevé	<input type="radio"/>	<input type="radio"/>	<input type="radio"/>	<input type="radio"/>	<input type="radio"/>	bas
Je me sentais	endormi(e)	<input type="radio"/>	<input type="radio"/>	<input type="radio"/>	<input type="radio"/>	<input type="radio"/>	réveillé(e)
La tâche m'a paru	ennuyeuse	<input type="radio"/>	<input type="radio"/>	<input type="radio"/>	<input type="radio"/>	<input type="radio"/>	motivante
L'effort mental que j'ai fourni m'a paru	élevé	<input type="radio"/>	<input type="radio"/>	<input type="radio"/>	<input type="radio"/>	<input type="radio"/>	bas
De mon point de vue le feedback était un signal	que j'observais	<input type="radio"/>	<input type="radio"/>	<input type="radio"/>	<input type="radio"/>	<input type="radio"/>	qui venait de moi
Je me sentais	heureux(se)	<input type="radio"/>	<input type="radio"/>	<input type="radio"/>	<input type="radio"/>	<input type="radio"/>	triste
Lorsque mon esprit s'égarait, j'arrivais à me reconcentrer	facilement	<input type="radio"/>	<input type="radio"/>	<input type="radio"/>	<input type="radio"/>	<input type="radio"/>	difficilement
Je me sentais	tendu(e)	<input type="radio"/>	<input type="radio"/>	<input type="radio"/>	<input type="radio"/>	<input type="radio"/>	relaxé(e)

Dans quelle mesure avez-vous dû travailler dur pour accomplir votre niveau de performance ?



A quel point étiez-vous incertain, découragé, irrité, stressé, et ennuyé ?



Bibliography

- [1] F. Pichiorri, G. Morone, M. Petti, J. Toppi, I. Pisotta, M. Molinari, S. Paolucci, M. Inghilleri, L. Astolfi, F. Cincotti, and D. Mattia, “Brain-computer interface boosts motor imagery practice during stroke recovery,” *Annals of Neurology*, vol. 77, pp. 851–865, 2015.
- [2] S. Rayegani, S. Raeissadat, L. Sedighipour, I. Rezaazadeh, M. Bahrani, D. Eliaspour, and S. Khosrawi, “Effect of neurofeedback and electromyographic-biofeedback therapy on improving hand function in stroke patients,” *Topics in Stroke Rehabilitation*, vol. 21, pp. 137–151, 2014.
- [3] A. Ramos-Murguialday, D. Broetz, M. Rea, L. Läer, Özge Yilmaz, F. L. Brasil, G. Liberati, M. R. Curado, E. Garcia-Cossio, A. Vyziotis, W. Cho, M. Agostini, E. Soares, S. Soekadar, A. Caria, L. G. Cohen, and N. Birbaumer, “Brain-machine-interface in chronic stroke rehabilitation: A controlled study,” *Annals of neurology*, vol. 74, p. 100, 7 2013.
- [4] C. Schneider, R. Marquis, J. Jöhr, M. L. da Silva, P. Ryvlin, A. Serino, M. D. Lucia, and K. Diserens, “Disentangling the percepts of illusory movement and sensory stimulation during tendon vibration in the eeg,” *NeuroImage*, vol. 241, 11 2021.
- [5] N. Cheng, K. S. Phua, H. S. Lai, P. K. Tam, K. Y. Tang, K. K. Cheng, R. C. H. Yeow, K. K. Ang, C. Guan, and J. H. Lim, “Brain-computer interface-based soft robotic glove rehabilitation for stroke,” *IEEE transactions on bio-medical engineering*, vol. 67, pp. 3339–3351, 12 2020.
- [6] P. Arpaia, D. Coyle, F. Donnarumma, A. Esposito, A. Natalizio, and M. Parvis, “Visual and haptic feedback in detecting motor imagery within a wearable brain–computer interface,” *Measurement*, vol. 206, p. 112304, 1 2023.
- [7] R. Leeb, K. Gwak, D. S. Kim, and J. D. R. Millan, “Freeing the visual channel by exploiting vibrotactile bci feedback,” *Proceedings of the Annual International Conference of the IEEE Engineering in Medicine and Biology Society, EMBS*, pp. 3093–3096, 2013.
- [8] M. Easterday, D. R. Lewis, and E. Gerber, “Design-based research process: Problems, phases, and applications,” *Proceedings of International Conference of the Learning Sciences, ICLS*, vol. 1, pp. 317–324, 10 2014.
- [9] V. L. Feigin, M. Brainin, B. Norrving, S. Martins, R. L. Sacco, W. Hacke, M. Fisher, J. Pandian, and P. Lindsay, “World stroke organization (wso): Global stroke fact sheet 2022,” *International Journal of Stroke*, vol. 17, pp. 18–29, 1 2022.
- [10] M. O. Owolabi, A. G. Thrift, A. Mahal, M. Ishida, S. Martins, *et al.*, “Primary stroke

- prevention worldwide: translating evidence into action,” *The Lancet Public Health*, vol. 7, pp. e74–e85, 1 2022.
- [11] S. Allain, D. Naouri, and C. de Peretti, “En france, les AVC sont plus fréquents, plus graves et moins souvent pris en charge en unité spécialisée pour les personnes les plus modestes,” 2 2022.
- [12] R. W. Teasell, “Long-term sequelae of stroke: How should you handle stroke complications?,” *Canadian family physician Medecin de famille canadien*, vol. 38, pp. 381–8, 2 1992.
- [13] A. Yelnik, “Récupération de la motricité après accident vasculaire cérébral. facteurs pronostiques et rééducation,” *Bulletin de l’Académie Nationale de Médecine*, vol. 206, pp. 594–603, 5 2022.
- [14] D. Nowak, “The impact of stroke on the performance of grasping: Usefulness of kinetic and kinematic motion analysis,” *Neuroscience & Biobehavioral Reviews*, vol. 32, pp. 1439–1450, 10 2008.
- [15] P. Aqueveque, P. Ortega, E. Pino, F. Saavedra, E. Germany, and B. Gómez, *After Stroke Movement Impairments: A Review of Current Technologies for Rehabilitation*. InTech, 6 2017.
- [16] L. Oujamaa, I. Relave, J. Froger, D. Mottet, and J.-Y. Pelissier, “Rehabilitation of arm function after stroke. literature review,” *Annals of Physical and Rehabilitation Medicine*, vol. 52, pp. 269–293, 4 2009.
- [17] S. Anwer, A. Waris, S. O. Gilani, J. Iqbal, N. Shaikh, A. N. Pujari, and I. K. Niazi, “Rehabilitation of upper limb motor impairment in stroke: A narrative review on the prevalence, risk factors, and economic statistics of stroke and state of the art therapies,” *Healthcare*, vol. 10, p. 190, 1 2022.
- [18] Physiopedia, “Stroke: Hand rehabilitation — physiopedia,,” 2022. [Online; accessed 13-July-2023].
- [19] J. D. R. Millán, “Combining brain-computer interfaces and assistive technologies: state-of-the-art and challenges,” *Frontiers in Neuroscience*, vol. 1, 2010.
- [20] J. Millan, F. Galan, D. Vanhooydonck, E. Lew, J. Philips, and M. Nuttin, “Asynchronous non-invasive brain-actuated control of an intelligent wheelchair,” in *2009 Annual International Conference of the IEEE Engineering in Medicine and Biology Society*, pp. 3361–3364, IEEE, 9 2009.
- [21] N. Birbaumer, N. Ghanayim, T. Hinterberger, I. Iversen, B. Kotchoubey, A. Kübler, J. Perelmouter, E. Taub, and H. Flor, “A spelling device for the paralysed,” *Nature*, vol. 398, pp. 297–298, 3 1999.
- [22] E. Donchin, K. Spencer, and R. Wijesinghe, “The mental prosthesis: assessing the speed of a p300-based brain-computer interface,” *IEEE Transactions on Rehabilitation Engineering*, vol. 8, pp. 174–179, 6 2000.
- [23] B. Obermaier, G. Muller, and G. Pfurtscheller, “"virtual keyboard" controlled by spontaneous eeg activity,” *IEEE Transactions on Neural Systems and Rehabilitation Engineering*, vol. 11, pp. 422–426, 12 2003.

-
- [24] G. R. Müller-Putz, R. Scherer, G. Pfurtscheller, and R. Rupp, "Eeg-based neuroprosthesis control: A step towards clinical practice," *Neuroscience Letters*, vol. 382, pp. 169–174, 7 2005.
- [25] G. R. Müller-Putz, R. Scherer, G. Pfurtscheller, and R. Rupp, "Brain-computer interfaces for control of neuroprostheses: from synchronous to asynchronous mode of operation / brain-computer interfaces zur steuerung von neuroprothesen: von der synchronen zur asynchronen funktionsweise," *Biomedizinische Technik/Biomedical Engineering*, vol. 51, pp. 57–63, 7 2006.
- [26] E. Monge-Pereira, J. Ibañez-Pereda, I. M. Alguacil-Diego, J. I. Serrano, M. P. Spottorno-Rubio, and F. Molina-Rueda, "Use of electroencephalography brain-computer interface systems as a rehabilitative approach for upper limb function after a stroke: A systematic review," *PM and R*, vol. 9, pp. 918–932, 2017.
- [27] E. López-Larraz, A. Sarasola-Sanz, N. Irastorza-Landa, N. Birbaumer, and A. Ramos-Murguialday, "Brain-machine interfaces for rehabilitation in stroke: A review," *NeuroRehabilitation*, vol. 43, pp. 77–97, 2018.
- [28] R. Carvalho, N. Dias, and J. J. Cerqueira, "Brain-machine interface of upper limb recovery in stroke patients rehabilitation: A systematic review," *Physiotherapy Research International*, vol. 24, p. e1764, 4 2019.
- [29] Z. Bai, K. N. Fong, J. J. Zhang, J. Chan, and K. H. Ting, "Immediate and long-term effects of bci-based rehabilitation of the upper extremity after stroke: A systematic review and meta-analysis," *Journal of NeuroEngineering and Rehabilitation*, vol. 17, pp. 1–20, 4 2020.
- [30] I. Yoo, "Electroencephalogram-based neurofeedback training in persons with stroke: A scoping review in occupational therapy," *NeuroRehabilitation*, vol. 48, pp. 9–18, 2021.
- [31] S. Mansour, K. K. Ang, K. P. S. Nair, K. S. Phua, and M. Arvaneh, "Efficacy of brain-computer interface and the impact of its design characteristics on poststroke upper-limb rehabilitation: A systematic review and meta-analysis of randomized controlled trials," *Clinical EEG and Neuroscience*, vol. 53, pp. 79–90, 2022. Complete.
- [32] G. Pfurtscheller and F. Lopes da Silva, "Event-related EEG/MEG synchronization and desynchronization: basic principles," *Clinical Neurophysiology*, vol. 110, pp. 1842–1857, 11 1999.
- [33] G. Pfurtscheller and F. Lopes da Silva, "Eeg event-related desynchronization (erd) and event-related synchronization (ers)," in *Electroencephalography: basic principles, clinical applications, and related fields* (E. Niedermeyer and F. Lopes da Silva, eds.), Philadelphia: Lippincott Williams & Wilkins, 5 ed., 2005.
- [34] C. Neuper, R. Scherer, S. Wriessnegger, and G. Pfurtscheller, "Motor imagery and action observation: Modulation of sensorimotor brain rhythms during mental control of a brain-computer interface," *Clinical Neurophysiology*, vol. 120, pp. 239–247, 2 2009.
- [35] N. Callow and A. Waters, "The effect of kinesthetic imagery on the sport confidence of flat-race horse jockeys," *Psychology of Sport and Exercise*, vol. 6, pp. 443–459, 7 2005.
- [36] E. E. V. Caenegem, G. Hamoline, B. M. Waltzing, and R. M. Hardwick, "Consistent

- under-reporting of task details in motor imagery research,” *Neuropsychologia*, vol. 177, p. 108425, 12 2022.
- [37] A. Guillot, C. Collet, V. A. Nguyen, F. Malouin, C. Richards, and J. Doyon, “Brain activity during visual versus kinesthetic imagery: An fmri study,” *Human Brain Mapping*, vol. 30, pp. 2157–2172, 2009.
- [38] F. Cincotti, L. Kauhanen, F. Aloise, T. Palomäki, N. Caporusso, P. Jylänki, D. Mattia, F. Babiloni, G. Vanacker, M. Nuttin, M. G. Marciani, and J. D. R. Millán, “Vibrotactile feedback for brain-computer interface operation,” *Computational Intelligence and Neuroscience*, vol. 2007, 2007.
- [39] X. Shu, L. Yao, X. Sheng, D. Zhang, and X. Zhu, “Enhanced motor imagery-based bci performance via tactile stimulation on unilateral hand,” *Frontiers in Human Neuroscience*, vol. 11, pp. 1–12, 2017.
- [40] W. Zhang, A. Song, H. Zeng, B. Xu, and M. Miao, “Closed-loop phase-dependent vibration stimulation improves motor imagery-based brain-computer interface performance,” *Frontiers in Neuroscience*, vol. 15, pp. 1–13, 2021.
- [41] S. Rimbart, L. Bougrain, R. Orhand, J. Nex, S. Gaborit, and S. Fleck, “Grasp’it : une interface cerveau-ordinateur pour l’amélioration de l’apprentissage d’une tâche d’imagination motrice kinesthésique,” 2017.
- [42] C. Jeunet, C. Vi, D. Spelmezan, B. N’Kaoua, F. Lotte, and S. Subramanian, *Continuous Tactile Feedback for Motor-Imagery Based Brain-Computer Interaction in a Multitasking Context*, vol. 9298. 2015.
- [43] American Stroke Association, *Explaining Stroke*, 2020.
- [44] C. W. Tsao, A. W. Aday, Z. I. Almarzooq, C. A. Anderson, P. Arora, C. L. Avery, C. M. Baker-Smith, A. Z. Beaton, A. K. Boehme, A. E. Buxton, Y. Commodore-Mensah, M. S. Elkind, K. R. Evenson, C. Eze-Nliam, S. Fugar, G. Generoso, D. G. Heard, S. Hiremath, J. E. Ho, R. Kalani, D. S. Kazi, D. Ko, D. A. Levine, J. Liu, J. Ma, J. W. Magnani, E. D. Michos, M. E. Mussolino, S. D. Navaneethan, N. I. Parikh, R. Poudel, M. Rezk-Hanna, G. A. Roth, N. S. Shah, M.-P. St-Onge, E. L. Thacker, S. S. Virani, J. H. Voeks, N.-Y. Wang, N. D. Wong, S. S. Wong, K. Yaffe, and S. S. Martin, “Heart Disease and Stroke Statistics—2023 Update: A Report From the American Heart Association,” *Circulation*, vol. 147, feb 2023.
- [45] P. M. Kelly-Hayes, J. T. Robertson, J. P. Broderick, P. W. Duncan, L. A. Hershey, E. J. Roth, W. H. Thies, and C. A. Trombly, “The american heart association stroke outcome classification,” *Stroke*, vol. 29, pp. 1274–1280, 6 1998.
- [46] J. Byrne, ed., *Neuroscience Online: An Electronic Textbook for the Neurosciences*. Department of Neurobiology and Anatomy. McGovern Medical School at The University of Texas Health Science Center at Houston (UTHealth), 1997.
- [47] E. P. Gardner, J. H. Martin, and T. M. Jessell, “The bodily senses,” in *Principles of Neural Science* (E. R. Kandel, J. H. Schwartz, and T. M. Jessell, eds.), McGraw-Hill, 4 ed., 2000.
- [48] E. P. Gardner and E. R. Kandel, “Touch,” in *Principles of Neural Science* (E. R. Kandel, J. H. Schwartz, and T. M. Jessell, eds.), McGraw-Hill, 4 ed., 2000.

-
- [49] J. M. Ferro, L. Caeiro, and M. L. Figueira, “Neuropsychiatric sequelae of stroke,” *Nature Reviews Neurology*, vol. 12, pp. 269–280, may 2016.
- [50] M. L. Hackett, C. Yapa, V. Parag, and C. S. Anderson, “Frequency of depression after stroke,” *Stroke*, vol. 36, pp. 1330–1340, 6 2005.
- [51] S. Chohan, P. Venkatesh, and C. How, “Long-term complications of stroke and secondary prevention: an overview for primary care physicians,” *Singapore Medical Journal*, vol. 60, pp. 616–620, 12 2019.
- [52] J. Bernhardt, K. S. Hayward, G. Kwakkel, N. S. Ward, S. L. Wolf, K. Borschmann, J. W. Krakauer, L. A. Boyd, S. T. Carmichael, D. Corbett, and S. C. Cramer, “Agreed Definitions and a Shared Vision for New Standards in Stroke Recovery Research: The Stroke Recovery and Rehabilitation Roundtable Taskforce,” *Neurorehabilitation and Neural Repair*, vol. 31, pp. 793–799, sep 2017.
- [53] T. H. Murphy and D. Corbett, “Plasticity during stroke recovery: from synapse to behaviour,” *Nature Reviews Neuroscience*, vol. 10, pp. 861–872, 12 2009.
- [54] D. Corbetta, V. Sirtori, G. Castellini, L. Moja, and R. Gatti, “Constraint-induced movement therapy for upper extremities in people with stroke,” *Cochrane Database of Systematic Reviews*, vol. 2017, oct 2015.
- [55] A. Saavedra-García, J. A. Moral-Munoz, and D. Lucena-Anton, “Mirror therapy simultaneously combined with electrical stimulation for upper limb motor function recovery after stroke: a systematic review and meta-analysis of randomized controlled trials,” *Clinical Rehabilitation*, vol. 35, pp. 39–50, jan 2021.
- [56] C. Marquez-Chin and M. R. Popovic, “Functional electrical stimulation therapy for restoration of motor function after spinal cord injury and stroke: A review,” *BioMedical Engineering Online*, vol. 19, pp. 1–25, 5 2020.
- [57] J. Wu, H. Cheng, J. Zhang, S. Yang, and S. Cai, “Robot-Assisted Therapy for Upper Extremity Motor Impairment After Stroke: A Systematic Review and Meta-Analysis,” *Physical Therapy*, vol. 101, apr 2021.
- [58] K. E. Laver, B. Lange, S. George, J. E. Deutsch, G. Saposnik, and M. Crotty, “Virtual reality for stroke rehabilitation,” *Cochrane Database of Systematic Reviews*, vol. 2018, nov 2017.
- [59] K. Barreto Monteiro, M. dos Santos Cardoso, V. Rodrigues da Costa Cabral, A. Oliveira Barros dos Santos, P. Soares da Silva, J. Brandão Pinto de Castro, and R. Gomes de Souza Vale, “Effects of motor imagery as a complementary resource on the rehabilitation of stroke patients: A meta-analysis of randomized trials,” *Journal of Stroke and Cerebrovascular Diseases*, vol. 30, pp. 1–11, 2021.
- [60] E. Villa-Berges, A. A. Laborda Soriano, O. Lucha-López, J. M. Tricas-Moreno, M. Hernández-Secorún, M. Gómez-Martínez, and C. Hidalgo-García, “Motor Imagery and Mental Practice in the Subacute and Chronic Phases in Upper Limb Rehabilitation after Stroke: A Systematic Review,” *Occupational Therapy International*, vol. 2023, pp. 1–12, jan 2023.
- [61] N. Murillo, J. Valls-Sole, J. Vidal, E. Opisso, J. Medina, and H. Kumru, “Focal vibration

- in neurorehabilitation.,” *European journal of physical and rehabilitation medicine*, vol. 50, pp. 231–42, 4 2014.
- [62] A. R. Alashram, E. Padua, C. Romagnoli, and G. Annino, “Effectiveness of focal muscle vibration on hemiplegic upper extremity spasticity in individuals with stroke: A systematic review,” *NeuroRehabilitation*, vol. 45, pp. 471–481, 12 2019.
- [63] Y. J. Park, S. W. Park, and H. S. Lee, “Comparison of the effectiveness of whole body vibration in stroke patients: A meta-analysis,” *BioMed Research International*, vol. 2018, pp. 1–10, 2018.
- [64] B. J. Martin and H.-S. Park, “Analysis of the tonic vibration reflex: influence of vibration variables on motor unit synchronization and fatigue,” *European Journal of Applied Physiology*, vol. 75, pp. 504–511, 5 1997.
- [65] H. Wang, R. Chandrashekhar, J. Rippetoe, and M. Ghazi, “Focal muscle vibration for stroke rehabilitation: A review of vibration parameters and protocols,” *Applied Sciences*, vol. 10, p. 8270, 11 2020.
- [66] V. F. Bento, V. T. Cruz, D. D. Ribeiro, and J. P. Cunha, “The vibratory stimulus as a neurorehabilitation tool for stroke patients: Proof of concept and tolerability test,” *NeuroRehabilitation*, vol. 30, pp. 287–293, 6 2012.
- [67] G. M. Goodwin, D. I. McCloskey, and P. B. C. Matthews, “Proprioceptive illusions induced by muscle vibration: Contribution by muscle spindles to perception?,” *Science*, vol. 175, pp. 1382–1384, 3 1972.
- [68] J.-P. Roll, “1.1. physiologie de la kinesthèse. la proprioception musculaire : sixième sens, ou sens premier ?,” *Intellectica. Revue de l’Association pour la Recherche Cognitive*, vol. 36, pp. 49–66, 2003.
- [69] E. Tidoni, G. Fusco, D. Leonardis, A. Frisoli, M. Bergamasco, and S. M. Aglioti, “Illusory movements induced by tendon vibration in right- and left-handed people,” *Experimental Brain Research*, vol. 233, pp. 375–383, 2 2015.
- [70] C. Klaes, “Chapter 28 - invasive brain-computer interfaces and neural recordings from humans,” in *Handbook of in Vivo Neural Plasticity Techniques* (D. Manahan-Vaughan, ed.), vol. 28 of *Handbook of Behavioral Neuroscience*, pp. 527–539, Elsevier, 2018.
- [71] S. L. Franc, G. H. Altamira, M. Guillen, S. Butet, S. Fleck, A. Lécuyer, L. Bougrain, and I. Bonan, “Toward an adapted neurofeedback for post-stroke motor rehabilitation: State of the art and perspectives,” *Frontiers in Human Neuroscience*, vol. 16, 7 2022.
- [72] G. H. Glover, “Overview of Functional Magnetic Resonance Imaging,” *Neurosurgery Clinics of North America*, vol. 22, pp. 133–139, apr 2011.
- [73] A. Paggiaro, N. Birbaumer, M. Cavinato, C. Turco, E. Formaggio, A. Del Felice, S. Masiero, and F. Piccione, “Magnetoencephalography in Stroke Recovery and Rehabilitation,” *Frontiers in Neurology*, vol. 7, mar 2016.
- [74] E. Buch, C. Weber, L. G. Cohen, C. Braun, M. A. Dimyan, T. Ard, J. Mellinger, A. Caria, S. Soekadar, A. Fourkas, and N. Birbaumer, “Think to Move: a Neuromagnetic Brain-Computer Interface (BCI) System for Chronic Stroke,” *Stroke*, vol. 39, pp. 910–917, mar 2008.

-
- [75] L. F. Nicolas-Alonso and J. Gomez-Gil, “Brain computer interfaces, a review,” *Sensors*, vol. 12, pp. 1211–1279, 2012.
- [76] J. N. Acharya, A. Hani, J. Cheek, P. Thirumala, and T. N. Tsuchida, “American clinical neurophysiology society guideline 2: Guidelines for standard electrode position nomenclature,” *Journal of Clinical Neurophysiology*, vol. 33, pp. 308–311, 8 2016.
- [77] P. D. E. Baniqued, E. C. Stanyer, M. Awais, A. Alazmani, A. E. Jackson, M. A. Mon-Williams, F. Mushtaq, and R. J. Holt, “Brain–computer interface robotics for hand rehabilitation after stroke: a systematic review,” *Journal of NeuroEngineering and Rehabilitation*, vol. 18, pp. 1–25, 12 2021. It has a table summing up some of the BCI characteristics we want to consider.
- [78] M. A. Cervera, S. R. Soekadar, J. Ushiba, J. del R. Millán, M. Liu, N. Birbaumer, and G. Garipelli, “Brain-computer interfaces for post-stroke motor rehabilitation: a meta-analysis,” *Annals of Clinical and Translational Neurology*, vol. 5, pp. 651–663, 5 2018.
- [79] M. A. Khan, R. Das, H. K. Iversen, and S. Puthusserypady, “Review on motor imagery based bci systems for upper limb post-stroke neurorehabilitation: From designing to application,” *Computers in Biology and Medicine*, vol. 123, p. 103843, 8 2020.
- [80] A. Kruse, Z. Suica, J. Taeymans, and C. Schuster-Amft, “Effect of brain-computer interface training based on non-invasive electroencephalography using motor imagery on functional recovery after stroke - a systematic review and meta-analysis,” *BMC Neurology* 2020 20:1, vol. 20, pp. 1–14, 10 2020.
- [81] W. Yang, X. Zhang, Z. Li, Q. Zhang, C. Xue, and Y. Huai, “The effect of brain–computer interface training on rehabilitation of upper limb dysfunction after stroke: A meta-analysis of randomized controlled trials,” *Frontiers in Neuroscience*, vol. 15, 2 2022.
- [82] K. K. Ang, C. Guan, K. S. Phua, C. Wang, L. Zhou, K. Y. Tang, G. J. E. Joseph, C. W. K. Kuah, and K. S. G. Chua, “Brain-computer interface-based robotic end effector system for wrist and hand rehabilitation: Results of a three-armed randomized controlled trial for chronic stroke,” *Frontiers in Neuroengineering*, vol. 7, p. 30, 7 2014.
- [83] K. K. Ang, K. S. G. Chua, K. S. Phua, C. Wang, Z. Y. Chin, C. W. K. Kuah, W. Low, and C. Guan, “A randomized controlled trial of eeg-based motor imagery brain-computer interface robotic rehabilitation for stroke,” *Clinical EEG and Neuroscience*, vol. 46, pp. 310–320, 10 2015.
- [84] M. Barsotti, D. Leonardis, C. Loconsole, M. Solazzi, E. Sotgiu, C. Procopio, C. Chisari, M. Bergamasco, and A. Frisoli, “A full upper limb robotic exoskeleton for reaching and grasping rehabilitation triggered by mi-bci,” in *IEEE International Conference on Rehabilitation Robotics*, vol. 2015-September, pp. 49–54, IEEE Computer Society, 9 2015.
- [85] A. Biasiucci, R. Leeb, I. Iturrate, S. Perdikis, A. Al-Khodairy, T. Corbet, A. Schneider, T. Schmidlin, H. Zhang, M. Bassolino, D. Viceic, P. Vuadens, A. G. Guggisberg, and J. D. Millán, “Brain-actuated functional electrical stimulation elicits lasting arm motor recovery after stroke,” *Nature Communications* 2018 9:1, vol. 9, pp. 1–13, 6 2018.
- [86] D. T. Bundy, L. Souders, K. Baranyai, L. Leonard, G. Schalk, R. Coker, D. W. Moran, T. Huskey, and E. C. Leuthardt, “Contralesional brain-computer interface control of a pow-

- ered exoskeleton for motor recovery in chronic stroke survivors,” *Stroke*, vol. 48, pp. 1908–1915, 7 2017.
- [87] R. I. Carino-Escobar, P. Carrillo-Mora, R. Valdés-Cristerna, M. A. Rodríguez-Barragan, C. Hernandez-Arenas, J. Quinzaños-Fresnedo, M. A. Galicia-Alvarado, and J. Cantillo-Negrete, “Longitudinal analysis of stroke patients’ brain rhythms during an intervention with a brain-computer interface,” *Neural Plasticity*, vol. 2019, pp. 1–11, 4 2019.
- [88] S. Chen, L. Cao, X. Shu, H. Wang, L. Ding, S. H. Wang, and J. Jia, “Longitudinal electroencephalography analysis in subacute stroke patients during intervention of brain–computer interface with exoskeleton feedback,” *Frontiers in Neuroscience*, vol. 14, p. 809, 8 2020.
- [89] A. Chowdhury, H. Raza, Y. K. Meena, A. Dutta, and G. Prasad, “Online covariate shift detection-based adaptive brain-computer interface to trigger hand exoskeleton feedback for neuro-rehabilitation,” *IEEE Transactions on Cognitive and Developmental Systems*, vol. 10, pp. 1070–1080, 12 2018.
- [90] A. Chowdhury, Y. K. Meena, H. Raza, B. Bhushan, A. K. Uttam, N. Pandey, A. A. Hashmi, A. Bajpai, A. Dutta, and G. Prasad, “Active physical practice followed by mental practice using bci-driven hand exoskeleton: A pilot trial for clinical effectiveness and usability,” *IEEE Journal of Biomedical and Health Informatics*, vol. 22, pp. 1786–1795, 11 2018.
- [91] M. R. Curado, E. G. Cossio, D. Broetz, M. Agostini, W. Cho, F. L. Brasil, O. Yilmaz, G. Liberati, G. Lepski, N. Birbaumer, and A. Ramos-Murguialday, “Residual upper arm motor function primes innervation of paretic forearm muscles in chronic stroke after brain-machine interface (bmi) training,” *PLOS ONE*, vol. 10, p. e0140161, 10 2015.
- [92] A. A. Frolov, O. Mokienko, R. Lyukmanov, E. Biryukova, S. Kotov, L. Turbina, G. Nadareyshvily, and Y. Bushkova, “Post-stroke rehabilitation training with a motor-imagery-based brain-computer interface (bci)-controlled hand exoskeleton: A randomized controlled multicenter trial,” *Frontiers in Neuroscience*, vol. 11, p. 400, 7 2017.
- [93] Y. Jang, T. Kim, and B. Lee, “Effects of brain–computer interface-controlled functional electrical stimulation training on shoulder subluxation for patients with stroke: A randomized controlled trial,” *Occupational Therapy International*, vol. 23, pp. 175–185, 6 2016.
- [94] Y. Kasashima-Shindo, T. Fujiwara, J. Ushiba, Y. Matsushika, D. Kamatani, M. Oto, T. Ono, A. Nishimoto, K. Shindo, M. Kawakami, T. Tsuji, and M. Liu, “Brain-computer interface training combined with transcranial direct current stimulation in patients with chronic severe hemiparesis: Proof of concept study,” *Journal of Rehabilitation Medicine*, vol. 47, no. 4, pp. 318–324, 2015.
- [95] T. Kim, S. Kim, and B. Lee, “Effects of action observational training plus brain-computer interface-based functional electrical stimulation on paretic arm motor recovery in patient with stroke: A randomized controlled trial,” *Occupational therapy international*, vol. 23, pp. 39–47, 3 2016.
- [96] Y. Miao, S. Chen, X. Zhang, J. Jin, R. Xu, I. Daly, J. Jia, X. Wang, A. Cichocki, and T.-P. Jung, “Bci-based rehabilitation on the stroke in sequela stage,” *Neural Plasticity*, vol. 2020, pp. 1–10, 12 2020.

-
- [97] S. L. Norman, D. J. McFarland, A. Miner, S. C. Cramer, E. T. Wolbrecht, J. R. Wolpaw, and D. J. Reinkensmeyer, “Controlling pre-movement sensorimotor rhythm can improve finger extension after stroke,” *Journal of Neural Engineering*, vol. 15, 8 2018.
- [98] Y. Ono, T. Tominaga, and T. Murata, “Digital mirror box: An interactive hand-motor bmi rehabilitation tool for stroke patients,” in *2016 Asia-Pacific Signal and Information Processing Association Annual Summit and Conference (APSIPA)*, pp. 1–7, IEEE, 12 2016.
- [99] S. Tsuchimoto, K. Shindo, F. Hotta, T. Hanakawa, M. Liu, and J. Ushiba, “Sensorimotor connectivity after motor exercise with neurofeedback in post-stroke patients with hemiplegia,” *Neuroscience*, vol. 416, pp. 109–125, 9 2019.
- [100] B. Várkuti, C. Guan, Y. Pan, K. S. Phua, K. K. Ang, C. W. K. Kuah, K. Chua, B. T. Ang, N. Birbaumer, and R. Sitaram, “Resting State Changes in Functional Connectivity Correlate With Movement Recovery for BCI and Robot-Assisted Upper-Extremity Training After Stroke,” *Neurorehabilitation and Neural Repair*, vol. 27, pp. 53–62, jan 2013.
- [101] X. Wang, W. W. Wong, R. Sun, W. C. W. Chu, and K. Y. Tong, “Differentiated effects of robot hand training with and without neural guidance on neuroplasticity patterns in chronic stroke,” *Frontiers in Neurology*, vol. 9, 10 2018.
- [102] Q. Wu, Z. Yue, Y. Ge, D. Ma, H. Yin, H. Zhao, G. Liu, J. Wang, W. Dou, and Y. Pan, “Brain functional networks study of subacute stroke patients with upper limb dysfunction after comprehensive rehabilitation including bci training,” *Frontiers in Neurology*, vol. 10, p. 1419, 1 2020.
- [103] G. Rizzolatti, L. Fogassi, and V. Gallese, “Neurophysiological mechanisms underlying the understanding and imitation of action,” *Nature Reviews Neuroscience*, vol. 2, pp. 661–670, 9 2001.
- [104] I. Nojima, S. Koganemaru, T. Kawamata, H. Fukuyama, and T. Mima, “Action observation with kinesthetic illusion can produce human motor plasticity,” *European Journal of Neuroscience*, vol. 41, pp. 1614–1623, 6 2015.
- [105] S. Chen, X. Shu, H. Wang, L. Ding, J. Fu, and J. Jia, “The Differences Between Motor Attempt and Motor Imagery in Brain-Computer Interface Accuracy and Event-Related Desynchronization of Patients With Hemiplegia,” *Frontiers in Neurobotics*, vol. 15, nov 2021.
- [106] L. Avanzino, A. Giannini, A. Tacchino, E. Pelosin, P. Ruggeri, and M. Bove, “Motor imagery influences the execution of repetitive finger opposition movements,” *Neuroscience Letters*, vol. 466, pp. 11–15, 2009.
- [107] M. Lotze and U. Halsband, “Motor imagery,” *Journal of Physiology-Paris*, vol. 99, pp. 386–395, 6 2006.
- [108] G. Pfurtscheller and C. Neuper, “Motor imagery activates primary sensorimotor area in humans,” *Neuroscience Letters*, vol. 239, pp. 65–68, 12 1997.
- [109] S. Kraeutner, A. Gionfriddo, T. Bardouille, and S. Boe, “Motor imagery-based brain activity parallels that of motor execution: Evidence from magnetic source imaging of cortical oscillations,” *Brain Research*, vol. 1588, pp. 81–91, 11 2014.

- [110] S. M. Kosslyn and W. L. Thompson, “When is early visual cortex activated during visual mental imagery?,” *Psychological Bulletin*, vol. 129, pp. 723–746, 2003.
- [111] C. M. Stinear, W. D. Byblow, M. Steyvers, O. Levin, and S. P. Swinnen, “Kinesthetic, but not visual, motor imagery modulates corticomotor excitability,” *Experimental Brain Research*, vol. 168, pp. 157–164, 1 2006.
- [112] M. Kilintari, S. Narayana, A. Babajani-Feremi, R. Rezaie, and A. C. Papanicolaou, “Brain activation profiles during kinesthetic and visual imagery: An fmri study,” *Brain Research*, vol. 1646, pp. 249–261, 9 2016.
- [113] D. J. McFarland, L. M. McCane, S. V. David, and J. R. Wolpaw, “Spatial filter selection for EEG-based communication,” *Electroencephalography and Clinical Neurophysiology*, vol. 103, pp. 386–394, sep 1997.
- [114] H. Ramoser, J. Müller-Gerking, and G. Pfurtscheller, “Optimal spatial filtering of single trial EEG during imagined hand movement,” *IEEE Transactions on Rehabilitation Engineering*, vol. 8, no. 4, pp. 441–446, 2000.
- [115] B. Blankertz, R. Tomioka, S. Lemm, M. Kawanabe, and K.-R. Müller, “Filters for Robust EEG,” *IEEE Signal Processing Magazine*, no. January 2008, pp. 41–56, 2008.
- [116] E. D. Adrian and B. H. C. Matthews, “The berger rhythm: Potential changes from the occipital lobes in man,” *Brain*, vol. 57, pp. 355–385, 1934.
- [117] W. Klimesch, M. Doppelmayr, H. Russegger, T. Pachinger, and J. Schwaiger, “Induced alpha band power changes in the human eeg and attention,” *Neuroscience Letters*, vol. 244, pp. 73–76, 3 1998.
- [118] H. Gastaut, “Electrocorticographic study of the reactivity of rolandic rhythm.,” *Revue neurologique*, vol. 87, pp. 176–82, 1952.
- [119] B. Fisch, *Fisch and Spehlmann’s EEG Primer*. Elsevier, 3 ed., 12 1999.
- [120] G. Pfurtscheller and A. Aranibar, “Evaluation of event-related desynchronization (erd) preceding and following voluntary self-paced movement,” *Electroencephalography and Clinical Neurophysiology*, vol. 46, pp. 138–146, 2 1979.
- [121] D. J. McFarland, “Mu and beta rhythm topographies during motor imagery and actual movements.,” *Brain Topography*, vol. 12, pp. 177–186, 2000.
- [122] L. Dugué, D. McLelland, M. Lajous, and R. VanRullen, “Attention searches nonuniformly in space and in time,” *Proceedings of the National Academy of Sciences*, vol. 112, pp. 15214–15219, 12 2015.
- [123] A. N. Landau, H. M. Schreyer, S. van Pelt, and P. Fries, “Distributed attention is implemented through theta-rhythmic gamma modulation,” *Current Biology*, vol. 25, pp. 2332–2337, 8 2015.
- [124] K. K. Ang, Z. Y. Chin, C. Wang, C. Guan, and H. Zhang, “Filter Bank Common Spatial Pattern Algorithm on BCI Competition IV Datasets 2a and 2b,” *Frontiers in Neuroscience*, vol. 6, 2012.
- [125] F. Lotte, M. Congedo, A. Lécuyer, F. Lamarche, B. Arnaldi, L. Anatole, F. Lotte, M. Congedo, L. Anatole, E. Abdulhay, R. Oweis, A. Mohammad, L. Ahmad, R. T. Schirrmeister,

-
- J. T. Springenberg, L. D. J. Fiederer, M. Glasstetter, K. Eggenberger, M. Tangermann, F. Hutter, W. Burgard, T. Ball, Z. Jiao, X. Gao, Y. Wang, J. Li, H. Xu, U. R. Acharya, S. L. Oh, Y. Hagiwara, J. H. Tan, and H. Adeli, “A review of classification algorithms for EEG-based brain – computer interfaces,” *Human brain mapping*, vol. 38, no. 11, pp. 270–278, 2018.
- [126] H. Yuan and B. He, “Brain–computer interfaces using sensorimotor rhythms: Current state and future perspectives,” *IEEE Transactions on Biomedical Engineering*, vol. 61, pp. 1425–1435, 5 2014.
- [127] M. J. Vansteensel and B. Jarosiewicz, “Chapter 7 - brain-computer interfaces for communication,” in *Handbook of Clinical Psychology*, vol. 168, pp. 67–85, Elsevier, 2020.
- [128] P. Herman, G. Prasad, T. M. McGinnity, and D. Coyle, “Comparative Analysis of Spectral Approaches to Feature Extraction for EEG-Based Motor Imagery Classification,” *IEEE Transactions on Neural Systems and Rehabilitation Engineering*, vol. 16, pp. 317–326, aug 2008.
- [129] N. Brodu, F. Lotte, and A. Lecuyer, “Comparative study of band-power extraction techniques for Motor Imagery classification,” in *2011 IEEE Symposium on Computational Intelligence, Cognitive Algorithms, Mind, and Brain (CCMB)*, pp. 1–6, IEEE, apr 2011.
- [130] L. Leocani, C. Toro, P. Manganotti, P. Zhuang, and M. Hallett, “Event-related coherence and event-related desynchronization/synchronization in the 10 hz and 20 hz eeg during self-paced movements,” *Electroencephalography and Clinical Neurophysiology/Evoked Potentials Section*, vol. 104, pp. 199–206, 5 1997.
- [131] K. J. Miller, G. Schalk, E. E. Fetz, M. den Nijs, J. G. Ojemann, and R. P. N. Rao, “Cortical activity during motor execution, motor imagery, and imagery-based online feedback,” *Proceedings of the National Academy of Sciences*, vol. 107, pp. 4430–4435, 3 2010.
- [132] G. Pfurtscheller, “Central beta rhythm during sensorimotor activities in man,” *Electroencephalography and Clinical Neurophysiology*, vol. 51, pp. 253–264, 3 1981.
- [133] G. Pfurtscheller, A. Stancák, and C. Neuper, “Post-movement beta synchronization. A correlate of an idling motor area?,” *Electroencephalography and Clinical Neurophysiology*, vol. 98, pp. 281–293, apr 1996.
- [134] G. Pfurtscheller, “Functional brain imaging based on ERD/ERS,” *Vision Research*, vol. 41, pp. 1257–1260, may 2001.
- [135] G. Pfurtscheller, C. Neuper, C. Brunner, and F. Lopes Da Silva, “Beta rebound after different types of motor imagery in man,” *Neuroscience Letters*, vol. 378, pp. 156–159, apr 2005.
- [136] J. R. Stieger, S. Engel, H. Jiang, C. C. Cline, M. J. Kreitzer, and B. He, “Mindfulness improves brain-computer interface performance by increasing control over neural activity in the alpha band,”
- [137] G. Pfurtscheller, C. Brunner, A. Schlögl, and F. L. da Silva, “Mu rhythm (de)synchronization and eeg single-trial classification of different motor imagery tasks,” *NeuroImage*, vol. 31, pp. 153–159, 5 2006.

- [138] Y. Jeon, C. S. Nam, Y.-J. Kim, and M. C. Whang, “Event-related (de)synchronization (erd/ers) during motor imagery tasks: Implications for brain–computer interfaces,” *International Journal of Industrial Ergonomics*, vol. 41, pp. 428–436, 9 2011.
- [139] R. O. Duda, P. E. Hart, and D. G. Stork, *Pattern Classification*. Wiley, second ed., 2000.
- [140] C. Burges, “A Tutorial on Support Vector Machines for Pattern Recognition,” in *Data Mining and Knowledge Discovery 2*, pp. 121–167, Kluwer Academic Publishers, 1998.
- [141] C. Jeunet, B. N’Kaoua, S. Subramanian, M. Hachet, and F. Lotte, “Predicting mental imagery-based bci performance from personality, cognitive profile and neurophysiological patterns,” *PLOS ONE*, vol. 10, p. e0143962, 12 2015.
- [142] G. Prasad, P. Herman, D. Coyle, S. McDonough, and J. Crosbie, “Applying a brain–computer interface to support motor imagery practice in people with stroke for upper limb recovery: a feasibility study,” *Journal of NeuroEngineering and Rehabilitation*, vol. 7, p. 60, dec 2010.
- [143] D. Wen, Y. Fan, S.-H. Hsu, J. Xu, Y. Zhou, J. Tao, X. Lan, and F. Li, “Combining brain–computer interface and virtual reality for rehabilitation in neurological diseases: A narrative review,” *Annals of Physical and Rehabilitation Medicine*, vol. 64, p. 101404, jan 2021.
- [144] A. Vourvopoulos, O. M. Pardo, S. Lefebvre, M. Neureither, D. Saldana, E. Jahng, and S.-L. Liew, “Effects of a Brain-Computer Interface With Virtual Reality (VR) Neurofeedback: A Pilot Study in Chronic Stroke Patients,” *Frontiers in human neuroscience*, vol. 13, p. 210, 2019.
- [145] M. Fleury, G. Lioi, C. Barillot, and A. Lécuyer, “A Survey on the Use of Haptic Feedback for Brain-Computer Interfaces and Neurofeedback,” *Frontiers in Neuroscience*, vol. 14, no. June, 2020.
- [146] C. Marquez-Chin and M. R. Popovic, “Functional electrical stimulation therapy for restoration of motor function after spinal cord injury and stroke: A review,” *BioMedical Engineering Online*, vol. 19, pp. 1–25, 5 2020.
- [147] D. B. Popovic, “Advances in functional electrical stimulation (FES),” *Journal of Electromyography and Kinesiology*, vol. 24, pp. 795–802, dec 2014.
- [148] T. Corbet, I. Iturrate, M. Pereira, S. Perdikis, and J. d. R. Millán, “Sensory threshold neuromuscular electrical stimulation fosters motor imagery performance,” *NeuroImage*, vol. 176, no. March, pp. 268–276, 2018.
- [149] X. Shu, S. Chen, J. Meng, L. Yao, X. Sheng, J. Jia, D. Farina, and X. Zhu, “Tactile Stimulation Improves Sensorimotor Rhythm-Based BCI Performance in Stroke Patients,” *IEEE Transactions on Biomedical Engineering*, vol. 66, pp. 1987–1995, jul 2019.
- [150] M. Barsotti, D. Leonardis, N. Vanello, M. Bergamasco, and A. Frisoli, “Effects of continuous kinaesthetic feedback based on tendon vibration on motor imagery bci performance,” *IEEE TRANSACTIONS ON NEURAL SYSTEMS AND REHABILITATION ENGINEERING*, vol. 26, pp. 105–114, 1 2018.
- [151] S. L. Franc, *Etude du neurofeedback avec retour visuo-proprioceptif pour la rééducation post-AVC*. PhD thesis, Université de Rennes 1, 9 2022.

-
- [152] H. Gürkök and A. Nijholt, “Brain–Computer Interfaces for Multimodal Interaction: A Survey and Principles,” *International Journal of Human-Computer Interaction*, vol. 28, pp. 292–307, may 2012.
- [153] W. Ishihara, K. Moxon, S. Ehrman, M. Yarborough, T. L. Panontin, and D. Nathan-Roberts, “Feedback Modalities in Brain–Computer Interfaces: A Systematic Review,” *Proceedings of the Human Factors and Ergonomics Society Annual Meeting*, vol. 64, no. 1, pp. 1186–1190, 2020.
- [154] T. Sollfrank, A. Ramsay, S. Perdakis, J. Williamson, R. Murray-Smith, R. Leeb, J. Millán, and A. Kübler, “The effect of multimodal and enriched feedback on smr-bci performance,” *Clinical Neurophysiology*, vol. 127, pp. 490–498, 1 2016.
- [155] W. Ishihara, K. Moxon, S. Ehrman, M. Yarborough, T. L. Panontin, and D. Nathan-Roberts, “Feedback Modalities in Brain–Computer Interfaces: A Systematic Review,” *Proceedings of the Human Factors and Ergonomics Society Annual Meeting*, vol. 64, no. 1, pp. 1186–1190, 2020.
- [156] L. Pillette, B. N’kaoua, R. Sabau, B. Glize, and F. Lotte, “Multi-session influence of two modalities of feedback and their order of presentation on mi-bci user training,” *Multimodal Technologies and Interaction*, vol. 5, 2021.
- [157] D. McFarland, L. McCane, and J. Wolpaw, “Eeg-based communication and control: short-term role of feedback,” *IEEE Transactions on Rehabilitation Engineering*, vol. 6, pp. 7–11, 3 1998.
- [158] S. P. Swinnen, R. A. Schmidt, D. E. Nicholson, and D. C. Shapiro, “Information feedback for skill acquisition: Instantaneous knowledge of results degrades learning.,” *Journal of Experimental Psychology: Learning, Memory, and Cognition*, vol. 16, pp. 706–716, 7 1990.
- [159] D. J. McFarland and J. R. Wolpaw, “Brain–computer interface use is a skill that user and system acquire together,” *PLOS Biology*, vol. 16, p. e2006719, 7 2018.
- [160] S. Steinert, C. Bublitz, R. Jox, and O. Friedrich, “Doing things with thoughts: Brain-computer interfaces and disembodied agency,” *Philosophy & Technology*, vol. 32, pp. 457–482, 9 2019.
- [161] M. Li, D. He, C. Li, and S. Qi, “Brain-computer interface speller based on steady-state visual evoked potential: A review focusing on the stimulus paradigm and performance.,” *Brain sciences*, vol. 11, 4 2021.
- [162] Y. Li, J. Pan, F. Wang, and Z. Yu, “A hybrid bci system combining p300 and ssvep and its application to wheelchair control,” *IEEE Transactions on Biomedical Engineering*, vol. 60, pp. 3156–3166, 11 2013.
- [163] X. Chen, B. Zhao, Y. Wang, and X. Gao, “Combination of high-frequency ssvep-based bci and computer vision for controlling a robotic arm,” *Journal of Neural Engineering*, vol. 16, p. 026012, 4 2019.
- [164] Y. Punsawad and Y. Wongsawat, “Multi-command ssaep-based bci system with training sessions for ssvep during an eye fatigue state,” *IEEJ Transactions on Electrical and Electronic Engineering*, vol. 12, 6 2017.

- [165] X. Zheng, G. Xu, Y. Zhang, R. Liang, K. Zhang, Y. Du, J. Xie, and S. Zhang, “Anti-fatigue performance in ssvep-based visual acuity assessment: A comparison of six stimulus paradigms,” *Frontiers in Human Neuroscience*, vol. 14, 7 2020.
- [166] J. Petit, J. Rouillard, and F. Cabestaing, “Eeg-based brain–computer interfaces exploiting steady-state somatosensory-evoked potentials: a literature review,” *Journal of Neural Engineering*, vol. 18, p. 051003, 10 2021.
- [167] G. Muller-Putz, R. Scherer, C. Neuper, and G. Pfurtscheller, “Steady-state somatosensory evoked potentials: suitable brain signals for brain-computer interfaces?,” *IEEE Transactions on Neural Systems and Rehabilitation Engineering*, vol. 14, pp. 30–37, 3 2006.
- [168] K.-T. Kim, H.-I. Suk, and S.-W. Lee, “Commanding a brain-controlled wheelchair using steady-state somatosensory evoked potentials,” *IEEE TRANSACTIONS ON NEURAL SYSTEMS AND REHABILITATION ENGINEERING*, vol. 26, pp. 654–665, 3 2018.
- [169] M. L. Chen, D. Fu, J. Boger, and N. Jiang, “Age-related changes in vibro-tactile eeg response and its implications in bci applications: A comparison between older and younger populations,” *IEEE Transactions on Neural Systems and Rehabilitation Engineering*, vol. 27, pp. 603–610, 4 2019.
- [170] E. López-Larraz, M. Creatura, I. Iturrate, L. Montesano, and J. Minguéz, “Eeg single-trial classification of visual, auditive and vibratory feedback potentials in brain-computer interfaces,” *Proceedings of the Annual International Conference of the IEEE Engineering in Medicine and Biology Society, EMBS*, pp. 4231–4234, 2011.
- [171] L. Yao, J. Meng, D. Zhang, X. Sheng, and X. Zhu, “Combining motor imagery with selective sensation toward a hybrid-modality bci,” *IEEE TRANSACTIONS ON BIOMEDICAL ENGINEERING*, vol. 61, pp. 2304–2312, 8 2014.
- [172] L. Hehenberger, A. I. Sburlea, and G. R. Müller-Putz, “Assessing the impact of vibrotactile kinaesthetic feedback on electroencephalographic signals in a center-out task,” *Journal of Neural Engineering*, vol. 17, 2020.
- [173] L. Batistic, D. Susanj, D. Pincic, and S. Ljubic, “Motor imagery classification based on eeg sensing with visual and vibrotactile guidance,” *SENSORS*, vol. 23, 5 2023.
- [174] K. Won, H. Kim, D. Gwon, M. Ahn, C. S. Nam, and S. C. Jun, “Can vibrotactile stimulation and tdcS help inefficient bci users?,” *JOURNAL OF NEUROENGINEERING AND REHABILITATION*, vol. 20, 5 2023.
- [175] Y. Zhong, L. Yao, J. Wang, and Y. Wang, “Tactile sensation assisted motor imagery training for enhanced bci performance: A randomized controlled study,” *IEEE TRANSACTIONS ON BIOMEDICAL ENGINEERING*, vol. 70, pp. 694–702, 2 2023.
- [176] A. Chatterjee, V. Aggarwal, A. Ramos, S. Acharya, and N. V. Thakor, “A brain-computer interface with vibrotactile biofeedback for haptic information,” *Journal of NeuroEngineering and Rehabilitation*, vol. 4, pp. 1–12, 2007.
- [177] L. Schiatti, G. Barresi, J. Tessadori, L. C. King, and L. S. Mattos, “The effect of vibrotactile feedback on errp-based adaptive classification of motor imagery,” *Proceedings of the Annual International Conference of the IEEE Engineering in Medicine and Biology Society, EMBS*, pp. 6750–6753, 2019.

-
- [178] N. A. Grigorev, A. O. Savosenkov, Maksim, U. A. L. V, N. N. Shusharina, A. E. K. A. Ya, Hramov, V. B. Kazantsev, and S. Gordleeva, “A bci-based vibrotactile neurofeedback training improves motor cortical excitability during motor imagery,” *IEEE TRANSACTIONS ON NEURAL SYSTEMS AND REHABILITATION ENGINEERING*, vol. 29, pp. 1583–1592, 2021.
- [179] M. E. Thurlings, J. B. van Erp, A.-M. Brouwer, B. Blankertz, and P. Werkhoven, “Control-display mapping in brain-computer interfaces,” *Ergonomics*, vol. 55, pp. 564–580, 5 2012.
- [180] Y. G. Chung, J. Kim, S. W. Han, H.-S. Kim, M. H. Choi, S.-C. Chung, J.-Y. Park, and S.-P. Kim, “Frequency-dependent patterns of somatosensory cortical responses to vibrotactile stimulation in humans: A fMRI study,” *Brain Research*, pp. 47–57, 2013.
- [181] J. Zimmerman, J. Forlizzi, and S. Evenson, “Research through design as a method for interaction design research in hci,” in *Proceedings of the SIGCHI Conference on Human Factors in Computing Systems*, pp. 493–502, ACM, 4 2007.
- [182] S. Rimbart, *Apport de la stimulation du nerf médian dans la conception d’une BCI basée sur l’activité cérébrale motrice : vers l’amélioration de la détection des réveils peropératoires au cours de l’anesthésie générale*. PhD thesis, Université de Lorraine, 7 2020.
- [183] Y. Renard, F. Lotte, G. Gibert, M. Congedo, E. Maby, V. Delannoy, O. Bertrand, and A. Lécuyer, “Openvibe: An open-source software platform to design, test, and use brain-computer interfaces in real and virtual environments,” *Presence: Teleoperators and Virtual Environments*, vol. 19, pp. 35–53, 2 2010.
- [184] S. Rimbart, L. Bougrain, and S. Fleck, “Learning how to generate kinesthetic motor imagery using a bci-based learning environment: A comparative study based on guided or trial-and-error approaches,” *IEEE Transactions on Systems, Man, and Cybernetics: Systems*, pp. 2483–2489, 2020.
- [185] G. Herrera Altamira, N. Skiba, A. Lécuyer, L. Bougrain, and S. Fleck, “Multisensory neurofeedback design for kmi embodiment,” in *ACM International Conference on Interactive Media Experiences Workshops (IMXw ’23)*, ACM, 6 2023.
- [186] M. Ziat, *Haptics for Human-Computer Interaction: From the Skin to the Brain*, vol. 17. Now Publishers, 2023.
- [187] K. O. Johnson, “The roles and functions of cutaneous mechanoreceptors,” *Current Opinion in Neurobiology*, vol. 11, pp. 455–461, 2001.
- [188] M. E. Johanson, M. A. James, and S. R. Skinner, “Forearm muscle activation during power grip and release,” *Journal of Hand Surgery*, vol. 23, pp. 938–944, 1998.
- [189] X. Huang, S. Liang, Z. Li, C. Y. Y. Lai, and K.-S. Choi, “Eeg-based vibrotactile evoked brain-computer interfaces system: A systematic review,” *PLOS ONE*, vol. 17, 2022.
- [190] G. A. Gescheider, R. R. Edwards, E. A. Lackner, S. J. Bolanowski, and R. T. Verrillo, “The effects of aging on information-processing channels in the sense of touch: Iii. differential sensitivity to changes in stimulus intensity,” *Somatosensory & Motor Research*, vol. 13, pp. 73–80, 1 1996.
- [191] P. Sagastegui Alva, S. Muceli, S. F. Atashzar, L. William, and D. Farina, “Wearable

- multichannel haptic device for encoding proprioception in the upper limb,” *Journal of Neural Engineering*, vol. 17, p. 056035, 10 2020.
- [192] G. A. Gescheider, “Resolving of successive clicks by the ears and skin.,” *Journal of Experimental Psychology*, vol. 71, pp. 378–381, 1966.
- [193] M. C. Duffy, S. P. Lajoie, R. Pekrun, and K. Lachapelle, “Emotions in medical education: Examining the validity of the medical emotion scale (mes) across authentic medical learning environments,” *Learning and Instruction*, vol. 70, p. 101150, 12 2020.
- [194] D. MP, K. D, W. D, L. R, K. MT, A. A, and P. A, “Four-item fatigue screen: replacing the brief fatigue index,” *The American journal of hospice & palliative care*, vol. 30, pp. 652–656, 11 2013.
- [195] C. Lallemand, V. Koenig, G. Gronier, and R. Martin, “Création et validation d’une version française du questionnaire attrakdiff pour l’évaluation de l’expérience utilisateur des systèmes interactifs,” *Revue Europeenne de Psychologie Appliquée*, vol. 65, pp. 239–252, 2015.
- [196] R. T. Verrillo, S. J. Bolanowski, and G. A. Gescheider, “Effect of aging on the subjective magnitude of vibration,” *Somatosensory & Motor Research*, vol. 19, pp. 238–244, 1 2002.
- [197] R. W. Cholewiak and A. A. Collins, “Vibrotactile localization on the arm: Effects of place, space, and age,” *Perception & Psychophysics 2003 65:7*, vol. 65, pp. 1058–1077, 2003.
- [198] L. Pillette, F. Lotte, B. N’Kaoua, P.-A. Joseph, C. Jeunet, and B. Glize, “Why we should systematically assess, control and report somatosensory impairments in bci-based motor rehabilitation after stroke studies,” *NeuroImage: Clinical*, vol. 28, p. 102417, 2020.
- [199] C. M. Stinear, W. D. Byblow, M. Steyvers, O. Levin, and S. P. Swinnen, “Kinesthetic, but not visual, motor imagery modulates corticomotor excitability,” *Experimental Brain Research*, vol. 168, pp. 157–164, 1 2006.
- [200] C. Marquez-Chin and M. R. Popovic, “Functional electrical stimulation therapy for restoration of motor function after spinal cord injury and stroke: A review,” *BioMedical Engineering Online*, vol. 19, pp. 1–25, 5 2020.
- [201] L. Yao, J. Meng, D. Zhang, X. Sheng, and X. Zhu, “Combining motor imagery with selective sensation toward a hybrid-modality bci,” *IEEE TRANSACTIONS ON BIOMEDICAL ENGINEERING*, vol. 61, pp. 2304–2312, 8 2014.
- [202] C. E. Seim, S. L. Wolf, and T. E. Starner, “Wearable vibrotactile stimulation for upper extremity rehabilitation in chronic stroke: clinical feasibility trial using the vts glove,” *Journal of NeuroEngineering and Rehabilitation*, vol. 18, pp. 1–11, 2021.
- [203] K. Gwak, R. Leeb, J. D. R. Millan, and D. S. Kim, “Quantification and reduction of visual load during bci operation,” *Conference Proceedings - IEEE International Conference on Systems, Man and Cybernetics*, vol. 2014-Janua, pp. 2795–2800, 2014.
- [204] N. Grigorev, A. Savosenkov, A. Udoratina, V. Kazantsev, M. Lukoyanov, and S. Gordleeva, “Influence of vibrotactile feedback on the motor evoked potentials (meps) induced by motor imagery,” *Conference Proceedings - 4th Scientific School on Dynamics of Complex Networks and their Application in Intellectual Robotics, DCNAIR 2020*, pp. 94–96, 2020.

-
- [205] C. Neuper, M. Wörtz, and G. Pfurtscheller, “Erd/ers patterns reflecting sensorimotor activation and deactivation,” in *Event-Related Dynamics of Brain Oscillations* (C. Neuper and W. Klimesch, eds.), vol. 159 of *Progress in Brain Research*, pp. 211–222, Elsevier, 2006.
- [206] W. Li, Q. Xu, Y. Li, C. Li, F. Wu, and L. Ji, “Eeg characteristics in “eyes-open” versus “eyes-closed” condition during vibrotactile stimulation,” *Biomedical Signal Processing and Control*, vol. 68, p. 102759, 7 2021.
- [207] B. Stephens-Fripp, R. Mutlu, and G. Alici, “Using vibration motors to create tactile apparent movement for transradial prosthetic sensory feedback,” in *Proceedings of the IEEE RAS and EMBS International Conference on Biomedical Robotics and Biomechanics*, vol. 2018-Augus, pp. 213–218, 2018.
- [208] S. G. Hart and L. E. Staveland, “Development of nasa-tlx (task load index): Results of empirical and theoretical research,” *Advances in Psychology*, vol. 52, pp. 139–183, 1 1988.
- [209] M. Minge, M. Thüring, I. Wagner, and C. V. Kuhr, “The mecue questionnaire: A modular tool for measuring user experience,” *Advances in Intelligent Systems and Computing*, vol. 486, pp. 115–128, 2017.
- [210] A. Delorme and S. Makeig, “EEGLAB: an open source toolbox for analysis of single-trial EEG dynamics including independent component analysis,” *Journal of Neuroscience Methods*, vol. 134, pp. 9–21, 2004.
- [211] N. P. Holmes and L. Tamè, “Locating primary somatosensory cortex in human brain stimulation studies: systematic review and meta-analytic evidence,” *Journal of Neurophysiology*, vol. 121, pp. 152–162, 1 2019.
- [212] C. B. Saper, S. Iversen, and R. Frackowiak, “Integration of sensory and motor function: The association areas of the cerebral cortex and the cognitive capabilities of the brain,” in *Principles of Neural Science* (E. R. Kandel, J. H. Schwartz, and T. M. Jessell, eds.), McGraw-Hill, 4 ed., 2000.
- [213] The jamovi project, “jamovi,” 2023.
- [214] G. Pfurtscheller, C. Neuper, and W. Mohl, “Event-related desynchronization (erd) during visual processing,” *International Journal of Psychophysiology*, vol. 16, pp. 147–153, 5 1994.
- [215] E. Niedermeyer, “The normal eeg of the walking adult,” in *Electroencephalography: basic principles, clinical applications, and related fields* (E. Niedermeyer and F. Lopes da Silva, eds.), Philadelphia: Lippincott Williams & Wilkins, 5 ed., 2005.
- [216] B. Reilly, “Mu rhythm,” in *Encyclopedia of Autism Spectrum Disorders* (F. Volkmar, ed.), pp. 1940–1941, Springer New York, 2013.
- [217] F. H. L. da Silva, “Event-related neural activities: what about phase?,” *Progress in Brain Research*, vol. 159, pp. 3–17, 1 2006.
- [218] C. Babiloni, F. Babiloni, F. Carducci, F. Cincotti, G. Coccozza, C. D. Percio, D. V. Moretti, and P. M. Rossini, “Human cortical electroencephalography (eeg) rhythms during the observation of simple aimless movements: A high-resolution eeg study,” *NeuroImage*, vol. 17, pp. 559–572, 10 2002.

- [219] W. Gaetz and D. Cheyne, “Localization of sensorimotor cortical rhythms induced by tactile stimulation using spatially filtered meg,” *NeuroImage*, vol. 30, pp. 899–908, 4 2006.
- [220] W. Li, C. Li, Q. Xu, L. Ji, and S. Cunningham, “Effects of focal vibration over upper limb muscles on the activation of sensorimotor cortex network: An eeg study,” *Journal of Healthcare Engineering*, vol. 2019, 2019.
- [221] A. Streltsova, C. Berchio, V. Gallese, and M. A. Umiltà, “Time course and specificity of sensory-motor alpha modulation during the observation of hand motor acts and gestures: a high density EEG study,” *Experimental Brain Research*, no. 205, pp. 363–373, 2010.
- [222] P. Avanzini, M. Fabbri-Destro, R. Dalla Volta, E. Daprati, G. Rizzolatti, and G. Cantalupo, “The Dynamics of Sensorimotor Cortical Oscillations during the Observation of Hand Movements: An EEG Study,” *PLoS ONE*, vol. 7, p. e37534, 5 2012.
- [223] C. W. Simon and W. H. Emmons, “EEG, consciousness, and sleep,” *Science*, vol. 124, no. 3231, pp. 1066–1069, 1956.
- [224] M. Saleh, J. Reimer, R. Penn, C. L. Ojakangas, and N. G. Hatsopoulos, “Fast and Slow Oscillations in Human Primary Motor Cortex Predict Oncoming Behaviorally Relevant Cues,” *Neuron*, vol. 65, pp. 461–471, 2 2010.
- [225] V. Nácher, A. Ledberg, G. Deco, and R. Romo, “Coherent delta-band oscillations between cortical areas correlate with decision making,” *Proceedings of the National Academy of Sciences of the United States of America*, vol. 110, pp. 15085–15090, 9 2013.
- [226] E. Kirmizi-Alsan, Z. Bayraktaroglu, H. Gurvit, Y. H. Keskin, M. Emre, and T. Demiralp, “Comparative analysis of event-related potentials during Go/NoGo and CPT: Decomposition of electrophysiological markers of response inhibition and sustained attention,” *Brain Research*, vol. 1104, pp. 114–128, 8 2006.
- [227] J. F. Cavanagh, L. Zambrano-Vazquez, and J. J. B. Allen, “Theta lingua franca: A common mid-frontal substrate for action monitoring processes,” *Psychophysiology*, vol. 49, pp. 220–238, 2 2012.
- [228] C. C. Williams, T. D. Ferguson, C. D. Hassall, B. Wright, and O. E. Krigolson, “Dissociated neural signals of conflict and surprise in effortful decision making: Theta activity reflects surprise while alpha and beta activity reflect conflict,” *Neuropsychologia*, vol. 155, p. 107793, 5 2021.
- [229] J. Jacobs, G. Hwang, T. Curran, and M. J. Kahana, “Eeg oscillations and recognition memory: Theta correlates of memory retrieval and decision making,” *NeuroImage*, vol. 32, pp. 978–987, 8 2006.
- [230] F. Lotte, F. Larrue, and C. Mühl, “Flaws in current human training protocols for spontaneous brain-computer interfaces: lessons learned from instructional design,” *Frontiers in Human Neuroscience*, vol. 7, 2013.
- [231] M. Alimardani, S. Nishio, and H. Ishiguro, *Brain-Computer Interface and Motor Imagery Training: The Role of Visual Feedback and Embodiment*. InTech, 10 2018.
- [232] K. K. Ang and C. Guan, “Brain-computer interface for neurorehabilitation of upper limb after stroke,” *Proceedings of the IEEE*, vol. 103, pp. 944–953, 6 2015.

-
- [233] R. Sigrist, G. Rauter, R. Riener, and P. Wolf, “Augmented visual, auditory, haptic, and multimodal feedback in motor learning: A review,” *Psychonomic Bulletin & Review*, vol. 20, pp. 21–53, 2 2013.
- [234] G. Gargiulo, Mohamed, McEwan, Bifulco, Cesarelli, Jin, Ruffo, Tapson, and van Schaik, “Investigating the role of combined acoustic-visual feedback in one-dimensional synchronous brain computer interfaces, a preliminary study,” *Medical Devices: Evidence and Research*, p. 81, 9 2012.
- [235] S. Ainsworth, “Deft: A conceptual framework for considering learning with multiple representations,” *Learning and Instruction*, vol. 16, pp. 183–198, 6 2006.
- [236] S. Rimbart, N. Gayraud, L. Bougrain, M. Clerc, and S. Fleck, “Can a subjective questionnaire be used as brain-computer interface performance predictor?,” *Frontiers in Human Neuroscience*, vol. 12, 2019.
- [237] S. D. Muthukumaraswamy, B. W. Johnson, and N. A. McNair, “Mu rhythm modulation during observation of an object-directed grasp,” *Cognitive Brain Research*, vol. 19, pp. 195–201, 4 2004.
- [238] G. Chen, S. M. Gully, and D. Eden, “Validation of a new general self-efficacy scale,” *Organizational Research Methods*, vol. 4, pp. 62–83, 6 2001.
- [239] H. Walach, N. Buchheld, V. Buittenmüller, N. Kleinknecht, and S. Schmidt, “Measuring mindfulness—the freiburg mindfulness inventory (fmi),” *Personality and Individual Differences*, vol. 40, pp. 1543–1555, 6 2006.
- [240] J. Bismuth, F. Vialatte, and J.-P. Lefaucheur, “Relieving peripheral neuropathic pain by increasing the power-ratio of low- β over high- β activities in the central cortical region with eeg-based neurofeedback: Study protocol for a controlled pilot trial (smrpain study),” *Neurophysiologie Clinique*, vol. 50, pp. 5–20, 2 2020.
- [241] L. P. McAvinue and I. H. Robertson, “An evaluation of a movement imagery training scheme,” *Imagination, Cognition and Personality*, vol. 29, pp. 99–114, 10 2009.
- [242] B. Z. Allison and C. Neuper, “Could anyone use a bci?,” in *Brain-Computer Interfaces* (D. S. Tan and A. Nijholt, eds.), London: Springer London, 2010.
- [243] J. Thievenaz, *De l’étonnement à l’apprentissage. Enquêter pour mieux comprendre*. De Boeck Supérieur, 2017.
- [244] E. Vogl, R. Pekrun, K. Murayama, K. Loderer, and S. Schubert, “Surprise, curiosity, and confusion promote knowledge exploration: Evidence for robust effects of epistemic emotions,” *Frontiers in Psychology*, vol. 10, 11 2019.
- [245] J. R. Stieger, S. Engel, H. Jiang, C. C. Cline, M. J. Kreitzer, and B. He, “Mindfulness improves brain-computer interface performance by increasing control over neural activity in the alpha band,” *Cerebral Cortex*, vol. 31, pp. 426–438, 1 2021.
- [246] N. Ramli, S. S. Kuok, L. K. Tan, Y. Q. Tan, L. F. Tan, K. J. Goh, K. A. A. Kadir, P. C. Seow, and S. Y. Goh, “Effect of mindfulness meditation on brain-computer interface,” *Neurology Asia*, vol. 24, pp. 343–353, 12 2019.
- [247] R Core Team, *R: A Language and Environment for Statistical Computing*. R Foundation for Statistical Computing, Vienna, Austria, 2022.

- [248] D. Zapala, P. Iwanowicz, P. Francuz, and P. Augustynowicz, “Handedness effects on motor imagery during kinesthetic and visual-motor conditions,” *Scientific Reports*, vol. 11, 12 2021.
- [249] A. Vuckovic and B. A. Osuagwu, “Using a motor imagery questionnaire to estimate the performance of a brain-computer interface based on object oriented motor imagery,” *Clinical Neurophysiology*, vol. 124, pp. 1586–1595, 8 2013.
- [250] A. Vourvopoulos, F. Liarokapis, and M.-C. Chen, “The effect of prior gaming experience in motor imagery training for brain-computer interfaces: A pilot study,” in *2015 7th International Conference on Games and Virtual Worlds for Serious Applications (VS-Games)*, pp. 1–8, IEEE, 9 2015.
- [251] A. Vourvopoulos, S. Bermudez i Badia, and F. Liarokapis, “Eeg correlates of video game experience and user profile in motor-imagery-based brain-computer interaction,” *Visual Computer*, vol. 33, pp. 533–546, 4 2017.
- [252] E. M. Hammer, T. Kaufmann, S. C. Kleih, B. Blankertz, and A. Kübler, “Visuo-motor coordination ability predicts performance with brain-computer interfaces controlled by modulation of sensorimotor rhythms (smr),” *Frontiers in Human Neuroscience*, vol. 8, 8 2014.
- [253] A. B. Randolph, “Not all created equal: Individual-technology fit of brain-computer interfaces,” in *2012 45th Hawaii International Conference on System Sciences*, pp. 572–578, IEEE, 1 2012.
- [254] N. Leeuwis, A. Paas, and M. Alimardani, “Vividness of visual imagery and personality impact motor-imagery brain computer interfaces,” *Frontiers in Human Neuroscience*, vol. 15, 4 2021.
- [255] C. Ferrel-Chapus and P. Tahej, “Processus attentionnels et apprentissage moteur,” *Movement & Sport Sciences*, vol. n° 71, p. 71, 2010.
- [256] R. M. Ryan and E. L. Deci, “Self-determination theory and the facilitation of intrinsic motivation, social development, and well-being,” *American Psychologist*, vol. 55, pp. 68–78, 2000.
- [257] M. E. Thurlings, A.-M. Brouwer, J. B. F. V. Erp, B. Blankertz, and P. J. Werkhoven, “Does bimodal stimulus presentation increase erp components usable in bcis?,” *Journal of Neural Engineering*, vol. 9, p. 045005, 8 2012.
- [258] O. Bai, Z. Mari, S. Vorbach, and M. Hallett, “Asymmetric spatiotemporal patterns of event-related desynchronization preceding voluntary sequential finger movements: a high-resolution eeg study,” *Clinical Neurophysiology*, vol. 116, pp. 1213–1221, 5 2005.
- [259] L. N. Singh, S. Higano, S. Takahashi, N. Kurihara, S. Furuta, H. Tamura, Y. Shimanuki, S. Mugikura, T. Fujii, A. Yamadori, M. Sakamoto, and S. Yamada, “Comparison of ipsilateral activation between right and left handers,” *NeuroReport*, vol. 9, pp. 1861–1866, 6 1998.
- [260] T. Wang, J. Deng, and B. He, “Classifying eeg-based motor imagery tasks by means of time–frequency synthesized spatial patterns,” *Clinical Neurophysiology*, vol. 115, pp. 2744–2753, 12 2004.

-
- [261] S. Ezquerro, J. A. Barios, A. Bertomeu-Motos, J. Diez, J. M. Sanchez-Aparicio, L. Donis-Barber, E. Fernández-Jover, and N. Garcia-Aracil, “Bihemispheric beta desynchronization during an upper-limb motor task in chronic stroke survivors,” in *From Bioinspired Systems and Biomedical Applications to Machine Learning* (J. M. Ferrández Vicente, J. R. Álvarez-Sánchez, F. de la Paz López, J. Toledo Moreo, and H. Adeli, eds.), (Cham), pp. 371–379, Springer International Publishing, 2019.
- [262] S. Rimbart and S. Fleck, “Long-term kinesthetic motor imagery practice with a bci: Impacts on user experience, motor cortex oscillations and bci performances,” *Computers in Human Behavior*, vol. 146, p. 107789, 9 2023.
- [263] M. Crotti, K. Koschutnig, and S. C. Wriessneger, “Handedness impacts the neural correlates of kinesthetic motor imagery and execution: A fmri study,” *Journal of Neuroscience Research*, vol. 100, pp. 798–826, 3 2022.
- [264] G. Pfurtscheller, C. Neuper, and W. Mohl, “Event-related desynchronization (erd) during visual processing,” *International Journal of Psychophysiology*, vol. 16, pp. 147–153, 5 1994.
- [265] C. Benaim, J. Barnay, G. Wauquiez, H. Bonnin-Koang, C. Anquetil, D. Pérennou, C. Piscicelli, B. Lucas-Pineau, L. Muja, E. le Stunff, X. de Boissezon, C. Terracol, M. Rousseaux, Y. Bejot, D. Antoine, C. Biquet, and H. Devilliers, “The Cognitive Assessment scale for Stroke Patients (CASP) vs. MMSE and MoCA in non-aphasic hemispheric stroke patients,” *Annals of Physical and Rehabilitation Medicine*, vol. 58, pp. 78–85, apr 2015.
- [266] J. C. Borod, H. Goodglass, and E. Kaplan, “Normative data on the boston diagnostic aphasia examination, parietal lobe battery, and the boston naming Test,” *Journal of Clinical Neuropsychology*, vol. 2, pp. 209–215, nov 1980.
- [267] J. Gregson, M. J. Leathley, A. P. Moore, T. L. Smith, A. K. Sharma, and C. L. Watkins, “Reliability of measurement of muscle tone and muscle power in stroke patients,” *Age and Ageing*, vol. 29, pp. 223–228, may 2000.
- [268] L. Smith, “Activetwo system operating guidelines,” 2009.
- [269] O. Alkoby, A. Abu-Rmileh, O. Shriki, and D. Todder, “Can We Predict Who Will Respond to Neurofeedback? A Review of the Inefficacy Problem and Existing Predictors for Successful EEG Neurofeedback Learning,” *Neuroscience*, vol. 378, pp. 155–164, may 2018.

My publications

Journals

1. Le Franc, S., **Herrera Altamira, G.**, Guillen, M., Butet, S., Fleck, S., Lécuyer, A., Bougrain, L., & Bonan, I. (2022). "Toward an Adapted Neurofeedback for Post-stroke Motor Rehabilitation: State of the Art and Perspectives." *Frontiers in Human Neuroscience* 16:917909. doi: 10.3389/fnhum.2022.917909

Conferences

1. **Herrera Altamira, G.**, Bougrain, L., Lécuyer, A., & Fleck, S. (2022). "Grasp-IT Xmod: A Multisensory Brain-Computer Interface for Post-Stroke Motor Rehabilitation." *33ème Conférence Francophone Pour l'Interaction Humain Machine IHM'22*. April 2022. Namur, Belgium. ****Award for the Best Demonstration.**
2. **Herrera Altamira, G.**, Fleck, S., Lécuyer, A., & Bougrain, L. (2023). "User test and EEG insights of bimodal, visual and vibrotactile, stimuli." *Journées CORTICO 2023* May 9-10, 2023. Paris, France.
3. **Herrera Altamira, G.**, Fleck, S., Lécuyer, A., & Bougrain, L. (2023). "Design and Evaluation of Vibrotactile Stimulus to Support a KMI-based Neurofeedback." *Proceedings of the 10th International Brain-Computer Interface Meeting 2023* (p. 113). Verlag der Technischen Universität Graz. doi: 10.3217/978-3-85125-962-9-108.
4. **Herrera Altamira, G.**, Skiba, N., Lécuyer, A., Bougrain, L., & Fleck, S. (2023). "Multi-sensory neurofeedback design for KMI embodiment." *In SensoryX'23: Workshop on Multisensory Experiences, together with IMX 2023: ACM International Conference on Interactive Media Experiences*. June 12-15, 2023. Nantes, France ACM, New York, NY, USA, 3 pages. <https://doi.org/10.1145/3604321.3604352>
5. **Altamira, G.**, Fleck, S., Lécuyer, A., & Bougrain, L. (2023). "EEG Modulations Induced by a Visual and Vibrotactile Stimulation". *IEEE SMC 2023 - International IEEE Conference on Systems, Man, and Cybernetics 2023*. October 1-4, 2023. Oahu, Hawaii, USA. ****Co-chair of the Special Session in the BMI workshop: "Multimodal and Multisensory Information in BMIs".**

Abstract

Motor imagery-based brain-computer interfaces (BCI) offer promising solutions for post-stroke motor rehabilitation. Kinesthetic motor imagery (KMI) consists of imagining the sensations of a movement (such as temperature, pressure, roughness, muscular contraction, and nerve activation) rather than visualizing the movement. However, KMI lacks sensory or kinesthetic feedback, making this task challenging to understand, learn, and perform. This absence of feedback hinders performance evaluation and therapeutic guidance for post-stroke patients. To address this issue, feedback is provided to both patients and therapists, based on the patient's performance.

Various feedback modalities, including visual, functional electrical stimulation, exoskeletons, and robotic assistance, have been explored to bridge this gap. Vibrotactile feedback is an underexplored alternative, that offers skin stimulation, targeting patients with limited mobility. Combining different feedback modalities has emerged as a promising approach to provide more effective feedback and enhance the rehabilitation process.

The development of BCI feedback has often prioritized technological advancement over patient-centric considerations, resulting in limited clinical adoption. This thesis adopts a novel design-based research (DBR) approach, placing the user at the core of feedback system development. The objective is to design and evaluate vibrotactile feedback, complemented with visual feedback and integrated it with a KMI-based BCI to improve post-stroke motor rehabilitation.

We start by identifying the needs and objectives of patients undergoing BCI training, leading to the hypothesis that bimodal feedback (combining vibrotactile and visual modalities) can enhance KMI within the BCI context. We tailor the vibrotactile stimulation to provide precise sensory feedback during grasping KMI. The vibrotactile device is then built considering the anatomical and physical limitations of post-stroke patients.

Then, the vibrotactile stimulation is built in two phases: establishing vibration sensory thresholds for age-dependent groups and synchronizing a visual environment with vibrotactile stimulation. Different vibration patterns are compared to determine the one that better corresponds to the graphic animation. The stimulation was designed, drawing inspiration from the natural muscle activation of the muscles during grasping.

Following the validation of the stimulation, the BCI is assessed with a group of neurotypical participants to measure its efficacy in improving KMI and evaluate its acceptability, usability, and reliability. Three feedback modalities (vibrotactile, visual and bimodal - vibrotactile and visual) are compared to determine their effectiveness.

This research highlights the potential of a user-centered approach for developing feedback solutions that enhance motor imagery and rehabilitation outcomes. Furthermore, an experimental protocol is presented for future studies with post-stroke patients to assess the acceptability and usability of the meticulously designed BCI with bimodal feedback. The findings of this work lay the foundation for translating the resulting BCI into practical clinical applications, ultimately benefiting post-stroke patients.

Keywords: vibrotactile feedback, brain-computer interface, kinesthetic motor imagery, user-centered design, stroke, motor rehabilitation.

Résumé

Les interfaces cerveau-ordinateur (ICOs) basées sur l'imagination motrice offrent des solutions prometteuses pour la rééducation motrice des patients après un accident vasculaire cérébrale (AVC). L'imagerie motrice kinesthésique (IMK) consiste à imaginer les sensations d'un mouvement, telles que la température, la pression, la rugosité, la contraction musculaire et l'activation nerveuse, plutôt que de visualiser le mouvement. Cependant, l'IMK ne comporte pas de retour sensoriel ou kinesthésique, ce qui rend cette tâche difficile à comprendre, à apprendre et à réaliser. Cette absence de retour d'information, ou feedback en anglais, restreint l'évaluation de la performance et l'orientation thérapeutique des patients post-AVC. Pour faire face à ce problème, un retour d'information est fourni aux patients et aux thérapeutes en fonction de la performance du patient.

Diverses modalités de feedback ont été étudiées pour résoudre ce problème, notamment visuelles, la stimulation électrique fonctionnelle, les exosquelettes et les robots. Le feedback vibrotactile est une alternative peu explorée, qui vise à stimuler la peau et s'adresse aux patients avec une mobilité très réduite qui ne peuvent pas profiter des autres solutions. La combinaison des différents feedbacks est révélée comme une approche prometteuse pour fournir un retour d'information plus efficace et améliorer le processus de réadaptation.

Le développement du feedback pour les ICOs a souvent donné la priorité au progrès technologique plutôt qu'aux considérations centrées sur le patient, ce qui a eu pour conséquence une adoption clinique limitée. Cette thèse adopte une nouvelle approche de recherche basée sur la conception (design-based research en anglais, DBR), plaçant l'utilisateur au coeur du développement du système du retour d'information. L'objectif est de concevoir et d'évaluer un feedback vibrotactile, complété par un feedback visuel, et de l'intégrer à une ICO basée sur l'IMK pour améliorer la rééducation motrice post-AVC.

Nous commençons par identifier les besoins et les objectifs des patients post-AVC qui suivent un entraînement par une ICO. Comme résultat, nous avons formulé l'hypothèse que le feedback bimodal (intégrant les modalités vibrotactiles et visuelles) peut améliorer l'IMK dans le contexte d'interaction avec une ICO. Le dispositif vibrotactile est ensuite construit en tenant compte des limitations anatomiques et physiques des patients post-AVC.

Ensuite, la stimulation vibrotactile est construite en deux phases : établissement des seuils sensoriels de vibration pour trois groupes des âges différents et synchronisation d'un environnement visuel avec la stimulation vibrotactile. Différents modèles de vibration sont comparés pour déterminer celui qui correspond le mieux à l'animation graphique. La stimulation a été conçue en s'inspirant de l'activation des muscles lors d'un mouvement de préhension.

Après la validation de la stimulation, l'ICO est évaluée auprès d'un groupe de participants neurotypiques afin de mesurer l'efficacité, l'utilisabilité et la fiabilité du système. Trois modalités de feedback (vibrotactile, visuelle, bimodal — vibrotactile et visuelle) sont comparées pour évaluer leur efficacité à soutenir l'exécution de l'IMK.

Cette recherche met en évidence le potentiel d'une approche centrée sur l'utilisateur pour développer des solutions de feedback qui améliorent l'IMK et la rééducation. Un protocole

expérimental est présenté pour une future étude chez les patients post-AVC afin d'évaluer l'acceptabilité et l'utilisabilité de l'ICO avec un feedback bimodal méticuleusement conçu. Les résultats de ce travail offrent les bases pour l'application de notre ICO dans la pratique clinique, avec le potentiel de bénéficier les patients post-AVC.

Mots-clés: retour vibrotactile, interface cerveau-ordinateur, imagerie motrice kinesthésique, conception centrée utilisateur, accident vasculaire cérébral, rééducation motrice.

